

Design of a Business Jet

a project presented to
The Faculty of the Department of Aerospace Engineering
San José State University

in partial fulfillment of the requirements for the degree
Master of Science in Aerospace Engineering

by

Nicholas Dea

August 2018

approved by

Dr. Nikos Mourtos
Faculty Advisor



Chapter 1

Introductory Literature Review

1.1 Motivation

Currently, there are several factors that contribute to the negative connotations that come with air travel. Some issues that are most often negatively associated with flying are personal space and safety. These issues are at the forefront of today's topics as airlines are doing their best to maximize profits, while leaving passengers in the rear-view mirror. One example of a reduction in one's personal space would be in the journal article presented by Govindaraju and Crossley [1]. In their observations and analysis, they determined that the most profitable travel for airlines were not on large passenger transports with maximized seating, but rather with smaller regional jets whom are able to fly shorter distances, yet make a higher number of trips between the destinations. Others may argue that a reduction in personal space may be a hinderance on emergency evacuations as the volume of passengers that must exit the plane in confined spaces will take considerably more time than fewer passengers in wider more open aisles and seats.

Safety refers to a multitude of factors, for instance, security checkpoints as well as turbulence or airplane mechanical or technical issues. Safety is an issue as the public and those setting the regulations have a distance between the two as to what the objective of the security measures are meant for, as discussed in the article by David Caskey [2]. Within this report, Caskey reports one case in which many luxuries once in place and now removed has irked passengers, thus causing rifts between the two sides.

These issues are of importance as passenger air travel has progressed by leaps and bounds since first being introduced. Steps and measures must be taken to have continued success and longevity that will have the industry last a multitude of lifetimes with continued demand.

1.2 Literature Review

When flying in any aircraft, safety is always an issue. In aerospace engineering a common saying is that mistakes are written in blood. This statement is true as a minor mistake to the design, build or flight process could lead to catastrophic failure that may result in death. During the flight process, the most dangerous segment of a flight plan occurs during the takeoff and landing sequences, as explained in the journal article written by Patrick Veillette [3]. In this article, observations were made in 2004 that observed business jets on approach and landing. Of the accidents that did occur during these sequences, a majority were caused by human error. A possible solution to this issue that was suggested is to have a greater training experience for both the pilot and air traffic controller.

Another possible solution to this issue is presented by John Griswold [4]. In Griswold's journal article, feedback systems were used as a way to improve the safety of the flight. From this study, the system was observed to have increased the safety of the flight, decrease the workload of the pilot, as well as be used to plot a more effective flight path to the intended destination. A system such as the one employed for this article utilized a six degree of freedom simulation to achieve a stable flight. This system would improve the safety by taking in factors which a pilot may miss from gauges or general feel of the plane. The feedback system is a very powerful tool that can be used as a backup for the pilot if they were to miss judge or overlook a factor which may put themselves and the passengers at risk of an accident.

The design process is also a very integral part that takes into account the overall safety a plane will have during certain situations. In the journal article presented by Bruce A. Noble [5], the design and development of the plane strongly correlate to the plane's overall structural integrity. In the beginning steps, the materials and intended mission requirements must comply with one another. The next steps that must be considered are the different loading scenarios and fail safeties. This article displays the importance of how the overall design choices must relate to the desired mission requirements to provide a safe and effective aircraft.

The design process also must take into account the tradeoffs that are presented when selecting different mission requirements. In this first example, written by Paul Kalberber and Andy Supinie [6], the development of the Cessna Citation line had an instance where a tradeoff decision was made. The Citation was developed from the first design the Fanjet 500. This objective was to produce a lighter weight business jet that would appeal to the light to mid weight turboprop rather than the existing business jet. The objective was to be able to utilize shorter runways. To meet this requirement the decision was made to sacrifice speed for safety, as well as to account for the elimination of pilot error.

The consistent reduction of seat space has caused a recent uproar amongst the public. This is an issue in which the airlines are doing their best to compensate for the ever-increasing operating costs. Yet, this may be doing more bad than good for its passengers. Passenger health is often a topic which is not looked upon when air travel is discussed as most flights average a time of approximately two hours. Yet if the frequency of the number of flights is increased, the hours will add up, as evidenced by in the article Health & Safety at Work [7]. Amongst British subjects observed, with a closer proximity among fellow passengers, the likely hood of catching or infecting others is increased. Another issue that was brought to light was more than just bodily harm, but psychological harm that may be caused. With the increased business travel, language barriers and cultural shocks can lead to issues of a passenger's health and safety.

With a reduction in space and the high volume of passengers on commercial airliners, the overall feeling is that airplanes are pressure vessels of contamination flying at 35,000 ft in the air. One issue observed is in the *Journal of Occupational and Environmental Hygiene* [8], was the possibility of fungal infections being transferred in the air. From the results, it was concluded that the possibility of obtaining the fungal infection through air spores was unlikely during flight. It was determined passengers would be at a higher risk in the terminals and even higher risk once leaving the airports. The data also concluded that the greatest chance of catching the fungal infection would be during the boarding and deplaning processes as at these times, passenger activity and motion is at its highest, as well as having the necessary ventilation for the air spores to spread.

Fungal infection pores are not the only airborne health concern that should be considered. In the journal article presented by the Center for Energy & Environ. Res. & Services, CEERs [9], Viral infections are also transported through droplets in the air. Planes are equipped with air recirculation systems which are a mixture of recycled and bleed air. From the observation and results, the recirculation system tended to deposit virus droplets at the front and rear rows. The findings also determined that the droplets typically were dispersed on the side of the aisle of which they originated from. If someone were to have a contagious disease on a commercial flight, it is very likely that the passengers at the front and rear of the aisle contaminate will be affected.

Another issue that has arose and will continue to gain momentum as an issue is the number of signals that are emitted by electronic devices. As presented in the journal article

presented at IEEE Africon [10], radio frequencies, RF, were observed in metal enclosures which have small metallic areas, such as elevators and planes, for the frequencies to escape. The results concluded that small children were at higher risk of bodily harm being done from RF waves, as opposed to adults. Yet these values were still able to not exceed the acceptable amount of RF guidelines. With the continued improvement of technology and society becoming more reliant on cellular devices, it is an inevitable fact that one day cell phone usage will be allowed on planes. RF waves may not be an issue today, but the likelihood of cell phone companies changing the way the RF is given from a phone and the duration of an international business flight, the likelihood of RF causing bodily harm increases dramatically. \

One argument that is universally agreed upon are the comfortability of airplane seats. Sitting for long periods of times is a fact which is often associated as having no effect on the human body. This statement is false as sitting for long periods is detrimental to one's health. Possible health issues that may arise during flights are sore joints or loss of blood flow to areas which are not being utilized. Presented in Personal and Ubiquitous Computing [11], unobtrusive monitoring airplane seats are proposed to solve such an issue. The seats would measure electrocardiogram, electrodermal activity, skin temperature, and respiration. These results would help to determine the health of each passenger as they rest on their flight and alert the crew if emergency measures are needed to be taken.

The business jet market is one which is often overlooked as they are typically not used commercial, but rather for personal and leisure use. The market will trend as to the cost profit margin trends. If costs to operate surpasses the profit, the demand will decline. As opposed to a low fleet of business jets will increase profits as there are fewer competitors, which will lead to possible reinvestments into business jets to meet the demand. In the article written by Lawrie Jones [12], the tradeoff between efficiency and cost and profit were observed. Jones observed one such tradeoff that continues to improve as technology helps to aid the issue. The tradeoff between engine selection and profits were discussed. As engines rely heavily on the technology used, improving efficiency, minimizing environmental impact and improving efficiency to reduce the operating costs. These engines can be built using composites, advanced high-pressure compressors and 3D printed components amongst other possible solutions.

Boeing has conducted its own studies of the expected airplane market for more than just their well-known passenger jets. It is anticipated that the market for regional jets will be able to maintain a steady market of the number of units sold within the next 20 years. This trend is expected because after the large decline in the number of units sold in 2009, the market is expected to return to a level and steady market [13].

Another source that was analyzed to determine the need for a medium sized jet would be the market expectations by Jet Stream [14]. In the article, it mentions there are several factors influencing the market, "GDP growth, fleet replacement, and the expansion and most importantly the globalization of international business and commerce". One such example was the number of Chinese companies expanding their businesses and using private jets to reach their destinations rather than using passenger airliners to travel. With this trend, companies other than those located in China have followed suit, therefore bolstering the private jet market. The final analysis estimates that private jet manufacturing companies expect to see a 13% to 25% increase in the number of units sold through 2024.

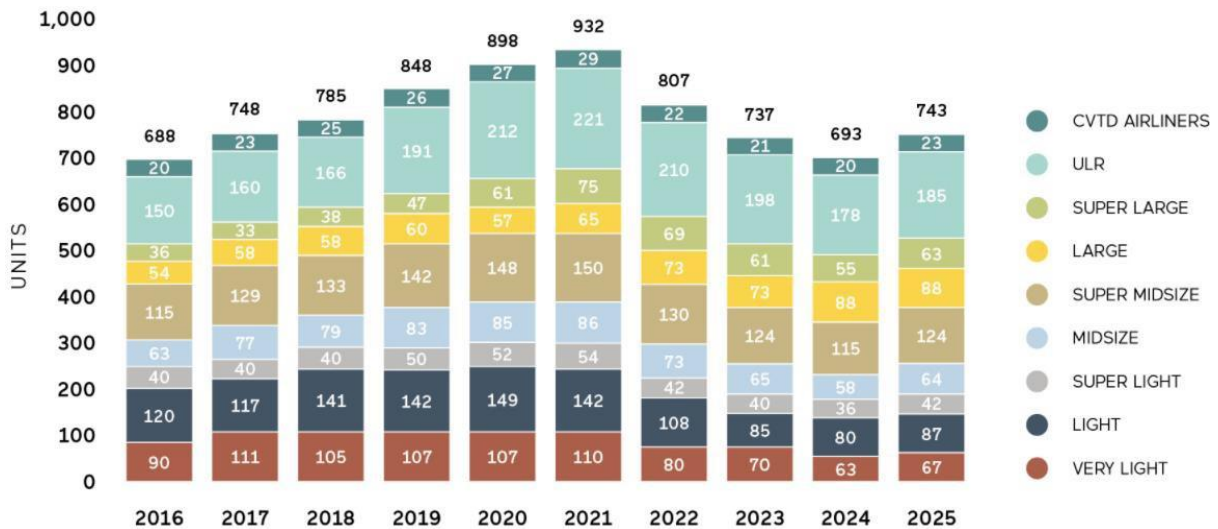


Figure 1: Expected units to be sold by size category. [15]

CNN has also written an article that more companies are beginning to utilize private jets for their own personal leisure business trips [16]. The article mentions that businesses have been converting or purchasing passenger sized aircraft, such as Airbus A380 or Boeing 737 or 747, as their way of transit. But with these large planes that have the capacity to carry upwards of 100 people, the companies should fill the plane to capacity to be worth the operating costs. With these businesses and who is most likely to travel on the company plane, the number one priority is money. With a larger plane and the need to only carry the executive staff, the need for such a large plane may outweigh the benefits of an extra roomy cabin. This trend should therefore lead companies in the future to purchase smaller luxury jets.

1.3 Project Proposal

The objective goal of this project is to expand my personal knowledge of the design process which goes into the design process of an airplane. To enhance my knowledge, a business jet was chosen to be the main subject. A business jet was chosen as it is similar to a passenger airliner, yet a smaller scale. The design process of an airplane requires that mission requirements are met, while also complying with FAA regulations. A business jet will also allow for flexibility as to the overall interior and exterior appearance. This will be a unique business jet as it will consider several of the solutions presented above to the problems presented regarding the safety, personal space and marketability.

1.4 Methodology

The steps that will be taken throughout this project will build upon the prior business jet design performed in Advanced Aircraft Design class, AE 271. The project will build upon the Class I method of sizing and performance to advance to Class II methods of sizing and performance, in regards to the processes set forth by Jan Roskam's Airplane Design. The steps that will be taken are as follows:

1. Completion of Class I sizing

2. Landing gear re-design
3. Aircraft subsystems
4. Weight estimation
5. V-n diagram
6. Weight and balance analysis
7. Drag Polar

References

- [1] Govindaraju, P., & Crossley, W. A. (2013). Profit motivated airline fleet allocation and concurrent aircraft design for multiple airlines. Paper presented at the *2013 AIAA Aviation Technology, Integration, and Operations Conference (ATIO 2013)*, 19 pp.
- [2] D. L. Caskey. (1992). The problem with security: Public perception versus reality. Paper presented at the *Proceedings 1992 International Carnahan Conference on Security Technology: Crime Countermeasures*, 99-102. 10.1109/CCST.1992.253764
- [3] Veillette, P. R. (2004). A human factors analysis of business jet approach and landing accidents. Paper presented at the *49th Annual Corporate Aviation Safety Seminar, CASS - Quality Safety: Oasis in the Desert, April 27, 2004 - April 29, , 49 25-42.*
- [4] Griswold, J. (2000). Integrated flight and propulsion control system design for a business jet. Paper presented at the *AIAA Guidance, Navigation, and Control Conference and Exhibit 2000, August 14, 2000 - August 17.*
- [5] Noble, B. A. (1966). Design and development of the structural integrity of a jet executive, D.H. 125. Paper presented at the *Business Aircraft Conference, March 30, 1966 - April 1*, 10.4271/660216
- [6] Kalberer, P., & Supinie, A. (2003). Development of the citation line of business jets. Paper presented at the *AIAA\ICAS International Air and Space Symposium and Exposition: The Next 100 Years, 2003, July 14, 2003 - July 17,*
- [7] Leaving on a jet plane business travel health and safety]. (2007). *Health & Safety at Work*, 29(12), 18-21.
- [8] McKernan, L. T., Hein, M. J., Wallingford, K. M., Burge, H., & Herrick, R. (2008). Assessing total fungal concentrations on commercial passenger aircraft using mixed-effects modeling. *Journal of Occupational and Environmental Hygiene*, 5(1), 48-58. 10.1080/15459620701766817
- [9] Taherian, S., Rahai, H., Bonifacio, J. R., & Hortsman, R. (2014). Virus transport aboard commercial regional aircraft. Paper presented at the *44th AIAA Fluid Dynamics Conference*, 1-13.
- [10] A. Y. Simba, S. Watanabe, T. Hikage, & T. Nojima. (2009). A review of mobile phone usage in enclosed areas and RF safety guideline. Paper presented at the *Africon 2009*, 1-6. 10.1109/AFRCON.2009.5308075

- [11] Schumm, J., Setz, C., Bachlin, M., Bachler, M., Arnrich, B., & Troster, G. (2010). Unobtrusive physiological monitoring in an airplane seat. *Personal and Ubiquitous Computing*, 14(6), 541-50. 10.1007/s00779-009-0272-1
- [12] L. Jones. (2015). Battle for the skies. *Engineering & Technology*, 10(5), 72-75. 10.1049/et.2015.0511
- [13] CURRENT MARKET OUTLOOK 2016–2035. (2017). [ebook] Boeing, pp.5 -19. Available at: http://www.boeing.com/resources/boeingdotcom/commercial/about-our-market/assets/downloads/cmo_print_2016_final_updated.pdf [Accessed 1 Sep. 2017].
- [14] Brenner, C. (2017). *Large, Long-Range Business Jets Driving Industry Growth* | Jetcraft. [online] Jetcraft. Available at: <https://www.jetcraft.com/jetstream/2016/04/large-long-range-business-jets-driving-industry-growth/> [Accessed 2 Sep. 2017].
- [15] Jetcraft. (2017). *Market Forecast* | Jetcraft. [online] Available at: <https://www.jetcraft.com/knowledge/market-forecast/> [Accessed 2 Sep. 2017].
- [16] Ros, M. (2017). *Luxury VIP jets: How the super-rich fly*. [online] CNN Travel. Available at: <http://www.cnn.com/travel/article/flying-palaces-vip-airliners/index.html> [Accessed 2 Sep. 2017].

Chapter 2

Class I Design Methodology

LIST OF SYMBOLS

- A – Regression coefficient
AAA – Advanced Aircraft Analysis Version 3.7
AEO – All engines operative
AR – Aspect ratio
B - Regression coefficient
b - Wing span
c – Regression line coefficient c
 \bar{c} – Mean geometric chord length of wing
 c_r – Chord at the root
CG - center of gravity
CGR – Climb gradient requirement
CG_{WE} – Center of gravity of empty weight load
CG_{WOE} – Center of gravity of operating empty weight
CG_{WTO} – Center of gravity takeoff weight
 C_D – Coefficient of drag
 C_{D_0} – Zero lift drag coefficient
 c_f – Equivalent skin friction coefficient
 $c_{j_{cr}}$ – Specific fuel consumption for jet during cruise
 $c_{j_{ltr}}$ – Specific fuel consumption for jet during loiter
 c_j – Specific fuel consumption for jet plane
 C_L – Coefficient of lift
 $C_{L_{MAX_L}}$ – Maximum coefficient of lift during landing
 $C_{L_{MAX_{TO}}}$ – Maximum coefficient of lift during takeoff
 $C_{L_{MAX}}$ – Maximum coefficient of lift
 $C_{L_{max_{W_{swept}}}}$ – Maximum coefficient of lift of the swept wing
 $C_{L_{max_{W_{unswept}}}}$ – Maximum coefficient of lift of the unswept wing
 $C_{L_{max_W}}$ – Maximum coefficient of lift of the wing
 $C_{L_{max_r}}$ – Maximum coefficient of lift at the root
 $C_{L_{max_t}}$ – Maximum coefficient of lift at the tip
 $C_{L_{max}}$ – Maximum coefficient of lift of clean airplane
 $C_{l_{\alpha_v}}$ – Lift curve slope of vertical stabilizer
 $C_{l_{\alpha_h}}$ – Lift curve slope of horizontal stabilizer
 $C_{l_{\alpha_w}}$ – Lift curve slope of wing
 $C_{l_{\delta_f}}$ – Coefficient of lift at deflection angle of flap
 C_{n_β} – Yaw moment with respect to sideslip angle
 $C_{n_\beta_{wb}}$ – Yaw moment with respect to sideslip angle of wing and body

D - Regression coefficient
 d - Regression line coefficient
 dB - Decibels
 D_{ef} - Fan cowling exit width
 D_{eg} - exit width of gas generator
 D_f - Equivalent diameter
 D_g - Width of leading edge of gas generator
 D_{hl} - Inlet width of fan cowling
 D_n - Max width of fan cowling
 D_n - Outer width of fan cowling
 D_p - Width of plug
 dα - Change of angle of attack
 dε - Downwash angle
 dε_h - Downwash angle of horizontal stabilizer
 E - Endurance
 e - Oswald efficiency
 f - Equivalent parasite area
 F - factor
 F - Fahrenheit
 FAR - Federal Aviation Requirements
 ft - foot or feet
 ft/s - feet per second
 g - Gravity (ft/s)
 h_{Crit} - max certified altitude
 h_{cr} - Critical max height (max service ceiling)
 i_h - Incidence angle of horizontal stabilizer
 in - Inches
 km - Kilometers
 knts - knots
 k_λ - Taper ratio
 lbf - pound force
 lbs - pounds
 $\frac{L}{D}$ - Lift to drag ratio
 $\frac{L}{D_{cr}}$ - Lift to drag ratio during cruise
 $\frac{L}{D_{ltr}}$ - Lift to drag ratio during loiter
 l₁ - Distance from leading edge to max height of exterior of fan cowling
 lbs - pounds
 l_f - Length of fuselage
 l_g - Length of gas generator
 l_m - Distance between center of gravity and main landing gear in longitudinal direction
 l_n - Distance between nose landing gear and center of gravity in longitudinal direction
 l_n - Length of fan cowling
 LNDG - Landing gear
 l_p - Length of plug

m – meter
 M – Maximum operating Mach number
 M_{cc} – Crest critical Mach
 M_{cruise} – Cruise Mach
 M_{Div} – Divergence Mach
 M_{ff} – Mission fuel fraction
 M_{res} – Reserve fuel regarding mission fuel fraction
 M_{tfo} – Trapped fuel and oil referenced to takeoff gross weight
 MFW – Maximum fuel weight
 MLW – Maximum landing weight
 mph - Miles per hour
 MTL – Maximum thrust loading
 MTOW – Maximum takeoff weight
 MWL – Maximum wing loading
 MZFW – Maximum zero fuel weight
 N – Number of engines
 NP – Max number of passengers (excluding crew)
 NTSB – National Transportation Safety Board
 N_D – Drag induced yawing moment
 n_s – Number of main gear struts
 $N_{t,crit}$ – Critical one-engine out yawing moment
 N_{ult} – Ultimate load according to FAR 25
 OEI – One engine inoperative
 P_m – Main landing gear load
 P_n – Nose landing gear load
 psf – per square foot
 q – Dynamic pressure
 R – Range
 R_{n_r} – Reynolds number at root
 R_{n_t} – Reynolds number at tip
 R/C – Max rate of climb
 RTL – Runway length to land (at MLW, with max passengers)
 r_{min} – Minimum turn radius (ft)
 S - Wing area
 $S_{Elevator}$ – Area of elevator
 $S_{exp,plf}$ – Wetted exposed planform
 S_{FL} – Safety field length
 S_h – Area of horizontal stabilizer
 S_h – Wing area of horizontal stabilizer
 S_{Rudder} – Area of rudder
 S_{TOFL} – Takeoff field length
 S_v – Area of vertical stabilizer
 S_v – Wing area of vertical stabilizer
 S_{wet} – Wetted area of plane
 S_{wet_emp} – Wetted area of empennage
 $S_{wet_fan\ cowling}$ – Wetted area of fan cowling

S_{wet_fus} – Wetted area of fuselage
 S_{wet_plf} – Wetted area of planform
 S_{wg} – Area of wing
 S_{wing} – Wing area
 S_{wing} – Area of the wing only
 T – Thrust force
 T_{TO_e} – Thrust to takeoff
 t/c – Thickness ratio
 $(t/c)_{avg}$ – Average thickness ratio
 $(t/c)_r$ – Thickness ratio at root
 T/W – Thrust to weight ratio
 $(\frac{T}{W})_L$ – Thrust to weight ratio during landing
 $(\frac{T}{W})_{TO}$ – Thrust to weight ratio during takeoff
 TOL – Takeoff Length (balanced field length, at MTOW)
 $(TOP)_{25}$ – Takeoff parameter of FAR 25
 TOW – Takeoff weight
 Type of PL - type of payload
 v – Velocity
 V_A – Velocity upon approach
 V_{crit} – Stall speed
 V_{cruise} – Cruise velocity (above FL310, at long range)
 \bar{V}_h - Volume coefficient of horizontal stabilizer
 \bar{V}_v - Volume coefficient of vertical stabilizer
 V_{Max} – Maximum operating speed
 V_{mc} – Minimum controllable velocity
 V_S – Stall speed
 V_{S_A} – Approach stall speed
 V_{S_L} – Stall speed during landing
 V_{S_L} – Stall velocity for landing
 $V_{S_{TO}}$ – Stall speed during takeoff
 V_{wf} – Volume of fuel in wing
 W/S – Wing loading
 $(W/S)_L$ – Wing loading during landing
 $(W/S)_{TO}$ – Wing loading during takeoff
 $W_{E_{tent}}$ – Tentative empty weight
 $W_{OE_{tent}}$ – Tentative operating empty weight
 W_E – Empty weight
 W_F – Weight of fuel
 W_{FEQ} – Fixed equipment weight
 W_L – Landing weight
 W_{ME} – Manufacturer's empty weight
 W_O – Initial weight (takeoff weight)
 W_{PL} – Payload weight
 W_{TO} – Takeoff weight

W_{crew} – Crew weight
 W_{tfo} – Weight of trapped fuel and oil
 W_{wing} – Weight of the wing
 $\frac{W_1}{W_1}$ – Weight fraction from takeoff to stage 1
 $\frac{W_{TO}}{W_2}$ – Weight fraction from stage 1 to stage 2
 $\frac{W_1}{W_3}$ – Weight fraction from stage 2 to stage 3
 $\frac{W_2}{W_4}$ – Weight fraction from stage 3 to stage 4
 $\frac{W_3}{W_5}$ – Weight fraction from stage 4 to stage 5
 $\frac{W_4}{W_6}$ – Weight fraction from stage 5 to stage 6
 $\frac{W_5}{W_7}$ – Weight fraction from stage 6 to stage 7
 $\frac{W_6}{W_8}$ – Weight fraction from stage 7 to stage 8
 W_7
 x_{ac_A} – Aerodynamic center of aircraft
 x_{ac_h} – Aerodynamic center of horizontal stabilizer
 x_{ac_wb} – Aerodynamic center of wing and body(fuselage) x_h – moment arm of horizontal stabilizer
 x_v – Distance of center of gravity to aerodynamic center of vertical stabilizer
 x_v – moment arm of vertical stabilizer
 y_t – Lateral thrust moment arm of critical engine
ZFW – Zero fuel weight

 η_{max} – Max load factor
 ρ_{SL} – Air density of sea level
 ρ_{TO} – Air density during takeoff
 γ – Specific heat
 Γ_h – Dihedral angle of horizontal stabilizer
 Γ_w – Dihedral angle
 θ – Angle between longitudinal axis and main landing gear with relation to nose gear
 λ – Ratio between chord at tip to root
 ΔC_L – Change in coefficient of lift
 $\Delta C_{L_{maxL}}$ – Change in maximum coefficient of lift during landing
 $\Delta C_{L_{maxTO}}$ – Change in maximum coefficient of lift during takeoff
 Λ – Sweep angle
 $\Lambda_{c/4}$ – Sweep angle at the quarter chord
 $\Lambda_{c/4_h}$ – Sweep angle at quarter chord of horizontal stabilizer
 λ_f – Fuselage fineness ratio
 λ_h – Taper ratio of horizontal stabilizer
 λ_w – Taper ratio of wing
 π – Pi, 3.14...
 τ – Ratio between thickness ratio at root to tip
 ϕ – Angle between ground and lowest part of wing, in relation to main landing gear

ψ – Angle between ground and aft most center of gravity

ω – Rate of turn

ρ – Air density

σ – Ratio of air density at takeoff over sea level

δ_f – deflection angle of flap

$^{\circ}$ - Degree

$\frac{\partial W_{TO}}{\partial L/D}$ – Sensitivity of takeoff weight to lift to drag ratio

$\frac{\partial W_{TO}}{\partial W_P}$ – Sensitivity of takeoff weight to empty weight

$\frac{\partial W_{TO}}{\partial W_E}$ – Sensitivity of takeoff weight to weight of payload

$\frac{\partial W_{TO}}{\partial W_{PL}}$ – Sensitivity of takeoff weight to specific fuel consumption

$\frac{\partial W_{TO}}{\partial c_j}$ – Sensitivity of takeoff weight to endurance

$\frac{\partial W_{TO}}{\partial R}$ – Sensitivity of takeoff weight to range

$\frac{\partial W_{TO}}{\partial v}$ – Sensitivity of takeoff weight to velocity

In this chapter, the steps of a Class I design method will be discussed and explained. The initial steps that will be taken are defining mission specifications and a comparative study, configuration design, weight sizing and weight sensitivity, performance constraints and overall fuselage design.

1.0 Mission Specification and Comparative Study

1.1 Introduction

The purpose of this subchapter is to begin identifying and outlining the steps to fill the void in the airplane market. The mission requirements will be set to design the plane around. The plane will then be compared against other preexisting planes that fit the desired mission requirements.

1.2 Mission Specification

In this section, mission requirements, flight profile, anticipated market, economic feasibility and possible pitfalls will be discussed in further detail.

1.2.1 Mission Requirements

The main objective of this aircraft is the transportation of passengers to their desired destination in a luxurious manor. The aircraft is intended to carry in the range of 10 to 14 people, the exact number will be determined later on, with the inclusion of any crew members. There will be enough space in the cargo hold to carry the baggage of the passengers and crew and any extra necessities needed for safety or emergencies. This plane will primarily consist of a minimum of 2 crew, a pilot and co-pilot, and if necessary a stewardess to attend to the guests if desired by the passengers. With a stewardess, one less passenger will be able to be seated on the plane as it will affect the weights, which will be discussed later.

For this plane to be worth purchasing, the statistical numbers of range, cruise speed, and other noteworthy flight parameters must be met. For range, the plane should be able to fly for a cruising time of 5 hours and attain a range of 3000 miles, which is suitable for a continental US flight from coast to coast. With a cross country flight across the United States within the plane's capabilities, it makes it a viable purchase option with a wider range of possible destinations an investor may travel to. This plane will also be able to fly across continental Europe with the range of 3000 miles, equivalent to 4830 km. The approximated cruise speed is to be 530 mph, Mach .69, at an altitude between 30000 and 40000 ft, with a max ceiling of 45000 ft, depending on the need to conserve fuel on long duration flights.

The aircraft will generally takeoff and land at commercial airports and runways, but at the same time, will be able to utilize private airstrips with shorter runways, typical of remote areas. The plane will require a 6000 ft runway when taking off at sea level with an estimated maximum takeoff weight (MTOW) of 30000 lbs. With a takeoff occurring at altitude, the runway length will need to be increased by approximately two feet for every one foot of altitude experienced above sea level. This plane will require a runway of 2700 ft to land. The landing speed, stall speed when landing, required must be greater than 100 knots, 115 mph, Mach .15, this will ensure that the plane does not stall in the air when on approach for landing. To ensure this is met, a computer feedback alert system will be used to enhance the safety and warn the pilots if the airspeed is too low and stall flow begins.

The noise pollution generated from this aircraft will be at its maximum when taking off and its minimum when approaching for landing. The noise levels should not exceed 65 dB on average from an exterior standpoint. While in comparison to the noise levels within the aircraft, a

noise level of 75 dB on average should not be exceeded, with the greatest noise level during takeoff to not exceed 85 dB for an extended period of time.

1.2.2 Mission Profile

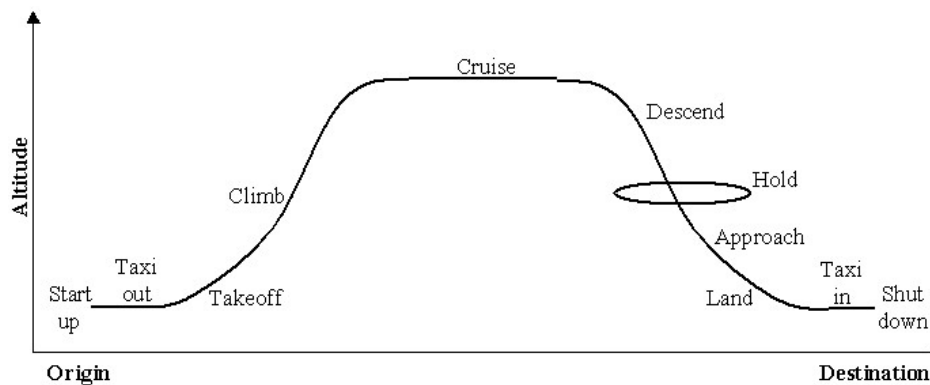


Figure 1.1: Sketch of mission profile. [1]

In the figure above, it shows the general flight pattern to be taken when the airplane is utilized as intended by the mission requirements. This flight plan follows the conventional path of planes when used. The figure is not to scale. The cruise length will take the majority of the flight distance from origin to destination. The holding pattern is not scaled correctly as the frequency of planes landing at private air strips may be less than that of a commercial airport, as well as other possibilities of runways being obstructed for landing. Thus, the holding pattern may not exist or may need several circular flight maneuvers for a landing slot to open.

1.2.3 Market Analysis

The intended market for this plane is directed towards super star athletes, private holders or startup CEO's rather than for large commercial airliners to add to their larger passenger fleet. The plane is anticipated to be priced between 10 and 50 million dollars in the market place, depending on the fine details such as the type of technology used in the avionics portion or the number and type of engines used as the propulsion system just for example as many other options are available.

The need for this type of plane fits with several findings that a new medium sized jet design is warranted. The first point of evidence that a plane such as the one being presented in this report is the relationship with star athletes, presented by The Christian Science Monitor [2]. In this article, it states that athletes are using private jets as a status symbol rather than their intended usage of air travel. This may not appeal to the case for building this plane in the beginning, but if it sells a plane, that is all that matters. This can also be applied to celebrities who star in movies or those who feature their music on the radio, essentially those who are well known public figures that want to portray themselves and lifestyles in a certain manner. The market from a potential buyer's standpoint can seem to be limitless as there are always new and emerging stars coming from all horizons.

The potential buyer market can be further explained by PrivateFly, a booking service for private jets. The article depicts the markets between the United States and Europe. It portrays the difference in economies of the US and Europe [3]. It shows that the market for private jets is larger in the US than that in Europe, but the two markets combined make up over 90% of the world's private jet fleet. The private jet market is anticipated to decline in the European market, but the US market is expected to grow within that same time span. This shows that there is a significant market Europe, with an expanding market in the United States.

1.2.4 Technical and Economic Feasibility

When designing, developing, and building a plane, a realistic point of view must be taken. The plane's mission requirements will direct the plausibility of the plane being built from technologies that already exist or plan on being developed in the near future. From a technical standpoint, there is nothing in particular that will limit the plane from taking off the ground. To design and develop the plane, no new programs or processes will have to be invented in. The technology that will be used in the building process of the plane are standard options, such as navigation, altimeter and the remaining avionics used in the plane.

From an economical viewpoint, the plane will be limited by the type of technology that is implemented in the plane. The specific models of the technology used will dictate the pricing of the plane on the market. As the market projections mentioned in the previous section, the market seems to be stable over the next 10 years, as stated by JetStream, "forecasts \$178B worth of transactions to be executed over the next ten years for larger cabin aircraft" [5]. The best option would be to use the standard equipment used in other midsize jets.

1.2.5 Critical Mission Requirements

Of the mission requirements listed, the major items that may pose a problem are range, storage and safety of passenger and crew. These items will impact the design of the plane to ensure the mission requirements are met and satisfied with confidence. Each possible solution is looked at solving the issue individually without negatively impacting other aspects of the aircraft.

The range and endurance will impact several key design features of the plane. Range will likely have an influence on the wing's design, the wingspan, aspect ratio (AR) and the type of airfoil used. With these possible modifications made to the wing, it will help the design by increasing the amount of lift generated which will not require as much fuel to be consumed, therefore increasing the range. Range could also be increased to meet the mission requirements by reducing the weight of plane's structure or possibly utilizing a more efficient propulsion system. There are numerous design changes that can be made to enhance the range of the plane, these are just a select few possibilities to consider.

The storage and ability to move around the cabin for passengers could also be a limiting factor that may dissuade potential buyers from purchasing the plane. The amount of space in a small luxury jet likely impacts a potential buyer's decision by limiting the number of passengers they may want to accompany them on the trip while remaining comfortable with the amount of personal space each is given. With the number of passengers, the individuals will most likely have baggage that will be brought along on the trip. The most likely solution will be to either place the baggage in the cabin closest or in the cargo hold on the underside of the plane. The best way to combat this potential flaw in the design would be to increase the size of the fuselage. This will likely have an effect on the distance as the plane is now heavier and will require more lift. Another possible option would be to use a low wing configuration to create extra space in the cargo hold for passenger and crew luggage to be stored.

The safety of the passengers will always be an important factor in the design process of a plane. With a smaller jet, safety will be much more key as the number of accidents of small jets is quite significant. In an article by Live Science, "the fatality rate hovers just over 1 death per every 100,000 hours", in reference to a 2010 NTSB report [4]. It was also stated that, "the accident rate in personal flights has increased by 20 percent in the past decade, and the fatality rate for personal flights is up 25 percent" [4]. These statistics show that private planes may be luxurious in that there is less hassle of public airports and waiting time, but the danger level is heightened over passenger planes significantly. A possible design option to increase the safety of

passengers may be to have a stronger structure that will hold up upon heavy ground impact. Depending on how these accidents are occurring, there are a few different design modifications that can be made to improve the safety of passengers. One feature that should be standard to help reduce injury possibilities during accidents would be to ensure that passengers are buckled in with a seat belt or another similar safety device.

1.3 Comparative Study of Similar Airplanes

With the design outlook for this plane, it is anticipated to be categorized as either a midsize or super midsize jet. In the following sections, the planes below fit into either of those two categories. These statistics will be able to help determine the design outlook for the plane to either be a larger or smaller luxury jet. The planes being analyzed will consist of three midsize jets and three super midsize jets to help determine which category will best fit. The three midsize jets to be analyzed are the Cessna 560 Citation Excel/ XLS, Hawker 800XP and Learjet 60 [5]. The super midsize jets are comprised of the Cessna 680 Citation Sovereign, Bombardier Challenger 300 and Gulfstream G200 [5].

1.3.1 Mission capabilities and configuration selection

Table 1.1: Critical mission requirements and design characteristics of select jets. [5][6]

Plane	Range (miles)	Cruise Speed (mph)	Max Number of Passengers	Wing Position	Engine Position	Empennage Design
Cessna 560 Citation Excel/ XLS	2416	507	9	Low	Rear of Cabin	Cruciform
Hawker 800XP	3202	505	8	Low	Rear of Cabin	Cruciform
Learjet 60	2772	483	10	Low	Rear of Cabin	T - tail
Cessna 680 Citation Sovereign	3682	529	12	Low	Rear of Cabin	Cruciform
Bombardier Challenger 300	3527	527	9	Low	Rear of Cabin	T - tail
Gulfstream G200	3510	608	10	Low	Rear of Cabin	Cruciform

1.3.2 Comparison of Important Design Parameters

Table 1.2: Specific flight characteristic parameters of midsize and super midsize jets. [5][6]

Plane	WTO (lbs)	WPL (lbs)	WE (lbs)	WF (lbs)	T (lbf)	Vcr (mph)	R (miles)	hcr (ft)	S (ft^2)	B (ft)	AR	Type of PL
Cessna Citation Excel/XLS	20200	2240	12170	6740	4119	104	2416	41000	370	54.33	7.977	Passenger and baggage
Hawker 800XP	28000	2120	16330	7880	4660	106	3202	41000	381	54.33	7.7	Passenger and baggage
Learjet 60	23500	2104	14896	7910	4600	122	2772	51000	265.84	43.75	7.2	Passenger and baggage

Cessna 680 Citation Sovereign	30775	4065	17710	11332	5770	NA	3682	47000	543	72.33	7.7	Passenger and baggage
Bombardier Challenger 300	38849	3348	22749	14149	6826	NA	3527	45000	523	63.84	7.81	Passenger and baggage
Gulfstream G200	35450	3800	20200	15000	6040	129	3510	45000	369	58.08	9.1	Passenger and baggage

1.3.3 Discussion

From the statistical parameters illustrated in the tables above, the mission requirements will not match any one specific plane which has already been designed and manufactured. Rather it will consist of a mix of capabilities and configurations pulled from multiple planes.

With the mission requirements having been set at a cruising speed of 530 mph, with a range of 3000 miles, an altitude between 30000 ft and 40000 ft, a maximum takeoff weight of 30000 lbs and a stall speed of 100 knots, about 115 mph. Based off of these mission requirements being met, the plane appears to fall in between the two categories, either a larger scale midsize jet and a smaller scale super midsize jet. Based on which plane best matches the most important parameters of range and takeoff weight, the plane matches best with the Hawker 800XP, thus the proposed plane will be categorized as a midsize jet.

1.4 Conclusions and Recommendations

From this report, the design process can now begin. Upon declaring the mission requirements and analyzing the potential buyer market of a business jet, the process of analyzing planes already in the market may take place. The planes which were analyzed to compare with the potential design plane were categorized as midsize and super midsize jets. These jets were compared first by their abilities to match the mission requirements set by the potential design plane proposed, the configurations were also analyzed to determine what will best suit the proposed design plane. The established planes were then compared by their performance parameters to determine which planes general size and performance will best match the mission requirements set forth. Upon the collection of evidence of the potential market and competitor planes, the plane will best be set as a midsize jet to perform at numbers most similar to the Hawker 800XP.

With the statistics and data collected, the plane should be a midsize jet, with the closest comparison jet being the Hawker 800XP. The next step is to determine the configuration of the plane. The plane's mission requirements of range, 3000 miles, cruise speed, 500 mph, stall speed, 100 knots, payload, 8-12 passengers, and max takeoff weight, 30000 lbs, will be comprised to determine the configuration of the plane. The configuration process will consist of the fuselage size, wing placement and empennage shape. These will be used to achieve the mission requirements. If the configuration process is unable to meet the key mission requirements, the standards set will be changed accordingly without taking away too much of the performance from the plane.

1.5 References

- [1] Sigworth, A., Dávila, J., McNeil, T., Nicolalde, J., Scheve, D., & Funk, K. (200, March 14). Mission Analysis. Retrieved September 1, 2017, from <http://flightdeck.ie.orst.edu/ElectronicChecklist/HTML/mission.html>
- [2] McLaughlin, A. (1999). *Private jets have become crucial to star athletes*. [online] The Christian Science Monitor. Available at: <https://www.csmonitor.com/1999/1027/p1s2.html> [Accessed 1 Sep. 2017].
- [3] Privatefly. (2017). *Private jet market comparison: USA vs Europe | PrivateFly*. [online] Available at: <https://www.privatefly.com/us/inspirational-jet-flights/private-jet-market-in-europe-vs-usa-infographic> [Accessed 1 Sep. 2017].
- [4] Pappas, S. (2017). *Why Private Planes Are Nearly as Deadly as Cars*. [online] Live Science. Available at: <https://www.livescience.com/49701-private-planes-safety.html> [Accessed 3 Sep. 2017].
- [5] Airpartner.com. (2017). *Aircraft Guides | Private Jets | Airlines | Cargo aircraft | Air Partner USA*. [online] Available at: <http://www.airpartner.com/en-US/aircraft-guide/#privatejet> [Accessed 4 Sep. 2017].
- [6] Jane's Information Group. (1930). *Jane's All the World's Aircraft*.

2.0 Configuration Design

2.1 Introduction

The purpose of this subchapter is to determine a design configuration that works best for the plane to satisfy the mission requirements. The design configuration should meet the mission requirements while maintaining an appealing exterior and luxurious interior look that appeals to potential buyers of the proposed business jet.

2.2 Comparative Study of Airplanes with Similar Mission Performance

2.2.1 Comparison of Weights, Performance and Geometry of Similar Airplanes

The planes analyzed below are closely related to the mission requirements for range and the max number of passengers to be transported.

2.2.1.1 Weights and Loadings

Table 2.1: Weights and loads of planes. [1]

Plane	WE (lbs)	MTOW (lbs)	MLW (lbs)	MZFW (lbs)	MFW (lbs)	WPL (lbs)	MWL (lbs/ft ²)	MTL (lb/lb st)
Cessna 560XL Citation Excel/XLS	12,170	20,200	18,700	15,100	6,740	2,300	54.64	2.53
Cessna 560XL Citation XLS+	12,300	20,200	18,700	15,100	6,740	2,340	54.64	2.45
Cessna 680A Citation Latitude	18,656	30,800	27,575	21,200	11,344	2,544	56.77	2.70
Hawker 800/850	16,330	28,000	23,350	18,450	7,880	2,120	74.86	3.00
Hawker 900XP	16,020	28,000	23,350	18,450	10,000	1,950	73.49	2.95
Bombardier Learjet 60	14,896	23,500	19,500	17,000	7,910	2,104	88.85	2.55
Bombardier Learjet 85	22,850	36,700	30,150	25,250	12,100	2,100	88.65	2.91
Gulfstream G100	14,635	24,650	20,700	17,000	8,692	2,365	77.89	2.90
Gulfstream G150	15,200	26,100	21,700	17,500	10,300	2,300	82.34	2.95
Embraer Legacy 450	22,928	35,758	32,518	25,904	10,939	2,921	74.35	N/A
Embraer Legacy 500	23,437	38,360	34,524	26,499	13,146	2,800	78.55	2.73

2.2.1.2 Performance

Table 2.2: Performance statistics of planes. [1]

Plane	TOL (ft)	R/C (ft/min)	h_{Crit} (ft)	V_{MAX} (mph)	M	V_{Cruise} (mph)	V_{Crit} (mph)	RTL (ft)	R (miles)	NP
Cessna 560XL Citation Excel/XLS	3,590	3490	45,000	575	0.75	498	104	3,180	1,981	9
Cessna 560XL Citation XLS+	3560	3500	45,000	575	0.75	507	104	3,180	2,138	9
Cessna 680A Citation Latitude	3,668	N/A	45,000	613	0.80	509	N/A	3,901	3,107	9

Hawker 800/850	5,030	3,100	41,000	613	0.80	463	106	2,650	2,989	13
Hawker 900XP	5,030	N/A	41,000	613	0.80	513	126	2,650	3,242	15
Bombardier Learjet 60	5,450	4,500	51,000	621	0.81	536	122	3,420	2,767	8
Bombardier Learjet 85	4,800	N/A	49,000	629	0.82	516	N/A	2,700	3,107	8
Gulfstream G100	5,395	3,805	45,000	671	0.875	557	117	2,920	2,806	9
Gulfstream G150	5,015	N/A	45,000	652	0.85	495	126	2,445	2,761	8
Embraer Legacy 450	3,908	N/A	45,000	637	0.83	598	119	2,090	2,889	9
Embraer Legacy 500	4,085	N/A	45,000	637	0.83	536	N/A	2,123	3,392	12

2.2.1.3 Geometric dimensional parameters

Table 2.3: Dimensional values of external and internal fuselage. [1]

Plane	Dimension External				Dimension Internal				
	Length (ft)	Height (ft)	Wing Span (ft)	AR	Length (ft)	Width (ft)	Height (ft)	Cabin Volume (ft^3)	Baggage Volume (ft^3)
Cessna 560XL Citation Excel/XLS	59.79	17.37	56.31	8.4	18.66	5.58	5.66	N/A	80
Cessna 560XL Citation XLS+	52.5	17.16	56.33	8.4	18.5	5.5	5.66	N/A	90.2
Cessna 680A Citation Latitude	62.25	20.83	72.33	10.1	21.75	6.39	6	656	N/A
Hawker 800/850	51.16	18.08	54.33	7.7	21.33	6	5.75	604	76
Hawker 900XP	51.16	18.08	54.33	7.7	21.33	6	5.75	604	49.95
Bombardier Learjet 60	58.71	14.56	43.75	7.2	17.67	5.92	5.67	453	N/A
Bombardier Learjet 85	68.10	19.94	61.52	9.4	24.75	6.08	5.92	665	100
Gulfstream G100	55.58	19.5	54.58	8.8	17.08	4.75	5.58	367	64
Gulfstream G150	56.75	19.08	55.58	9.7	17.67	5.75	5.75	465	80
Embraer Legacy 450	64.56	21.10	66.44	10.3	23.98	6.83	5.98	678	148
Embraer Legacy 500	68.04	21.13	66.44	9.1	26.83	6.83	5.98	860	148

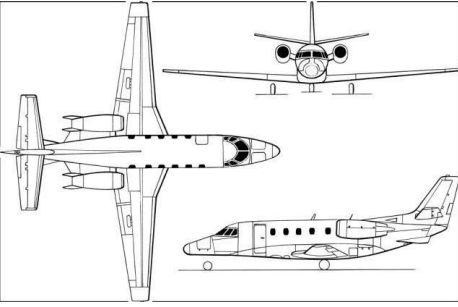

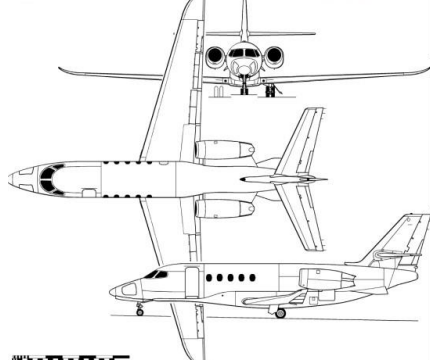
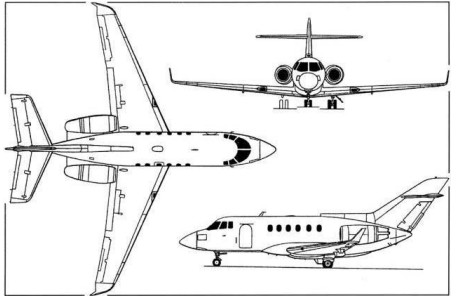
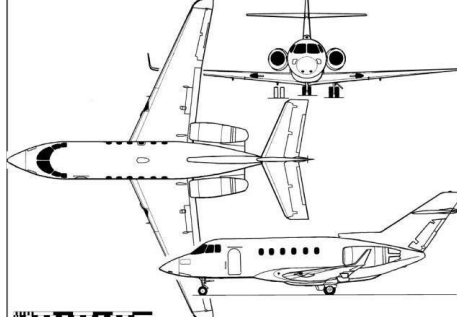
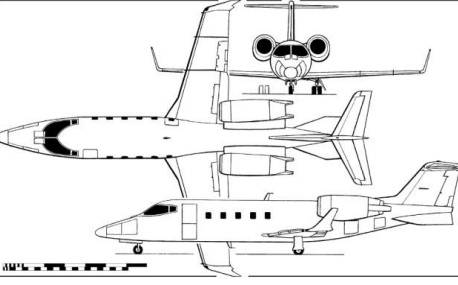
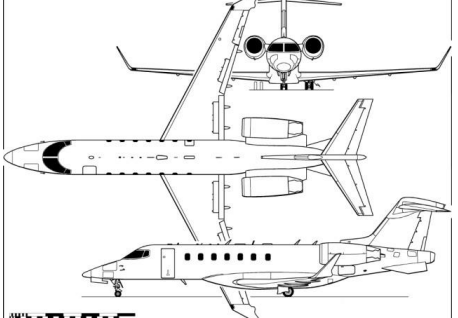
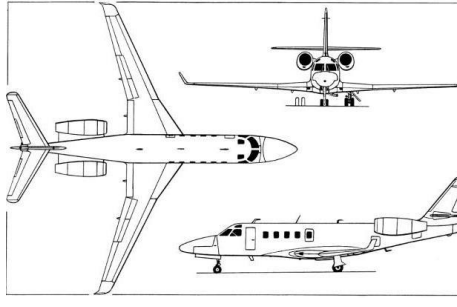
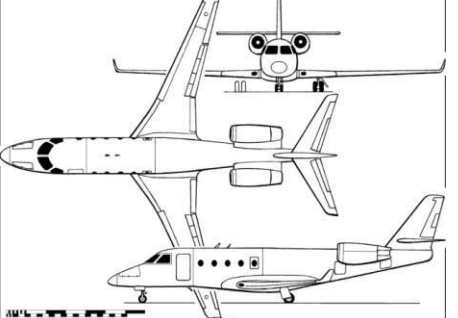
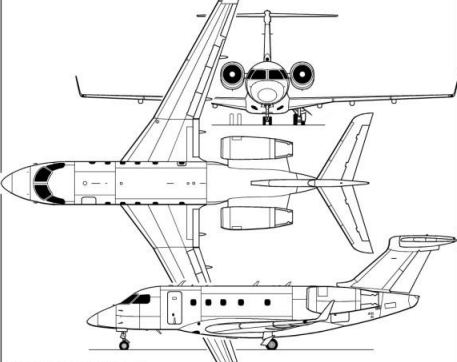
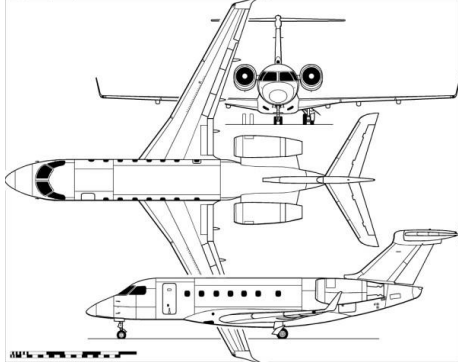
2.2.1.4 External Appearance

Table 2.4: External features highlighting key features of the planes. [1]

Plane	Wheel Base (ft)	Wheel Track (ft)	Wing Position	Tail Configuration	Engine Position
Cessna 560XL Citation Excel/XLS	21.90	14.90	Low	Cruciform	Pod-Mounted
Cessna 560XL Citation XLS+	21.98	14.98	Low	Cruciform	Pod-Mounted
Cessna 680A Citation Latitude	27	10	Low	Cruciform	Pod-Mounted
Hawker 800/850	21.04	9.17	Low	Cruciform	Pod-Mounted
Hawker 900XP	21.04	9.17	Low	Cruciform	Pod-Mounted
Bombardier Learjet 60	25.38	8.25	Low	T-tail	Pod-Mounted (45°)
Bombardier Learjet 85	N/A	N/A	Low	T-tail	Pod-Mounted (45°)
Gulfstream G100	24.08	9.08	Low	Cruciform	Pod-Mounted (45°)
Gulfstream G150	N/A	N/A	Low	Cruciform	Pod-Mounted (45°)
Embraer Legacy 450	N/A	N/A	Low	T-tail	Pod-Mounted
Embraer Legacy 500	N/A	N/A	Low	T-tail	Pod-Mounted

2.2.2 Configuration Comparison of Similar Airplanes

Table 2.5: 3-View images of planes similar to one being designed. [1]

Cessna 560XL Citation Excel/XLS	Cessna 560XL Citation XLS+	Cessna 680A Citation Latitude
		
Hawker 800/850	Hawker 900XP	Bombardier Learjet 60
		
Bombardier Learjet 85	Gulfstream G100	Gulfstream G150
		
Embraer Legacy 450		Embraer Legacy 500
		

2.2.3 Discussion

In general, all of the planes analyzed in this report maintain a similar exterior appearance in regards to the wing position, engine position and empennage configuration. Each will be further examined and discussed.

To begin, the wing positioning among all of the planes is the same, a low wing configuration. One key benefit to a low wing plane is that it utilizes ground effect, therefore allowing the plane to generate more lift than usual when close to the ground, in comparison to when the plane is in flight at altitude. This allows the plane to takeoff from shorter runways without requiring a larger wing to make up for the lift of a high wing configuration. The low wing also utilizes the space in the cargo hold, more efficiently as compared to a mid or high wing configuration, by allowing the wing to be structurally safer as it is able to be connected over a singular spar, which creates one connected wing rather than two separate halves if it were to be connected through the passenger cabin for a mid-wing configuration or lower head space for a high wing configuration. This creates a safer structure as the wing can distribute the load better, rather than having to rely on the wing root only being attached to the fuselage.

Next, the engine position on all of the planes being analyzed are the same, aft of the cabin area and pod-mounted to the fuselage. The more conventional positioning of a passenger airliner's engines is pod-mounted below the wings. This is not the case for private business jets as the clearance from the ground to the wings would not allow for the conventional configuration without risking possible damage when the plane is on the tarmac at any point. The benefits of having pod-mounted engines to the fuselage allows for a clean wing, thus maximizing the amount of lift generated without requiring extra fuel to accelerate the flow over the wing. The engine placement also allows for a low door level, which is useful for private jets as passengers typically board from the tarmac rather than walking up a jetway to board. This positioning also allows for a fairly accessible engine as they are primarily exposed, other than the side facing the fuselage, allowing for easy maintenance and service.

The final primary key configuration design is the empennage configuration. From the planes analyzed, there were two primary options used, a T-tail and cruciform empennage configuration. The two are similar as the engine placement forces the configuration. If the planes were to use a more conventional inverted T-tail and the engine's being placed where they are, the flow over the horizontal stabilizer would have been obstructed, resulting in a useless control surface. To further analyze the two empennage configurations, the T-tail will be analyzed first. The T-tail allows for better pitch control and is more efficient for low speed aircraft. The T-tail is prone to deep stall, when the plane is climbing, when the flow over the wing will disrupt the flow over the horizontal stabilizer causing it to stall. The cruciform is similar to the T-tail as it too may experience deep stall, but this allows for the horizontal stabilizer to be moved to the midpoint of the vertical stabilizer to ensure deep stall does not occur. Both empennage configurations are structural stiff with sufficient bracing and simplistic in the build process.

2.3 Configuration Selection

In this section, the configuration of the plane being designed will be laid out. Each configuration selection will be analyzed for its positives and negatives.

2.3.1 Overall Configuration

The overall configuration fits into the category of a land-based aircraft rather than the two other possible configurations, water and amphibious based aircraft. The land-based aircraft will be able to allow for a wing configuration other than a high wing to avoid the water. The use of

retractable landing gear over pontoons as the primary way of landing will aid in the reduction of the drag force during flight.

The design of a conventional aircraft, implies the utilization an aft tail. The other possible plane options are a flying wing, canard, three surfaces or joined wing. The canard may be a possible option in helping with the horizontal stabilizer to avoid deep stall. With a conventional aircraft, the fuselage can be utilized to carry passengers and baggage.

2.3.2 Wing Configuration

Based upon the mission requirements and the planes analyzed prior in this report, the wing will be classified as a cantilever wing. The wing will be positioned as a low wing, as well as being swept in the aft direction at approximately 15° to 25° , depending on further calculations that will warrant the exact value, to help reduce the effects of drag. With a low wing configuration, the plane will be unstable when using control surface to roll, thus dihedral effect must be incorporated into the wing. The wing will have a dihedral angle of approximately 10° to 20° , which will be refined later. Winglets will also be utilized to help improve tip recovery and increase maneuverability. The winglets can also be used by aiding the range and the mass of the payload the plane is able to cover and carry.

As for the precise numbers that go into the final configuration steps of weight and sizing, the numbers are based off values in Jan Roskam's Airplane Design Vol II [2]. The aspect ratio will be set at 9. The thickness ratio is directly related to the drag divergence Mach number, as thickness ratio increases, the drag divergence Mach number decreases. The thickness ratio should be minimized to elongate the time before critical Mach is reached, prolonging the amount of time before drag becomes critical and detrimental to the plane.

The taper ratio of the plane is the relation between the wing root to the wing tip. The taper ratio is to be set at .35, based off the values provided by Roskam [2], as well as based off the 3-view diagrams in table 2.5. The angle of twist to be incorporated within the wing is set at zero. This was deemed unnecessary as wing twist helps to ensure the tips of the wing do not stall. With winglets, they are used as a self-made wing twist to help prevent the tips from stalling too quickly during roll or climb phases of flight. Without incorporating twist into the wing, it will help by simplifying the manufacturability process, as well as simplifying the load analysis of the wing. The incidence angle is also another negligible feature as the aircraft does not require extra lift to be generated in order to takeoff or during flight. With the plane not requiring a generalized commercial runway and a lighter aircraft than a passenger airliner, the private business jet does not need to generate the extra lift, as well as the low wing experiences ground effect.

The airfoil shape will help to determine the final choices as it will determine the amount of lift and drag created as a standalone wing. This will also help to determine if the plane requires high lift devices or extra control surfaces. The NACA 64008a, as seen in the figure below, will be used for the business jet, as it has also been used in multiple small to midsize private business jets. With a thinner airfoil, the critical Mach is able to generate less drag at high speeds. The use of high lift devices will not be necessary as they will only add additional weight to the aircraft. An extra control surface may be necessary to account for the deep stall that is anticipated when the aircraft climbs. This topic will be examined further in the sections below.

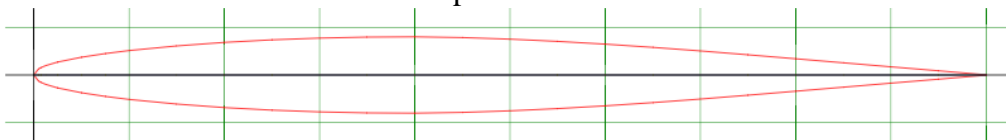


Figure 2.1: NACA 64008a airfoil shape. [3]

From this wing configuration, there are negatives that come about. With a low wing cantilever, the structure must have extra support as the wing is self-supported. The low wing is also unsafe if the plane was to have a forced landing. If the plane experiences a forced landing, the wing will likely impact the ground first. The most likely consequence is that the fuel stored in the wing will act as an accelerant and make the situation worse.

2.3.3 Empennage Configuration

The empennage is an important control surface as it contributes to all three directions of movement, roll, pitch and yaw. The vertical stabilizer is critical in the rolling and yawing moment. The vertical stabilizer is to be mounted to the fuselage. This ensures simplicity and is structurally strong. The horizontal stabilizer is to be attached at or near the top of the vertical tail. This is necessary as if it were to be fuselage mounted, the engine wake would force the surface to be negligible. The horizontal stabilizer will be mounted high creating a T-tail configuration. This will help to eliminate deep stall as when the plane is climbing, the plane will typically climb at an angle of 25° . With a shorter fuselage length, the angle should measure out that the T-tail horizontal stabilizer will not be affected by the flow over the wing to avoid deep stall.

With a T-tail configuration, the structural strength of the empennage is key. With a T-tail, the horizontal stabilizer is placed on the top of the vertical stabilizer and must be stable and not flutter to ensure the control surface is utilized to its maximum potential. The horizontal stabilizer is placed as high for a T-tail rather than a cruciform because it allows for clearance of the proposed placement of the engine exhaust. This will eliminate the possibility of heat causing the structure to deform during flight. Additionally, the vertical tail will need to be strengthened to support the loads generated by the horizontal stabilizer, this will in effect add additional weight to the plane.

2.3.4 Integration of the Propulsion System

The plane will be configured as a pusher aircraft, rather than a tractor or a combination of the two. Placing the engine on the rear of the fuselage helps with the stability in the pitching and yawing moment. This will also allow for a smaller empennage configuration, which will reduce the weight of the aircraft, allowing the possibility for a longer range.

Placing the engines in the rear will help to reduce the amount of noise created within the cabin. Compared to passenger planes, such as a Boeing 747 or an Airbus A319, the engines are pod-mounted, but under the wing. Placing the engines under the wing, the exhaust of the engine forces the air to exit past the back half of the fuselage, creating noise in the passenger cabin. With the engines proposed to be placed in the rear, this potential noise disturbance will not be an issue as the exhaust of the engines is at the location of the empennage, past the placement of any passenger seats.

The engine placement in the rear of the plane also has its negatives. The first negative that comes with placing the engines in the rear would be the movement of the CG position over the duration of the flight. The most likely placement of the fuel is to be stored within the wing. As the plane flies and fuel is burned, the CG will slowly move further aft. This will influence the plane to want to pitch nose up during flight. This must be accounted for by either employing a fuel redistribution system or the enlargement of the empennage's horizontal stabilizer to generate more lift to maintain a level flight or possibly placing heavier items near the cockpit of the plane. Another negative would be the missing propwash over the wing. Although the plane is set to use jet engines, if the engines were mounted below the wing, the exhaust flow could have been redirected to generate extra lift by the ailerons.

2.3.5 Landing Gear Disposition

Of the possible landing gear configurations, the conventional tricycle landing gear configuration will be used. The tricycle landing gear was chosen because it is the safest of the possible options, single, bicycle or quadricycle, while being weight effective. The tricycle configuration places two landing gears aft of the CG point and one near the nose of the plane, creating a triangular base. Some of the benefits that come with a tricycle landing gear include the ability to land at a crab angle, low drag during initial takeoff and allowing a good viewpoint for the pilot while taxiing. The landing gear will be retractable to help reduce the drag during cruise.

The tricycle configuration does come with negatives, such as weight balance and storage issues. The weight of the nose landing gear is required to be strong as it acts as a lone point of the plane which impacts the ground with force, compared to the two rear landing gears that can distribute the load between each other. With small aircraft, storage of the underside of the aircraft is limited. The storage of the landing gear may take away valuable space for passenger baggage in the cargo hold of the plane, as well as possible space within the wing or fuselage for fuel to be stored.

2.3.6 Proposed Configuration

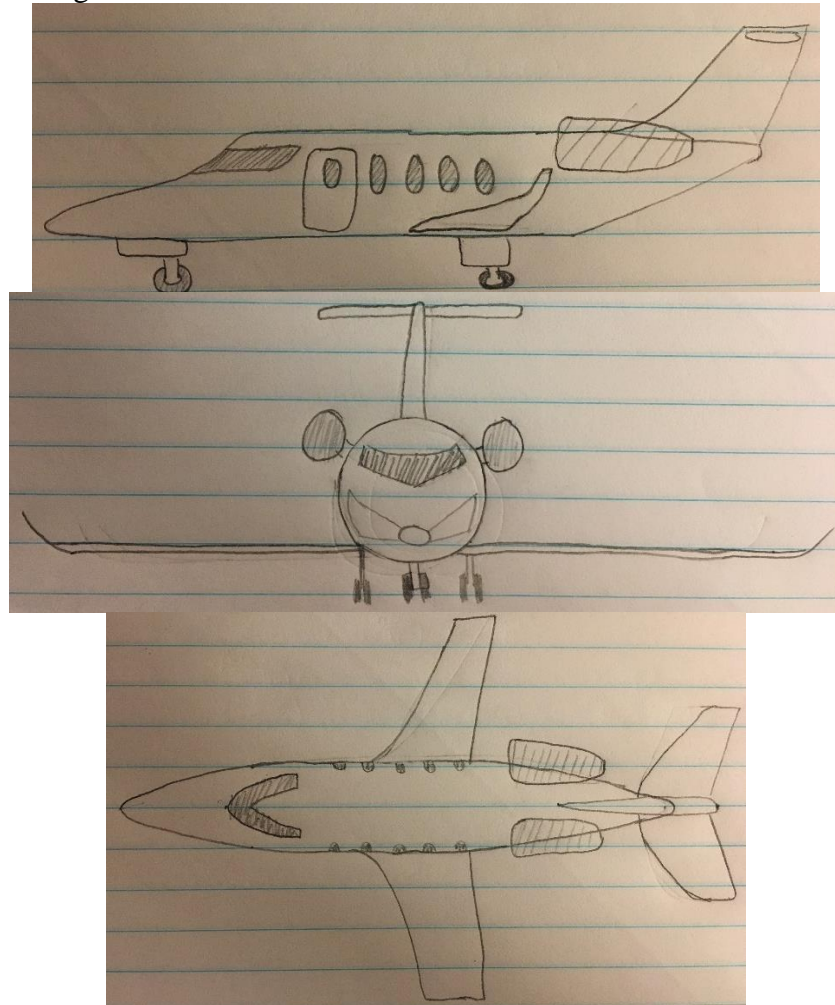


Figure 2.2: Preliminary 3-view sketch of proposed airplane design.

2.4 Discussion

The configuration proposed is the most optimal combination of design configurations to fulfill the mission requirements. The configuration of a land based conventional aircraft best fits the mission requirements as the plane is not intended to make a water landing. The choice of a low cantilever wing is the best option because it will allow for a strong wing to utilize the forces of ground effect. The empennage design configuration of a T-tail is the best option because it will be able to be put to its greatest potential in reference to the placement of the engines. The engines are to be placed at the rear of the fuselage as to minimize the noise in the cabin and to maximize the lift of the wing without creating extra drag forces. The engine placement will also help to reduce the need for the wing to account for extra structural support and added weight to the plane. The landing gear best suited for the plane's mission requirements is the tricycle landing gear as it is the most stable and utilizes the space within the wing and cargo hold the best. The landing gear will also be retractable to reduce drag during cruise. Although a number of different design configurations could be altered, this configuration will best accomplish the mission requirements without requiring extra structural supports, weights or other negative impacts to be accounted for.

2.5 References

- [1] Jane's Information Group. (1930). *Jane's All the World's Aircraft*.
- [2] Roskam, J. (1985). *Airplane design*. Ottawa, Kan.: Roskam Aviation and Engineering.
- [3] Airfoiltools.com. (2017). NACA 64-008A AIRFOIL (n64008a-il). [online] Available at: <http://airfoiltools.com/airfoil/details?airfoil=n64008a-il> [Accessed 14 Sep. 2017].

3.0 Weight Sizing and Weight Sensitivities

3.1 Introduction

The purpose of this subchapter is to determine the optimal weight size and weight sensitivities of the plane. The weight sizing will be determined by the process of examining previously manufactured planes of similar mission profile and approximate size, as well as performing calculations to determine the precise size and weight of the plane. The weight sensitivities will be analyzed by equations that relate two key flight parameters to how they affect maximum takeoff weight.

3.2 Mission Weight Estimates

3.2.1 Data Base for Takeoff Weight and Empty Weight of Similar Airplanes

The 11 planes examined in the table below are categorized within the mid-size jet category. The mid-size jet is categorized as having the ability to carry seven to eight passengers and an endurance of five to six hours.

Table 3.1: Weights and loads of planes. [1]

Plane	WE (lbs)	MTOW (lbs)	MLW (lbs)	MZFW (lbs)	MFW (lbs)	WPL (lbs)	MWL (lbs/ft ²)	MTL (lb/lb st)
Cessna 560XL Citation Excel/XLS	12,170	20,200	18,700	15,100	6,740	2,300	54.64	2.53
Cessna 560XL Citation XLS+	12,300	20,200	18,700	15,100	6,740	2,340	54.64	2.45
Cessna 680A Citation Latitude	18,656	30,800	27,575	21,200	11,344	2,544	56.77	2.70
Hawker 800/850	16,330	28,000	23,350	18,450	7,880	2,120	74.86	3.00
Hawker 900XP	16,020	28,000	23,350	18,450	10,000	1,950	73.49	2.95
Bombardier Learjet 60	14,896	23,500	19,500	17,000	7,910	2,104	88.85	2.55
Bombardier Learjet 85	22,850	36,700	30,150	25,250	12,100	2,100	88.65	2.91
Gulfstream G100	14,635	24,650	20,700	17,000	8,692	2,365	77.89	2.90
Gulfstream G150	15,200	26,100	21,700	17,500	10,300	2,300	82.34	2.95
Embraer Legacy 450	22,928	35,758	32,518	25,904	10,939	2,921	74.35	N/A
Embraer Legacy 500	23,437	38,360	34,524	26,499	13,146	2,800	78.55	2.73

3.2.2 Determination of Regression Coefficients A and B

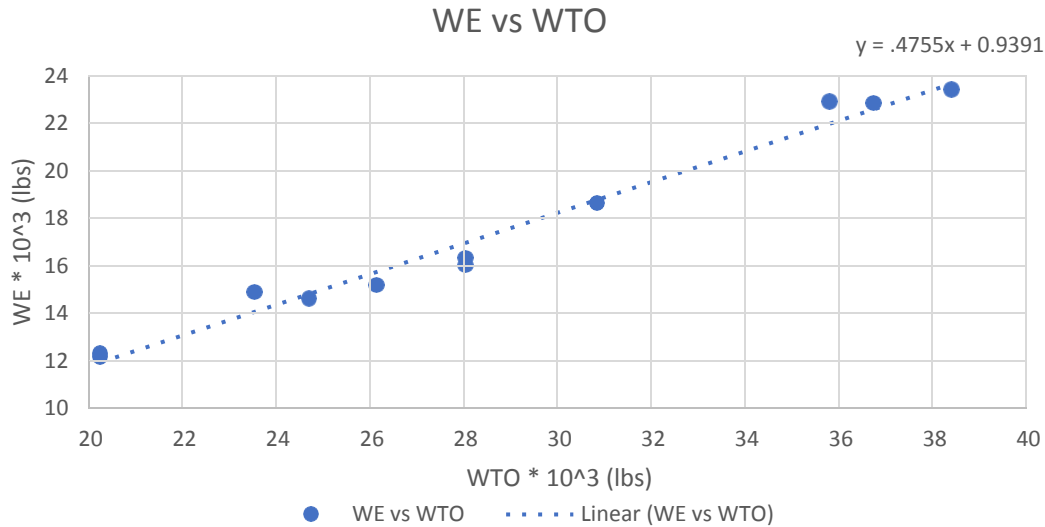


Figure 3.1: Empty weight vs the takeoff weight of the previous planes analyzed.

After the analysis of previous planes, the A and B regression coefficients of the log-log plot can be determined. Following the best fit line of the data points of the previous planes, the values of A and B are .4755 and .9391, respectively. In comparison to the results provided by Roskam for a business jet, the regression line coefficient A and B are .2670 and .9979, respectively [2]. Using the log-log A and B coefficients, the empty weight can be computed from the takeoff weight to observe how the difference in the regression coefficients between Roskam’s values and the hand calculated values.

Using the log-log equation, the regression coefficients can be verified.

$$\log(W_E) = \frac{\log(W_{To}) - A}{B} \quad (1)$$

Table 3.2: Displaying the results of the log-log plot of previous data in comparison to the regression coefficients presented by Roskam.

	Roskam Values A=.2678 B=.9979	Previous Data Values A=.4755 B=.9391
WTO (lbs)	WE (lbs)	WE (lbs)
20,200	11118.55	11973.32
20,200	11118.55	11973.32
30,800	16968.09	18762.66
28,000	15422.44	16951.86
28,000	15422.44	16951.86
23,500	12939.06	14066.72
36,700	20225.93	22612.35
24,650	13573.62	14800.88
26,100	14373.79	15729.71
35,758	19705.7	21994.83
38,360	21142.75	23703.05

From these results, the method of using previous data and placing the values into a log-log plot are fairly accurate in obtaining the A and B regression coefficients. The empty weight values are within reason, but are not a precise match to Roskam’s, but are better matched to the actual weights presented in table 3.1. With such a small sample analyzed in the previous planes

graph in figure 3.1, the regression coefficients A and B will be skewed to accommodate these planes in this analysis. Compared to Roskam which analyzed private business jets that range in takeoff weight from 13,500 lbs to 43,750 lbs. In Roskam's book, the planes analyzed in table 3.1 are all above the trend line computed by Roskam.

3.2.3 Determination of Mission Weights

3.2.3.1 Manual Calculation of Mission Weights

The process to determine the appropriate weights was described in Jan Roskam's Airplane Design Part I: Preliminary Sizing of Airplanes [2]. The process will output the mission fuel weights: takeoff weight, empty weight and weight of the fuel. To obtain the weights, the mission fuel fraction equation was used to begin the process. To begin the determination of the mission fuel fraction values, the flight plan is separated into stages.

Each stage is in relation to the plane's predicted flight path, as shown in the figure below. The values for stages 1,2,3,7 and 8 were pulled from Roskam's book [2]. The sketch is relatively simple, as it does not specify the time for climb and acceleration, range of a plane during cruise or the amount of time required for loiter.

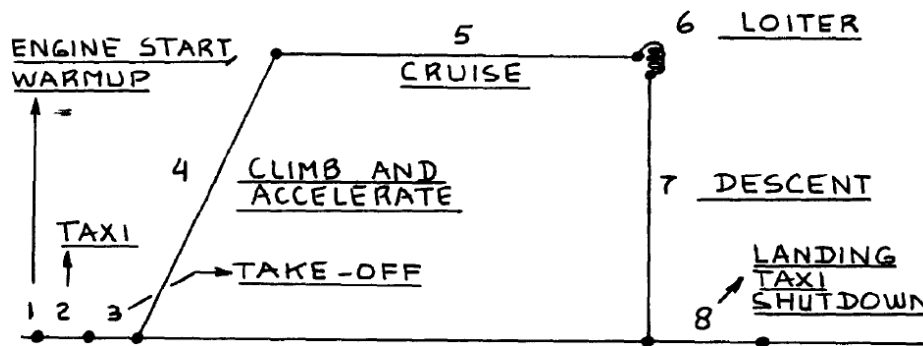


Figure 3.2: Mission profile sketch. [2]

For a more accurate weight fraction value of stages four, five and six, the equations presented below were used for five and six, while stage four was obtained by observing the fuel fraction graph in Roskam. At a cruise speed of Mach .69, the fuel fraction value was roughly .970 [2]. For stage 5, the range set during the mission requirements was 3000 miles, 2606.929 nautical miles and a cruise velocity of 530 mph, 460.6 knots. The c_j and $\frac{L}{D}$ values during cruise were provided as .7 and 11, respectively [2]. For stage 6, the loiter section, of the mission profile is intended as extra fuel in case of emergency to divert to another airport. The minimum requirement for time of loiter is 30 minutes, therefore the loiter time was set at double for precautionary reasons. The c_j and $\frac{L}{D}$ values differ between loiter and cruise. During loiter, the c_j and $\frac{L}{D}$ values are .5 and 13, respectively.

The Breguet range equation was used to determine the weight fraction value of stage five.

$$\text{Stage 5: } R = \left(\frac{v}{c_j}\right) \left(\frac{L}{D}\right) \ln\left(\frac{W_4}{W_5}\right) \quad (2)$$

After manipulation of the equation to determine the weight fuel fraction, $\frac{W_5}{W_4}$,

$$\frac{W_5}{W_4} = e^{-\left(\frac{R \cdot c_j}{v \cdot \left(\frac{L}{D}\right)}\right)} \quad (3)$$

$$\frac{W}{W_4} = e^{-\left(\frac{2606.929 \cdot 7}{460.6 \cdot (11)}\right)} = .698$$

The endurance equation was used to determine the weight fraction value of stage six.

$$\text{Stage 6: } E = \left(\frac{1}{c_j}\right) \left(\frac{L}{D}\right) \ln\left(\frac{W_5}{W_6}\right) \quad (4)$$

After manipulation of the equation to determine the weight fuel fraction, $\frac{W_6}{W_5}$,

$$\frac{W_5}{W_6} = e^{-\left(\frac{E \cdot c_j \cdot L}{D \cdot \ln}\right)} \quad (5)$$

$$\frac{W_5}{W_6} = e^{-\left(\frac{1 \cdot 5}{13}\right)} = .962$$

$$M_{ff} = \left(\frac{W_1}{W_{TO}}\right) \left(\frac{W_2}{W_1}\right) \left(\frac{W_3}{W_2}\right) \left(\frac{W_4}{W_3}\right) \left(\frac{W_5}{W_4}\right) \left(\frac{W_6}{W_5}\right) \left(\frac{W_7}{W_6}\right) \left(\frac{W_8}{W_7}\right) \quad (6)$$

From the more accurate method of determining the weight fraction values of stages four, five and six, all of the mission fuel fraction weight values are presented in the table 3.3 below. These values are then inputted into equation 6 to determine the mission fuel fraction of the plane.

Table 3.3: Weight fraction values used in mission fuel fraction equation. [2]

Stage	1	2	3	4	5	6	7	8
Weight Fraction	$\frac{W_1}{W_{TO}}$	$\frac{W_2}{W_1}$	$\frac{W_3}{W_2}$	$\frac{W_4}{W_3}$	$\frac{W_5}{W_4}$	$\frac{W_6}{W_5}$	$\frac{W_7}{W_6}$	$\frac{W_8}{W_7}$
Value	.990	.995	.995	.970	.698	.962	.990	.992

$$M_{ff} = (.990)(.995)(.995)(.970)(.698)(.962)(.990)(.992) = .6267$$

Upon finding the mission fuel fraction value, the fuel weight can be calculated by the equation presented below.

$$W_F = (1 - M_{ff}) * W_{TO} \quad (7)$$

$$W_F = (1 - .6267) * W_{TO} = .3733W_{TO}$$

The next step is to find the empty weight of the plane. This is obtained by using the two equations below.

$$W_{OE_{tent}} = W_{TO} - W_F - W_{PL} \quad (8)$$

$$\text{and } W_{E_{tent}} = W_{OE_{tent}} - W_{tfo} - W_{crew} \quad (9)$$

These two equations are tentative equations as they are based on the takeoff weight of the plane being iterated to an acceptable error difference between the two equations. For the tentative empty operating weight, the payload weight must be defined. There will be 8 passengers, with an average weight of 200 lbs. Each passenger will have 2 bags, each weighing 25 lbs. For the tentative empty weight, the weight of trapped fuel and oil is set at .5% of the takeoff weight and the crew weight of two people at 200 lbs each.

$$W_{OE_{tent}} = W_{TO} - .3733W_{TO} - [(8 * 200) + (8 * 2 * 25)]$$

$$W_{OE_{tent}} = .6267W_{TO} - 2000$$

$$W_{E_{tent}} = .6267W_{TO} - 2000 - (.005 * W_{TO}) - (2 * 200)$$

$$W_{E_{tent}} = .6217W_{TO} - 2400$$

To determine the appropriate takeoff weight of this plane, the $W_{E_{tent}}$ and W_E is to be within a .5% difference of each other. To find the empty weight of the plane, the equation below, equation 10, can be used. The manufacturers empty weight and the fixed equipment weight were

not found for the planes in table 3.1. The manufacturers empty weight and fixed equipment weight were estimated at 15000 lbs and 1000 lbs, respectively, thus amounting to an empty weight of 16,000 lbs.

$$W_E = W_{ME} + W_{FEQ} \quad (10)$$

$$W_E = 15000 + 1000 = 16,000\text{lbs}$$

With the calculations complete, the analysis begins to determine what is the best appropriate takeoff weight by iteration. To determine a takeoff weight, the tentative empty weight and empty weight should be within .5% of each other. The yellow cells present weights that are within 1% of the empty weight. The green cells present values that match the tentative empty weight and the empty weight of the aircraft the closest.

Table 3.4: Takeoff weight, operating weight and empty weight in relation to the empty weight by percent error.

W_{TO} (lbs)	$W_{OE_{tent}}$ (lbs)	$W_{E_{tent}}$ (lbs)	Error %
29300	16362.355	15815.86	1.150905
29350	16393.69	15846.94	0.956623
29400	16425.025	15878.03	0.762342
29450	16456.36	15909.11	0.56806
29500	16487.695	15940.2	0.373778
29550	16519.031	15971.28	0.179497
29600	16550.366	16002.37	0.014785
29650	16581.701	16033.45	0.209067
29700	16613.036	16064.54	0.403349
29750	16644.371	16095.62	0.59763
29800	16675.706	16126.71	0.791912
29850	16707.041	16157.79	0.986194
29900	16738.376	16188.88	1.180476

Upon the values calculated, the decision is made that the final weight of the plane corresponds to the values listed below.

Table 3.5: Final takeoff, empty and fuel weights.

W_{TO} (lbs)	W_E (lbs)	W_F (lbs)
29600	16002.37	11049.63

3.2.3.2 Calculation of Mission Weights using the AAA Program

In the Advanced Aircraft Analysis Version 3.7 program, the mission weights were able to be calculated in a similar manner to that of the hand calculations above. This will help to compare the hand calculations to computerized calculations to compare possible errors. This will also help to determine which parameters may have a larger effect on the mission weights.

The first step was to determine the mission fuel fraction value of the aircraft. The mission profile stages had to be defined, as shown in figure 3 below.

Mission Profile	M_{ff}
Warmup	0.9900
Taxi	0.9950
Take-off	0.9950
Climb	0.9800
Cruise	0.6973
Loiter	0.9623
Descent	0.9900
Land/Taxi	0.9920

Figure 3.3: Mission fuel fraction values.

When calculating the values for cruise and loiter, special methods were taken into account to obtain more accurate values, similar to the hand calculation process in section 3.2.3.1.

R	<input type="text" value="2606.0"/> nm	V	<input type="text" value="460.00"/> kts	c_j	<input type="text" value="0.700"/> $\frac{\text{lb/hr}}{\text{lb}}$	L/D	<input type="text" value="11.00"/>
Output Parameter							
M_{ff}	<input type="text" value="0.6973"/>						

Figure 3.4: Method to determine the mission fuel fraction value for stage five, cruise.

E	<input type="text" value="60.0"/> min	c_j	<input type="text" value="0.500"/> $\frac{\text{lb/hr}}{\text{lb}}$	L/D	<input type="text" value="13.00"/>
Output Parameter					
M_{ff}	<input type="text" value="0.9623"/>				

Figure 3.5: Method to determine the mission fuel fraction value for stage six, loiter.

To begin the process of determining the mission weights, the input parameters must first be defined. The regression coefficients were obtained from Roskam [2]. The takeoff weight was estimated at 29,600 lbs, based off of the hand calculation completed above. The weight of the eight passengers is 200 lbs each, amounting to a total weight of 1,600 lbs. Each passenger carries one bag of 50 lbs, rather than in the hand calculation when each passenger had two bags at 25 lbs each. There are two pilots, each weighing 200 lbs. There are no additional crew members. Since the aircraft is a passenger business jet, it is not intended as a jet transport, therefore the cargo weight is zero. The mass of the trapped fuel and oil is .5% of the takeoff weight. There is not reserve fuel, as it is accounted for in the loiter stage of the mission profile. The takeoff weight min and max values are used to define the upper and lower limit of which the weight will be analyzed between.

Input Parameters									
A	<input type="text" value="0.2678"/>	$W_{\text{passenger}}$	<input type="text" value="200"/> lb	W_{pilot}	<input type="text" value="200"/> lb	$N_{\text{crew_other}}$	<input type="text" value="0"/>	$M_{F_{\text{res}}}$	<input type="text" value="0.000"/> %
B	<input type="text" value="0.9979"/>	N_{pax}	<input type="text" value="8"/>	N_{pilots}	<input type="text" value="2"/>	W_{cargo}	<input type="text" value="0"/> lb	$W_{\text{TO_min}}$	<input type="text" value="25000.0"/> lb
$W_{\text{TO_est}}$	<input type="text" value="29600.0"/> lb	W_{bag}	<input type="text" value="50"/> lb	$W_{\text{crew_other}}$	<input type="text" value="0.0"/> lb	$M_{\text{f/o}}$	<input type="text" value="0.500"/> %	$W_{\text{TO_max}}$	<input type="text" value="35000.0"/> lb

Figure 3.6: Input parameters used to determine the output parameters of the mission weights.

The output values show the final mission weights. The fuel weight is 11,673.3 lbs. The empty weight is 17,572.2 lbs. The takeoff weight is 31,804.6 lbs. The weights of trapped oil and fuel, crew and payload were also defined. The useful weight, defined as the payload weight plus the fuel weight, is 14,073.3 lbs.

M_{H_2}	0.6330	W_F	11673.3 lb	$W_{F_{res}}$	0.0 lb	W_{crew}	400.0 lb	W_{PL}	2000.0 lb	W_E	17572.2 lb
$W_{F_{used}}$	11673.3 lb	$W_{F_{max}}$	11673.3 lb	$W_{f_{to}}$	159.0 lb	N_{crew}	2	W_{useful}	14073.3 lb	W_{TO}	31804.6 lb

Figure 3.7: Output values of mission weights.

The graph shows the iteration process used in the program to find the optimal mission weights of takeoff, empty and fuel. The two equations used to produce this graph are the log-log equation used to find the regression coefficients and the sum of the takeoff weight, amassed by the empty, payload, crew and fuel weights.

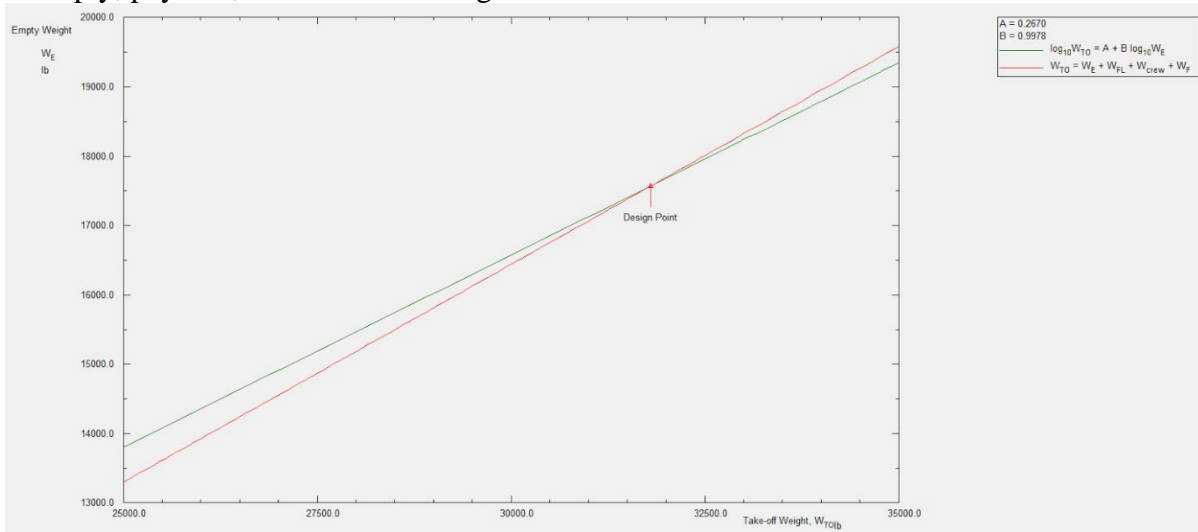


Figure 3.8: Iteration process to determine the accurate mission weights.

The figure below shows the stage to stage weights. This will help to illustrate the amount of fuel used during each stage.

	Mission Profile	W_{begn} lb	$\Delta W_{F_{used}}$ lb	$W_{F_{begn}}$ lb
1	Warmup	31804.6	318.0	11673.3
2	Taxi	31486.5	157.4	11355.3
3	Take-off	31329.1	156.6	11197.8
4	Climb	31172.5	623.4	11041.2
5	Cruise	30549.0	9246.6	10417.7
6	Loiter	21302.4	803.8	1171.1
7	Descent	20498.6	205.0	367.3
8	Land/Taxi	20293.6	162.3	162.3

Figure 3.9: The mission profile weights from stage to stage.

3.3 Takeoff Weight Sensitivities

3.3.1 Manual Calculation of Takeoff Weight Sensitivities.

Referencing the A and B regression coefficients from Roskam, A is .2678 and B is .9979 for business jets [2]. The C and D coefficients must be calculated to further analyze the sensitivity of takeoff weight to other key flight parameters.

$$A = .2678$$

$$B = .9979$$

$$C = 1 - (1 + M_{res})(1 - M_{ff}) - M_{tfo} \quad (11)$$

$$C = 1 - (1 + 0)(1 - .6267) - .005 = .6217$$

$$D = W_{PL} + W_{crew} \quad (12)$$

$$D = ((8 * 200) + (8 * 2 * 25)) + (2 * 200) = 2400$$

This log-log equation will be used to determine the takeoff weight in regards of the regression coefficients A, B, C and D. The takeoff weight will be found through iteration, similar to the method in section 3.2.3.1.

$$\log(W_{TO}) = A + (B * \log((C * W_{TO}) - D)) \quad (13)$$

From this equation, the takeoff weight is calculated as 29,700 lbs through iteration, rather than the iterated weight of 29,600 lbs calculated in section 3.2.3.1. These values are within reason of one another that it should provide sufficient values for sensitivity.

3.3.1.1 Sensitivity of Takeoff Weight to Payload

$$\frac{\partial W_{TO}}{\partial W_{PL}} = (B * W_{TO}) * (D - (C * (1 - B) * W_{TO}))^{-1} \quad (14)$$

$$\frac{\partial W_{TO}}{\partial W_{PL}} = 12.55 \text{ lbs}$$

For every pound of payload added, such as passenger baggage or other supplies, the airplane's takeoff weight will be increased by 12.55 lbs.

3.3.1.2 Sensitivity of Takeoff Weight to Empty Weight

$$\frac{\partial W_{TO}}{\partial W_E} = \frac{B * W_{TO}}{\text{invlog}(\frac{W_{TO} - A}{B})} \quad (15)$$

$$\frac{\partial W_{TO}}{\partial W_E} = .9765 \text{ lbs}$$

For every pound of empty weight, such as the structure weight or fixed equipment weight, that is added for the plane, the takeoff weight will increase by .9765 lbs.

3.3.1.3 Sensitivity of Takeoff Weight to Range, Endurance and Velocity

$$F = \frac{-B * W_{TO}^2}{(C * W_{TO} * (1 - B)) - D} * (1 + M_{Res}) * M_{ff} \quad (16)$$

$$F = 245307.9489 \text{ lbs}$$

Range Sensitivity:

The specific fuel consumption value and lift to drag ratio are those during cruise.

$$\frac{\partial W_{TO}}{\partial R} = \frac{F * c_j}{v * \frac{L}{D}} \quad (17)$$

$$\frac{\partial W_{TO}}{\partial R} = 33.89 \text{ lbs/nm}$$

For every nautical mile added to the range of the flight's mission, the plane's takeoff weight will increase by 33.89 lbs.

Endurance Sensitivity:

The specific fuel consumption value and lift to drag ratio are those during loiter.

$$\frac{\partial W_{TO}}{\partial E} = \frac{F * c_j}{\frac{L}{D}} \quad (18)$$

$$\frac{\partial W_{TO}}{\partial F} = 9434.92 \text{ lbs/hr}$$

For every hour of endurance added to the flight's mission, the plane's takeoff weight will have to add an additional 9,434.92 lbs.

Velocity Sensitivity:

The specific fuel consumption value and lift to drag ratio are those during cruise.

$$\frac{\partial W_{TO}}{\partial V} = -\frac{F \cdot R \cdot c_i}{v^2 \cdot \frac{L}{D}} \quad (19)$$

$$\frac{\partial W_{TO}}{\partial V} = -191.857 \text{ lbs/kt}$$

For every one knot increase to the cruise velocity, the plane is able to lose 191.857 lbs.

3.3.1.4 Specific Fuel Consumption and Lift to Drag Ratio Sensitivity

With respect to range requirements, the specific fuel consumption rate and lift to drag ratio will affect the takeoff weight as shown below:

$$\frac{\partial W_{TO}}{\partial c_j} = \frac{F \cdot R}{v \cdot \frac{L}{D}} \quad (20)$$

$$\frac{\partial W_{TO}}{\partial c_i} = 126230.49 \text{ lbs/lbs/lbs/hr}$$

The takeoff weight will increase by 126,230 lbs for every one-unit increase of the specific fuel consumption rate.

$$\frac{\partial W_{TO}}{\partial \frac{L}{D}} = -\frac{F \cdot R \cdot c_i}{v \cdot \frac{L^2}{D}} \quad (21)$$

$$\frac{\partial W_{TO}}{\partial \frac{L}{D}} = -8032.85 \text{ lbs}$$

The takeoff weight will increase by 8,032.85 lbs for every one-unit increase of lift to drag ratio.

With respect to endurance requirements, the specific fuel consumption rate and lift to drag ratio will affect the takeoff weight as shown below:

$$\frac{\partial W_{TO}}{\partial c_j} = \frac{F \cdot E}{\frac{L}{D}} \quad (22)$$

$$\frac{\partial W_{TO}}{\partial c_i} = 18869.84 \text{ lbs/lbs/lbs/hr}$$

The takeoff weight will increase by 18,869.84 lbs for every one-unit increase of the specific fuel consumption rate.

$$\frac{\partial W_{TO}}{\partial \frac{L}{D}} = -\frac{F \cdot E \cdot c_i}{\frac{L^2}{D}} \quad (23)$$

$$\frac{\partial W_{TO}}{\partial \frac{L}{D}} = -725.76 \text{ lbs}$$

The takeoff weight will increase by 725.76 lbs for every one-unit increase of the lift to drag ratio.

3.3.2 Calculation of Takeoff Weight Sensitivities using the AAA Program

Utilizing the Advanced Aircraft Analysis Version 3.7 program, the flight sensitivities in regards to the takeoff weight were analyzed. The input parameters must be defined first. The regression coefficient b value was the same value used in the determination of the plane's mission weights by the program. The mission fuel fraction was taken from the previous section, section 3.2.3.2. The payload and crew weight were also taken from the values found in section 3.2.3.2. The mass of the trapped fuel and oil and the reserve fuel were .5% and zero percent, respectively. The takeoff and empty weight were taken from the results of section 3.2.3.2.

Input Parameters							
B	0.9979	W_{PL}	2000.0 lb	M_{tfo}	0.500 %	W_{TO}	31071.3 lb
M_{ff}	0.6332	W_{crew}	400.0 lb	M_{res}	0.000 %	W_E	17117.9 lb

Figure 3.10: Input parameters to determine the takeoff weight sensitivities.

Upon the final calculations, the takeoff weight sensitivities were outputted, as shown in the figure below.

Output Parameters			
$\partial W_{TO} / \partial W_{PL}$	13.43	$\partial W_{TO} / \partial W_{crew}$	13.43
		$\partial W_{TO} / \partial W_E$	1.81

Mission Sensitivity Table: Output								
	Mission Prctile	$\partial W_{TO} / \partial W_{FL_{exp}}$	$\partial W_{TO} / \partial W_{FL_{reoad}}$	$\partial W_{TO} / \partial W_{F_{retuel}}$	$\partial W_{TO} / \partial c_j$ lb-hr	$\partial W_{TO} / \partial R$ $\frac{lb}{nm}$	$\partial W_{TO} / \partial L/D$ lb	$\partial W_{TO} / \partial E$ $\frac{lb}{hr}$
1	Warmup							
2	Taxi							
3	Take-cf							
4	Climb							
5	Cruise				138838.3	37.3	-8835.2	
6	Loiter				20754.5		-798.3	10377.3
7	Descent							
8	Land/Taxi							

Figure 3.11: Output of takeoff weight sensitivities.

3.3.3 Trade Studies

3.3.3.1 Range Versus Payload Tradeoff

In order to conduct this study, the takeoff weight must be defined and remain constant, thus it was made to be 29,600 lbs, from the calculation in section 3.2.3.1.

$$M_{ff} = (.990)(.995)(.995)(.970) e^{-\left(\frac{R \cdot c_{jcr}}{v \cdot \left(\frac{L}{D_{cr}}\right)}\right)} (.962)(.990)(.992)$$

$$M_{ff} = .9074 * e^{-\left(\frac{R \cdot c_{jcr}}{v \cdot \left(\frac{L}{D_{cr}}\right)}\right)}$$

$$W_F = 1 - .9074 * e^{-\left(\frac{R \cdot c_{jcr}}{v \cdot \left(\frac{L}{D_{cr}}\right)}\right)} * 29600$$

$$W_F = 29600 - 26860.9326 e^{-\left(\frac{R \cdot c_{jcr}}{v \cdot \left(\frac{L}{D_{cr}}\right)}\right)}$$

$$W_{OE_{tent}} = 29600 - 29600 - 26860.9326 e^{-\left(\frac{R \cdot c_{jcr}}{v \cdot \left(\frac{L}{D_{cr}}\right)}\right)} - W_{PL}$$

Since the takeoff weight is defined, the mission fuel weights were also calculated with the defined takeoff weight in section 3.2.3.1. The empty weight is 16002.37 lbs. The trapped fuel and oil weight is .5% of the takeoff weight. The crew of two each weighs 200 lbs.

$$W_{OE_{tent}} = 16002.37 + (.005 * 29600) + (2 * 200) = 16550.37$$

The two equations are equated together to make the equation a function of range and payload.

$$16550.37 = 29600 - (29600 - 26860.9326e^{-\left(\frac{R * c_{jcr}}{v * \left(\frac{L}{D_{cr}}\right)}\right)} - W_{PL}$$

$$16550.37 = 26860.9326e^{-\left(\frac{R * c_{jcr}}{v * \left(\frac{L}{D_{cr}}\right)}\right)} - W_{PL}$$

$$\frac{16550.37 + W_{PL}}{26860.9326} = e^{-\left(\frac{R * c_{jcr}}{v * \left(\frac{L}{D_{cr}}\right)}\right)}$$

$$\ln\left(\frac{16550.37 + W_{PL}}{26860.9326}\right) = -\left(\frac{R * c_{jcr}}{v * \left(\frac{L}{D_{cr}}\right)}\right)$$

$$R = -\ln\left(\frac{16550.37 + W_{PL}}{26860.9326}\right) * \frac{v}{c_{jcr}} * \left(\frac{L}{D_{cr}}\right) \quad (24)$$

After inputting this equation into excel, the following data was collected. The maximum payload is about 11,000 lbs, based off of the payload weight and the estimated extra space of the cabin area not occupied. With a maximum payload, the plane will amount to a range of zero nautical miles. Without a payload, the plane can maximize its range to about 3,600 nautical miles.

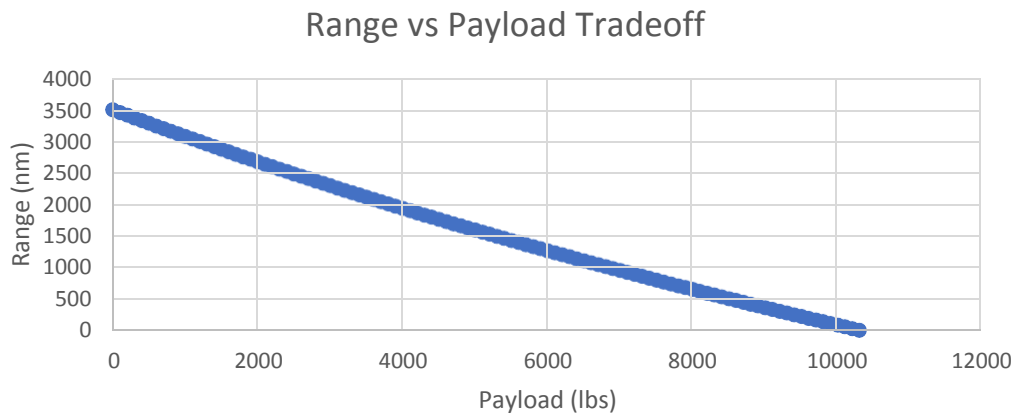


Figure 3.12: Range vs Payload tradeoff.

To verify these results, the Advanced Aircraft Analysis program was utilized. To find the trend of the tradeoff between range and payload, the input parameters are based off of the weights of the payload, thus the number of passengers, crew and their weights. The following data were the results computed by the program.

Output Parameters								
W_{crew}	400.0	lb	W_{PL}	2000.0	lb	$W_{PL@R=0}$	10709.2	lb

Output: Useful Load Sizing Table						
#	N_{pilots}	N_{pax}	W_{PL} lb	W_F lb	M_{if}	R_{cruise} nm
1	2	0	0.0	13636.6	0.5701	3366.1
2	2	1	250.0	13386.6	0.5780	3266.7
3	2	2	500.0	13136.6	0.5859	3168.7
4	2	3	750.0	12886.6	0.5938	3072.0
5	2	4	1000.0	12636.6	0.6016	2976.5
6	2	5	1250.0	12386.6	0.6095	2882.4
7	2	6	1500.0	12136.6	0.6174	2789.4
8	2	7	1750.0	11886.6	0.6253	2697.6
9	2	8	2000.0	11636.6	0.6332	2606.9

Figure 3.13: Values to plot the range vs payload tradeoff graph.

From these results, the absolute maximum payload weight is 10,790 lbs, which will amount in a range of zero nautical miles. The output table in the figure shows the different possible payload configurations. These data points are shown in the figure of the graph below, displaying the range vs payload tradeoff for the plane.

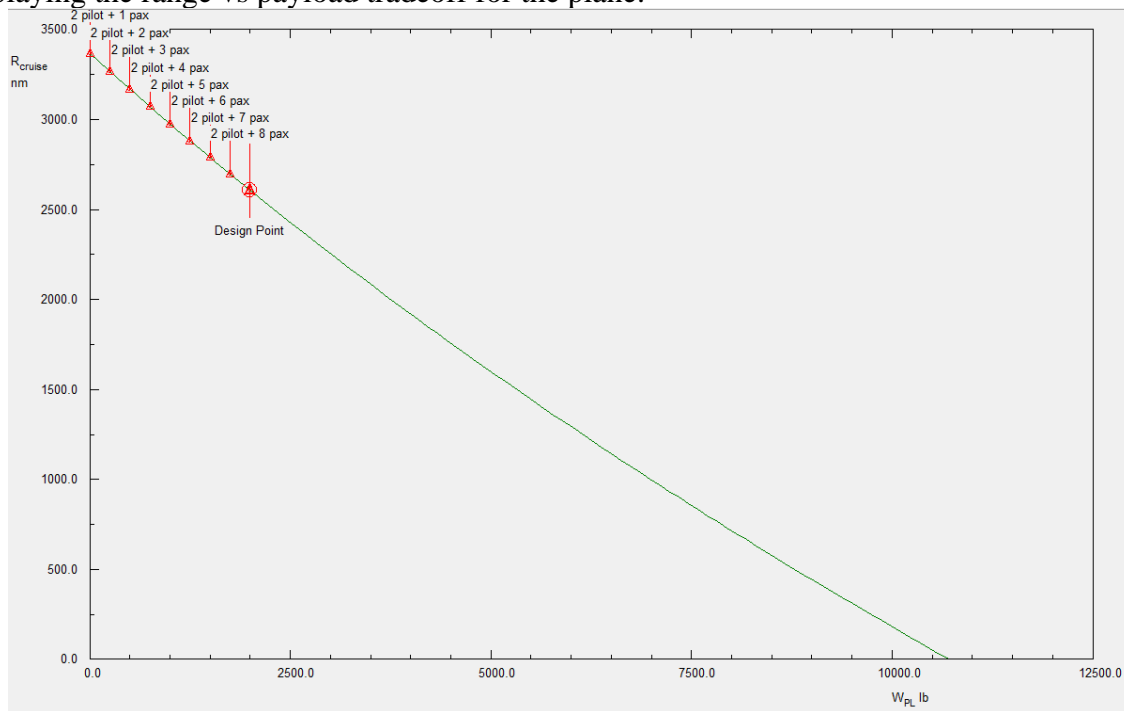


Figure 3.14: Advanced Aircraft Analysis output tradeoff graph of range vs payload.

3.4 Discussion

The calculation of takeoff weight between the hand calculation result and the AAA program result, of section 3.2.3, are different. The hand calculation takeoff weight results in

29,600 lbs. The AAA results yielded a takeoff weight of 31, 804 lbs. The two results differ by about 2,000 lbs. Although this is a significant amount of weight, they are still close enough to determine that either takeoff weight will suffice.

After the hand calculation of takeoff weight in section 3.2.3.1 and the takeoff weight of section 3.3.1, the two weights are nearly identical as well. This shows that either process will yield an accurate process of determining the takeoff weight for this plane.

The process of section 3.3.1, which also uses the results of sections 3.2.1 and 3.2.2, to calculate the takeoff weight depends on the selection of previous planes that have the most similar mission requirements to the plane that is being designed, otherwise the regression coefficients will be skewed. The more accurate method would be that of section 3.2.3.1 as it will act independent of mission requirements set forth. To obtain a more precise takeoff weight with the hand calculation of section 3.2.3.1, the iteration process could be more precise, such as increments of 10 lbs for the takeoff weight. The method taken was iterate the equations with the takeoff weight in intervals of 50 to 100 lbs to closely match the empty allowable and empty tolerable weights to match.

For the sensitivities between the aircraft’s takeoff weight and to the many flight parameters, the table below presents all of the values together.

Table 3.6: Sensitivity to takeoff weight values.

Sensitivity to Takeoff Weight	Value (Hand Calculation)	Value (AAA Program)
$\frac{\partial W_{TO}}{\partial W_{PL}}$	12.55 lbs	13.43 lbs
$\frac{\partial W_{TO}}{\partial W_E}$.9765 lbs	1.81 lbs
$\frac{\partial W_{TO}}{\partial R}$	33.89 lbs/nm	37.3 lbs/nm
$\frac{\partial W_{TO}}{\partial E}$	9,434.92 lbs/hr	10,377.3 lbs/hr
$\frac{\partial W_{TO}}{\partial V}$	-191.857 lbs/kt	N/A

Range (Cruise Stage)			Endurance (Loiter Stage)		
Sensitivity to Takeoff Weight	Value (Hand Calculation)	Value (AAA Program)	Sensitivity to Takeoff Weight	Value (Hand Calculation)	Value (AAA Program)
$\frac{\partial W_{TO}}{\partial c_j}$	126,230.49 lbs/lbs/lbs/hr	138,838. 3 lbs/lbs/lbs/hr	$\frac{\partial W_{TO}}{\partial c_j}$	18,869.84 lbs/lbs/lbs/hr	20,754.7 lbs/lbs/lbs/hr
$\frac{\partial W_{TO}}{\partial L}$	-8,032.85 lbs	-8835.2 lbs	$\frac{\partial W_{TO}}{\partial L}$	-725.76 lbs	-798.3 lbs

From this table, the change in fuel consumption will have the greatest impact upon the takeoff weight of the aircraft. The fuel consumption during the range portion of flight, the cruise stage, has a greater impact upon the weight rather than loiter because the range consists of a much longer period of fuel being burned. The sensitivity between velocity and takeoff weight is the lone parameter that allows for the plane to lose weight when the flight parameter is increased, rather than having to add more to the takeoff weight of the aircraft. The values calculated by hand and using the AAA program are similar in value that the two results verify one another.

These takeoff weight sensitivities show how the slightest change in flight parameters can influence the takeoff weight of the plane in a positive or negative manner.

The trade study shows that as the payload is increased the range will decrease. This makes sense as more power will need to be generated to create the equal amount of thrust as if the plane had no payload.

From completing this report, one questionable result did appear. The regression coefficients of A and B were of interest. The value of B was relatively close to that of Roskam, but A differed by nearly a factor of 2. This raises the question of whether there was another defined method that should have been used to obtain these values.

3.5 Conclusions and Recommendations

The mission weights follow the data weights of the previous planes expected trend. From the analysis conducted, the mission weights are as follows:

- $W_{TO} = 29,600$ lbs
- $W_E = 16,002$ lbs
- $W_F = 11,050$ lbs

Weight sensitivities can help to determine the what flight parameters will have a significant effect on a specific flight parameter. This will allow for a more in-depth analysis of what will have a positive or negative effect on the plane's performance. Another conclusion that is also able to be made is the fact that either a hand calculation or the AAA program can be used to obtain an accurate value for the desired variable.

To improve upon the design of the plane, the powerplant system should be upgraded to allow for a greater cruise velocity, while maintaining the flight parameters and weights. In theory, the greater cruise velocity allows for a lighter aircraft at takeoff weight, but the practicality of this occurring will not yield the results calculated as the engine will likely be heavier and require more fuel to generate the extra thrust needed to counter the weight.

If one factor of the plane was to be enhanced technologically without compromising any other design or performance characteristics, the best thing to do would be to obtain a more efficient engine. With a more efficient engine, the fuel consumption would decrease. This would help with the fuel weight, requiring less fuel to obtain an equal range.

Another possible change that could be made would be to choose an engine that will allow for a higher cruising velocity. The higher cruising velocity will help with the range. As shown in the tradeoff study, it displays the trend that the higher velocity will yield a greater range.

3.6 References

[1] Jane's Information Group. (1930). *Jane's All the World's Aircraft*.

[2] Roskam, J. (1985). *Airplane design*. Ottawa, Kan.: Roskam Aviation and Engineering.

4.0 Performance Constraint Analysis

4.1 Introduction

The purpose of this report is to meet the desired performance standards in order to help determine the size of the aircraft being designed. This will allow for the performance characteristics to be met rather than the size of the plane limiting the performance of the plane. The plane will follow the standards under the Federal Aviation Regulations (FAR) part 25 requirements.

The most important flight performance characteristics that must be met will be used to help size the plane the best regarding wing loading, W/S , and thrust to weight ratio, T/W . The flight performance characteristics which will determine the size of the plane are:

- Takeoff Distance
- Landing Distance
- Stall Speed
- Drag Polar Estimation
- Climb Constraints
- Maneuvering Constraints and
- Speed Constraints

4.2 Manual Calculation of Performance Constraints

The following flight performance characteristics are based off of the FAR 25 requirements. The plane falls under the FAR 25 category because it has a maximum takeoff weight, MTOW, over 12,500 lbs.

According to Roskam, the coefficients of lift value are a range of values depending on what stage of flight the plane is in. Thus, the following coefficients of lift will be used throughout the report depending on the stage of flight:

- CL max range: 1.4 – 1.8
- CL max takeoff range: 1.6 – 2.2
- CL max landing range: 1.6 - 2.6

4.2.1 Takeoff Distance

According to the requirements, the takeoff distance required for a plane to follow the FAR 25 guidelines, specifically FAR 25.113, the takeoff distance is 115% of the distance required for the plane to be able to clear a 35 ft obstacle at the end of the runway [1].

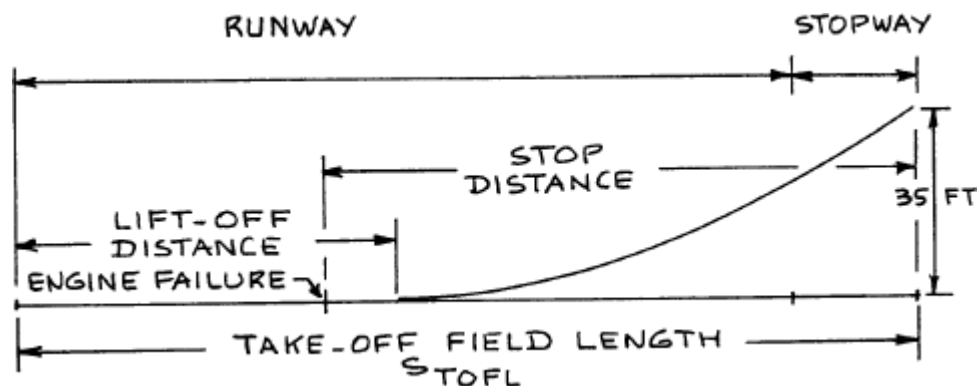


Figure 4.1: Takeoff field length as defined by Roskam. [2]

As the FAR rules state a runway distance of no more than 5000 ft at an altitude of 8000 ft is allowed, according to Roskam [2]. As the actual runway length is not what is being sought, the

figure from Roskam will be used to determine the relation between wing loading and thrust to weight ratio.

$$S_{TOFL} = 37.5 * (TOP)_{25} = 37.5 * \frac{(W/S)_{TO}}{\sigma * C_{L_{MAX_{TO}}} * (W)_{TO}} \quad (1)$$

$$5000 = 37.5 * \frac{(W/S)_{TO}}{\sigma * C_{L_{MAX_{TO}}} * (W)_{TO}}$$

$$\sigma = \frac{\rho_{TO}}{\rho_{SL}} \quad (2)$$

$$\sigma = \frac{.0018684 \frac{slugs}{ft^3}}{.002377 \frac{slugs}{ft^3}} = .786$$

$$\frac{T}{W_{TO}} = \frac{37.5}{5000} * \frac{(W/S)_{TO}}{.786 * C_{L_{MAX_{TO}}}}$$

The wing loading values, a range from 40 psf to 100 psf, are used to create a linear set of data points to create a line in regards to different maximum coefficients of lift at takeoff. The maximum coefficient of lift during takeoff ranges from 1.6 to 2.2. The following calculation will be done for a wing loading of 40 psf and coefficient of lift value of 1.6.

$$\left(\frac{T}{W}\right)_{TO} = \frac{37.5}{5000} * \frac{40}{.786 * 1.6} = .2385$$

Takeoff Distance

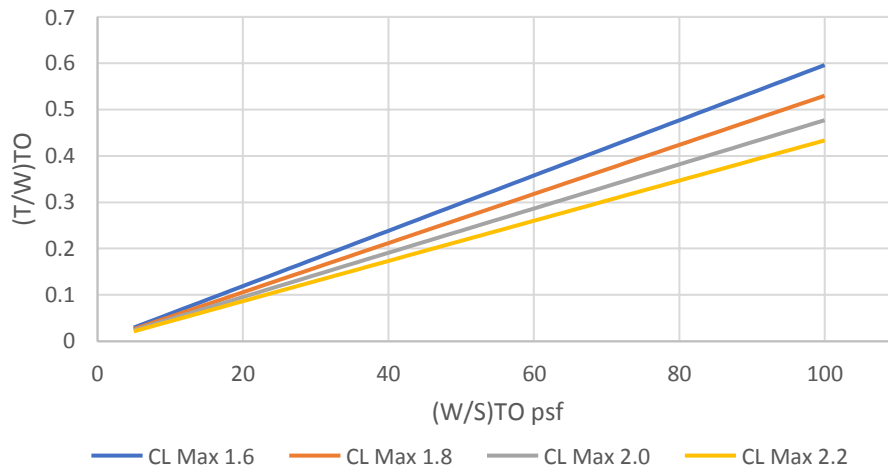


Figure 4.2: Thrust to weight ratio versus wing loading of takeoff distance.

4.2.2 Landing Distance

In order for a safe landing, the landing distance begins when the plane is still able to clear a 50 ft obstacle until the point at which the plane comes to a stop or to a speed of approximately 3 knots. The FAR landing field length is the landing length divided by 0.6. This will allow for a safety range in the case of pilot preference or flying style. FAR 25 requires the plane to be able to land in 5,000 ft at sea level.

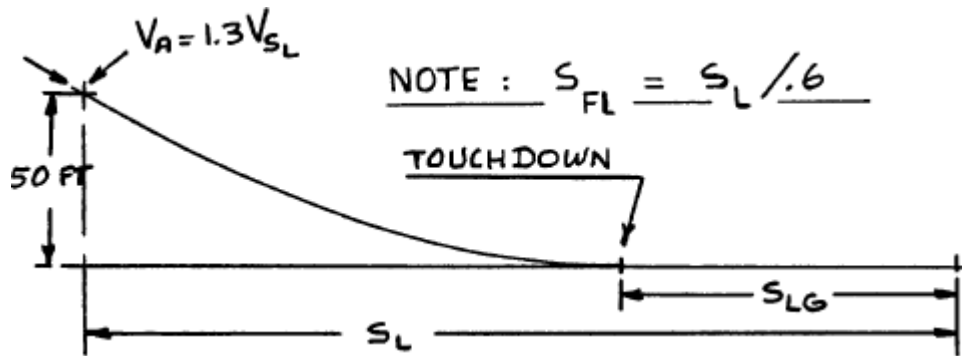


Figure 4.3: Landing distance requirement. [2]

The landing distance is in relation to the approach and stall speed of the aircraft. The following equations will be used to determine the relation between landing field length to the wing loading during takeoff.

$$S_{FL} = .3 * V_A^2 \quad (3)$$

$$V_A = \sqrt{\frac{5000}{.3}} = 129.099 \text{ knts}$$

$$V_A = 1.3 * V_{SL} \quad (4)$$

$$V_{SL} = \frac{129.099}{1.3} = 99.307 \text{ knts}$$

Referencing the stall speed equation, the landing distance is able to be related to the wing loading of the aircraft.

$$V_S = \sqrt{\frac{2 * (W/S)_{TO}}{\rho * C_{L_{MAX}}}} \quad (5)$$

$$99.307 \text{ knts} * 1.686 \frac{ft}{s} = \sqrt{\frac{2 * (W/S)_L}{.002377 * C_{L_{MAX_L}}}}$$

$$33.317 * C_{L_{MAX_L}} = \left(\frac{W}{S}\right)_L$$

To relate all of the flight performance characteristics together, the relation between takeoff and landing must be defined.

$$W_L = .85 W_{TO} \quad (6)$$

$$\left(\frac{W}{S}\right)_{TO} = \frac{33.317}{.85} * C_{L_{MAX_L}}$$

The coefficient of max during landing has a range of values. The relation between landing distance and wing loading will have a range of coefficient of lift values between 1.6 and 2.6. The following calculation will be done for a coefficient of lift of 1.6.

$$\left(\frac{W}{S}\right)_{TO} = \frac{33.317}{.85} * 1.6 = 62.714 \text{ psf}$$

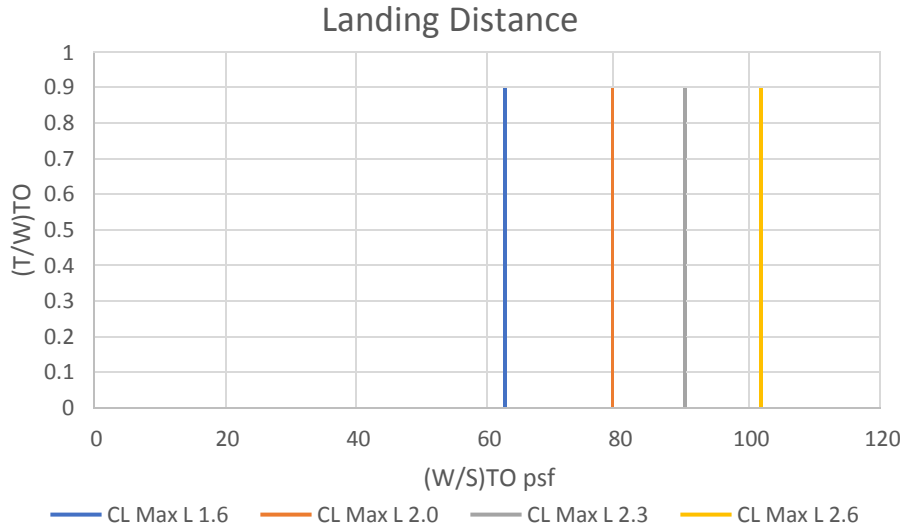


Figure 4.4: Thrust to weight ratio versus wing loading of landing distance.

4.2.3 Stall Speed

According to the FAR 25 requirements, there is no minimum defined stall speed, such as that defined for a FAR 23 aircraft. With that said, there is a stall speed that can be referenced as a target stall speed. The reference stall speed is the stall speed found during the landing distance, section 4.2.2. The stall speed cannot be more than 99.307 knots, 167.431 ft/s, at sea level.

$$V_s > \sqrt{\frac{2 * (W/S)_{TO}}{\rho * C_{L_{MAX}}}} \quad (7)$$

$$99.307 * 1.686 > \sqrt{\frac{2 * (W/S)_{TO}}{0.002373 * C_{L_{MAX}}}}$$

$$(W/S)_{TO} < 167.431^2 * \frac{0.002373 * C_{L_{MAX}}}{2}$$

The stall velocity can be conducted at all three stages of coefficient of lift values, clean, takeoff and landing. Since the stall velocity was found during landing, the coefficient of lift values will be analyzed during landing, which range from 1.6 to 2.6. The following hand calculation will be conducted at a coefficient of max of 1.6.

$$(W/S)_{TO} < 167.431^2 * \frac{0.002373}{2} * 1.6 < 53.308 \text{ psf}$$

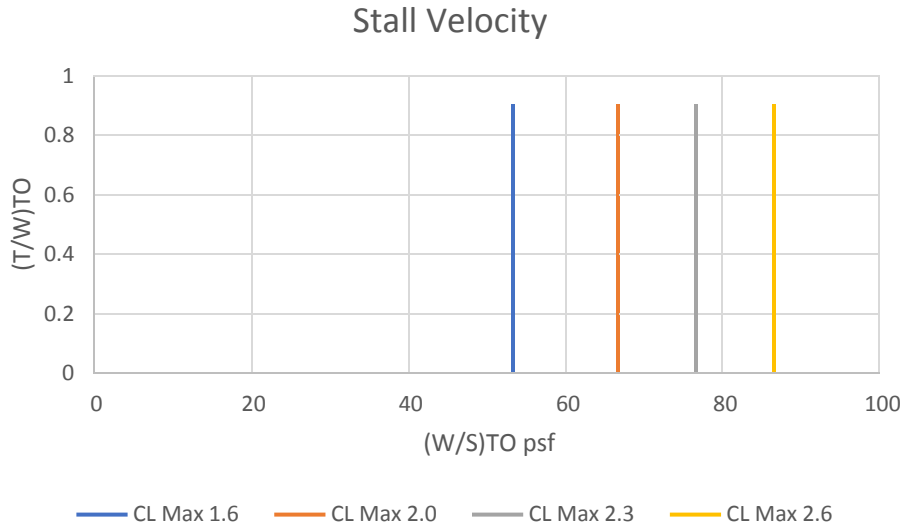


Figure 4.5: Thrust to weight ratio versus wing loading of stall speed.

4.2.4 Drag Polar Estimation

The drag polar estimation is useful because it is helpful to use in determining the relationship between the coefficient of lift and coefficient of drag. There are a number of different conditions that drag polar equations are able to analyze. The drag polar equations will be used for:

- Clean aircraft
- Takeoff flaps and landing gear up
- Takeoff flaps and landing gear down
- Landing flaps and landing gear up
- Landing flaps and landing gear down

The following equation will be used to find the coefficient of drag at each of the plane configurations listed above.

$$C_D = C_{D_0} + \frac{C_L^2}{\pi A R e} \quad (8)$$

To find an accurate value for the zero lift drag coefficient, the following equations will be used.

$$C_{D_0} = \frac{f}{S} \quad (9)$$

$$\log(f) = a + [b * \log(S_{wet})] \quad \text{and} \quad (10)$$

$$\log(S_{wet}) = c + [d * \log(W_{TO})] \quad (11)$$

The takeoff weight is the value found in the previous report, Weight Sizing and Weight Sensitivity, 29,600 lbs. The a, b, c and d values are the regression coefficients, pulled from Roskam's book [2].

$$\log(S_{wet}) = .2263 + [.6977 * \log(29600)]$$

$$S_{wet} = 2217.789 \text{ ft}^2$$

$$\log(f) = -2.3979 + [1 * \log(2217.789)]$$

$$f = 8.87197 \text{ ft}^2$$

Now that f, the equivalent parasite area has been found, the wing area, S, must be defined as the wetted wing area is representative of a different value. To determine the wing area, the

following equation is used, along with the wing loading value being a middling value within the range of 40 psf to 100 psf, the typical range evaluated throughout the report.

$$S_{wing} = \frac{W_0}{W/S} = \frac{29600}{75.75} = 390.759 \text{ ft}^2 \quad (12)$$

Thus,

$$C_{D_0} = \frac{8.87197}{390.759} = .0227$$

$$C_D = .0227 + \frac{C_L^2}{\pi * 7.5 * .83}$$

$$C_D = .0227 + .0514 C_L^2$$

This equation is for a clean aircraft without any flaps or landing gear being exposed. There are multiple drag polar scenarios as previously stated, those that will be analyzed are based off of the clean coefficient of drag equation found. The conditions of flaps or landing gear are as follows:

- Clean
 - $\Delta C_{D_0} = 0$
 - $e = .8 - .85$
- Takeoff Flaps
 - $\Delta C_{D_0} = .01 - .02$
 - $e = .75 - .8$
- Landing Flaps
 - $\Delta C_{D_0} = .055 - .075$
 - $e = .7 - .75$
- Landing Gear
 - $\Delta C_{D_0} = .015 - .025$
 - $e = \text{no effect}$

The coefficients of drag can be found for clean, takeoff flaps, takeoff flaps and landing gear, landing flaps and landing flaps and landing gear. The following coefficient of drag equations are presented below. The changes in zero lift drag coefficients and Oswald efficiency values are averaged values of the projected changes.

Clean Aircraft:

$$C_D = .0227 + .0514 C_L^2$$

Takeoff Flaps:

$$C_D = (.0227 + .015) + \frac{C_L^2}{\pi * 7.5 * .775}$$

$$C_D = .0377 + .05476 C_L^2$$

Takeoff Flaps and Landing Gear:

$$C_D = (.0377 + .02) + \frac{C_L^2}{\pi * 7.5 * .775}$$

$$C_D = .0577 + .05476 C_L^2$$

Landing Flaps:

$$C_D = (.0227 + .065) + \frac{C_L^2}{\pi * 7.5 * .725}$$

$$C_D = .0877 + .0585 C_L^2$$

Landing Flaps and Landing Gear:

$$C_D = (.0877 + .02) + \frac{C_L^2}{\pi * 7.5 * .725}$$

$$C_D = .1077 + .0585 C_L^2$$

Using the five coefficient of drag equations, the following figure below can be constructed. The maximum coefficient of lift values are based off of the values in Roskam during cruise, takeoff and landing [2].

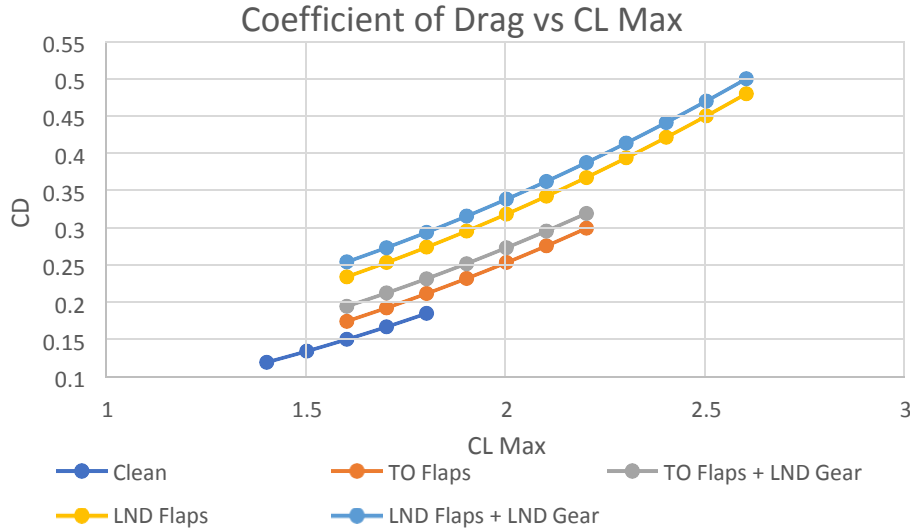


Figure 4.6: Drag polar graph of the multiple plane configurations.

4.2.5 Climb Constraints

The climb constraints of a FAR 25 aircraft follow 6 unique qualifications, four during takeoff and two during landing. The climb requirements occur when either one engine is inoperative, OEI, or all engines are operative, AEO. The climb requirements are in relation to the thrust to weight ratio. Two equations are used to define the relationship, one for OEI and the other for AEO.

$$\text{OEI: } \frac{T}{W} = \frac{N}{N-1} * \left(\frac{1}{L/D} + CGR \right) \quad (13)$$

$$\text{AEO: } \frac{T}{W} = \left(\frac{1}{L/D} + CGR \right) \quad (14)$$

The number of engines on the plane is two. The climb gradient requirement will be defined in each scenario.

FAR 25.111: With OEI, the initial climb segment requirement must have a climb gradient of 1.2% under the following conditions:

- Take off flaps
- Landing gear retracted
- Speed is $1.2V_{S_{TO}}$
- Remaining engine at takeoff thrust
- Altitude between 35 ft and 400 ft
- Ground effect
- Analyzed at maximum takeoff weight

$$\frac{T}{W} = \frac{2}{2-1} * \left(\frac{1}{L/D} + .012 \right)$$

The lift to drag ratio must first be defined under this circumstance.

$$\frac{L}{D} = \frac{C_{LqS}}{C_{DqS}} = \frac{C_L}{C_D} \quad (15)$$

$$\frac{C_L}{C_{L_{MAXTO}}} = \frac{2.0}{1.44} = 1.4$$

$$C_D = .0377 + .05476C_L^2$$

$$C_D = .0377 + .05476(1.4)^2 = .145$$

$$\frac{L}{D} = \frac{1.4}{.145} = 9.653$$

Substituting back into the thrust to weight ratio equation, the following is obtained. The change in temperature, 50°F, must also be taken into account. The maximum thrust of a turbofan at sea level will change by 50°F, a ratio of 0.8.

$$\frac{T}{W} = \frac{2}{2-1} * \left(\frac{1}{9.653} + .012 \right) = \frac{.2312}{.8} = .28898$$

FAR 25.121: With OEI, the transition segment climb requirement must have a positive climb gradient requirement under the following conditions:

- Takeoff flaps
- Landing gear down
- Speed between V LOF and $1.2V_{S_{TO}}$
- Remaining engine at takeoff thrust
- Ground effect
- Ambient atmospheric conditions
- Max takeoff weight

$$\frac{T}{W} = \frac{2}{2-1} * \left(\frac{1}{L/D} + 0 \right)$$

The lift to drag ratio must first be defined under this circumstance.

$$\frac{L}{D} = \frac{C_{LqS}}{C_{DqS}} = \frac{C_L}{C_D} \quad (15)$$

$$\frac{C_L}{C_{L_{MAXTO}}} = \frac{2.0}{1.1^2} = 1.65$$

$$C_D = .0577 + .05476C_L^2$$

$$C_D = .0577 + .05476(1.65)^2 = .2068$$

$$\frac{L}{D} = \frac{1.65}{.2068} = 7.979$$

Substituting back into the thrust to weight ratio equation, the following is obtained. The change in temperature, 50°F, must also be taken into account. The maximum thrust of a turbofan at sea level will change by 50°F, a ratio of 0.8.

$$\frac{T}{W} = \frac{2}{2-1} * \left(\frac{1}{7.979} + 0 \right) = \frac{.2508}{.8} = .3135$$

Under FAR 25.121, with OEI, the second segment climb requirement must have a climb gradient requirement of 2.4% under the following conditions:

- Takeoff flaps
- Landing gear retracted
- Remaining engine at takeoff thrust
- Speed of $1.2V_{S_{TO}}$
- Out of ground effect
- Ambient atmospheric conditions
- Maximum takeoff weight

$$\frac{T}{W} = \frac{2}{2-1} * \left(\frac{1}{L/D} + .024 \right)$$

The lift to drag ratio must first be defined under this circumstance.

$$\frac{L}{D} = \frac{C_{LqS}}{C_{DqS}} = \frac{C_L}{C_D} \quad (15)$$

$$C_{L_{MAX}} = \frac{2.0}{1.44} = 1.4$$

$$C_D = .0377 + .05476C_L^2$$

$$C_D = .0377 + .05476(1.4)^2 = .145$$

$$\frac{L}{D} = \frac{1.4}{.145} = 9.655$$

Substituting back into the thrust to weight ratio equation, the following is obtained. The change in temperature, 50°F, must also be taken into account. The maximum thrust of a turbofan at sea level will change by 50°F, a ratio of 0.8.

$$\frac{T}{W} = \frac{2}{2-1} * \left(\frac{1}{9.655} + .024 \right) = \frac{.2552}{.8} = .3189$$

Under FAR 25.121, with OEI, the en-route climb requirement must have a climb gradient requirement of 1.2% under the following conditions:

- Flaps retracted
- Landing gear retracted
- Remaining engine at max continuous thrust
- Speed of $1.25V_{S_{TO}}$
- Ambient atmospheric conditions
- Maximum takeoff weight

$$\frac{T}{W} = \frac{2}{2-1} * \left(\frac{1}{L/D} + .012 \right)$$

The lift to drag ratio must first be defined under this circumstance.

$$\frac{L}{D} = \frac{C_{LqS}}{C_{DqS}} = \frac{C_L}{C_D} \quad (15)$$

$$C_{L_{MAX}} = \frac{1.6}{1.25^2} = 1.024$$

$$C_D = .0227 + .0514C_L^2$$

$$C_D = .0227 + .0514(1.024)^2 = .0766$$

$$\frac{L}{D} = \frac{1.024}{.0766} = 13.3687$$

Substituting back into the thrust to weight ratio equation, the following is obtained. The change in temperature, 50°F, must also be taken into account. The maximum thrust of a turbofan at sea level will change by 50°F, a ratio of 0.8. The previous climb requirements were conducted at maximum takeoff thrust, this condition is under maximum continuous thrust. The maximum continuous thrust is .94 for a turbofan engine.

$$\frac{T}{W} = \frac{2}{2-1} * \left(\frac{1}{13.3687} + .012 \right) = \frac{.1736}{.8} * .94 = .2309$$

AEO climb is not a problem as compared to severity of OEI requirements, thus AEO climb requirements were not analyzed for takeoff.

FAR 25.119: With AEO, the go around or balked landing requirements must have a climb gradient greater than 3.2% at a thrust level equivalent to eight seconds after moving the throttle from flight idle to the takeoff position. The following conditions must be met:

- Landing flaps

- Landing gear down
- Speed of $1.3V_{S_{T0}}$
- Ambient atmospheric conditions
- Max landing weight

$$\frac{T}{W} = \left(\frac{1}{L/D} + .032 \right)$$

The lift to drag ratio must first be defined under this circumstance.

$$\frac{L}{D} = \frac{C_{LqS}}{C_{DqS}} = \frac{C_L}{C_D} \quad (15)$$

$$C_{L_{MAXL}} = \frac{2.0}{1.3^2} = 1.18$$

$$C_D = .1077 + .0585C_L^2$$

$$C_D = .1077 + .0585(1.18)^2 = .1896$$

$$\frac{L}{D} = \frac{1.18}{.1896} = 6.224$$

Substituting back into the thrust to weight ratio equation, the following is obtained. The change in temperature, 50°F, must also be taken into account. The maximum thrust of a turbofan at sea level will change by 50°F, a ratio of 0.8.

$$\left(\frac{T}{W} \right)_L = \left(\frac{1}{6.224} + .032 \right) = \frac{.1927}{.8} = .2408$$

To convert from thrust to weight ratio during landing to thrust to weight ratio during takeoff, the ratio of takeoff to landing weight is used, while also accounting for the temperature.

$$\left(\frac{T}{W} \right)_{TO} = .2408 * \frac{W_{TO}}{W_L}$$

$$\left(\frac{T}{W} \right)_{TO} = .2408 * \frac{31804.6}{20293.6} = .3775$$

FAR 25.121: With OEI, the go around or balked landing requirements must have a climb gradient requirement greater than 2.1% under the following conditions:

- Approach flaps
- Landing gear
- Speed no more than $1.5V_{S_A}$
- Stall velocity must be greater than $1.1V_{S_L}$
- Remaining engine at takeoff thrust
- Ambient atmospheric conditions
- Maximum landing weight

$$\frac{T}{W} = \left(\frac{1}{L/D} + .021 \right)$$

The lift to drag ratio must first be defined under this circumstance.

$$\frac{L}{D} = \frac{C_{LqS}}{C_{DqS}} = \frac{C_L}{C_D} \quad (15)$$

$$C_{L_{MAXL}} = \frac{2.4}{1.5^2} = 1.0667$$

$$C_D = \left(\frac{.03774 + .0877}{2} + .02 \right) + .0585C_L^2$$

$$C_D = .0827 + .0585(1.0667)^2 = .1493$$

$$\frac{L}{D} = \frac{1.0667}{.1493} = 7.146$$

Substituting back into the thrust to weight ratio equation, the following is obtained. The change in temperature, 50°F, must also be taken into account. The maximum thrust of a turbofan at sea level will change by 50°F, a ratio of 0.8.

$$\left(\frac{T}{W}\right)_L = \left(\frac{1}{7.146} + .021\right) = \frac{.1609}{.8} = .2012$$

To convert from thrust to weight ratio during landing to thrust to weight ratio during takeoff, the ratio of takeoff to landing weight is used, while also accounting for the temperature.

$$\left(\frac{T}{W}\right)_{TO} = .2012 * \frac{W_{TO}}{W_L}$$

$$\left(\frac{T}{W}\right)_{TO} = .2012 * \frac{31804.6}{20293.6} = .3153$$

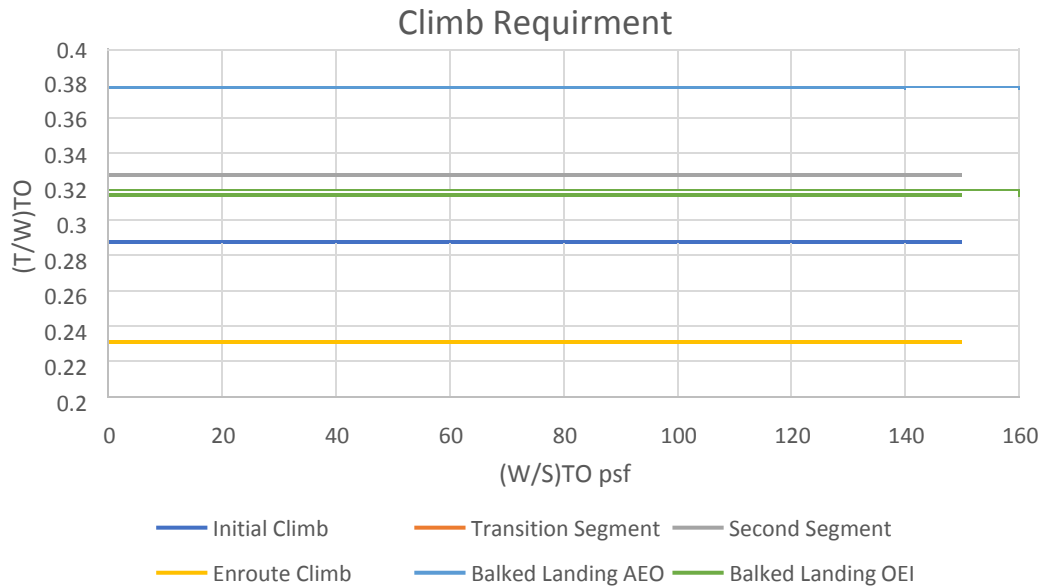


Figure 4.7: Climb requirement graph for multiple flight stages.

4.2.6 Maneuvering Constraints

According to FAR 25.337, the load factor may not be less than 2.5 and no greater than 3.8 the maximum takeoff weight. Maneuverability will relate both the wing loading and thrust to weight ratio to one another. Maneuverability can be determined by the following equation:

$$\frac{T}{W} = \frac{qC_{D0}}{W/S} + \left(\frac{W}{S} * \frac{\eta_{max}^2}{\pi * AR * e * q}\right) \quad (16)$$

The load factor ranges, thus the average load factor will be analyzed to determine the general trend on the effects of the wing loading and thrust to weight ratio. The maneuverability load will be conducted at sea level while at maximum cruise velocity of a clean aircraft.

$$\frac{T}{W} = \frac{(\frac{1}{2} * .002377 * 777.3332) * .0227}{W/S} + \left(\frac{W}{S} * \frac{3.15^2}{\pi * 7.15 * .825 * (\frac{1}{2} * .002377 * 777.333)^2}\right)$$

$$\frac{T}{W} = \frac{16.0276}{W/S} + (.000710792 * \frac{W^2}{S})$$

The wing loading will range from 40 psf to 100 psf, as this range was previously used to analyze the previous sections.

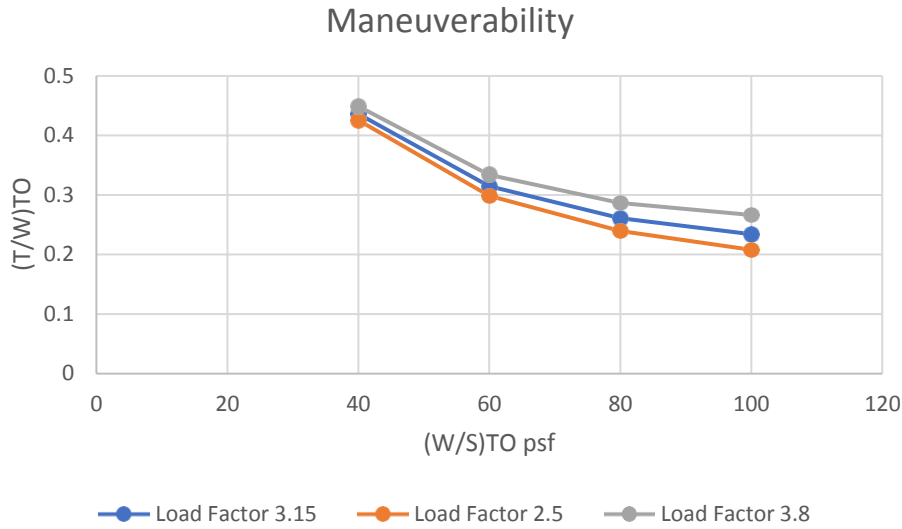


Figure 4.8: Maneuverability graph in relation to the wing loading and thrust to weight ratio. The turn radius and rate of turn are also important factors in the maneuverability of the aircraft. Both will be analyzed for the average load factor, 3.15.

Turn Radius:

$$r_{min} = \frac{v^2}{g} * \frac{1}{\sqrt{\eta_{max}^2 - 1}} \quad (17)$$

$$r_{min} = \frac{777.333^2}{32.2} * \frac{1}{\sqrt{3.15^2 - 1}} = 6282.247 \text{ ft}$$

Rate of Turn, ω :

$$\omega_{MAX} = \frac{g}{v} * \sqrt{\eta_{max}^2 - 1} \quad (18)$$

$$\omega_{MAX} = \frac{32.2}{777.333} * \sqrt{3.15^2 - 1} = .1237 \frac{\text{radians}}{\text{seconds}}$$

4.2.7 Speed Constraints

FAR 25 does not explicitly state a minimum nor a maximum cruise speed that must be met. Thus, the set cruise speed can be used to relate wing loading and thrust to weight ratio to each other.

$$\left(\frac{T_{cr}}{W_{cr}}\right)_{req} = \frac{C_{D0} q}{W_{cr}/S} + \frac{W_{cr}/S}{\pi q A R e} \quad (19)$$

$$\left(\frac{T_{cr}}{W_{cr}}\right)_{req} = \frac{.0227 * \left(\frac{1}{2} * .002377 * 777.333^2\right)}{W_{cr}/S} + \frac{W_{cr}/S}{\pi \left(\frac{1}{2} * .002377 * 777.333^2\right) (7.5) (8)}$$

$$\left(\frac{T_{cr}}{W_{cr}}\right)_{req} = \frac{16.3019}{W_{cr}/S} + \frac{W_{cr}/S}{13536.75}$$

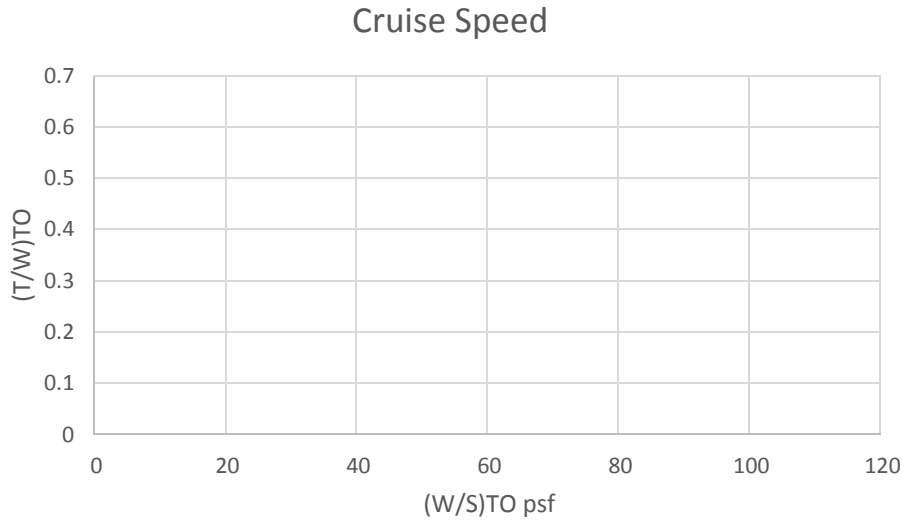


Figure 4.9: The cruise speed relationship of wing loading and thrust to weight during takeoff.

4.2.8 Matching Graph

The following matching graph was created using the hand calculation computed values.

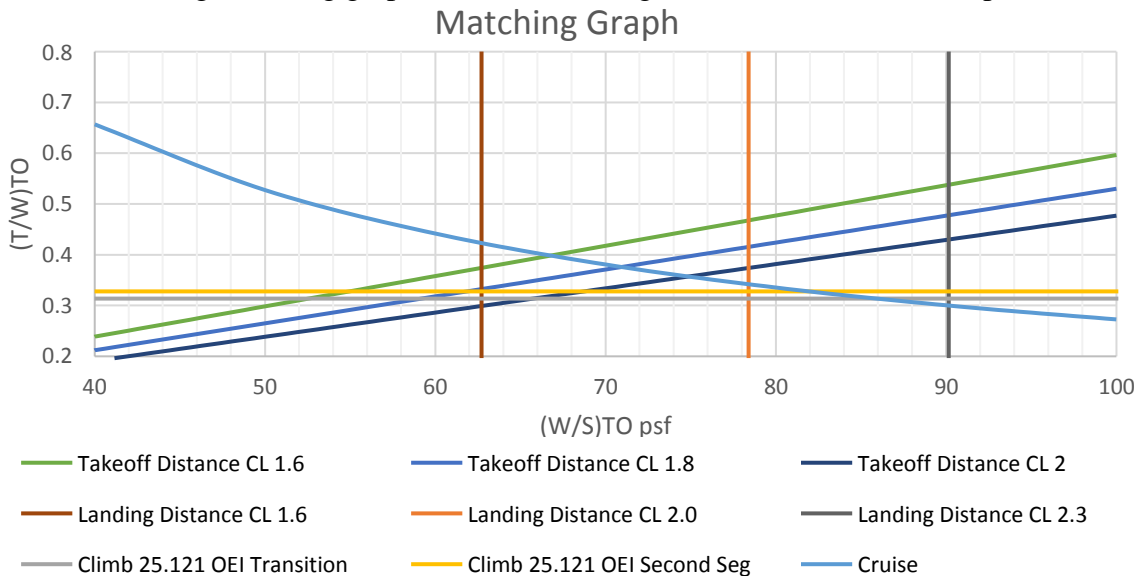


Figure 4.10: Matching graph from hand calculated values.

4.3 Calculation of Performance Constraints with the AAA Program

The same flight conditions as those used in the hand calculations above were used in the AAA program.

4.3.1 Stall Speed

The stall speed was analyzed at sea level without a change in temperature. The estimated clean stall speed and stall speed was needed and assumed to be 109 knts and 99 knts, respectively, based off of the hand calculations. The ratio of weight at stall weight and takeoff weight is .97, an estimate that stall will not occur immediately after takeoff. The maximum coefficient of lift was 2, the average of the range given by Roskam.

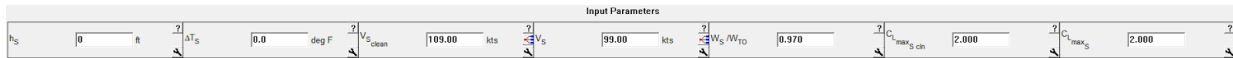


Figure 4.11: Input parameters to determine stall speed in AAA program.

The following values were outputted. The two values show the difference in wing loading between a clean aircraft during takeoff and an aircraft with either flaps or landing gear extended.

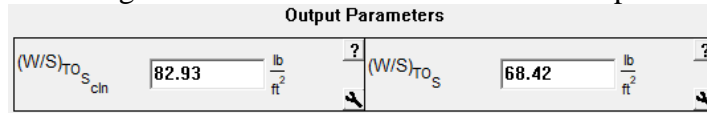
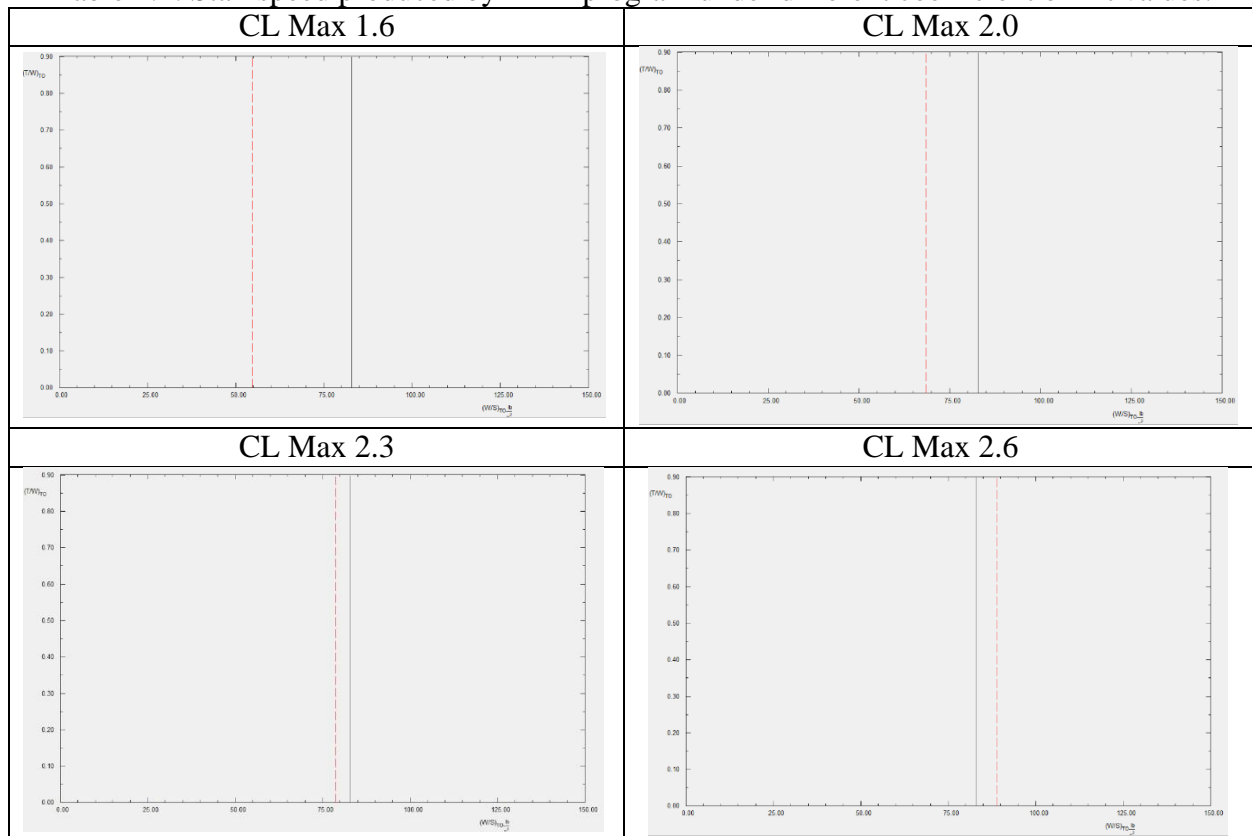


Figure 4.12: Output parameters of stall speed determined by the AAA program.

The table below presents the different stall speed requirements at different coefficient of lift values. The red dash line represents the wing loading at takeoff. The black line represents the wing loading at takeoff of a clean aircraft.

Table 4.1: Stall speed produced by AAA program under different coefficient of lift values.



4.3.2 Takeoff Distance

To determine the relationship of wing loading and thrust to weight ratio with takeoff distance, the AAA program was utilized. The input parameters are defined in the figure below. The altitude at which the takeoff occurs is at 8000 ft. The ratio of takeoff power at the desired altitude to the takeoff power at sea level is 1. The change in temperature at takeoff is 0°F. According to the FAR 25 requirements, the size of the takeoff runway is 5000 ft. The max coefficient of lift during takeoff is set at 1.9, the average of the range presented by Roskam.

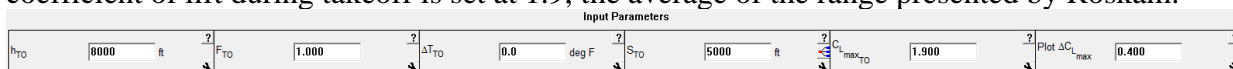


Figure 4.13: Input parameters to determine takeoff distance in AAA program.

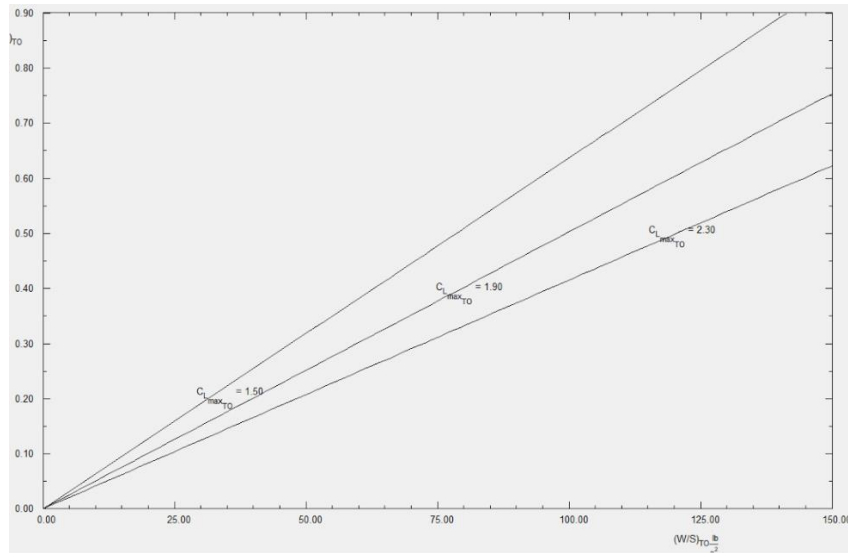


Figure 4.14: Takeoff distance produced by AAA program under different coefficient of lift values.

4.3.3 Landing Distance

The landing distance is used to determine a wing loading value at different coefficients of lift during the landing stage of flight. To begin the input parameters in the figure below were used in the AAA program. The landing process will be conducted at sea level with a temperature of 95°F. The landing weight to the takeoff weight ratio is 0.85. The coefficient of lift that was analyzed was at a coefficient of lift value during landing of 2.1, with a range of 0.4 in either direction to be plotted on the thrust to weight ratio vs wing loading graph. The landing distance length is 5000ft.

Input Parameters							
h_L	0	ft	ΔT_L	95.0	deg F	W_L/W_{TO}	0.850
$C_{L_{max_L}}$	2.100		Plot $\Delta C_{L_{max}}$	0.400		S_L	5000
							ft

Figure 4.15: Input parameters to determine landing distance in AAA program.

The following results were outputted. The field length required to land is 8333 ft at a wing loading of 105.13 lb/ft².

Output Parameters			
S_{FL}	8333	ft	$(W/S)_L$
			105.13
			lb/ft ²

Figure 4.16: Output parameters determined for landing distance by AAA program.

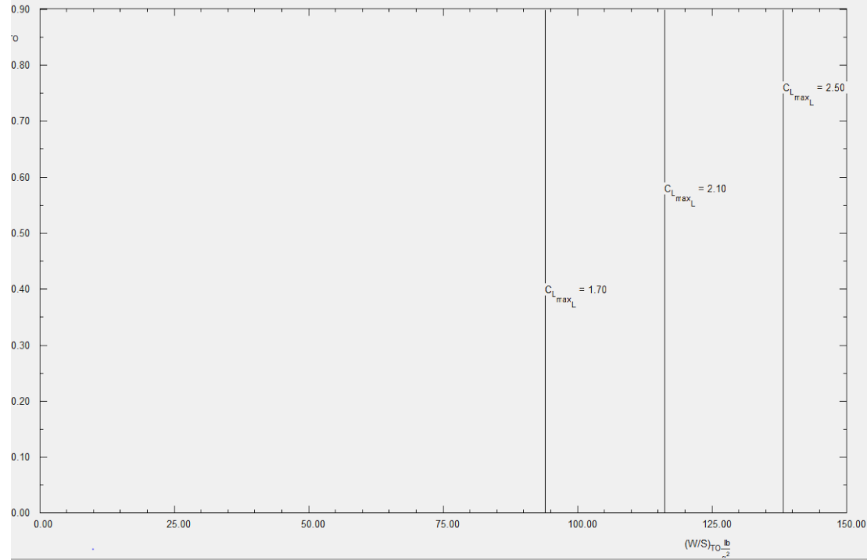


Figure 4.17: Landing distance produced by AAA program under different coefficient of lift values.

4.3.4 Drag Polar Estimation

The drag polar estimates were used to find the climb constraints. As the AAA program does not have a specific section for drag polar estimation, it was indirectly accounted for in the climb constraints section below.

4.3.5 Climb Constraints

The climb constraints had many parameter inputs that analyzed multiple sections of flight. There were inputs of coefficients of lift and Oswald's efficiency values for a clean aircraft during cruise, takeoff, approach and landing. The FAR 25 climb gradient requirement was also defined for the 6 possible climb scenarios.

Input Parameters											
$F_{maxCont}$	0.800	$C_{L_{max_A}}$	2.000	e_{clean}	0.8000	θ_L	0.7000	CGR	FAR 25	$CGR_{25.121_{ER}}$	0.012
F_{sec}	0.750	$C_{L_{max_L}}$	2.100	$C_{D_{clean,M}}$	0.0227	$C_{D_{L_{down}}}$	0.0377	$CGR_{25.111}$	0.012	$CGR_{25.121_L}$	0.021
$C_{L_{max_{clean}}}$	1.800	W_L/W_{TO}	0.850	θ_{TO}	0.7500	ΔC_{D_A}	0.0550	$CGR_{25.121_T}$	0.000	$CGR_{25.119}$	0.032
$C_{L_{max_{TO}}}$	1.900	AR_w	7.50	$C_{D_{TO_{down}}}$	0.0377	$C_{D_{wm}}$	0.1000	$CGR_{25.121_{SS}}$	0.024		

Figure 4.18: Input parameters to determine the climb requirement in the AAA program.

The following climb constraints were outputted.

Output Parameters			
$B_{DP_{clean}}$	0.0531	$B_{DP_{TO_{down}}}$	0.0566
$B_{DP_{L_{down}}}$	0.0606		

Figure 4.19: Output parameters for climb constraints in the AAA program.

4.3.6 Maneuvering Constraints

The maneuvering constraints were conducted under the maximum load factor of $3.8g$'s. The flight maneuvers were conducted at the cruise altitude, 35,000 ft, and maximum cruise velocity, 530 mph. The weight at maneuver to weight at takeoff ratio is not defined, therefore was assumed as .97. The ratio of maneuver power to takeoff power was assumed as 1. The aspect ratio of the wing is defined as 7.5. The zero lift drag coefficient of a clean wing is 0.0227 with an Oswald's efficiency value of 0.8.

Input Parameters							
h_M	35000	ft	n	3.80	g	F_M	1.000
V_M	460.56	kts	W_M/W_{TO}	0.970		AR_w	7.50
						$C_{D_0, clean, M}$	0.0227
						e_{clean}	0.8000

Figure 4.20: Input parameters to determine maneuverability limits in the AAA program.

The following results were outputted. The turn rate is the lone output that can be compared to the results found in the hand calculation section.

Output Parameters			
M_M	0.799	$B_{DP, clean}$	0.0531
		TurnRate	0.1501 rad/s

Figure 4.21: Output parameters for maneuverability limits in the AAA program.

4.3.7 Speed Constraints

The plane is limited to a certain cruise velocity. The altitude of the critical cruise velocity occurring was sea level. The ratio of thrust power to power at takeoff is 0.75. The maximum cruise velocity is 530 mph, 460.56 ft/s. The cruise weight to takeoff weight ratio is 0.95. The aspect ratio of the wing was previously defined as 7.5. The zero lift drag coefficient of a clean wing is 0.0227 with an Oswald's efficiency value of 0.8.

Input Parameters							
h_{Cr}	0	ft	F_{Cr}	0.750		$V_{Cr, max}$	460.56
						W_{Cr}/W_{TO}	0.950
						AR_w	7.50
						$C_{D_0, clean, M}$	0.0227
						e_{clean}	0.8000

Figure 4.22: Input parameters for speed constraints in the AAA program.

Output Parameters			
$M_{Cr, max}$	0.696	$B_{DP, clean}$	0.0531

Figure 4.23: Output parameters for speed constraints in the AAA program.

4.3.8 Summary of Performance Constraints

After the completion of the performance constraints, a matching graph can be made. The following figure shows the results of the AAA program. The optimal position for the aircraft is to be as close to the origin as possible.

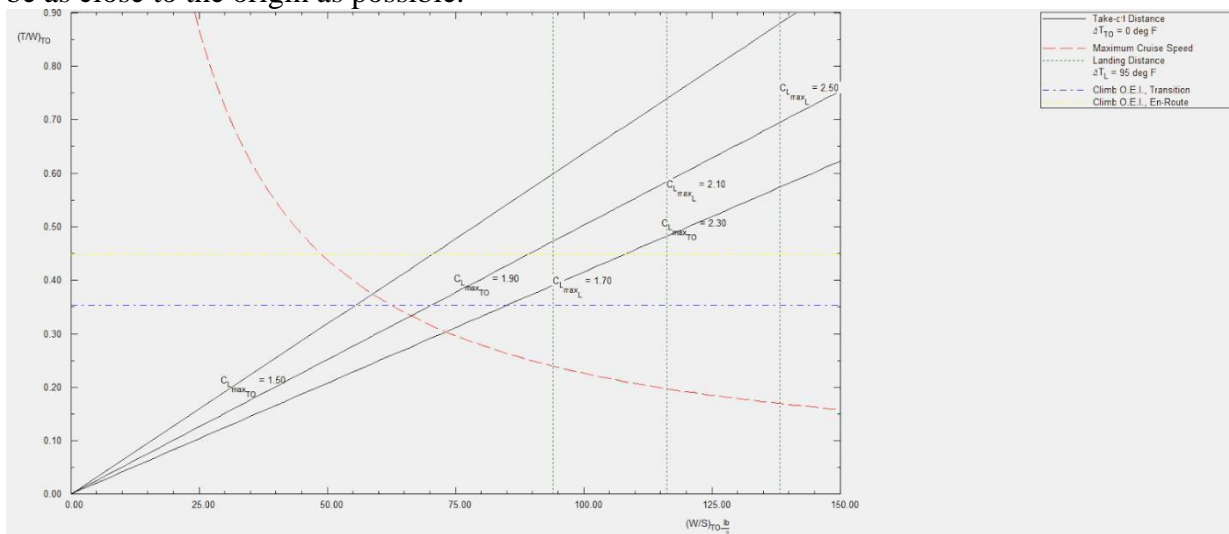


Figure 4.24: Matching graph of all results outputted by AAA program.

The figure below presents the results of defined coefficients of lift during multiple stages of the flight, as well as a defined aspect ratio. The following values are defined:

- CL Max Clean = 1.8
- CL Max Takeoff = 1.9
- CL Max Landing = 2.1
- AR = 7.5

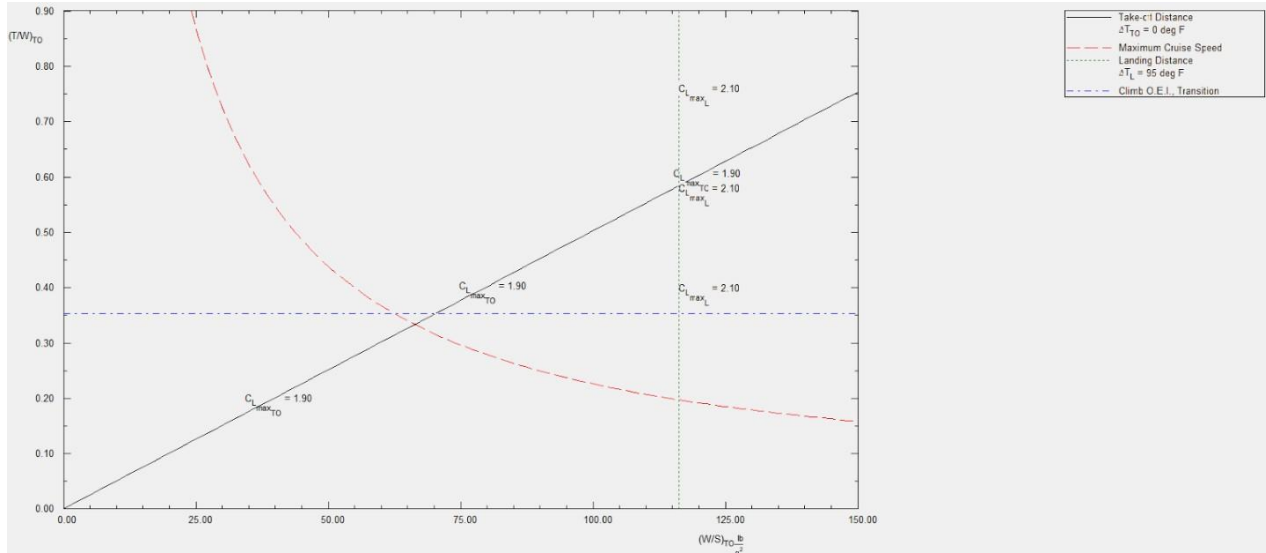


Figure 4.25: Matching graph of set coefficients of lift and aspect ratio outputted by AAA program.

From the AAA program matching graph and the hand calculated matching graph, the two are fairly similar. One of the prime differences is the landing distance. The hand calculation will be used to find an accurate wing loading and thrust to weight ratio as there were values that were assumed in the AAA program.

The following design point was chosen based off the hand calculated matching graph.

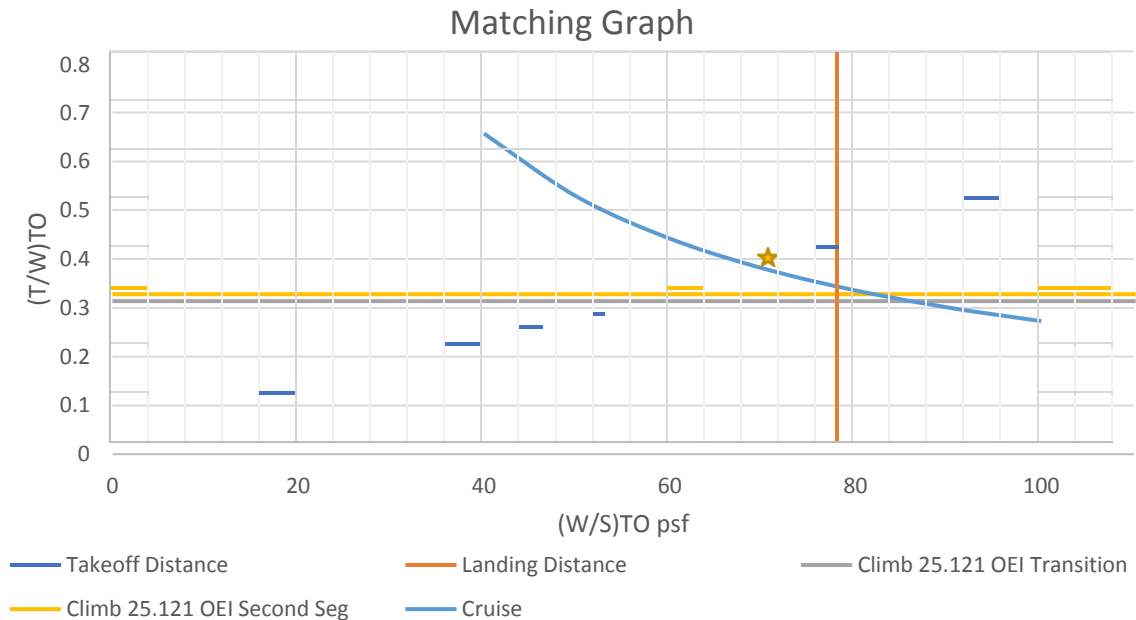


Figure 4.26: Cleaned up matching graph of hand calculations.

The wing loading value at takeoff is approximately 71 psf. The thrust to weight ratio at takeoff is approximately 0.4. From these values, the wing area and thrust can be calculated.

Wing area:

$$\begin{aligned} W/S_{TO} &= 71 \text{ psf} & (20) \\ S &= \frac{W_{TO}}{71} = \frac{29600}{71} = 416.9 \text{ ft}^2 \end{aligned}$$

Thrust:

$$\begin{aligned} T/W_{TO} &= 0.4 & (21) \\ T &= 0.4W_{TO} = .4(29600) = 11,840 \text{ lbs} \end{aligned}$$

4.4 Selection of Propulsion System

4.4.1 Selection of the Propulsion System Type

The selection of a propulsion system type has many factors to take into consideration. Arguably the most important factors are the performance and ability to certify. The engine capabilities must take into account the desired cruise speed, range, altitude, takeoff distance among other performance parameters that rely on the amount of thrust produced. The following will be taken into consideration:

- Required cruise speed: 530 mph
- Required max operating altitude: 45,000 ft
- Required range: 3000 miles
- FAR 36 noise regulations: 70 dB during takeoff, as found from similar aircraft
- Fuel weight: 11,000 lbs

Several other factors will be looked upon, but without definitive values being known:

- Installed weight
- Reliability and maintainability
- Fuel cost
- Fuel availability
- Specific customer or market demands
- Timely certification

The installed weight depends on the choice of engine. The reliability and maintainability are important as the upkeep is important to keep a good track record with potential buyers to have the ease of mind that they purchased a solid plane. The fuel cost and availability are also important that the plane is capable of being compatible with the ups and downs of the economy with how much jet fuel will cost and the ability to adapt to clean or dirty fuel.

For business jet, a turbojet or turbo fan works best as shown in Roskam's book [2]. The line illustrating the business jet's flight envelope shows that it is capable of reaching the desired cruise speed at a high altitude, at which the plane will cruise at.

4.4.2 Selection of the Number of Engines

The selection process of what engines will be used follows a set of rules. The first being whether to equip the plane with a newly developed engine or to use a preexisting design. The decision has been made that the plane will use an already existing engine. This will allow for maintenance familiarity and known statistics of reliability or potential issues that may occur and how to counter them.

From the previous section of the design point being chosen, the wing loading and thrust to weight ratio were defined. From the thrust to weight ratio, the amount of thrust was found to be 11,840 lbf, approximately 12,000 lbf. With a 12,000 lbf, two engines will be used to supply

the thrust necessary for the plane, amounting to each engine having the capability of producing 6,000 lbf.

A number of different engines were found that are able to obtain the desired thrust needed for the plane.

Table 4.2: Possible engines with thrust and application of each. [3][4]

Engine	Application	Max Thrust (lbf)
General Electric J47 (J47-GE-2)	Boeing B-47 Stratojet	6,000
Rolls Royce (Adour Mk 106)	BAE Systems Hawk	6,000 - 8,430
Lycoming ALF 502 (ALF 502R-3)	Bombardier Challenger 600	6,700
Pratt & Whitney PW300 (PW 306A)	Gulfstream G200	6,000
Pratt & Whitney PW300 (PW 306C)	Cessna Citation Sovereign	6,000
Pratt & Whitney PW300 (PW 307B)	Bombardier Learjet 85	6,100
Pratt & Whitney PW500 (PW 545B/C)	Cessna Citation XLS/XLS+	4,100
Honeywell TFE731 (TFE731-5BR-1H)	Hawker 800	4,660
Honeywell HTF7500 (AS-907-3-1E)	Embraer Legacy 450	6,300-7,100

In order to assure the amount of thrust necessary to meet the design point, the Honeywell HTF 7500 will be used for the plane. The mission requirements of the Embraer Legacy 450 are similar to that of the plane being designed. It will be able to meet the range desired at the desired cruise velocity. The choice to have two engines allows for a safety factor in case if one engine was to fail, the plane would still have a propulsion system.

4.5 Discussion

The following matching graph was created using the hand calculation computed values. The coefficient of lift values and aspect ratio were defined as:

- CL MAX TO 1.8
- CL MAX LND 2.0
- CL MAX 2.0
- Aspect Ratio 7.5

In order to meet the requirements, the design point must be above the takeoff distance line. The design point must also be above the climb requirement lines, as well as being above the cruise speed. The landing distance only relies on the coefficient of lift vale being met, which does not require being on either side of the line.

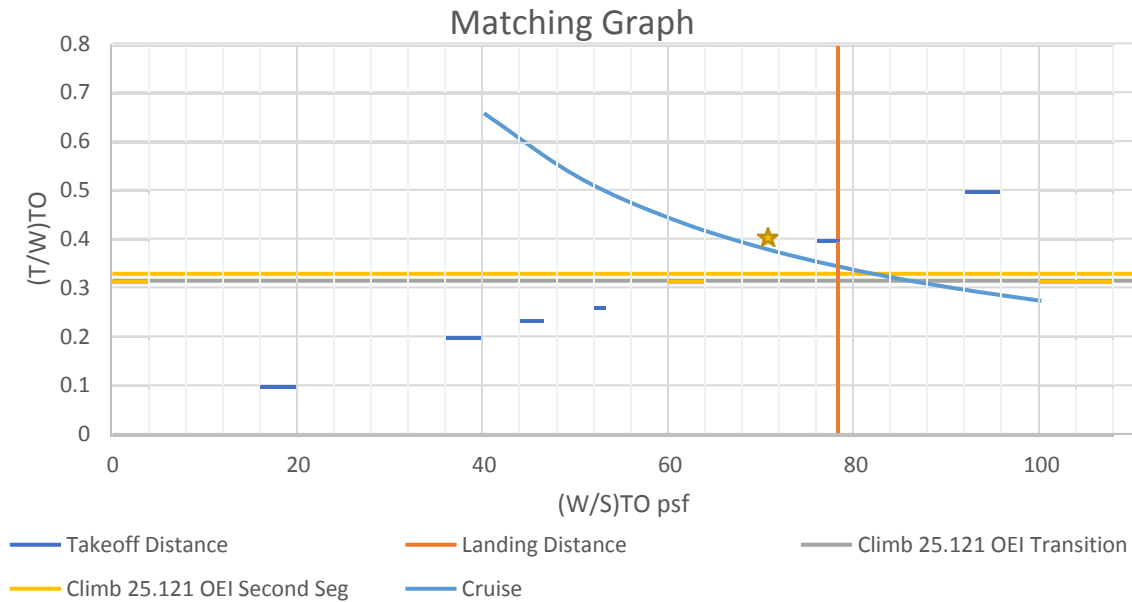


Figure 4.26: Cleaned up matching graph of hand calculations.

The wing loading value at takeoff is approximately 71 psf. The thrust to weight ratio at takeoff is approximately 0.4. From these values, the wing area and thrust can be calculated. The wing area corresponds to an area of 416.9 ft^2 . The thrust needed to satisfy this design point is 11,840 lbs.

Of the possible design configurations that significantly contributes to the design of the aircraft, the range, storage and safety were noted as being points of interest in the design process of the plane. The range would be the lone factor contributing to the production of the matching graph. The range would impact the selection of engines used for the plane's propulsion system. This will affect the amount of thrust needed to be generated. Another possible design that will have a large impact on the matching graph would be the sizing of the wing. The aspect ratio has a direct effect on the drag polar equations, climb requirements, maneuverability and cruise speed. The climb requirement and cruise speed have an effect on the matching graph. The larger AR produce larger climb requirement. The aspect ratio does affect the cruise speed, but not be a significantly large amount.

4.6 Conclusions and Recommendations

With a defined takeoff weight, the process of determining the finer details of the sizing of the plane. From this report, the performance of the plane is able to be defined allowing for a definitive design point being determined. The wing sizing is able to approximately be defined as an aspect ratio was used in the generation of the matching graph. The thrust is also able to be determined which will allow for the engine selection to be made.

From this data collected, the following recommendations can be made in order for the plane to perform in a safe manner:

- Stall velocity of 99 knts
- Takeoff distance of 5000 ft
- Landing distance of 8333 ft
- Ability to pull 3.8 g's during maneuver at max cruise velocity
- Turn radius of 6282 ft

- Turn rate of .1237 radians per second
- Cruise speed of 530 mph
- Wing area of 417 ft^2
- Thrust of 11, 840 lbf
- Selection of two Honeywell HTF7500 turbofan for propulsion

4.7 References

- [1] Ecf.gov. (2017). eCFR — Code of Federal Regulations. [online] Available at: <https://www.ecfr.gov/cgi-bin/text-idx?node=14:1.0.1.3.11> [Accessed 11 Oct. 2017].
- [2] Roskam, J. (1985). *Airplane design*. Ottawa, Kan.: Roskam Aviation and Engineering.
- [3] Pwc.ca. (2017). PW300 | Pratt & Whitney Canada. [online] Available at: <http://www.pwc.ca/en/engines/pw300> [Accessed 12 Oct. 2017].
- [4] Jane's Information Group. (1930). *Jane's All the World's Aircraft*.

5.0 Fuselage Design

5.1 Introduction

The purpose of this report is to determine the layout of the cockpit and fuselage. The layout of the cockpit is designed to be able to fit two pilots comfortably while at the same time maintaining the fact that the pilots are able to reach the controls, see all of the flight essential instruments, communicate effectively with one another and to have a good visibility of the surrounding areas. The fuselage layout is designed to be able to be functional and spacious at the taste of the passengers.

5.2 Layout Design of the Cockpit

Below, the cockpit is shown from multiple views of what it could potentially look like. The views shown are from the top, side, rear and front views. Both the hand sketches and computer aided design drawings are included.

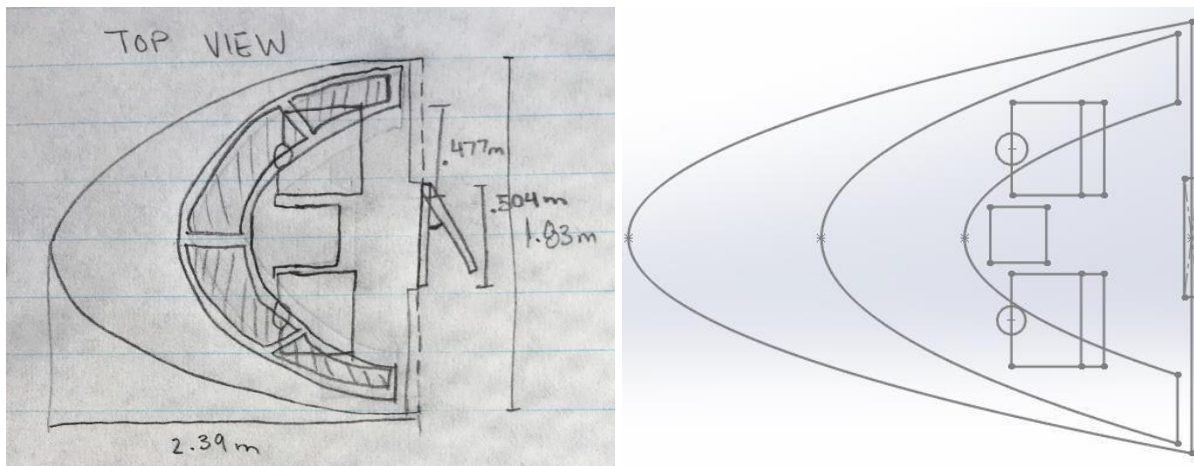


Figure 5.1: Top view of cockpit.

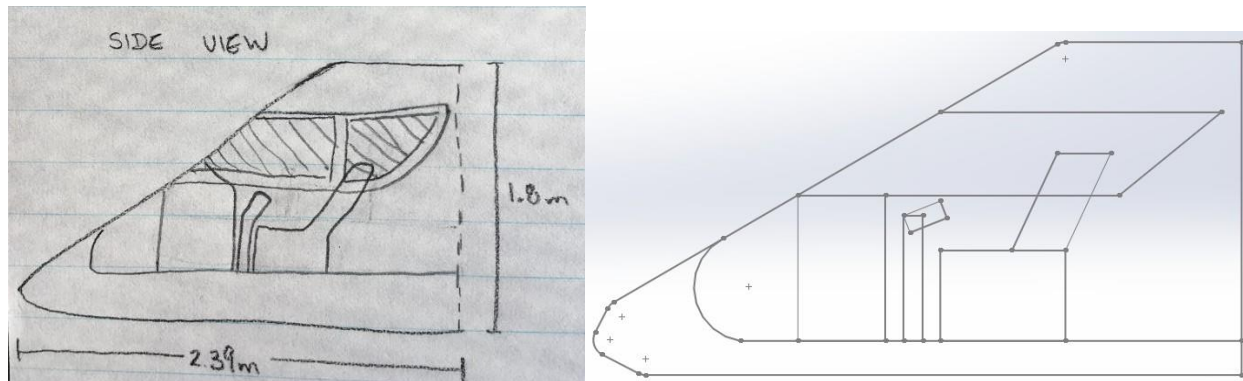


Figure 5.2: Side view of cockpit.

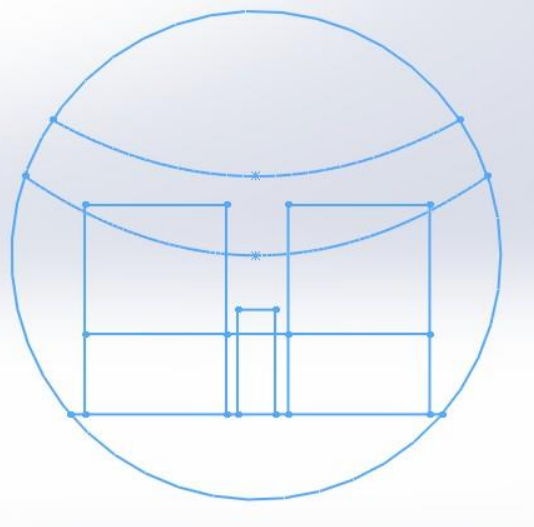
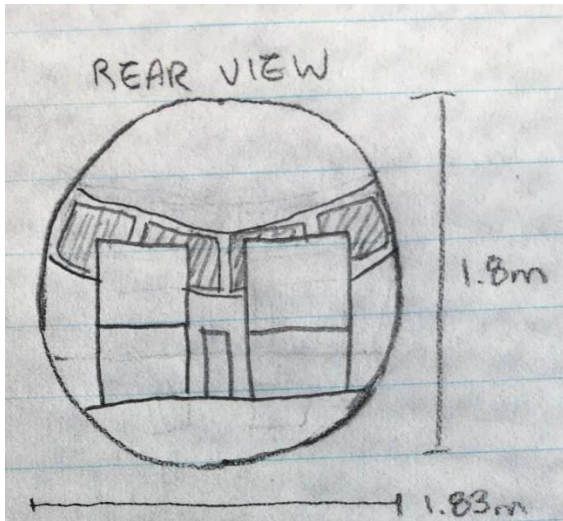


Figure 5.3: Rear view of cockpit.

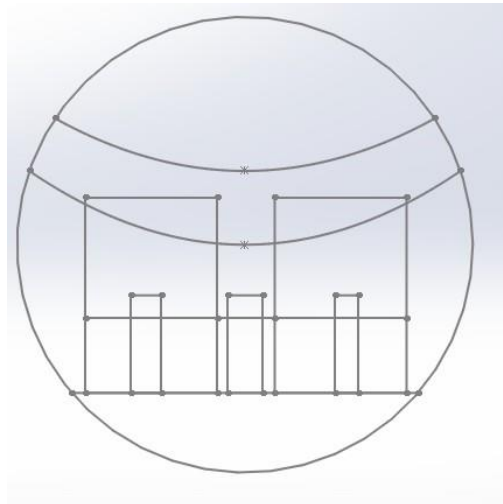
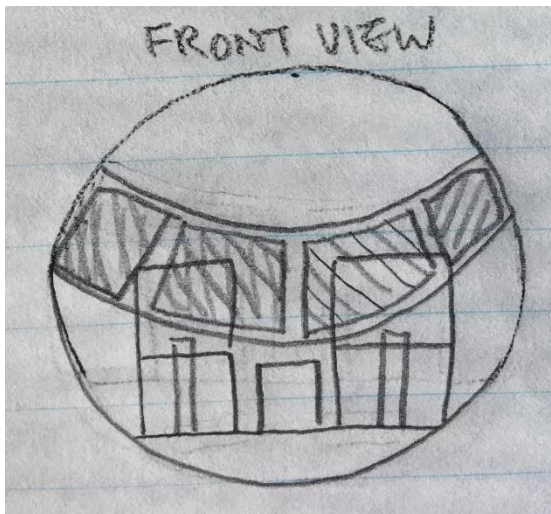


Figure 5.4: Front view of cockpit.

5.3 Layout Design of the Fuselage

Below, the fuselage is shown from multiple views of what it could potentially look like. The seating and closet areas can be rearranged and dimensioned if necessary to meet customer's desires. The views shown are from the top, side, rear and front views.

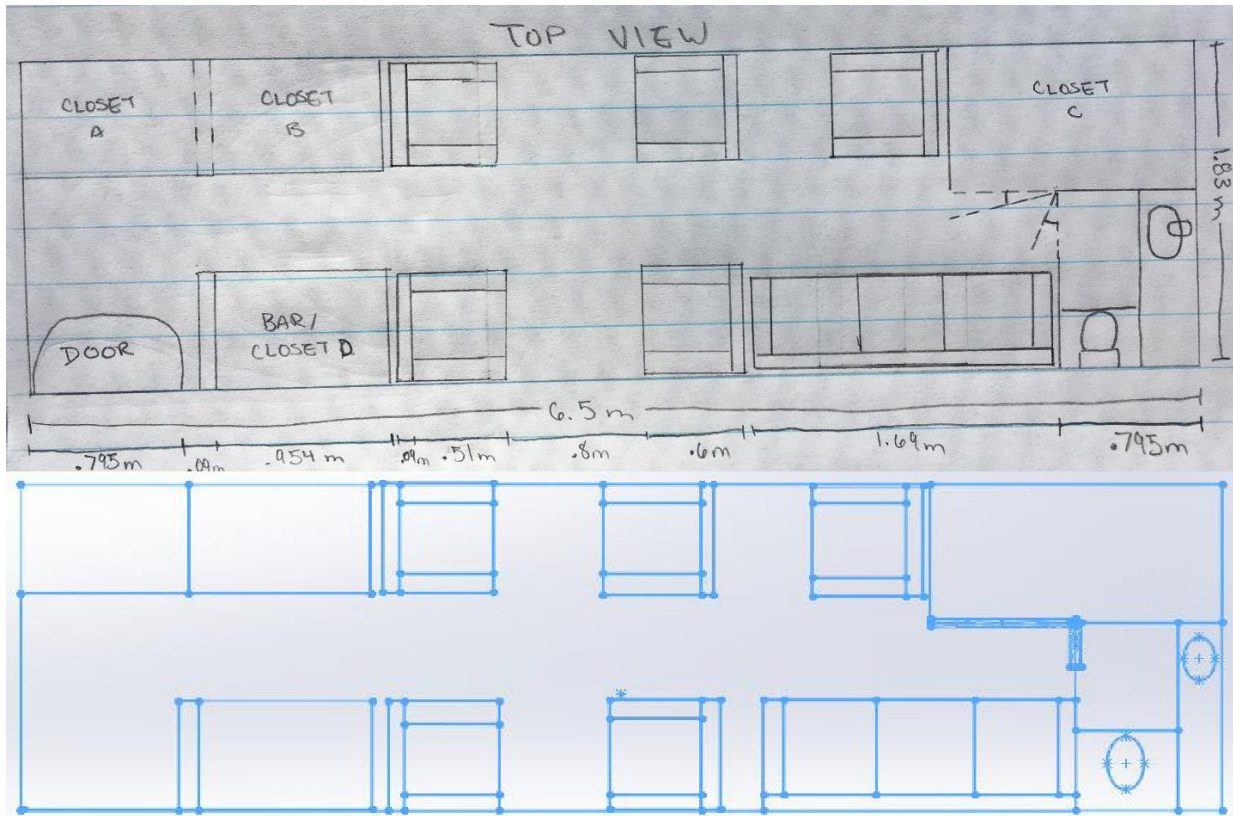


Figure 5.5: Top view of fuselage configuration.

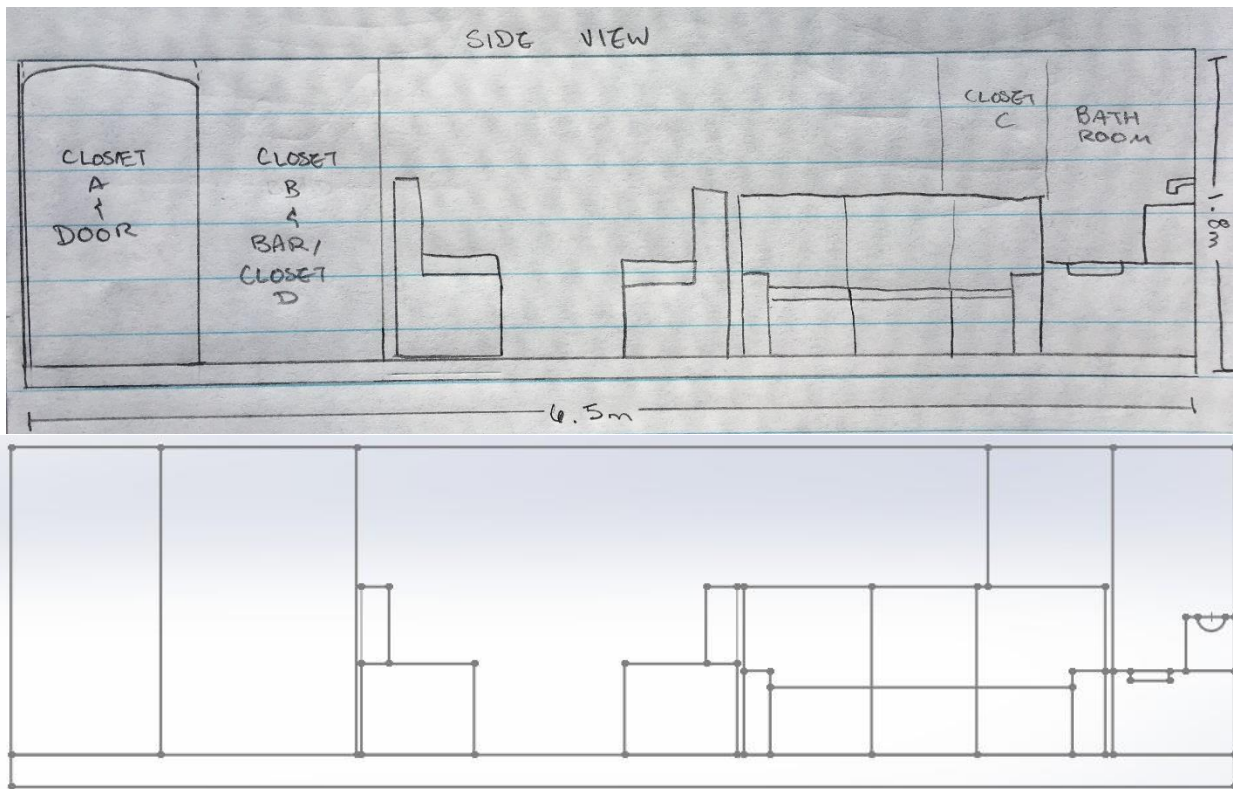


Figure 5.6: Side view of fuselage configuration.

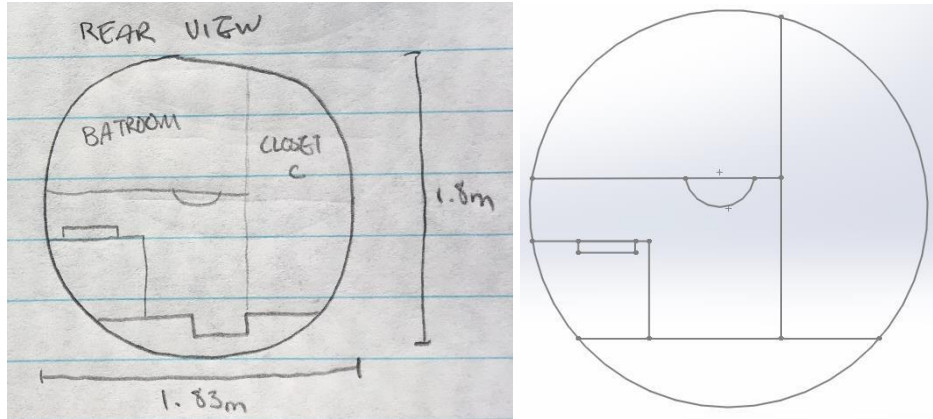


Figure 5.7: Rear view of fuselage configuration.

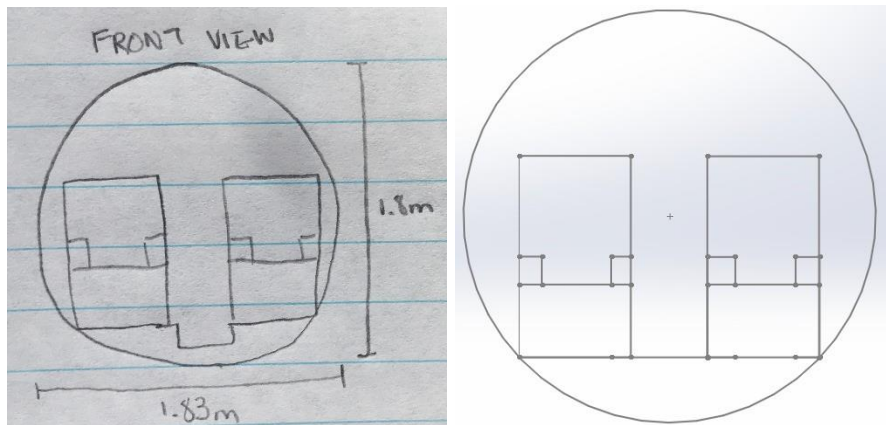


Figure 5.8: Front view of fuselage configuration.

5.4 Discussion

The figure below is the completed interior layout of the plane.

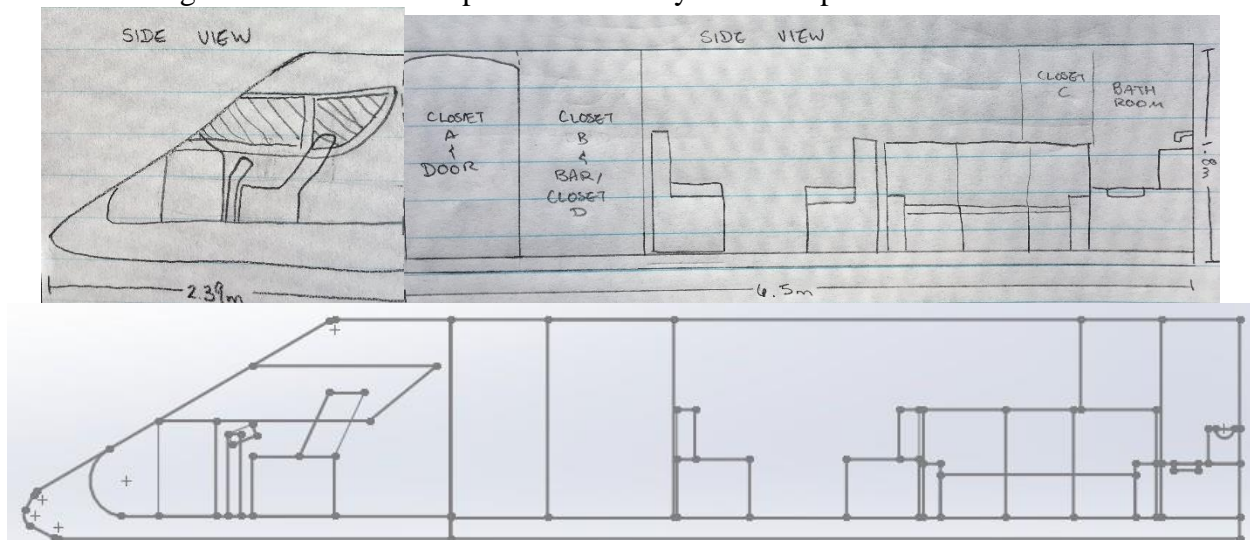


Figure 5.9: Complete side view of plane's cockpit and fuselage.

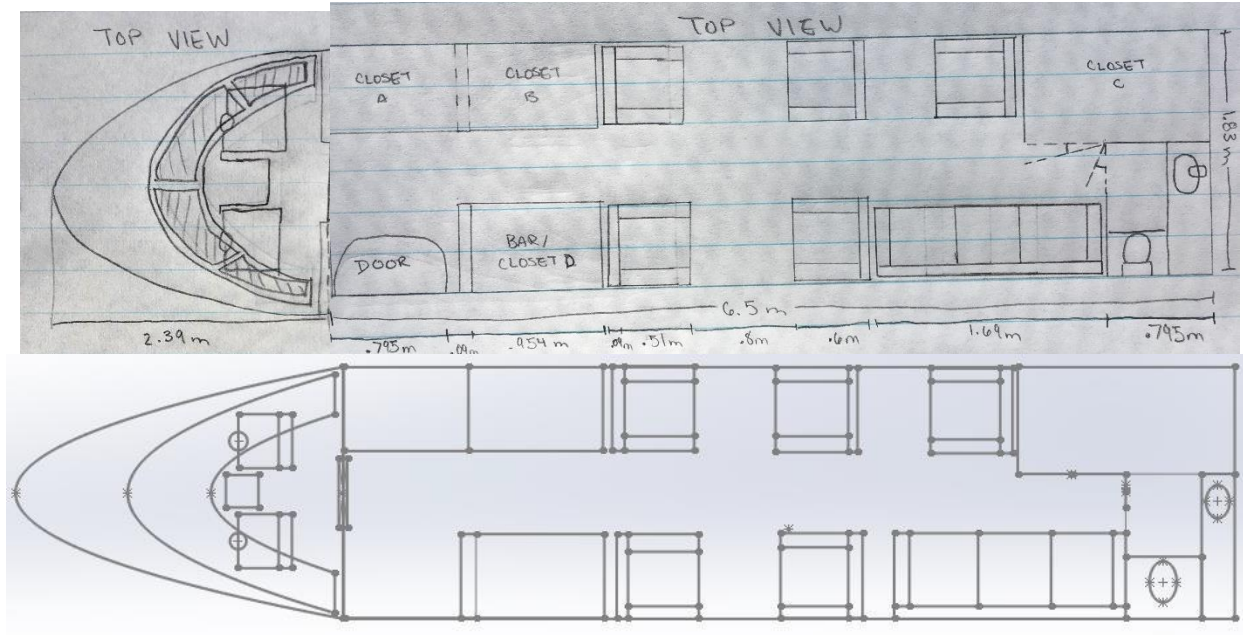


Figure 5.10: Complete top view of plane's cockpit and fuselage

From these planned configurations, there is room for adjustment as need be. The bar/closet D section shown in the top view sketches will give the customer the option of choosing to either have a self serve mini bar or an extra storage space for luggage. The total length of the plane's cockpit and fuselage will amount to 8.9 meters and a width of 1.83 meters at any point of the fuselage. The height within the cabin will be 1.8 meters.

6.0 Wing, High-Lift System & Lateral Control Design

6.1 Introduction

The purpose of this report is to determine an accurate wing geometry in order for this plane to have a successful flight. The wing geometry values will first be determined as to which will benefit the plane the most. The next step is the airfoil selection, this will determine the amount of lift and drag that will be generated by the wing. After the airfoil selection, this will determine if the maximum coefficient of lift during the takeoff or landing sequences is enough to match the plane's performance constraints. If the airfoil is not able to meet the desired coefficients of lift, high lift device systems will be utilized. The final step would be to determine the lateral control surfaces will be combined and analyzed as one.

6.2 Wing Planform Design

To begin, several variables pertaining to the geometry of the plane must be defined. The following wing geometric characteristics are determined as follows:

- Gross Area, S : 416.9 ft^2
- Aspect Ratio, AR : 7.5
- Taper Ratio, λ_w : .42
- Dihedral Angle, Γ_w : 2.9

The taper ratio and dihedral angles were values determined by Jan Roskam of previously designed and manufactured planes.

The plane's structure will be decided first before continuing. The wing will be a cantilever rather than a strut wing because it will help with the reduction of drag and it creates a more appealing look to a sleek plane. The wing will be configured as a low wing. This allows for the storage of the landing gear and the utilization of the cargo hold to place the cantilever to support the wing.

6.2.1 Sweep Angle - Thickness Ratio Combination

The thickness ratio, t/c , and sweep angle, Λ , are directly related to one another in determining how the two are able to benefit the wing of the plane. The two wing geometry options will affect the weight of the wing. The following calculation was conducted in order to find the relationship. To find the relationship of thickness ratio and sweep angle, the following equation was used.

$$\begin{aligned} & \frac{M_{cc}^2 \cdot \cos^2 \Lambda}{\sqrt{(1 - M_{cc}^2 \cdot \cos^2 \Lambda)}} \cdot \left[\left(\frac{\gamma + 1}{2} \right) \cdot \frac{2.64 \cdot (t/c)}{\cos \Lambda} + \left(\frac{\gamma + 1}{2} \right) \cdot \frac{2.64 \cdot (t/c) \cdot (0.34 \cdot C_L)}{\cos^3 \Lambda} \right] \\ & + \frac{M_{cc}^2 \cdot \cos^2 \Lambda}{1 - M_{cc}^2 \cdot \cos^2 \Lambda} \cdot \left[\left(\frac{\gamma + 1}{2} \right) \left(\frac{1.32 \cdot (t/c)}{\cos \Lambda} \right)^2 \right] + \\ & M_{cc}^2 \cdot \cos^2 \Lambda \cdot \left[1 + \left(\frac{\gamma + 1}{2} \right) \cdot \frac{(0.68 \cdot C_L)}{\cos^2 \Lambda} + \left(\frac{\gamma + 1}{2} \right) \cdot \left(\frac{(0.34 \cdot C_L)}{\cos^2 \Lambda} \right)^2 \right] - 1 = 0 \end{aligned} \quad (1)$$

This equation has several unknowns that must be accounted for before continuing. The crest critical Mach value and coefficient of lift during cruise must first be calculated.

Crest Critical Mach:

$$M_{Cruise} = M_{Div} \quad (2)$$

$$M_{Div} = 1.02M_{cc}$$

$$M_{cc} = \frac{.69}{1.02} = .676$$

Coefficient of Lift During Cruise at 35,000 ft:

$$C_{L_{cr}} = \frac{W_{TO} - 4W_F}{\rho \phi} \quad (3)$$

$$C_{L_{cr}} = \frac{29600 - 4(11050)}{1482(.2335)(.69^2)(416.9)} = .363$$

The relation between thickness ratio and sweep angle at zero degrees will be calculated showing the general process to analyze the relationship as the sweep angle increases by a matter of one degree until reaching 90 degrees.

$$1.77 \left(\frac{t}{c}\right)^2 + 2.22 \left(\frac{t}{c}\right) - .397 = 0$$

Solving with the quadratic formula:

$$\frac{t}{c} = \frac{-b \pm \sqrt{b^2 - 4ac}}{2a} \quad (4)$$

$$\frac{t}{c} = \frac{-2.22 \pm \sqrt{2.22^2 - 4(1.77)(-.397)}}{2(1.77)} = .159 \text{ and } -1.4$$

This process was executed by varying the sweep angle from 0° to 90°. The thickness ratio must be between .1 and .2 to be a viable option. This specific range is because the wing must have enough room for its own structural support, fuel and landing gear, as well as not to create a profile drag that will negatively impact to performance of the plane.

The ratio between weight of the wing and takeoff weight should also be considered when determining an accurate thickness ratio and sweep angle value. The takeoff weight was predetermined in the Weight Sizing and Weight sensitivities report. The weight of the wing is determined by the following equation [1]:

$$W_{wing} = 4.22 S_{wg} + 1.642 \times 10^{-6} \frac{N_{ult} b^3 \sqrt{TOW ZFW} (1+2\lambda)}{(\eta c)_{avg} \cos^2 \Delta_{ea} S_{wg} (1+\lambda)} \quad (5)$$

The wing area is 416.9 ft². The ultimate load factor is 3.8. the wing span is 55.92 ft. The takeoff weight and zero fuel weight are 29600 lbs and 18550 lbs, respectively. The taper ratio is .42, based off of other business jets presented in Roskam's book [2]. After inputting the necessary values at a sweep angle of zero degrees, the following was determined:

$$W_{wing} = 2046.382 \text{ lbs}$$

$$\frac{W_{wing}}{W_{TO}} = \frac{2046.382}{29600} = 0.0691$$

The following graph was able to be created showing the relation between thickness ratio and sweep angle and the ratio of weight of wing and takeoff weight.

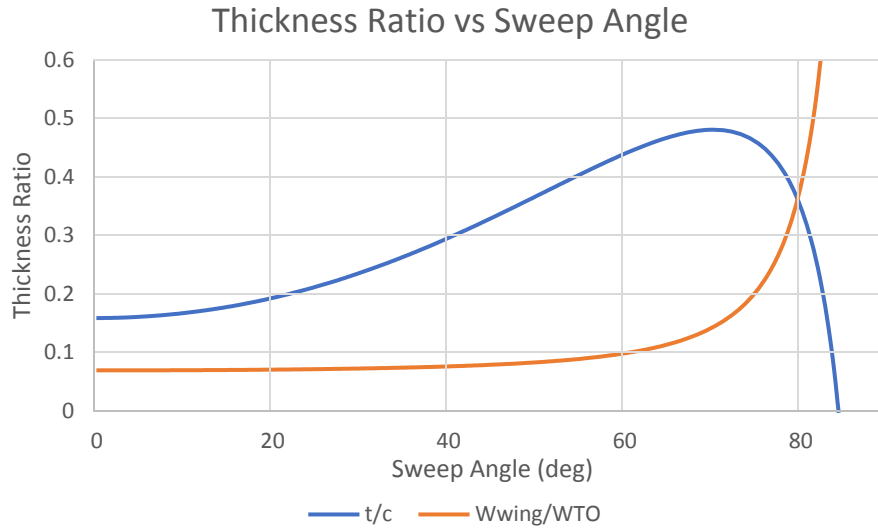


Figure 1: Tradeoff between sweep angle and thickness ratio in relation to the weight of the wing and takeoff weight ratio.

From the graph, the sweep angle should be approximately 20° along with a thickness ratio of .2. These decisions will be explained later in this report.

6.3 Airfoil Selection

There are a number of possible airfoil designs that can be used for the plane. Roskam illustrates this point in the tables presenting business jets and what airfoil shape is used.

Table 1: Airfoil type used by business jets. [2]

Plane	Type/Name of Airfoil(s)
Cessna Citation 500	NACA 23014 and NACA 23012
Cessna Citation III	NASA supercritical
Gates Learjet 24	NACA 64a109
Gates Learjet 33	NACA 64a109
Israel Aircraft Astra	Sigma 2
Israel Aircraft Westwind	NACA 64a212

From this table, it can be seen that these planes utilize different and multiple airfoils to create the wing. The decision is made that the plane will utilize a NACA 64008a. Although it is not listed in the table of a previous plane having used it, it will be able to provide sufficient data and statistics as it is relatively well known and has previous data on it.

The incidence and angle and angle of twist will be defined based off of Roskam’s values of previous business jets. The angle of twist, is to be set at 0°. The incidence angle is to be set at 1°. These two selections will be explained in further detail in the discussion section in the report.

6.4 Wing Design Evaluation

Using the Advanced Aircraft Analysis Version 3.7 Program, AAA, the wing geometry was plotted. The inputs needed to determine the geometry of the wing were AR, S, λ, Λ, the X-position of the wing and Y offset position of the wing.

Input Parameters					
AR_w	7.50	S_w	416.90 ft ²	t_w	0.42
$A_{c,d,w}$	30.0 deg	$x_{apex,w}$	-0.00 ft	$y_{offset,w}$	0.00 ft
Output Parameters					
$c_{r,w}$	10.50 ft	b_w	55.92 ft	$y_{mgc,w}$	12.08 ft
$c_{t,w}$	4.41 ft	\bar{c}_w	7.87 ft	$x_{mgc,w}$	7.63 ft
				$\alpha_{LE,w}$	32.3 deg
				$\alpha_{TE,w}$	22.5 deg
Straight Tapered Wing Geometry: Output Parameters					
Panel	c_r ft	c_t ft	X_r ft	X_t ft	Y_r ft
1	10.5009	4.4104	0.0000	17.6646	0.0000

Figure 2: Inputs and outputs of wing geometry determined by AAA.

It was determined the chord length at the root is 10.5 ft and the chord length at the tip is 4.4 ft. The average chord length of the wing is 7.87 ft at 7.63 ft in the x direction, with respect to the leading edge of the root, and 12.08 ft in the y direction, with respect to the root of the wing.

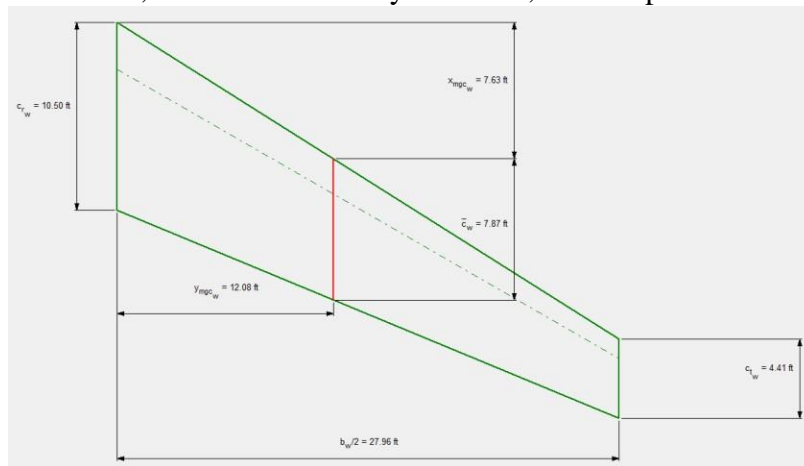


Figure 3: Outputted geometry of wing determined by AAA.

This wing is able to generate a clean coefficient of lift of 1.641. From this wing geometry, the use of a high lift device will be needed.

6.5 Design of the High-Lift Devices

From the Performance Sizing Report, the maximum coefficient of lift during takeoff, landing and clean airplane were determined. The max coefficient of lift during takeoff was defined as 1.8. The max coefficient of lift during landing was defined as 2.0. The max coefficient of lift for a clean plane was defined as 2.0.

To determine the Reynolds number of the root and tip, the following was used:

At the root:

$$R_{n_r} = \frac{\rho V c_r}{\mu} \quad (6)$$

$$R_{n_r} = \frac{.002377(777.333)(10.5)}{3.737 \cdot 10^{-7}} = 51.9 \cdot 10^6$$

At the tip:

$$R_{n_t} = \frac{\rho V c_t}{\mu} \quad (7)$$

$$R_{n_t} = \frac{.002377(777.333)(4.41)}{3.737 \cdot 10^{-7}} = 21.8 \cdot 10^6$$

With a high Reynolds number, the figures of Roskam do not show these needed values. Thus, it will be assumed that the maximum coefficient of lift will be 2.0 at thickness ratio of the root and tip of .14 and .18 respectively.

To verify if the wing can meet the unswept $C_{L_{max\ W}}$. For a taper ratio of .4, k_λ of 0.95, the following equations will be used:

$$C_{L_{max\ W}} = \frac{k_\lambda(C_{L_{max\ r}} + C_{L_{max\ t}})}{2} \quad (8)$$

$$C_{L_{max\ W}} = \frac{.95(2.0+2.0)}{2} = 1.9$$

The next step will correct for the swept wing, as shown below:

$$C_{L_{max\ W_{unswept}}} = C_{L_{max\ W_{swept}}} / \cos(\Lambda_c/4) \quad (9)$$

$$C_{L_{max\ W_{unswept}}} = \frac{1.9}{\cos(22)} = 2.049$$

The coefficient of lift of the wing must be able to obtain the coefficient of lift of the clean plane.

$$C_{L_{max\ W}} = 1.05 C_{L_{max\ W_{unswept}}} \quad (10)$$

$$C_{L_{max\ W}} = \frac{2.049}{1.05} = 1.95$$

This coefficient of lift value of 1.92 is within reason as there is a 2.5% difference between the values. This calculation provides the evidence that a high lift system is not required for this plane as all of the coefficients of lift are approximately the same value.

To determine the amount of the coefficient of lift that must still be generated is:

Takeoff:

$$\Delta C_{L_{max\ T_O}} = 1.05 (C_{L_{max\ T_O}} - C_{L_{max}}) \quad (11)$$

$$\Delta C_{L_{max\ T_O}} = 1.05(1.8 - 2) = -.21$$

Landing:

$$\Delta C_{L_{max\ L}} = 1.05 (C_{L_{max\ L}} - C_{L_{max}}) \quad (12)$$

$$\Delta C_{L_{max\ L}} = 1.05(2 - 2) = 0$$

To determine the size of the flaps to generate the extra coefficient of lift. The flap size parameter is not yet known, but will be assumed as two values to be analyzed .6 and .8. The following process will be used:

$$\Delta C_{L_{max\ T_O}} = \Delta C_{L_{max}} \left(\frac{S}{S_{wf}} \right) K_\Lambda \quad (13)$$

Where K_Λ is:

$$K_\Lambda = (1 - (.08 * \cos^2 \Lambda)) * \cos^{\frac{3}{4}}(\Lambda) \quad (14)$$

$$K_\Lambda = (1 - (.08 * \cos^2(22))) * \cos^{\frac{3}{4}}(22) = .87989$$

At $\frac{S}{S_{wf}} = .6$:

$$\Delta C_{L_{max\ T_O}} = (.21)(.6).87989 = .1109$$

At $\frac{S}{S_{wf}} = .8$:

$$\Delta C_{L_{max\ T_O}} = (.21)(.8).87989 = .1478$$

A plain flap will likely be able to do the job, as seen from the following process:

$$\Delta C_L = C_{l_{\delta_f}} * \delta_f * K' \quad (15)$$

$$\Delta C_L = 5.75 * 40^\circ * .6 = (5.75 * .6) * .698 \text{ radians} = 2.409$$

The flap will be able to change the coefficient of lift by 2.4, thus, the coefficient of lift required according to the performance constraints can be met.

6.6 Design of the Lateral Control Surfaces

Deciding upon the type, size and location of the lateral control devices will be done according to Roskam's tables of previous planes [2].

For the horizontal and vertical tail, the following wing geometries will be referenced and used in the future reports. These values are not definitive, however, will be used as a reference point. The values referenced are based off of the Learjet 55, as it closely resembles the intended mission requirements set for this plane.

Table 2: Horizontal tail geometry sizes according to Roskam [2].

Wing Area	Wing Mean Chord	Horizontal Tail Area (S_h)	S_e/S_h	x_h	\bar{V}_h	Elevator Chord (root/tip)
265 ft ²	6.88 ft	57.8 ft	.32	23.8	.76	.31/.35

Table 3: Vertical tail, rudder and aileron geometry sizes according to Roskam [2].

Wing Area	Wing Span	Vertical Tail Area (s_v)	S_r/S_v	x_v
265 ft ²	64.3 ft	96 ft ²	.26	19.2
\bar{V}_b	Rudder Chord (root/tip)	s_a/s	Aileron Span Location (in/out)	Aileron Chord (in/out)
.086	.26/.25	.062	.49/.71	.3/.3

6.7 Drawings

The following wing parameters can be calculated:

- Span, b: 55.92 ft
- Root chord, cr: 10.5 ft
- Tip chord, ct: 4.4 ft
- MAC, mean aerodynamic chord: 7.87 ft
- MGC, mean geometric chord: 7.455 ft
- Leading-edge sweep angle: 22°
- Trailing-edge sweep angle: 22°
- Coordinates of the aerodynamic center
 - X_{ac} : 1.97 ft
 - Y_{ac} : 12.08 ft from root

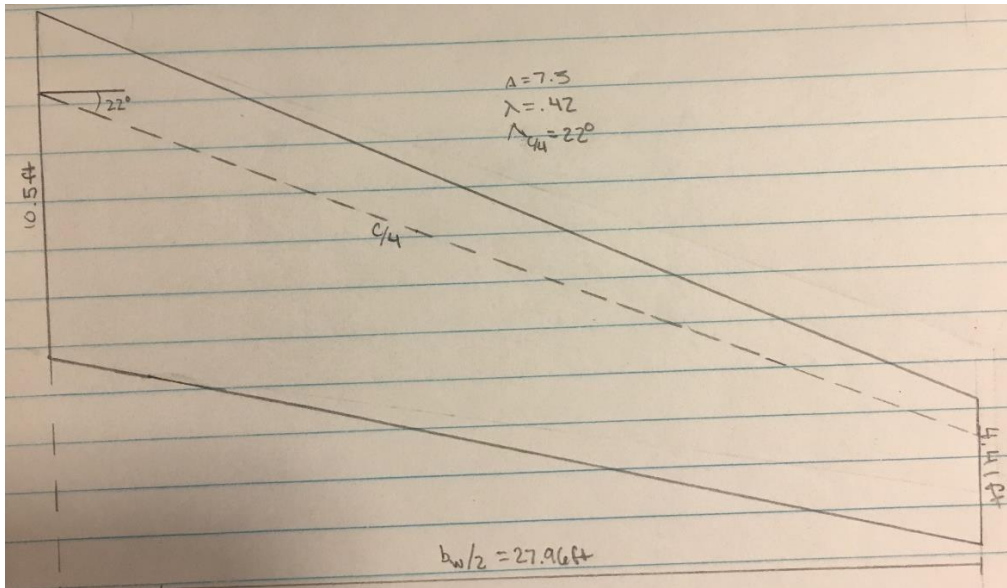


Figure 4: Wing planform.

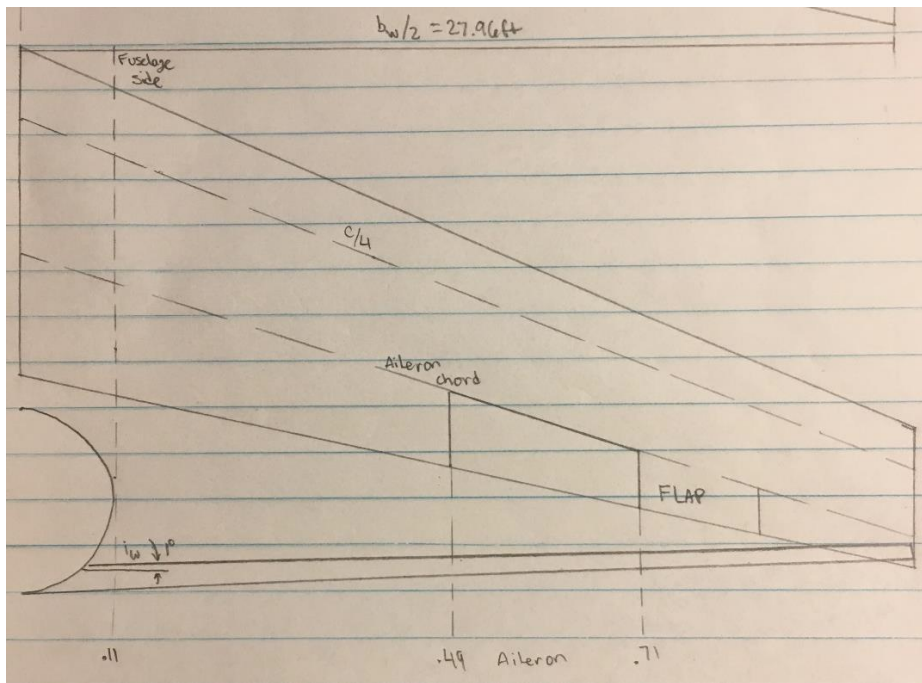


Figure 5: Flap and lateral control layout.

6.7.1 Wing Fuel Volume

The amount of fuel that can be stored in the wing can be found with the following equation:

$$V_{wf} = .54 * \left(\frac{s^2}{b}\right) \left(\frac{t}{c_r}\right) * \left[\frac{1 + \lambda\sqrt{\tau} + \lambda^2\tau}{(1 + \lambda)^2} \right] \quad (16)$$

Where τ is:

$$\tau = \frac{(t/c)t}{(t/c)r} \quad (17)$$

$$\tau = \frac{.13}{.16} = .8125$$

Thus, the amount of space for storable fuel is:

$$V_{wf} = .54 * \left(\frac{416.9^2}{55.92} \right) * .16 * \left[\frac{1 + (.42)\sqrt{.8125 + (.42)^2(.8125)}}{(1+.42)^2} \right]^3 = 202.68 \text{ ft}^3$$

The required amount of fuel for a maximum range from the maximum takeoff weight is 11,050 lbs. Converting this will result in $11050/44.9 = 246 \text{ ft}^3$. This results in the fact that not all of the fuel will be able to be stored in the wings. The placement of the excess fuel will be placed in an area of the cargo hold.

6.8 Discussion

The following figure shows the most up to date image configuration of what the plane is expected to look like from an exterior bird's eye point of view.

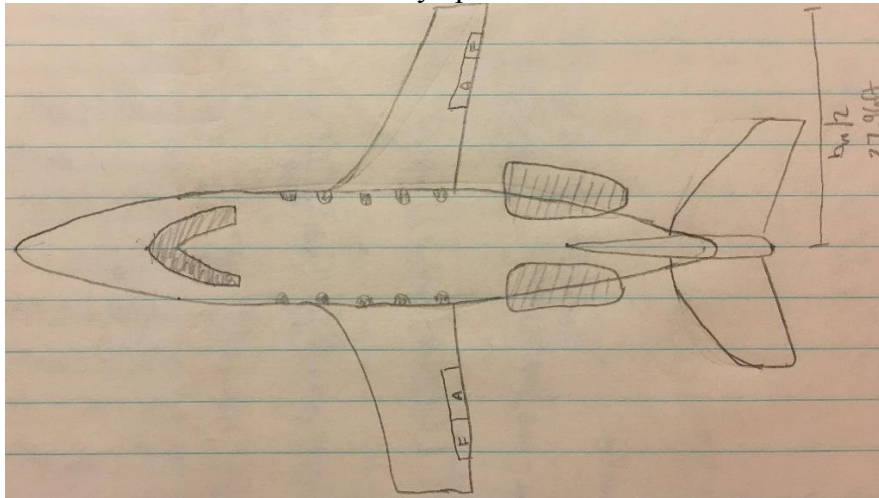


Figure 6: Most up to date plane configuration drawing.

From determining the relation between sweep angle and thickness ratio, the trend can be observed as to if one is increased, how the other will react. The choice of a viable sweep angle is to ensure that its corresponding thickness ratio is between .1 and .2. This range is necessary as the wing must be able to structurally support one's self and other parts that may need to be stored within it. The range is also important as if the wing thickness ratio is too large, the profile drag will become an issue of the plane. Thus, the sweep angle of 22° was chosen as it will correspond to the maximum thickness ratio of the desired range of .2.

The airfoil selection was based off of the fact that the previous planes analyzed by Roskam do not all use the same airfoil. This shows that for business jets, any airfoil may be used if it is within reason of enabling the plane to meet all of its mission requirements. The NACA 64008a was chosen because it is not a newly designed technology and has previous data about it, which may need to be referenced in future research and reports. The incidence angle and twist are to be 1° and 0° , respectively. The incidence angle was selected based off of previous data of business jets provide by Roskam. The angle of twist was chosen as it will reduce the complexity of the wing performance ratings and structural support needed.

The wing can generate most of its required lift alone. To ensure that the plane is able to meet the required performance constraints, more specifically the maximum coefficients of lift during takeoff and landing and for a clean aircraft. It was determined that the wing would require the plain flaps in order to sufficiently meet the requirements set by the performance constraints. The choice of a different flap or slat system could have been selected, but the complexity figure of merit was taken into consideration, thus the selection of the basic system was decided upon.

The lateral control surface geometry was determined off of Roskam's previous planes. This initial sizing was to determine what surfaces would be utilized. The configuration of plane only anticipated the use of ailerons, a rudder and elevator to be used. The sizing values were chosen based off of previous business jets provided by Roskam. The business jet's values that were used were based off of which plane similarly fit the mission requirements and size of the plane.

The wing fuel volume was determined to not have enough space to hold all of the fuel necessary for a maximum takeoff and maximum range flight. Approximately 2,000 lbs, 43ft³, of fuel must still be stored. The remainder of fuel may be stored in the cargo hold area of the plane. The plane has this ability because the space under the plane is too small for large passenger luggage, as well as the passengers are intended to store their luggage within the closest in the cabin of the aircraft. If more space is required, fuel may be placed in the empennage section, structure permitting.

6.9 Conclusions

The plane's wing geometry was able to be determined in this report. The wing will be a cantilever low wing with the following geometric values:

- $\Lambda_{c/4} = 22^\circ$
- $t/c = .2$
- $\Gamma_w = 2.9^\circ$
- $\lambda_w = .42$
- $i_w = 1$

The following features will be used:

- NACA 64008a
- Plain flaps
- Ailerons
- Horizontal tail with elevator
- Vertical tail with rudder

The empennage will be examined further in a future report.

6.10 References

- [1] Southampton.ac.uk. (2017). Component Weights. [online] Available at: <https://www.southampton.ac.uk/~jps7/Aircraft%20Design%20Resources/weight/Component%20Weights.htm> [Accessed 28 Oct. 2017].
- [2] Roskam, J. (1985). Airplane design. Ottawa, Kan.: Roskam Aviation and Engineering.

7.0 Design of Empennage & Longitudinal and Directional Control Bodies

7.1 Introduction

The purpose of this report is design the empennage section of the airplane. The empennage is an important factor as it will contribute to all three directional movements of the plane. The horizontal stabilizer will contribute to the pitch movement of the plane. The vertical tail will contribute to the yaw and roll moments generated as these two moments are coupled.

7.2 Overall Empennage Design

As stated in a previous report, Configuration Design, the empennage of the plane called for a conventional figuration. Rather than entertain the most recognizable configuration of an inverted t-tail, the plane will utilize a t-tail as to ensure the horizontal stabilizer is able to perform its duty as the engine placement would have negated the effects of an inverted t-tail's horizontal stabilizer surface.

The location, or moment arm, of the horizontal and vertical stabilizers is in reference to the plane's anticipated center of gravity to the horizontal and vertical's quarter chord position. The center of gravity should be at the quarter chord of the plane. The locations are as follows:

- x_h : 21.496 ft
- x_v : 18.425 ft

To determine the size of the horizontal and vertical stabilizer, it can be found by referencing previous business jets and the use of several equations. From the previous planes Roskam has provided, four of them will be used to obtain the surface area.

Table 1: Previous planes similar to design plane. [1]

Plane	\bar{V}_h	\bar{V}_v
Dassault Falcon 20	.65	.063
Dassault Falcon 50	.68	.064
Bombardier Challenger 601	.67	.083
Learjet 55	.76	.084
Average	.69	.074

To begin, the horizontal stabilizer's area will be determined. The following equation will be used:

$$S_h = \frac{\bar{V}_h * S * c}{x_h}$$

$$S_h = \frac{.69(416.9)(7.455)}{21.469} = 99.76 \text{ ft}^2$$

To determine the wing area of the vertical stabilizer, the process is as follows:

$$S_v = \frac{\bar{V}_v * S * b}{x_v}$$

$$S_v = \frac{(.074)(416.9)(55.92)}{18.425} = 93.63 \text{ ft}^2$$

7.3 Design of the Horizontal Stabilizer

Roskam informs that the design of the horizontal stabilizer is not found through equations, but rather through the comparison of similar aircraft's horizontal stabilizers. From these range of values, the following was decided upon for the plane's horizontal stabilizer to be sized after.

Table 2: Horizontal stabilizer geometry values presented by Roskam [1].

Dihedral Angle	Incidence Angle	Aspect Ratio	Sweep Angle	Taper Ratio
-4° to +9°	-3.5°	3.2 to 6.5	0° to 35°	.32 to .37

The dihedral angle, aspect ratio, sweep angle and taper ratio were chosen based on the average of the range presented. There was no evidence that warranted either utilizing the minimum or maximum values of each categories range. The incidence angle is a fixed value used with all business jets.

Table 3: Defined horizontal stabilizer geometry values to be used.

Dihedral Angle	Incidence Angle	Aspect Ratio	Sweep Angle	Taper Ratio
2.5°	-3.5°	4.8	17.5°	.34

7.4 Design of the Vertical Stabilizer

Similar to the horizontal stabilizer, the vertical stabilizer does not utilize equations to determine the planform geometry. The vertical stabilizer has its own set of values used to determine its geometrical shape. A similar method was taken in determining the wing planform of the vertical tail.

Table 4: Vertical stabilizer geometry values presented by Roskam [1].

Dihedral Angle	Incidence Angle	Aspect Ratio	Sweep Angle	Taper Ratio
90°	0°	.8 to 1.6	28° to 55°	.30 to .74

The dihedral and incidence angles are fixed values and evidence was not found that warranted a different set of values to be used. The aspect ratio, sweep angle and taper ratio were averages of the range provided by Roskam. The average of each categories range was taken because nothing was found that warranted either extreme of the range to be used or favored over the other.

Table 5: Defined vertical stabilizer geometry values to be used.

Dihedral Angle	Incidence Angle	Aspect Ratio	Sweep Angle	Taper Ratio
90°	0°	1.2	41.5°	.52

7.5 Empennage Design Evaluation

For the horizontal stabilizer, the following values were inputted and outputted by the AAA program. The program was then able to create the geometry planform of half of the horizontal stabilizer.

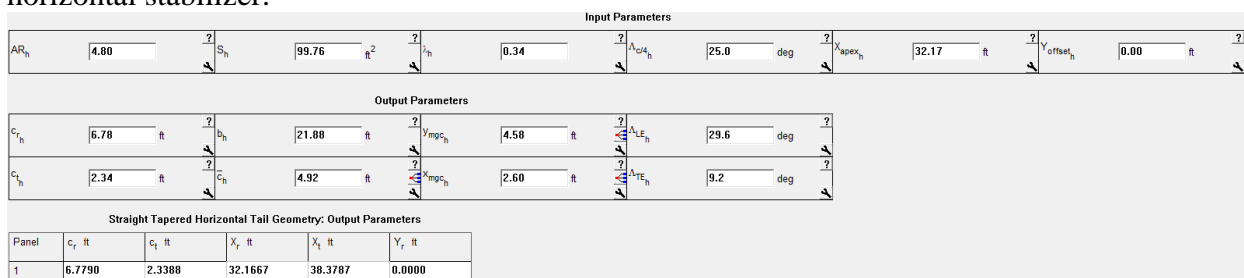


Figure 1: Inputs and outputs of AAA for horizontal stabilizer.

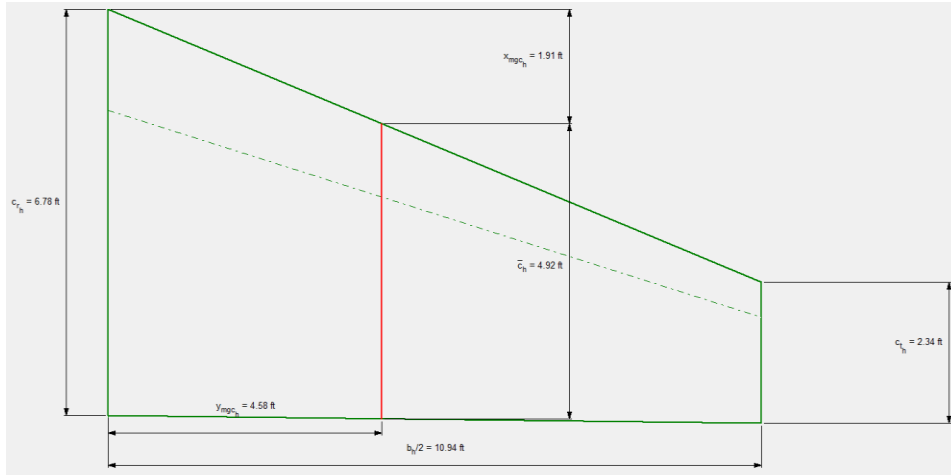


Figure 2: Wing planform generated by AAA of the horizontal stabilizer.

The following inputs and outputs were used in the AAA program for the vertical stabilizer. The program was then able to provide the wing geometry planform of the vertical stabilizer.

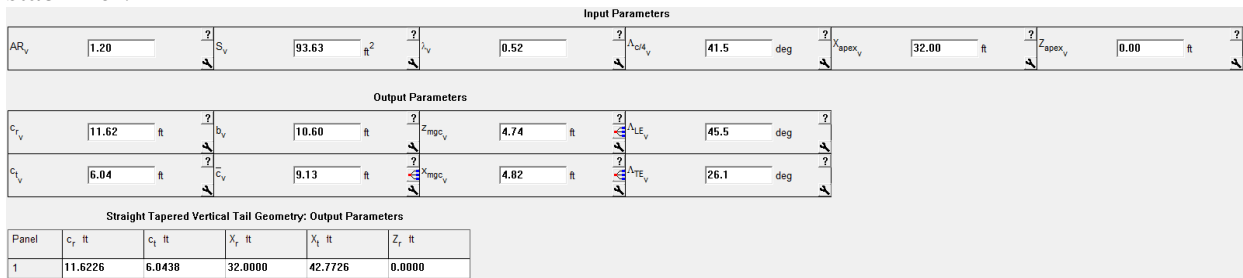


Figure 3: Inputs and outputs of AAA for vertical stabilizer.

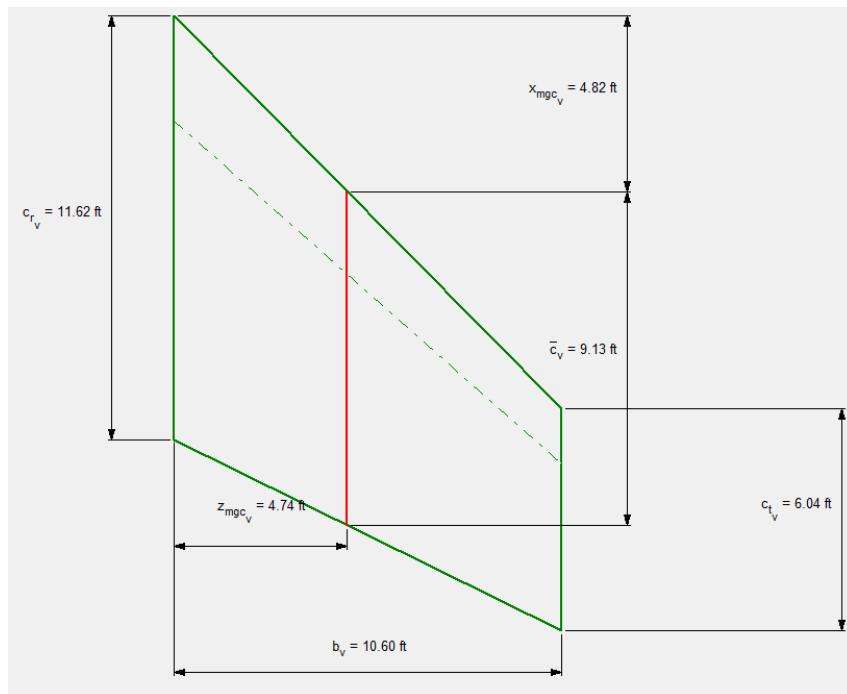


Figure 4: Wing planform generated by AAA of the vertical stabilizer.

7.6 Design of the Longitudinal and Directional Controls

To determine the size of the longitudinal and directional control surfaces relevant to the empennage of the plane, the method is similar to that of how the horizontal and vertical stabilizers were designed. The control surfaces are to be based off of other pre-existing planes of similar shape. An important thing to take into consideration would be to observe the empennage's that are of a t-tail. This will allow for more accurate measurements of the control surfaces relevant to the plane being designed.

The horizontal stabilizer will utilize an elevator control surface. The vertical stabilizer will utilize a rudder control surface.

Table 6: Control Surface sizing determined by previous plane data of Roskam. [1]

Horizontal Elevator			Vertical Rudder		
Size of Elevator	Chord at root	Chord at tip	Size of Rudder	Chord at root	Chord at tip
31.92 ft ²	1.722 ft	1.53 ft	15.92 ft ²	2.37 ft	2.28 ft

As the tail is a t-tail rather than the more common inverted tail, the position of the leading edge of the horizontal and vertical stabilizer will not be at the same position. As the vertical stabilizer is swept back, the leading edge of the horizontal stabilizer will be positioned after that of the vertical stabilizer. The position at which

7.7 Figure Drawings

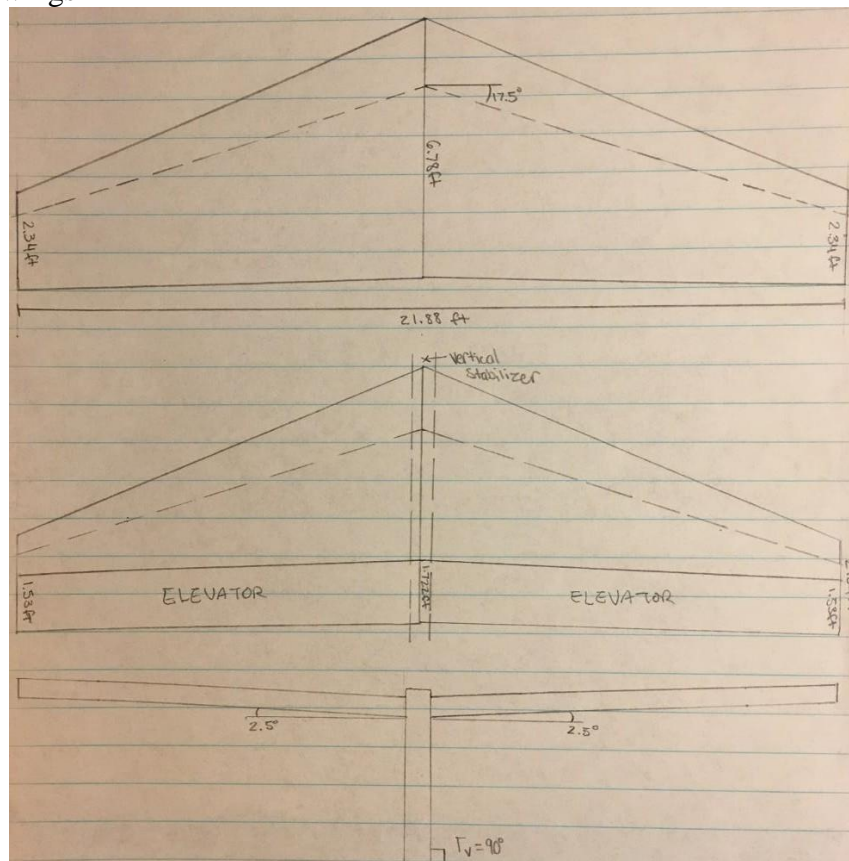


Figure 5: Wing planform and control surface of horizontal stabilizer.

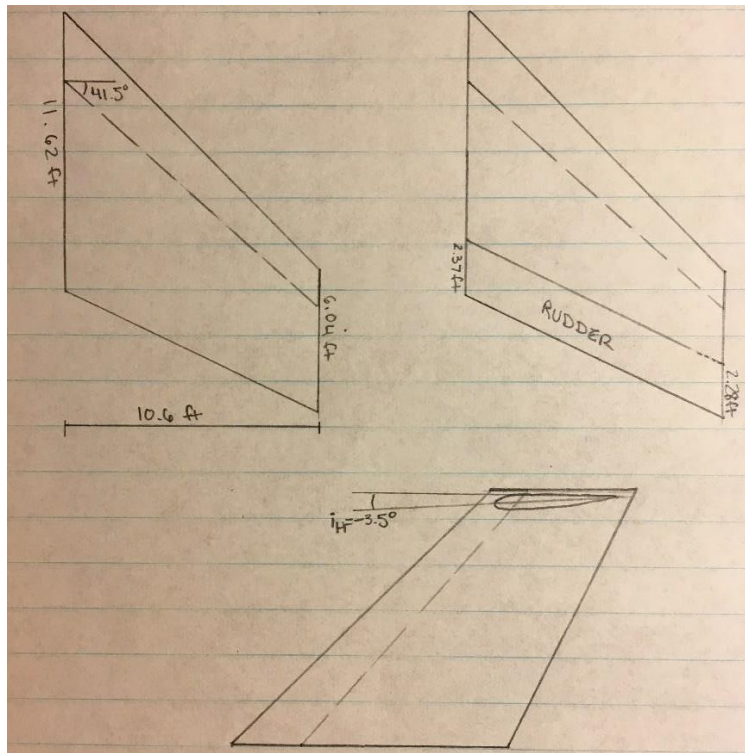


Figure 6: Wing planform and control surface of vertical stabilizer.

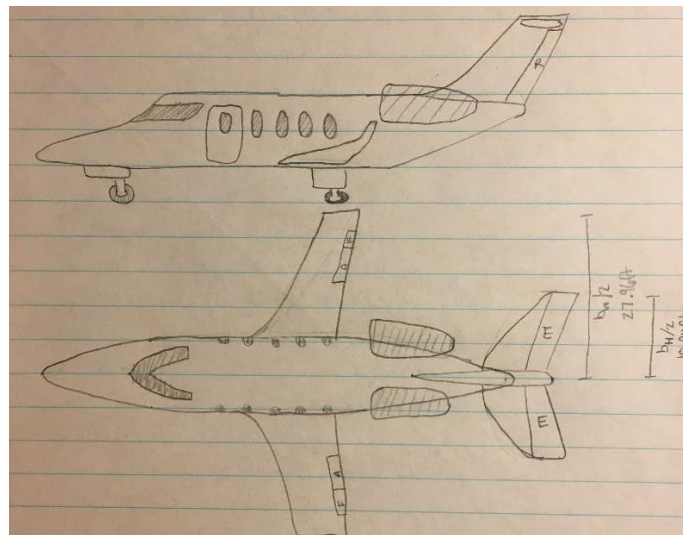


Figure 7: Plane configuration with revised empennage.

7.8 Discussion

The process of determining the wing structure of the empennage of plane is not as intense as the process of designing the primary wing of the plane. The empennage design process is a comparison of planes with similarly intentioned mission requirements and configurations.

The lone process which allowed for individuality in the design process was the sizing of the horizontal and vertical stabilizers. The sizing takes into consideration the distance between

the plane's center of gravity to the tail fin's aerodynamic center. This length is used to determine the moment arm that is generated to determine if a larger empennage is needed if closer to the plane's center of gravity or if a smaller empennage is needed if the tail is farther away from the center of gravity.

One point that must be taken into consideration is the fact that the tail is a t-tail. This is important structurally as the horizontal stabilizer is attached to the vertical stabilizer. To ensure that the horizontal stabilizer is effective, the vertical stabilizer should be strong and sturdy to ensure it will not cause flutter, which may diminish the effectiveness of the horizontal stabilizer. It is also important to consider the sizing of the control surfaces of the empennage section. As seen in the sketches, the control surfaces may need to be adjusted as the horizontal stabilizer will limit the height of the rudder. As well as the elevator's sizing may need to be adjusted to ensure the rudder has its full range of motion needed for pilots.

7.9 Conclusions

From this report, the following conclusions are able to be made:

- x_h : 21.496 ft
- x_v : 18.425 ft
- Horizontal Stabilizer
 - Γ_h : 2.5°
 - i_h : -3.5°
 - $\Lambda_{c/4_h}$: 17.5°
 - λ_h : .34
 - AR: 4.8
- Vertical stabilizer
 - Γ_v : 90°
 - i_v : 0°
 - $\Lambda_{c/4_v}$: 41.5°
 - λ_v : .52
 - AR: 1.2
- Elevator
 - S_{Elevator} : 31.92 ft²
 - Chord at root: 1.722 ft
 - Chord at tip: 1.53 ft
- Rudder
 - S_{Rudder} : 15.92 ft²
 - Chord at root: 2.37 ft
 - Chord at tip: 2.28 ft

7.10 References

[1] Roskam, J. (1985). Airplane design. Ottawa, Kan.: Roskam Aviation and Engineering.

8.0 Landing Gear Design; Weight & Balance Analysis

8.1 Introduction

The purpose of this report is to design a landing gear configuration that will satisfy the weight and balance analysis of the plane. The landing gear configuration is important as if it were to fail during takeoff or landing, the possibilities of injuring the passenger or cargo will increase exponentially. If the landing gear is to fail during flight, either it will not retract or breaks from the plane's structure, it would cause a significant amount of drag during flight to cause the plane's performance to

8.2 Estimation of the Center of Gravity Location of Airplane

Conducting a weight and balance analysis with an estimated landing gear position and height, the following was able to be determined based on the method used, and detailed further, in section 4.1 below.

Table 1: Weight and estimated position to find center of gravity of plane.

Plane Component	Component Weight (lbs)	X-position (ft)	Y-position (ft)	Z-position (ft)
Fuselage	10125.265	18.425	0	7.87
Wing	2046.38	20.582	0	5.97
Empennage	1023.19	41.063	0	16.13
Engine	1525	37.51	0	9.35
Landing Gear	280.165	19.93	0	3.28
Fixed Equipment	1000	4.31	0	6.4
Trapped Oil and Fuel	148	37.51	0	9.35
Crew	400	6.64	0	7.87
Fuel	11049.65	17.6	0	5.97
Passengers	1600	19.95	0	7.87
Baggage	400	13.87	0	7.87

Using the following equations, the center of gravity in the x, y and z directions can be determined.

$$x_{cg_{W_E}} = \frac{\sum_{i=1}^{i=6} W_i x_i}{W_E} \quad W_E = \sum_{i=1}^{i=6} W_i$$

$$x_{cg_{W_{OE}}} = \frac{\sum_{i=1}^{i=8} W_i x_i}{W_{OE}} \quad W_{OE} = \sum_{i=1}^{i=8} W_i$$

$$x_{cg_{W_{TO}}} = \frac{\sum_{i=1}^{i=13} W_i x_i}{W_{TO}} \quad W_{TO} = \sum_{i=1}^{i=13} W_i$$

Figure 1: Equations used to find the center of gravity of different loading scenarios of the x-position.

Table 2: X, Y and Z position of center of gravity of different loading scenarios.

	X-position (ft)	Y-position (ft)	Z-position (ft)
CG _{WE}	21.11	0	6.48
CG _{WOE}	20.91	0	6.49
CG _{WTO}	22.37	0	5.66

8.3 Landing Gear Design

The landing gear of a plane is very important as it is vital for the takeoff and landing portions of flight. The plane will utilize a retractable landing gear system. The overall landing gear configuration will be a conventional tricycle landing gear.

8.3.1 Landing Strut Disposition

In order for the landing gear to be safe, it must pass the tip over criteria in both the longitudinal and lateral directions, as well as the ground clearance criteria. To pass the longitudinal tip over criteria, the following must be met:

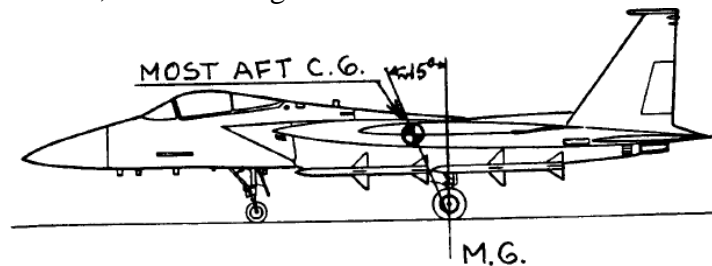


Figure 2: Longitudinal tip over criteria. [1]

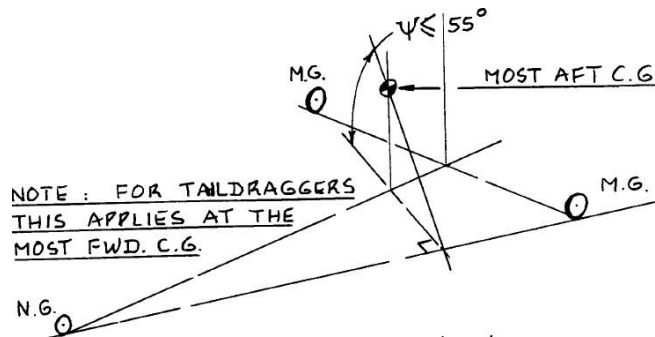


Figure 3: Lateral tip over criteria. [1]

The longitudinal tip over criteria of 15° is a typical value, but it is not a defined value that must always be met. To ensure that the longitudinal tip over criteria is met, the angle can be greater than 15° if it is able to be a point of productivity rather than negativity. Using the most aft center of gravity, the position of the main landing gear can be determined.

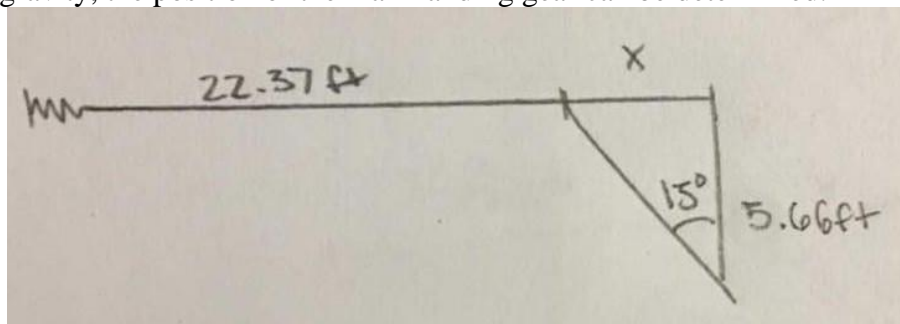


Figure 4: Main landing gear longitudinal disposition geometry.

$$22.37 + 5.66 \tan(15) = 23.87 \text{ ft}$$

Thus, the main landing gear position must be 23.87 ft or greater, in reference to the nose of the plane to satisfy the longitudinal tip over criteria.

In order to satisfy the lateral tip over criteria, the line perpendicular with the line between the nose and main landing gear that passes through the most aft center of gravity point must be less than 55°.

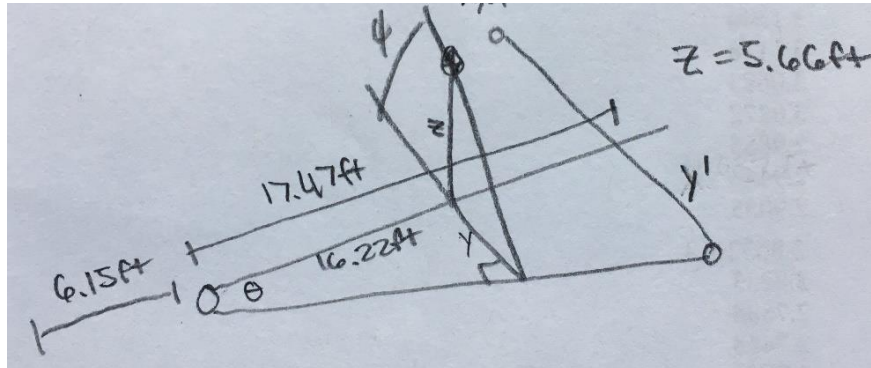


Figure 5: Main landing gear lateral disposition geometry.

$$\tan(\psi) = \frac{z}{y}$$

$$y = 5.66 / \tan(55) = 3.96 \text{ ft}$$

$$\tan(\theta) = \frac{y}{16.22}$$

$$\theta = \tan^{-1}\left(\frac{y}{16.22}\right) = 13.72^\circ$$

$$\tan(\theta) = \frac{y'}{17.47}$$

$$y' = 17.47 * \tan(13.72) = 4.265 \text{ ft} = 1.3 \text{ m}$$

Thus, the distance between the two main landing gears is 8.53 ft, 2.6 meters. To ensure an even safer main landing gear disposition, the distance between the two main landing gears should not recede past the distance found.

In order to satisfy the ground clearance criteria, the following criteria must be met to ensure the plane is of an effective height above the ground

:

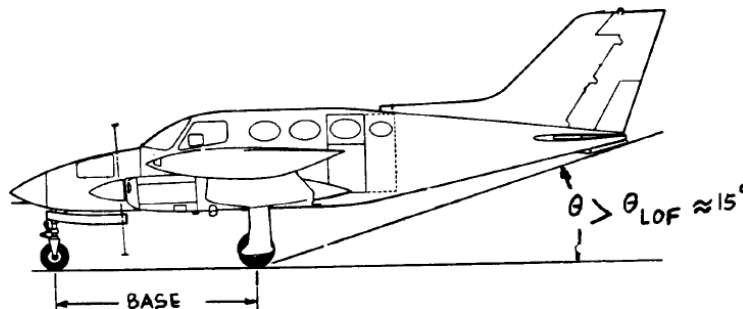


Figure 6: Longitudinal ground clearance criteria. [1]

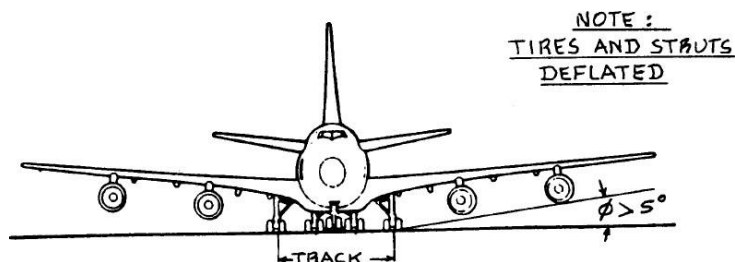


Figure 7: Lateral ground clearance criteria. [1]

To satisfy the longitudinal ground clearance criteria, the angle between the ground and rear of the fuselage should create a 15° angle or greater, with the origin being at the main landing gear.

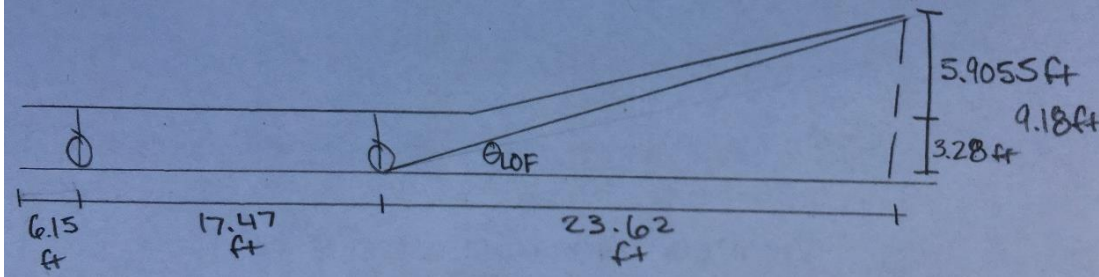


Figure 8: Longitudinal ground clearance geometry.

$$\tan(\theta) = \frac{y}{x}$$

$$\theta = \tan^{-1}\left(\frac{9.18}{23.62}\right) = 21.25^\circ$$

From this geometry and calculation, the proposed position of the main landing gear will help to satisfy the longitudinal ground clearance criteria.

To satisfy the lateral ground clearance criteria, the angle between the ground and the lowest point of the wing should be greater than 5°.

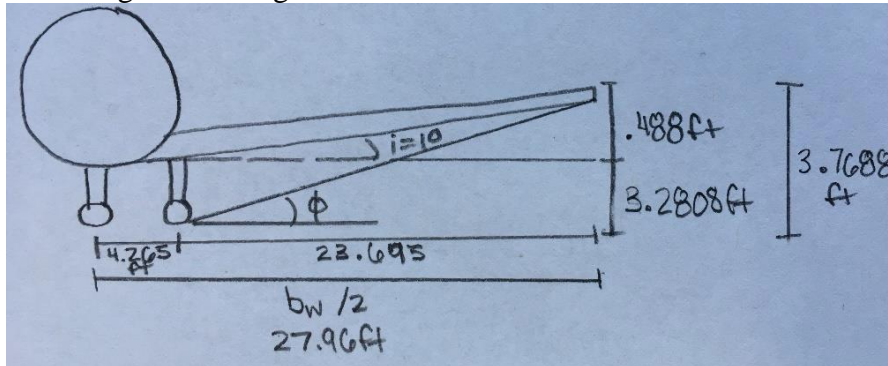


Figure 9: Lateral ground clearance geometry.

$$\tan(\phi) = \frac{y}{x}$$

$$\phi = \tan^{-1}\left(\frac{3.7688}{23.695}\right) = 9.037^\circ$$

The angle created of 9.037° satisfies and exceeds the minimum requirement needed of 5°. Thus, the placement of the landing gear gives sufficient lateral ground clearance.

8.3.2 Static Load per Strut

The load of the landing gear has limits as to how much each is able to support. Especially for a retractable landing gear, the pressure points must be taken seriously as if the load is too much, it may cause the landing gear to fail and buckle, which may cause serious injury to passengers or crew. The equations to find the maximum load able to be sustained by the nose gear and main gear are different, as well as varying under different load scenarios.

Nose Landing Gear Load Equation:

$$P_n = \frac{W_{TOL} l_m}{l_m + l_n}$$

$$P_n = \frac{29600 \cdot 2.51}{2.51 + 14.96} = 4249.78 \text{ lbs}$$

Table 3: Maximum load of nose gear under different loading scenarios.

Empty Weight	Operating Empty Weight	Takeoff Weight
4249.78 lbs	4593.99 lbs	2109.50 lbs

Main Landing Gear Load Equation:

$$P_m = \frac{W_{TO} l_n}{n_s(l_m + l_n)}, \text{ where } n_s = 2$$

$$P_m = \frac{29600 \cdot 14.96}{2 \cdot (2.51 + 14.96)} = 12675.11 \text{ lbs}$$

Table 4: Maximum load of main gear under different loading scenarios.

Empty Weight	Operating Empty Weight	Takeoff Weight
12675.11 lbs	12503.11 lbs	13745.25 lbs

8.3.3 Number of Tires

The number of tires to be used is determined based on similarly designed and sized planes. For business jets, the typical plane will consist of two wheels for the nose landing gear and two wheels for each main landing gear. Thus, the plane being designed will utilize a total of six wheels with each landing strut using two wheels.

3.4 Tire Size

To determine the appropriate tire size, the ratio between the nose landing gear load and takeoff weight and the main landing gear load and takeoff weight will be used to be compared to similar aircraft. The maximum takeoff weight will be used to analyze the tire size, as this is when the tires are under the most amount of pressure.

Nose Landing Gear:

$$\frac{P_n}{W_{TO}} = \frac{2109.54}{29600} = .072$$

Main Landing Gear:

$$\frac{n_s P_m}{W_{TO}} = \frac{2 \cdot 13745.25}{29600} = .9287$$

Comparing the ratios and takeoff weight in the tables presented by Roskam [1], The proposed tire size of the landing gears are as follows.

Table 5: Landing gear tire size.

Main Landing Gear		Nose Landing Gear	
Diameter (in.)	Thickness (in.)	Diameter (in.)	Thickness (in.)
26	6.6	14.5	5.5

8.3.5 Gear Retraction and Drawings

To allow for retractability of the landing gear, the placement and mechanism of the landing gear is important for storage during cruise.

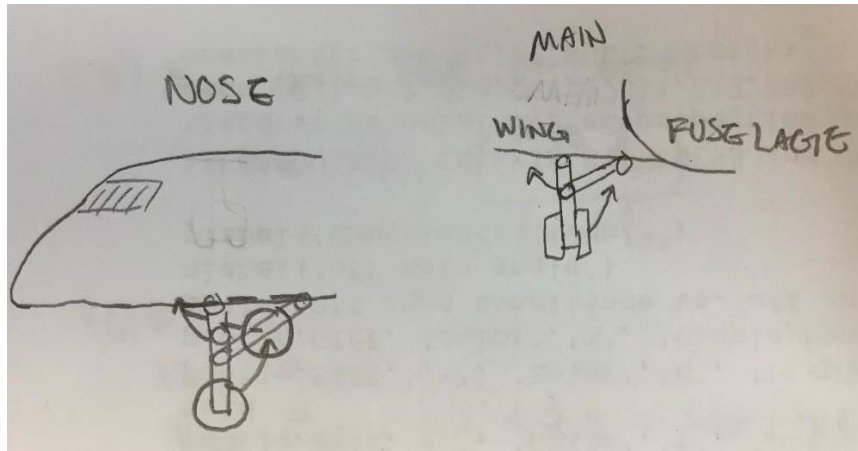


Figure 10: Landing gear retraction configuration.

8.4 Weight and Balance

The weight and balance of the plane is broken down and analyzed as separate entities that are used to build a plane. The plane was broken down into the following components:

1. Fuselage
2. Wing
3. Empennage
4. Engine
5. Landing Gear
6. Fixed Equipment
7. Trapped Oil and Fuel
8. Crew
9. Fuel
10. Passengers
11. Baggage
12. Cargo
13. Military Load

The plane being designed, a business jet, does not contain all of the components. Cargo and military load are options that may be used on jet transports or fighter jets, however, are not typically associated with business jets. The following three view center of gravity drawings can be made to determine the general position of these 13 subgroups. The placement of the subgroup numbers is an approximate position of each subgroup's center of gravity.

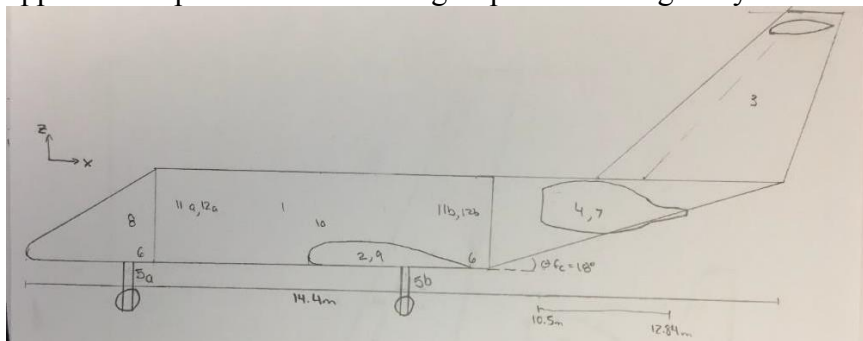


Figure 11: Longitudinal view of x-z plane.

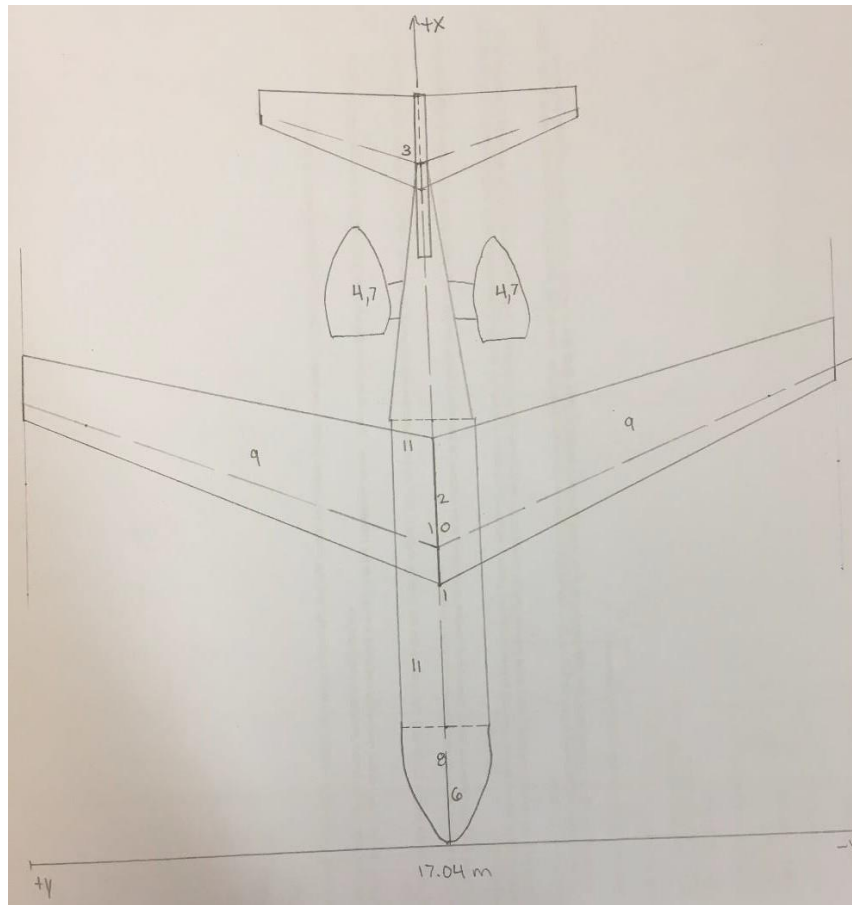


Figure 12: Top view of x y plane.

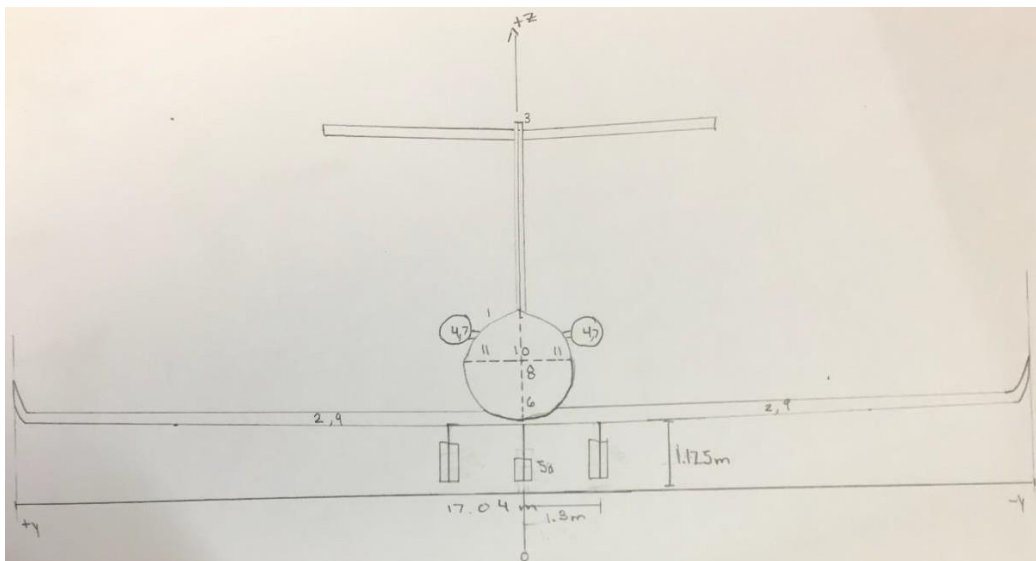


Figure 13: Front view of y z plane.

From these components, one through eleven, they can be arranged on the 3-view drawing to provide a general position of where each component is on the plane.

Table 6: Weight and estimated position to find center of gravity of plane.

Plane Component	Component Weight (lbs)	X-position (ft)	Y-position (ft)	Z-position (ft)
Fuselage	10125.265	18.425	0	6.23
Wing	2046.38	20.582	0	4.33
Empennage	1023.19	41.063	0	14.49
Engine	1525	37.51	0	7.71
Landing Gear	280.165	19.93	0	1.64
Fixed Equipment	1000	4.31	0	4.76
Trapped Oil and Fuel	148	37.51	0	7.71
Crew	400	6.64	0	6.23
Fuel	11049.65	25.23	0	4.33
Passengers	1600	19.95	0	6.23
Baggage	400	13.87	0	6.23

From these weight and position definitions of the plane's components, the following is center of gravity positions can be determined.

Table 7: Center of gravity position under basic loading scenarios.

	X-position (ft)	Y-position (ft)	Z-position (ft)
CG _{WE}	21.11	0	6.48
CG _{WOE}	20.91	0	6.49
CG _{WTO}	22.37	0	5.66

Thus, the landing gear design satisfies the tip over and ground clearance criteria.

8.4.1 CG Location for Various Loading Scenarios

From this table, the plane's center of gravity positions is able to be determined for the basic loading scenarios. The center of gravity excursion diagram, or the potato graph, is used to determine the most aft center of gravity point to determine if the main landing gear is in position in which it is still able to pass the tip over and ground clearance criteria.

The most aft center of gravity will change the center of gravity in the longitudinal x direction. To determine this point, the plane will be loaded from the aft forward, as the passenger and baggage will be loaded from the aft forward, without any crew being placed in the cockpit.

It is also important to determine where the most forward center of gravity point is as well. This point will help to determine that the nose landing gear is in a sufficient position as well. This will also help to determine that range that the center of gravity is able to move with the position of the plane's components.

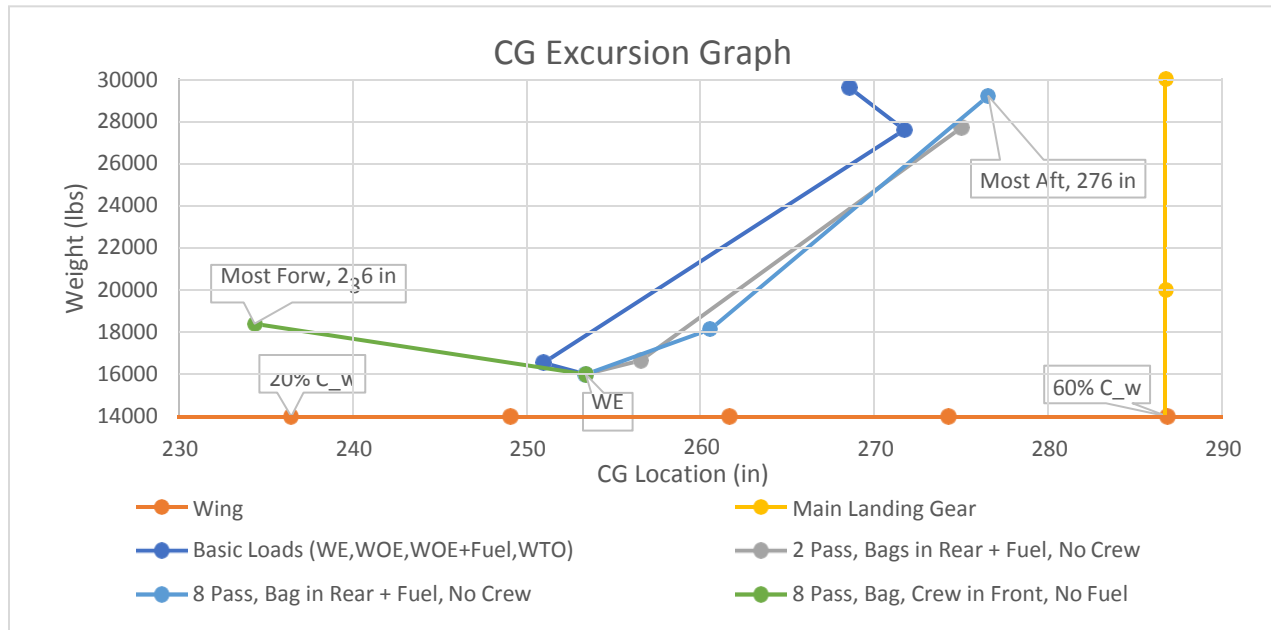


Figure 14: Center of gravity excursion graph.

8.5 Discussion

The tip over and ground clearance criteria are used to determine the positioning and size of the landing struts. Both the tip over and ground clearance criteria have a longitudinal and lateral component they must individually satisfy. Before beginning the design of the landing gear, a weight and balance analysis was conducted for an estimated landing gear position and size.

To design the position of the nose and main landing gear, the tip over criteria was used. The longitudinal tip over criteria calls for the main gear to be placed at an angle of 15° or greater in reference to the plane's most aft center of gravity position. This was satisfied with main landing gear being placed 1.52 ft aft of the center of gravity.

The lateral tip over criteria determines how far outward the main landing gear is to be placed, creating a 55° or less angle of the center of gravity in reference to the ground. This was satisfied with the main landing gears being placed 4.3 ft from the longitudinal axis of the plane.

The ground clearance was next to be determined. The longitudinal ground clearance requires the angle between the ground and the end of the fuselage to be greater than or equal to 15° in reference to the main landing gear. The main landing gear placed 23.35 ft from the nose of plane creates a 21.5° angle, thus satisfying the longitudinal ground clearance criteria.

The lateral ground clearance criteria requires the plane to create an angle of 5° or greater from the ground to the lowest plane component in the lateral direction in reference to the outboard main landing gear. With the engines being placed on the rear of the fuselage, the issue was not as great as with other low wing configurations. The angle created between the ground and tip of the wing was 8.8° in reference to the main landing gear, thus satisfying the lateral ground clearance criteria.

By satisfying the tip over and ground clearance criteria, the final weight and balance analysis was able to be conducted to determine how the plane's center of gravity will move as it is loaded or during flight.

As seen in the center of gravity excursion graph, the plane's most forward position was anticipated as the two crew in the cockpit, the passenger in the front hall with their baggage in closet A. The calculation was conducted without any trapped fuel or oil in the engines or fuel stored in the wing. These two components were excluded as it would have placed the center of gravity more aft. The most forward center of gravity was found as 236 inches. The most aft center of gravity will begin with the plane's manufacturer's empty weight, trapped fuel and oil in the engines and fuel in the wing, as well as with all 8 passengers congregated in the rear of the plane and their baggage all being stored in closet C. The most aft center of gravity position is at 276 inches in reference to the nose of the plane. This is still ahead of the main landing gear, which will ensure the plane will not tip over due to it being too tail heavy behind the main gear. Finding both the most forward and aft center of gravity allows for the crew to have a general idea of where the plane's center of gravity will be placed.

The overall design with landing gear retracted is as follows.

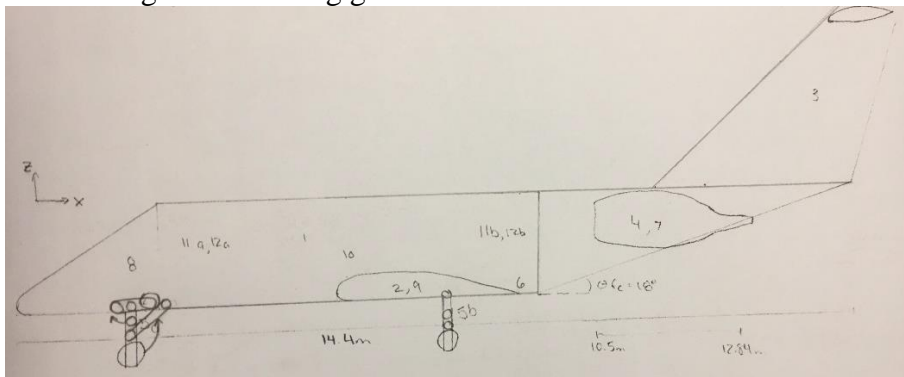


Figure 15: Longitudinal view of x-z plane with retracted landing gear.

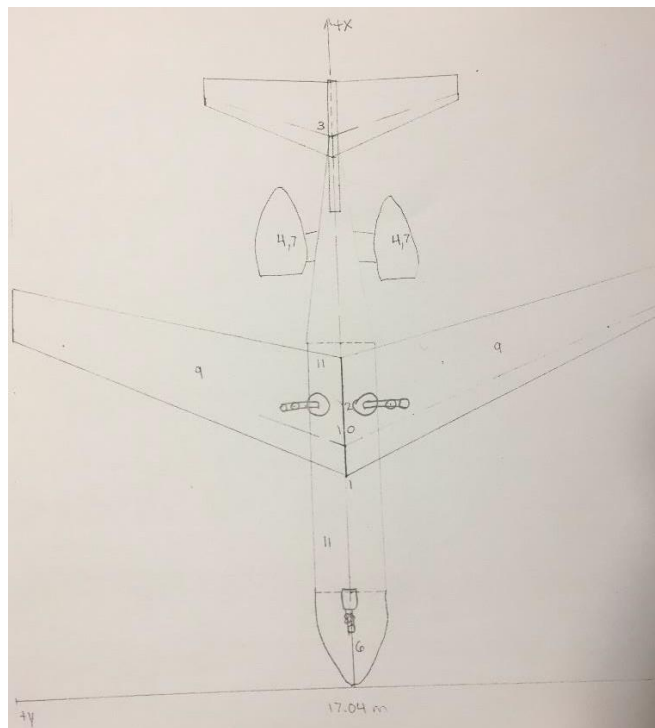


Figure 16: Top view of x y plane with retracted landing gear.

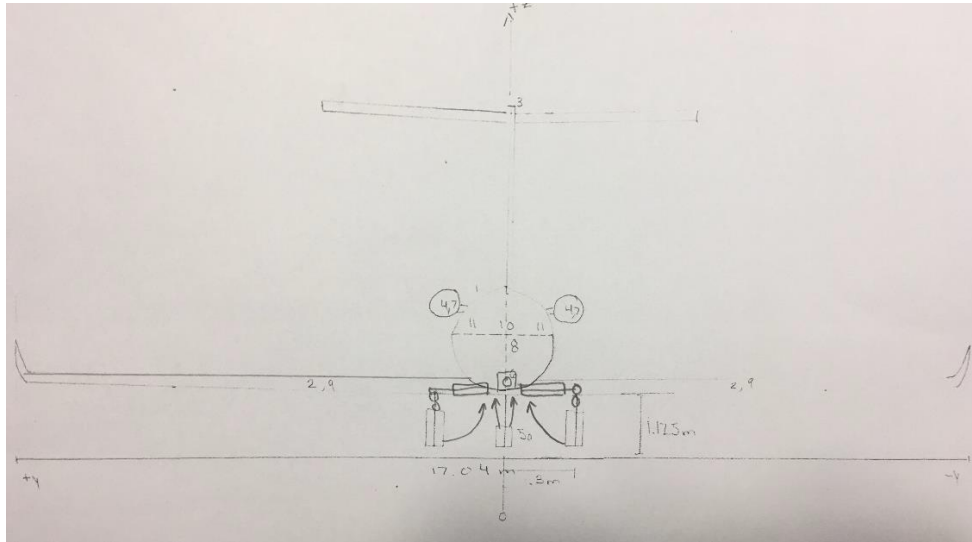


Figure 17: Front view of y z plane with retracted landing gear.

8.6 Conclusion

From this report, the plane's final landing gear size and position can be finalized based on the weight and balance analysis conducted. The positions of the landing gear are dependent on the tip over criteria and ground clearance criteria. The following geometrical statistics were determined for the landing gear:

- Height: 3.28 ft
- Width between main landing gear: 8.66 ft
- Distance between nose and main landing gear: 17.74 ft
- Load held by nose landing gear: 2532 lbs
- Load held by main landing gear: 13533 lbs
- Number of total tires: 6
- Tire size:
 - Nose:
 - Diameter: 26 in
 - Thickness: 6.6 in
 - Main:
 - Diameter: 14.5 in
 - Thickness 5.5 in

8.7 References

[1] Roskam, J. (1985). Airplane design. Ottawa, Kan.: Roskam Aviation and Engineering.

9.0 Stability and Control Analysis

9.1 Introduction

The purpose of this report is to determine if the plane being designed can be deemed a safe aircraft to satisfy its intended mission requirements. This will be done by determining the plane's longitudinal and directional stability. If the stability measures are not met, the possibility of the empennage, landing gear and weight and balance analysis will be reconfigured to satisfy the stability of the aircraft.

9.2 Static Longitudinal Stability

To determine if the plane is statically stable with the calculations in prior reports on the sizing of the plane, an X-plot will be generated to find the static margin between the plane's aft most center of gravity and aerodynamic center. To generate a stable aircraft in the longitudinal direction, the static margin that is of an acceptable standard is 10%. This standard is a widely recognized value for passenger aircraft.

To begin the center of gravity calculation was changed to a function of the horizontal tail size. This was conducted by using the overall weight determined for the empennage section as divided evenly among the horizontal and vertical tails as their sizing was nearly identical. This resulted in a formula which for every square foot of area added, the plane's empennage weight will increase by 5.11595 lbs. The center of gravity used is the aft most, determined in the previous report, when there is no crew aboard, no fuel in the wing, and the passengers and luggage are placed in the rear in the cabin.

The next step was to find a calculation that would find the plane's aerodynamic center. To determine the plane's aerodynamic center, the following equation was used:

$$x_{acA} = \frac{\{x_{acwb} + [C_{L\alpha_h} \left(\frac{1-d\epsilon}{d\alpha}\right) \left(\frac{S_h}{S}\right) x_{ach}]\}}{\{1 + [C_{L\alpha_h} \left(\frac{1-d\epsilon}{d\alpha}\right) \left(\frac{S_h}{S}\right)]\}} \quad (1)$$

To determine the aerodynamic center of the wing and body, the wing is at its 1/4 chord length and Munk's method was used to determine the aerodynamic center of the fuselage. The process calls for the plane to be divided into 13 sections, five sections ahead of the wing, six sections aft of the wing and two sections that comprise the wing.

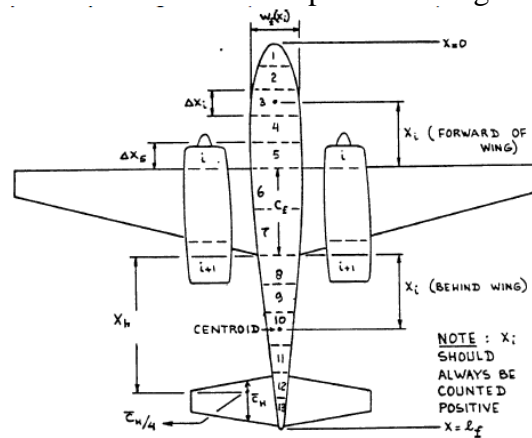


Figure 1: Monk's method.

Monk's method will give the change in the aerodynamic center. The dynamic pressure is calculated at sea level and cruise speed. The mean geometric chord length of the wing is 7.455 ft.

The coefficient of lift of the wing was 0.1, based on the coefficient of lift to alpha slope of the chosen airfoil shape [1].

$$\Delta x_{acf} = -\frac{\frac{dM}{d\alpha}}{\bar{\phi} \bar{c} C_{l_{\alpha w}}} \quad (2)$$

When using Monk's method, the sections ahead of the wing and behind the wing are used differently to calculate $d\bar{\epsilon}/d\alpha$.

$$\frac{dM}{d\alpha} = \frac{\bar{q}}{36.5} \cdot \frac{C_{l_{\alpha w}}}{0.08} \sum_{i=1}^{13} w_i^2 \left(\frac{d\bar{\epsilon}}{d\alpha} \right)_i \Delta x_i \quad (3)$$

Ahead of the wing, sections 1 thru 5, the figure is used to determine $d\bar{\epsilon}/d\alpha$. Curve 1 applies to sections 1 thru 4, while curve two applies to section 5.

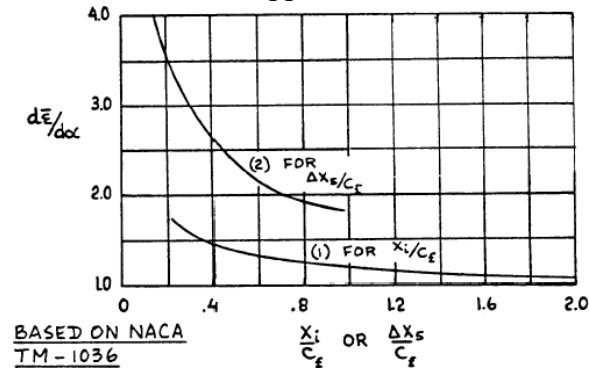


Figure 2: Downwash ahead of wing.

Behind the wing, the following equation is used to calculate $d\bar{\epsilon}/d\alpha$. Within the equation, $1 - \frac{d\bar{\epsilon}}{d\alpha}$ is an estimated value, between 0.6 and 0.7, thus the average was used, 0.65.

$$\left(\frac{d\bar{\epsilon}}{d\alpha} \right)_i = \frac{x_i}{x_h} \left(1 - \frac{d\bar{\epsilon}}{d\alpha} \right) \quad (4)$$

Upon finding the values needed, the aerodynamic center of the wing and body was able to be calculated to determine the aerodynamic center of the aircraft. The aerodynamic center of the aircraft equations was used as a function of the horizontal stabilizer's area.

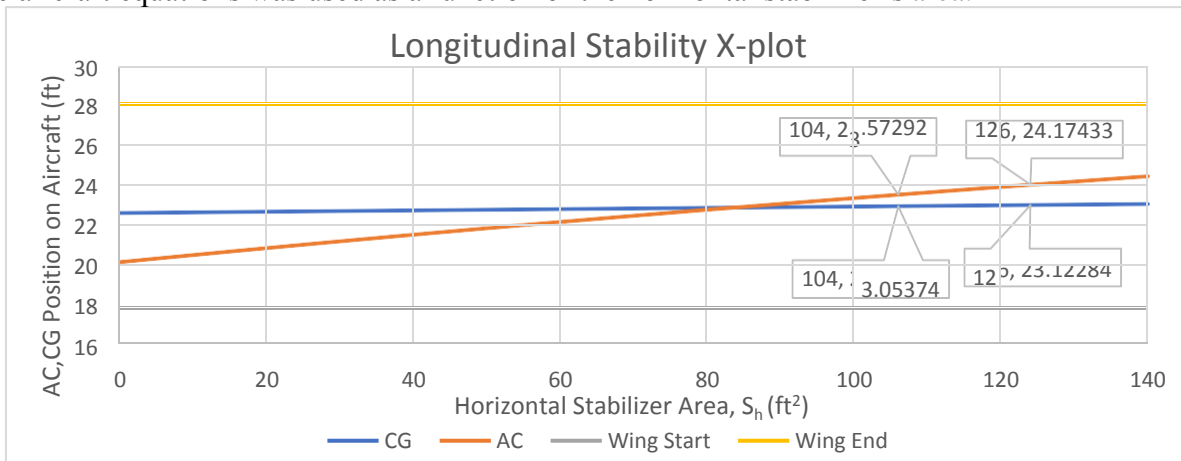


Figure 3: Longitudinal stability X-plot.

To create a longitudinally stable aircraft, the static margin should be 10% in reference to the distance between the aircraft's center of gravity and aerodynamic center to the chord of the wing. This point occurs when the aircraft's horizontal stabilizer amounts to 126 ft². Compared to the area found in report 7, of 99.76 ft². These two areas are within a reasonable distance from one another that this is an acceptable calculation. At a size of 99.76 ft² for the horizontal stabilizer, the plane will be able to maneuver, but will have difficulty maintaining an even flight if disturbed by a sudden gust. With a larger horizontal stabilizer, such as 126 ft², the plane will be safer.

The aircraft will be inherently stable, meaning the plane will have a natural tendency to return to a stable state in flight without needing a feedback system. Roskam states that for business jets, a static margin of 5% is acceptable. With a 5% static margin, the horizontal stabilizer area amounts to 104 ft². This value is closer to the previously found area of 99.7 ft².

9.3 Static Directional Stability

The plane's static directional stability is found by the following equation. Within the equation, the lift curve slope of the vertical stabilizer was found as .1 [1]. The size of wing is 416.9 ft². The distance between the plane's aft most center of gravity and aerodynamic center of the vertical stabilizer was measured as 17.8089 ft. The wing span was the value determined from a previous report, as 55.92 ft.

$$C_{n\beta} = C_{n\beta_{wb}} + C_{l\alpha_v} \left(\frac{S_v}{S} \right) \left(\frac{x_v}{b} \right) \quad (5)$$

To determine the yawing moment of the wing and body individually, the following equation was used [2].

$$C_{n\beta, wing+fuselage} = -K_1 K_2 \frac{S_f l_f}{S_w b} (\text{per degree}) \quad (6)$$

K_1 an empirical wing-body interference factor that is a function of the fuselage geometry

K_2 an empirical correlation factor that is a function of fuselage Reynolds number

S_f projected side area of the fuselage

l_f length of the fuselage

Once finding the value, -0.068, the following static directional stability plot was able to be generated as a function of the vertical stabilizer's wing area. The plane will be inherently stable, thus the directional stability must be 0.0010 per degree.

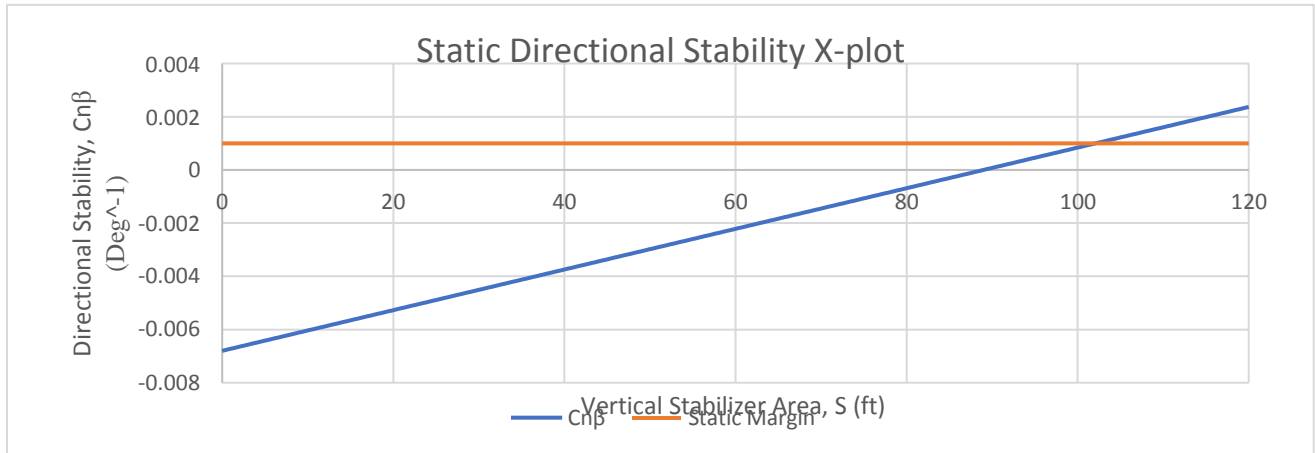


Figure 4: Static directional stability X-plot.

From the static directional stability x-plot, the results yielded a vertical stabilizer wing area of 102 ft². As compared to the previous method of determining a vertical stabilizer wing area of 93.63 ft². This difference is within reason that the results yielded by this process is of a reasonable value to be used.

With one engine out, the minimum control speed must be addressed. The first step is to determine the critical one-engine out yawing moment. To determine the yawing moment, the following equation was used.

$$N_{t_{crit}} = T_{TOe} * y_t \quad (7)$$

The thrust value is the max thrust needed to satisfy the plane's desired mission requirements, which amounted to 11,840 lbf combined, 5,920 lbs per engine. The moment arm of 1.5 m, 4.92 ft, from the engine's center line to the center of the engines.

$$N_{t_{crit}} = 5920 * 4.92$$

$$N_{t_{crit}} = 29,126.4 \text{ ft} * \text{lbs}$$

The next step is to determine the drag induced yawing moment due to an inoperative engine for a jet. For a jet driven plane with a wind milling engine with a high bypass ratio, the following equation was used.

$$N_D = 0.25 * N_{t_{crit}} \quad (8)$$

$$N_D = 0.25(29,126.4)$$

$$N_D = 7,281.6 \text{ ft} * \text{lbs}$$

The minimum control velocity is the next to be determined, using the following equation. The stall velocity, 99 knots, is the value found in a previous report.

$$V_{mc} = 1.2 * V_s \quad (9)$$

$$V_{mc} = 1.2 * 99$$

$$V_{mc} = 118.8 \text{ knots}$$

9.4 Empennage Design – Weight & Balance – Landing Gear Design – Longitudinal Static Stability & Control Check

By changing the size of the vertical and horizontal stabilizers, the plane's weight and balance will be affected. The affect may not be of a significant amount, however, is worth

exploring as the stability and safety measures are of importance. The topics that will be addressed are the tip over criteria being satisfied, the movement of the center of gravity, the amount of stability and a possible minimum control speed.

Table 1: Changes to critical safety measurements with new empennage design.

Measurement	Original	Recalculated	Difference
Most Aft Center of Gravity	23.04 ft	23.08 ft	.04 ft
Longitudinal Tip Over (Main LNDG position X-Axis)	23.89 ft	23.94 ft	.05 ft
Lateral Tip Over (Main LNDG Distance from Y-Axis)	4.34 ft	4.35 ft	.01 ft
Longitudinal Ground Clearance	21.47°	21.51°	.04°
Lateral Ground Clearance	8.88°	8.89°	.01°

With the change of the empennage configuration, the plane's center of gravity and landing gear position are affected. With the new empennage configuration, the most aft center of gravity will move aft by .04 ft. To satisfy the longitudinal tip over criteria of a minimum of 15° angle between the aft center of gravity, the main landing gear position must be moved back .05 ft. To satisfy the lateral tip over criteria, a minimum angle of 55° created between the center of gravity and imaginary line created between the nose and main landing gear. The main landing gear must be placed a distance of 4.25 ft from the y-axis to meet the criteria. The longitudinal ground clearance calls for an angle to be greater than 15°. The new landing gear position creates a longitudinal ground clearance of 21.51°. The lateral ground clearance criteria call for an angle to be greater than 5°. The new landing gear position creates an increased angle of 8.89°.

9.5 Discussion

The static longitudinal stability of the plane requires that for a business jet to be labeled as stable is to generate a 5% static margin between the plane's most aft center of gravity and aerodynamic center. A 5% static margin calls for a horizontal stabilizer area of 104 ft². The x-plot also displays that if the plane was to be categorized below a business jet, a 10% static margin would be needed for a stable aircraft. The horizontal stabilizer area would then be 126 ft².

The static directional stability of the plane is used to determine the sizing of the vertical stabilizer. The plane requires a yawing moment of .001 for the plane to be deemed statically stable. At this point, the x-plot calls for a vertical stabilizer area of 102 ft². The minimum controllable speed for the aircraft is calculated as 118.8 knots.

The x-plots call for a slight redesign of the empennage and landing gear by the reanalysis of the plane's weight and balance analysis. Upon the new design of the empennage, the size will affect the weight, which will move the plane's center of gravity aft as the new empennage is larger and heavier. The tip over criteria and ground clearance were both considered in the longitudinal and lateral direction. To satisfy the tip over criteria, the main landing gear was moved aft and spread further apart. The height of the landing gear was not of an issue as the ground clearance was able to be satisfied.

9.6 Conclusion

From this report, the conclusion is able to be made that the horizontal and vertical stabilizer will be redesigned to allow for the plane to be statically stable in the longitudinal and directional directions. The new calculations are as follows:

- S_h: 104 ft²
- S_v: 102 ft²

- Max Takeoff Weight: 29,664 lbs
- Most Aft CG: 23.08 ft
- Main Landing Gear Position: 23.94 ft
- Main Landing Gear Distance from Y-Axis: 4.35 ft

9.7 References

- [1] Airfoiltools.com. (2017). NACA 64-008A AIRFOIL (n64008a-il). [online] Available at: <http://airfoiltools.com/airfoil/details?airfoil=n64008a-il> [Accessed 12 Dec. 2017].
- [2] Anon, (2017). [online] Available at: [\[http://nptel.ac.in/courses/101104007/Module5/Lec23.pdf\]](http://nptel.ac.in/courses/101104007/Module5/Lec23.pdf) [Accessed 12 Dec. 2017].

10.0 Drag Polar Estimation

10.1 Introduction

The purpose of this report is to generate the plane's drag polar to allow for a visible confirmation of how the plane is expected to react, in regards to lift and drag. The airplane's zero lift drag will be used to create a relation between lift and drag with the use of drag polar equations and graph. Airplane zero lift drag will also be used to determine the relation between drag and lift during low speed flight. Compressibility drag and area ruling will also be used to determine if there are issues in which the airspeed or plane's geometry will negatively impact the plane's drag.

10.2 Airplane Zero Lift Drag

In this section, the goal is to determine the plane's zero lift drag value. In determining the zero lift drag, the steps that must be taken first are to determine the plane's S_{wet} and its equivalent parasite drag, f .

The first step of finding the S_{wet} area of the plane will be to divide the plane into sections to determine each section's wetted area. The plane was divided into the fuselage, wing, nacelle and the empennage.

Fuselage with cylindrical mid-section:

$$S_{wet.fus} = \pi D_f l_f \left(1 - \frac{2}{\lambda_f}\right)^{2/3} \left(1 + \frac{1}{\lambda_f^2}\right), \quad \text{where } \lambda_f = \frac{l_f}{D_f}$$

$$S_{wet fus} = \pi(1.83)(14.4) \left(1 - \frac{2}{1.83}\right)^{2/3} \left(1 + \frac{1}{(1.83)^2}\right)$$

$$S_{wet fus} = 69.19 \text{ m}^2 = 744.71 \text{ ft}^2$$

Wing:

$$S_{wet.plf} = 2S_{exp.plf} \left[1 + \frac{0.25 \left(\frac{t}{c}\right)_r (1 + \tau\lambda)}{1 + \lambda}\right]$$

$$\tau = \frac{(t/c)_r}{(t/c)_t} \quad \lambda = \frac{c_t}{c_r}$$

$$S_{wet plf} = 2 * 16.56 * \left[1 + \frac{.25(.16)(1 + \left(\frac{.16}{.13}\right)\left(\frac{4.4}{10.5}\right))}{1 + \left(\frac{4.4}{10.5}\right)}\right]$$

$$S_{wet plf} = 67.92 \text{ m}^2 = 731.12 \text{ ft}^2$$

Nacelle:

Fan Cowling:

$$S_{wet.fan.cowl} = l_n D_n \left(2 + 0.35 \frac{l_1}{l_n} + 0.81 \frac{l_1 D_{hl}}{l_n D_n} + 1.15 \left(1 - \frac{l_1}{l_n}\right) \frac{D_{ef}}{D_n}\right)$$

$$S_{wet fan cowl} = 1.2 \cdot 1.03 \left[2 + .35 \left(\frac{.514}{1.2}\right) + .81 \left(\frac{.514}{1.2}\right) \left(\frac{.69}{1.03}\right) + 1.15 \left(1 - \frac{.514}{1.2}\right) \left(\frac{.82}{1.03}\right)\right]$$

$$S_{wet fan cowl} = 3.59 \text{ m}^2 = 38.62 \text{ ft}^2$$

Gas Generator:

$$S_{wet, gas, gen} = \pi l_g D_g \left\{ 1 - \frac{1}{3} \left(1 - \frac{D_{eg}}{D_g} \right) \left[1 - 0.18 \left(\frac{D_g}{l_g} \right)^{5/3} \right] \right\}$$

$$S_{wet, gas, generator} = \pi (.69)(.58) \left\{ 1 - \frac{1}{3} \left(1 - \frac{.45}{.58} \right) \left[1 - .18 \left(\frac{.69}{.58} \right)^{5/3} \right] \right\}$$

$$S_{wet, gas, generator} = 1.16 \text{ m}^2 = 12.46 \text{ ft}^2$$

Plug:

$$S_{wet, plug} = 0.7 \pi l_p D_p$$

$$S_{wet, plug} = \pi (.7)(.51)(.27)$$

$$S_{wet, plug} = .31 \text{ m}^2 = 3.34 \text{ ft}^2$$

Empennage:

$$\text{Horizontal} = 104 \text{ ft}^2$$

$$\text{Vertical} = 102 \text{ ft}^2$$

With each component's wetted area found, the plane's total wetted area can be calculated. The total wetted area will be a summation of all the wetted areas.

$$S_{wet} = S_{wet, fus} + S_{wet, plf} + S_{wet, fan, cowl} + S_{wet, gas, gen} + S_{wet, plug} + S_{wet, emp}$$

$$S_{wet} = 69.19 + 67.92 + 3.59 + 1.16 + .31 + \frac{104+102}{.3048^2}$$

$$S_{wet} = 204.95 \text{ m}^2 = 2,206.10 \text{ ft}^2$$

With the total S_{wet} found, the equivalent parasite drag can now be found by referencing Roskam [1]. Roskam's figure displays results over a range of different skin friction coefficients, c_f , of an airplane. Based on the business jet's regression line coefficients, the skin friction line which will be used is .004. This yields an equivalent parasite area of approximately 8.8 ft².

Now that the wetted area of the plane and equivalent parasite drag have been found, the clean zero lift drag coefficient can now be calculated.

$$C_{D_0} = \frac{f}{S_{wing}}$$

$$C_{D_0} = \frac{8.8}{416.9} = .0211$$

10.3 Low Speed Drag Increments

The overall drag equation will be used to determine how takeoff flaps, landing flaps and the landing gear will affect the drag of the aircraft. All the drag equations will be based off the clean aircraft's drag equation.

$$C_D = C_{D_0} + \frac{L^2}{\pi * A R * e}$$

$$C_D = .0211 + \frac{C_L^2}{\pi * 7.5 * .825}$$

$$C_D = .0211 + .0514 C_L^2$$

10.3.1 High-lift device drag increments for takeoff and landing

During takeoff and landing, the plane will utilize flaps as part of its high lift device system. The takeoff flaps will add to the planes clean drag by a range of 0.01 to 0.02. The landing flaps will all to the planes clean drag by a range of 0.055 to 0.075. Without sufficient data to warrant the maximum or minimum of the range, the average was used.

Takeoff Flaps:

$$C_D = (.0211 + .015) + \frac{C_L^2}{\pi * 7.5 * .775}$$

$$C_D = .0361 + .0548 C_L^2$$

Landing Flaps:

$$C_D = (.0211 + .065) + \frac{C_L^2}{\pi * 7.5 * .725}$$

$$C_D = .0861 + .0585 C_L^2$$

3.2 Landing gear drag

The landing gear will also affect the amount of drag that is generated during takeoff and landing. The landing gear is used under both scenarios, takeoff and landing. The landing gear will be analyzed with takeoff and landing flaps extended.

Takeoff Flaps and Landing Gear:

$$C_D = (.0361 + .02) + \frac{C_L^2}{\pi * 7.5 * .775}$$

$$C_D = .0561 + .0548 C_L^2$$

Landing Flaps and Landing Gear:

$$C_D = (.0861 + .02) + \frac{C_L^2}{\pi * 7.5 * .725}$$

$$C_D = .1061 + .0585 C_L^2$$

10.4 Compressibility Drag

The compressibility drag of the plane can be determined by referring to the figure provided by Roskam which relates a plane's Mach number to zero lift drag rise [1]. Figure 12.6 of Part II of Roskam shows the typical compressibility drag behavior of multiple planes. The limited number of planes forces the hand of choosing a plane that is best suited to perform similarly with the plane being designed. The business jet follows the C-5A as a jet, rather than a propeller aircraft or passenger jet transport. At a cruise speed of Mach .69, it related to 4 counts of zero lift drag rise, .0004.

10.5 Area Ruling

The purpose of area ruling is to determine if there are areas of the plane which may disturb the desired elliptical lift distribution. The overall outline of the plane is as follows.

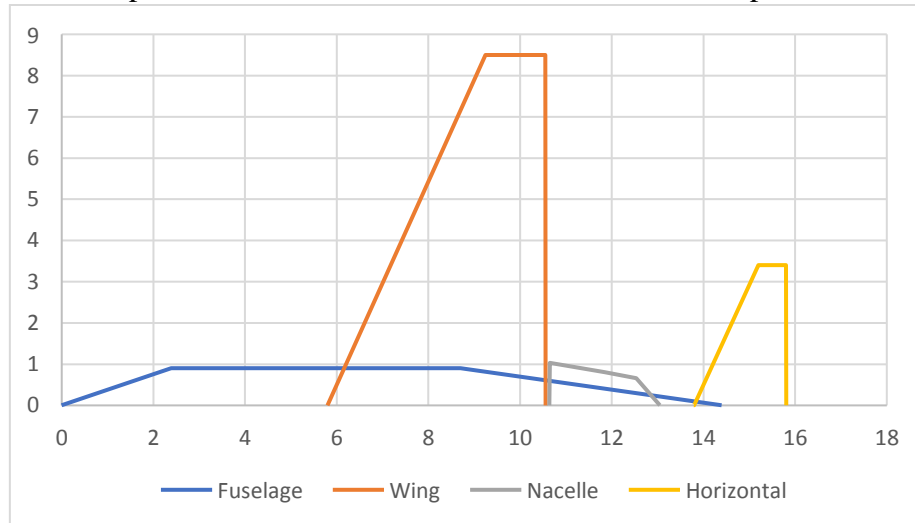


Figure 1: General outline of aircraft.

To simplify the process, the fuselage and wing will be analyzed, with the nacelle and horizontal being deemed negligent. From this, the following area ruling is determined for the fully cylindrical fuselage.

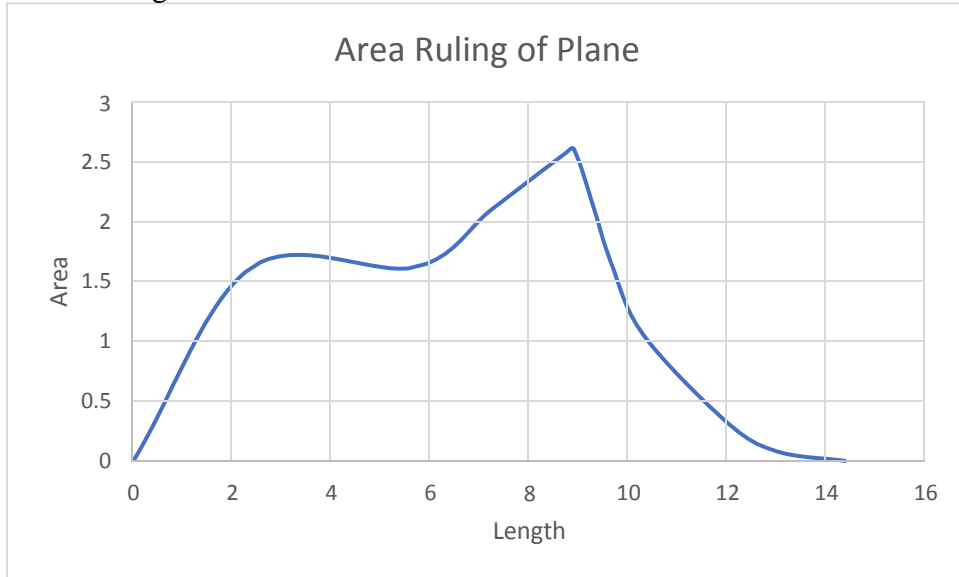


Figure 2: Area ruling of aircraft.

10.6 Airplane Drag Polars

For business jets, there are a range of possible coefficient of lift values typically reached. For clean aircraft, the coefficient of lift values range between 1.4 and 1.8, where the plane requires a value of 2.0. For a business jet during takeoff, the coefficient of lift values range between 1.6 and 2.2, where the plane requires a value of 1.8. During landing, the coefficient of lift value ranges between 1.6 and 2.6, where the plane requires a value of 2.0.

Table 1: Drag polar scenarios and equations.

Scenario	Equation
Clean	$C_D = .0211 + .0514C_L^2$
Takeoff Flaps	$C_D = .0361 + .0548C_L^2$
Landing Flaps	$C_D = .0861 + .0585C_L^2$
Takeoff Flaps, Landing Gear	$C_D = .0561 + .0548C_L^2$
Landing Flaps, Landing Gear	$C_D = .1061 + .0585C_L^2$

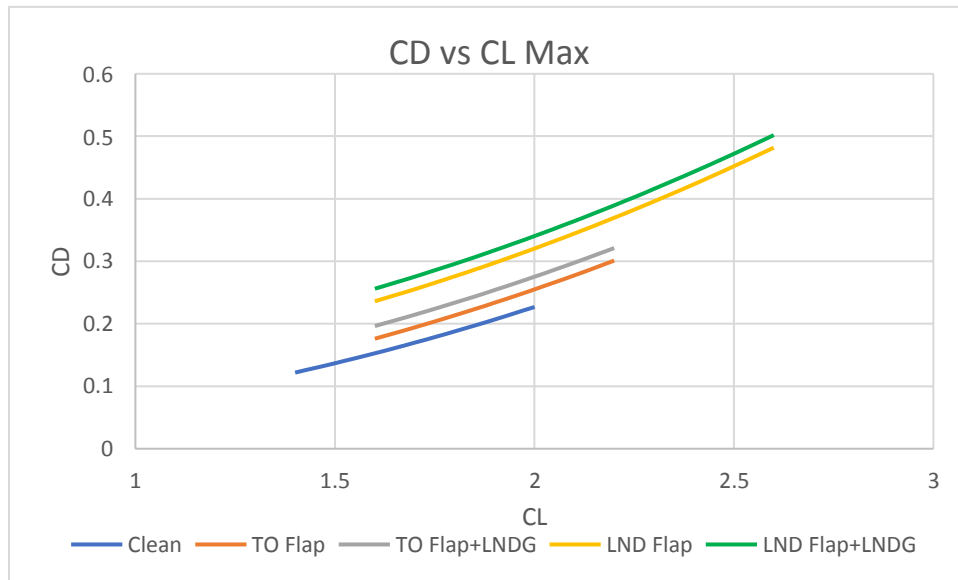


Figure 3: Drag polar for aircraft during takeoff, cruise and landing.

10.7 Discussion

The zero lift drag coefficient found in this report is a more accurate finding than that found in Report 4, Performance Constraints. This is due to the fact that the wetted area found through the process of several equations solely for finding wetted area proves to be more effective. This conclusion can be made because the difference between the previously found zero lift drag coefficient was .0227 to .0211 is rather miniscule. Thus, a new and more accurate drag polar can be found as to how the plane will perform during the critical parts of flight, takeoff and landing.

The area ruling process was used to determine possible issues at which the plane's desired elliptical lift distribution may jump or fall suddenly. Based on the results, the point at which the wing reaches its greatest distance from the fuselage, the elliptical lift distribution takes a sudden jump. To fix this issue, the best possible option would be to suck in the fuselage at that point to help smoothen out the lift distribution.

10.8 Conclusion

From this report, the conclusion can be made that following is acceptable:

- $S_{wet} = 204.95 \text{ m}^2 = 2,206.10 \text{ ft}^2$
- $C_{D0} = \frac{8.8}{416.9} = .0211$
- Clean: $C_D = .0211 + .0514C_L^2$
- Takeoff Flaps: $C_D = .0361 + .0548C_L^2$
- Landing Flaps: $C_D = .0861 + .0585C_L^2$
- Takeoff Flaps and Landing Gear: $C_D = .0561 + .0548C_L^2$
- Landing Flaps and Landing Gear: $C_D = .1061 + .0585C_L^2$

10.9 References

[1] Roskam, J. (1985). *Airplane design*. Ottawa, Kan.: Roskam Aviation and Engineering.

Chapter 3

Landing Gear

LIST OF SYMBOLS

a_x/g – braking constant
 A_g – Landing gear weight constant A
 B_g – Landing gear weight constant B
 C_g – Landing gear weight constant C
 D_g – Landing gear weight constant D
 D_o – Outside diameter
ESWL - Equivalent single wheel load
in – inches
LCN – Landing runway compatibility
 l_m – Distance from center of gravity to main landing gear struts
 l_n – Distance from center of gravity to nose landing gear struts
lbs - pounds
ft – feet
fps – feet per second
 $K_{g,r}$ – Wing to landing gear configuration
mph – miles per hour
MIL – Military
 N_g – Landing gear load factor
 n_s – number of struts
 n_t – number of tires on nose gear
 n_t – tire energy absorption constant
NS – New design
N/A – Not applicable
 P_n – Nose landing gear load
 P_m – Main Landing gear load
PR – Ply Rating
psi – pounds per square inch
 s_s – Stroke of shock absorber
 s_t – Max allowable tire deflection
 W_g – Weight of landing gear

1.0 Introduction

The landing gear is a vital component when designing an airplane, as it is what is used to keep the aircraft from damaging its outer shell, while also keep its cargo safe. There are many different landing gear configurations to choose from, whether it be land or water options or the number of landing gears to create a stable base for the plane. These will be considered in this section and will be explained in detail.

2.0 Landing Gear

The purpose of a designing a sturdy landing gear is to absorb landing and taxiing shocks, ground maneuverability, braking, towing and ground surface protection.

The vertical landing load the landing gear must be able to sustain, according to FAR 25 requirements is 12 fps. To account for this, landing gears will incorporate the use of tires and shock absorbers. The lateral and longitudinal loads must be accounted for as well. The use of drag or side braces, or struts, are used to help with the loads experienced.

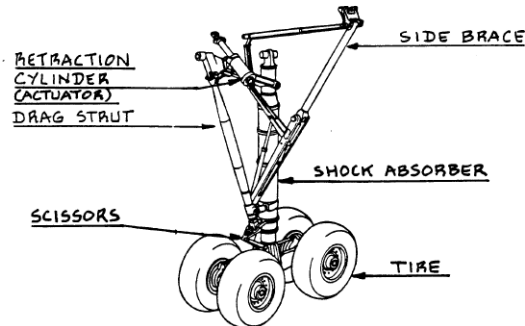


Figure 1: Illustration of landing gear layout. [1]

2.1 Type and Compatibility

As previously stated, there are several different landing gear configurations that can be chosen from. This business jet will use to retractable tricycle landing gear configuration as it is the most stable and will reduce the drag created by fixed landing gear during flight. The triangular landing gear provides good visibility, stability and favorable steering.

When selecting landing gear, it is important to account for tires which do not exceed weight limits which exceed values that may cause structural damage to gear, cause tire damage or cause runway damage. When accounting for these loads, the runway surfaces experienced by the plane must be considered. The business jet will utilize paved runways, whether asphalt or concrete, which categorizes as type 2 and 3 surfaces. Landing gear and tires must follow a certain LCN requirement. Based on the table in Roskam, the plane most similar would be the Fokker F-27 MK 500, with a tire pressure of 80 psi and a LCN of 19 [1]. Considering the intended destinations for the business jet being designed are large commercial airports, the LCN will most likely not be of issue. With multiple wheels on landing gear struts, the plane's equivalent single wheel load, ESWL, must be determined. As previously stated, each landing strut will have two wheels in the dual wheel configuration. The ESWL can then be found with the following equation set.

$$ESWL = P_n / 1.33 \text{ or } P_m / 1.33 \quad (1)$$

Where P_n , or P_m , is the load on the nose or main landing gear. As previously found, the P_n was found to be 2534.426 lbs. Thus, the ESWL was found to be 1905.584 lbs. It will be assumed the tire pressure will be set to 80 psi.

As shown in the table presented below from Roskam, the business jet will correspond to an LCN between 15 and 20. If an approximate value were to be determined, the LCN value would be about 19, as was predicted with a similar aircraft in Roskam.

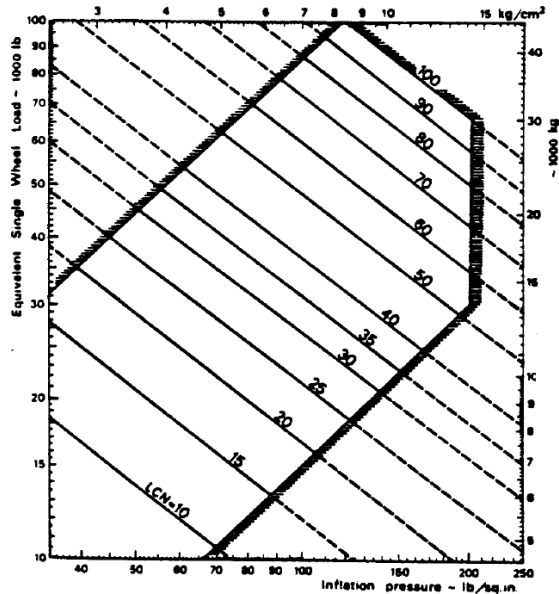


Figure 2: LCN value approximation based on ESWL and tire pressure. [1]

2.2 Tire Selection

The selection of tires is important as they will be used to safely land the plane without causing damage to the landing gear struts. The tire type, performance, clearance, size and load carrying capability will be covered. Type III tires will be used for this aircraft's landing gear, as shown below. The tires selected are considered for low pressure. The tire is similar to the Type I, yet it has smaller beads. This was selected as based on the previous example of a smaller jet which did not require a highly pressurized tire. The Type III tire will also follow the New Design, NS, tire requirements.



Figure 3: Type III tire tread pattern. [1]

The wear on the tires is greater than generally expected. Tires experience static and dynamics loads during taxiing, takeoff and landing, as well as shock absorption. The tires must also be able to expand and contract depending on weather conditions. The nosewheel tires will be designed for the maximum allowable dynamic load of 1.45. The allowable tire deflection can be found with the following equation.

$$s_t = D_o - 2(\text{loaded radius}) \quad (2)$$

Where D_o is the outside diameter of the wheel, as shown in the following diagram.

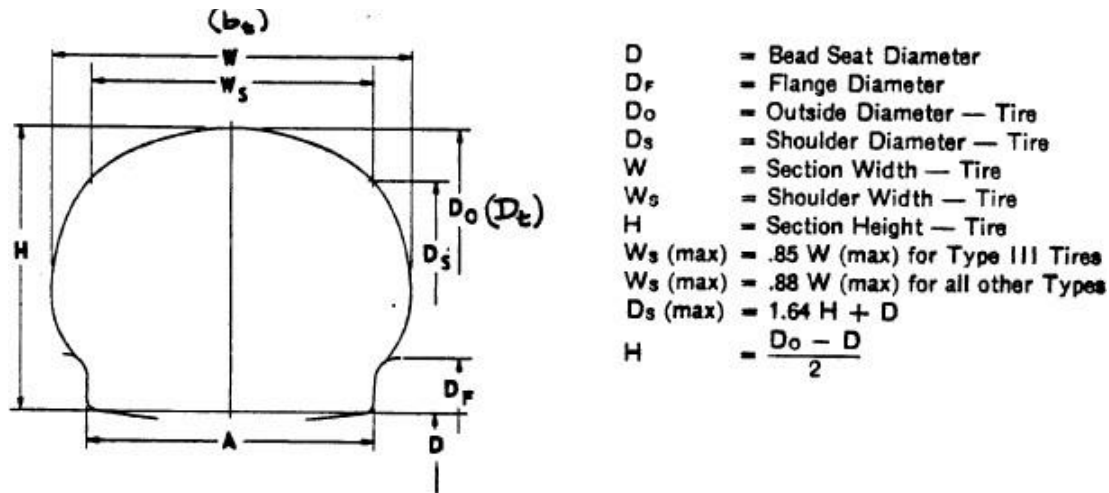


Figure 4: Tire geometry definition of values. [1]

The tires must meet a set of clearance requirements as well. The tires must fit within the wheel well for retraction, as well as tire to fork or strut and tire to tire clearance. It is important to consider that tire size will not remain constant as air pressure and temperatures will affect the tires size throughout the flight. A basic set of requirements is acceptable for the tires width and radius clearance values.

width: $0.04W + \text{lateral clearance due to centrifugal forces} + 1 \text{ inch}$

radius: $0.1D_o + \text{radial clearance due to centrifugal forces} + 1 \text{ inch}$

The main gear will first be sized following Roskam's procedure. First, the static load on each main landing gear was determined as 13,532.79 lbs. Since this plane falls under the FAR 25 requirements, the static load must be multiplied by a factor of 1.07. Thus, the load for each strut is 14480.08 lbs. This static load must also account for wheel growth during flight, this is accounted for by a factor of 1.25, thus, the new static weight experienced by each landing strut is 18,100 lbs. Each tire of the main landing gear will hold a static load of 4525.26 lbs.

The nose landing gear tires are next to be designed. The method of determining the static load on each tire is similar to the main landing gear, FAR 25 requirements and growth during flight. Thus, the nose landing gear tires have a static load of 3390 lbs, however, determining the load of each tire is different. The following equation is used to find the dynamic load on each nose gear tire. It is anticipated that the plane will use antiskid braking, resulting in an a_x/g value of .45.

$$P_{n_{dyn_t}} = W_{TO} \{ l_m + a_x/g(h_{cg}) \} / n_t (l_m + l_n) \quad (3)$$

The l_m and l_n values are determined from the center of gravity reference point to the main and nose landing gear positions. This resulted in a dynamic load of 4,234.579 lbs per tire of the main landing gear. This would then be divided by a factor of 1.5 based on the tire selection, resulting in a dynamic load of 2823.05 lbs per nose gear tire.

To determine the tires maximum tire operating speed, the speeds will vary between takeoff and landing. The following set of equations are used.

$$\text{For landing: } V_{\text{tire/max}} = 1.2V_{S_L}$$

$$\text{For take-off: } V_{\text{tire/max}} = 1.1V_{S_{TO}}$$

Referring to Class I design, the landing and takeoff stall speeds were recalled. With a stall speed of 99.307 knots, the max tire velocity during landing and takeoff are 119.17 knots and 109.24 knots, respectively. The tires can now be selected based off the Goodrich tire catalog provided in Roskam. The tire selection will be loosely based off the previously found tire sizing in Class I sizing. With a majority of the tire qualifications listing military, it will be assumed that military standards are set the highest, thus allowing for military worthy tires to be used commercially as well.

Table 1: Tire requirements

Main Gear		Nose Gear	
Tire static load	Tire dynamic load	Tire static load	Tire dynamic load
4,525 lbs	4,235 lbs	3,390 lbs	2,2823 lbs
Ground speed req.	119 knots	135 mph	

Table 2: Main landing gear tire options

Main Landing Gear Tire Selection						
Size (in)	PR	Load Rating (lbs)	Inflation Pressure (psi)	Speed Rating (mph)	Qualification	Weight (lbs)
25.3 x 6.50	8	5700	87	160	N/A	14.5
30.25 x 8.25	10	9250	90	160	MIL	23.0
30.35 x 13.2	10	8850	38	160	N/A	55.0

Table 3: Nose landing gear tire options

Nose Landing Gear Tire Selection						
Size (in)	PR	Load Rating (lbs)	Inflation Pressure (psi)	Speed Rating (mph)	Qualification	Weight (lbs)
17.7 x 5.85	8	3150	75	120	MIL	9.5
18.55 x 8.25	16	6650	125	150	MIL	9.0
13 x 4.85	14	3550	156	200	N/A	8.0

From these tire options of the main and nose landing gear, all will be able to satisfy the necessary conditions of static loads and max ground speed, apart from one nose gear tire. A selection of which tire to be used for the landing gear can be made. The objective remains to save weight while maintaining the safety of the plane. The main landing gear will utilize the 25.3 x 6.5 in tire as it satisfies the main landing gear static load significantly and is the most weight effective option. The nose landing gear will use the 13 x 4.85 in tire as it will satisfy both the nose gear's static and dynamic load, as well as surpass the maximum runway speed required of the tires.

2.3 Strut Interface

The main purpose of the struts is to absorb the shock when landing, as well as to help the aircraft maneuver around the tarmac and airport areas. This section will cover the shock and wheel interface, devices used for shock absorption and sizing of the struts.

When placing the wheel on the strut, it is important to take into consideration two unique terms, rake and trail. Rake is the struts ability to swivel at center of the wheel. Trail is related to rake as it the distance between the original strut position to the new imaginary vertical strut position at rake. When designing the strut, it is important to avoid shimmy, the continuous forward and backwards motion of the landing gear as it could cause unnecessary structural stresses.

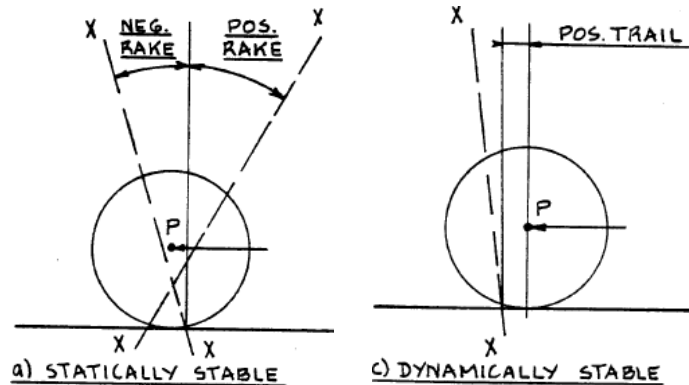


Figure 5: Stable rake and trail positioning of struts and wheels. [1]

The proposed airplane will use a telescoping mechanism as its primary strut, as shown in the figure below.

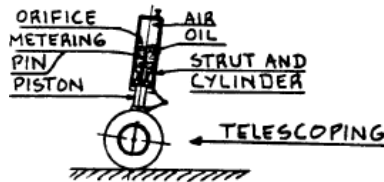


Figure 6: Proposed strut wheel configuration. [1]

There are a number of different options that can be chosen from to absorb the shock when landing the plane. Some of these options include tires, air springs, oleo pneumatic struts, shock chords and rubbers, cantilever springs and liquid springs. The oleo pneumatic spring system will be used as it is integrated as the strut rather than requiring several other components, which would add additional weight. As seen in the figure below, the recoil spring strength for a single versus a double is relatively similar for light loads. As the plane will experience a max of 18,000 lbs of the main landing gear during flight. The two remain fairly similar that a single shock may be used, but a double acting strut can be used if heavier loads are expected.

C) OLEO-PNEUMATIC STRUTS

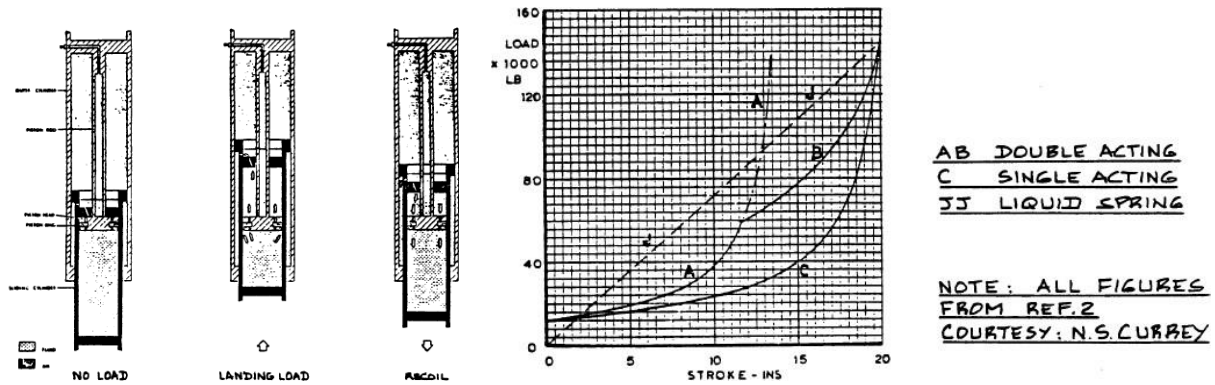


Figure 7: Oleo pneumatic spring recoil strength. [1]

To size the strut, the following process was outlined in Roskam. The first step is to determine the maximum kinetic energy with the following equation.

$$E_t = 0.5(W_L)(w_t)^2/g \quad (4)$$

$$E_t = .5*(18214)*(12^2)/32.2 = 40726.96 \text{ lb*fps}$$

From this value, it is assumed that the plane will initially land completely on its main landing gears. The following relation is used to find the stroke of the shock absorber, which then can be used to find the diameter required for the shock absorber.

$$E_t = n_s P_m N_g (\eta_t s_t + \eta_s s_s) \quad (5)$$

After manipulation, the following relation is shown. Several of the constants were defined by Roskam. The landing gear load factor, N_g , is defined by the FAR 25 requirements to be a range from 1.5 to 2.0, thus, an average of 1.75 will be used. The tire energy absorption, η_t , is .47. The energy absorption efficiency of shock absorbers is relative the selection of absorber, in this case the oleo pneumatic springs, which is .80. The max allowable tire deflection was defined earlier with a loaded static radius of 11.8 inches, and will be defined before continuing. It is important to convert fps to inches per second for an accurate calculation.

$$s_t = D_0 - 2(\text{loaded radius})$$

$$s_t = 25.3 - 2(11.8) = 1.7$$

$$s_s = \frac{\frac{E_t}{n_s P_m N_g} - \eta_t s_t}{\eta_s} = 11.899 \text{ in}$$

From this value, it is a suggested note to add one inch as an extended node of caution. Thus, the stroke is 12.899 inches. This rating is noted for only idealic conditions where the shock is directed completely in the direction of the shock absorber. The diameter of the shock absorber can now be estimated with the following equation.

$$d_s = 0.041 + 0.0025(P_m)^{1/2} \quad (6)$$

$$d_s = .041 + .0025(13532^{1/2}) = .3318 \text{ ft} = 3.98 \text{ in}$$

The next step will be to size nose landing gears shock absorbers. The process is similar to that of the main landing gear, with the substitution of several variables. The landing weight will be adjusted to the static nose gear load. The number of struts will be one as the nose is singular. The tire deflection will be that of the nose gear rather than the main landing gear tires.

$$E_t = .5(P_n)(w_t)^2/g$$

$$E_t = .5*(2534)*(12^2)/32.2 = 5667.04 \text{ lb*fps}$$

$$s_t = D_0 - 2(\text{loaded radius})$$

$$s_t = 13 - 2(6.1) = .8$$

$$s_s = \frac{\frac{E_t}{n_s} - n_s}{\frac{P_n * N_g}{t t}} = 14.956 \text{ in}$$

$$d_s = .041 + .0025(2534.43^{1/2}) = .167 \text{ ft} = 2.00 \text{ in}$$

2.4 Brakes

The purpose of having a sturdy and durable braking system as it is one of the many ways the plane will use to help stop the plane once landing on the runway. The usage of brakes are also important for steering enhancement, holding the plane when parked and while increasing engine power output for takeoff, as well as helping to have control over the plane's speed while taxiing.

With a majority of planes utilizing a disc braking system, this is what will be used for this aircraft. When braking, the plane is converting its kinetic energy into heat. With such a high kinetic energy value, a high amount of heat will be generated, thus, the heat must be dissipated away from the structure as to not cause unwanted warping or damage to the plane. The heat will dissipate into the wheel well, tire and surrounding air. Ultimately, the rolling friction caused between the runway and tires is what will cause the plane to slow and eventually come to a complete stop.

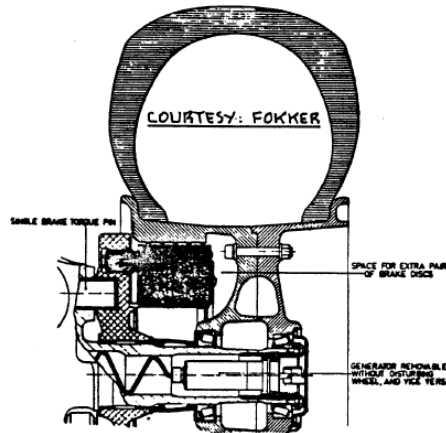


Figure 8: Cross sectional view of braking system. [1]

As the plane's pilot applies the brakes, the braking system should employ an anti-skid feature as this will avoid damages, such as a tire blow out. Roskam states that on dry surfaces, anti-skid brakes will slow the plane at a rate of .45g's. If the plane were to land on another undry surface, the braking capabilities would depreciate. In wet conditions, it is important to consider a plane hydroplaning. If this were to occur, the plane's tires would, in theory, lose contact with the runway forcing the plane to stop with only the use of reverse thrusters. The braking system will be deployed by the use of hydraulics to power their movement.

2.5 Landing gear layout geometry

In this section a brief overview of what has been covered will be reviewed, as well as any other pertinent notes that must be mentioned prior to continuing. The plane will utilize a retractable tricycle landing configuration. The following requirements must be met and satisfied.

Table 4: Tire requirements.

Main Gear	Nose Gear
-----------	-----------

Tire static load	Tire dynamic load	Tire static load	Tire dynamic load
4,525 lbs	4,235 lbs	3,390 lbs	2,2823 lbs
Ground speed req.	119 knots	135 mph	

The following table represents the selections made which satisfied what was asked of from the plane's mission requirements.

Table 5: Main landing gear component selections.

Main Landing Gear						
Tire Selection						
Size (in)	PR	Load Rating (lbs)	Inflation Pressure (psi)	Speed Rating (mph)	Qualification	Weight (lbs)
25.3 x 6.50	8	5700	87	160	N/A	14.5
Shock Absorber Sizing						
Length				Diameter		
12.899 in				3.98 in		

Table 6: Nose landing gear component selections.

Nose Landing Gear						
Tire Selection						
Size (in)	PR	Load Rating (lbs)	Inflation Pressure (psi)	Speed Rating (mph)	Qualification	Weight (lbs)
13 x 4.85	14	3550	156	200	N/A	8.0
Shock Absorber Sizing						
Length				Diameter		
14.956 in				2.00 in		

The following figures helps to illustrate the dimension lengths and sizing.

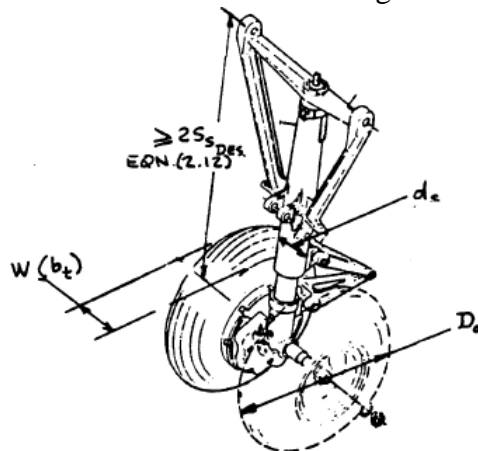


Figure 9: Landing gear with dimensioned variable lengths. [1]

2.6 Steering, turn radii and ground operations

Steering is an important factor in helping a plane maneuver around on the ground. Several options are to be chosen from, which include differential braking, rudder control

turning or nose gear turning. Differential braking will be used as it is the most common of the options. Rudder control is more typical of light aircraft. Nose gear steering is typical of transport aircraft, but requires a considerable amount of force to rotate the nose wheel. The differential braking system will be used as maintenance requirements do not require special training. This will also help to reduce extra weights of installing a large enough rotating mechanism to control the nose landing gear.

The plane's turning radius is important on larger aircraft, but the business jet being designed is smaller and is expected to operate out of large commercial airports. Thus, the plane's turning radius is not as important. The plane's turning radius will now be estimated off of the placements of the nose and main landing gear, as previously depicted in Class I sizing. With the main landing gear location being placed 23.94 ft aft of the nose of the plane, it is an estimate that the plane will have a minimum turning radius of about 25 feet.

2.7 Retraction Kinematics

With a large landing gear, the amount of drag it creates is quite large. Although it may not stop the plane from flying in the air, it will have a negative impact and decrease the plane's efficiency. This warrants the plane to utilize a retractable landing gear to get the most out of the plane. With the use of a retractable landing gear, it will provide a cleaner aircraft aerodynamically, while adding extra weight with the retraction mechanics. The following retraction kinematic will be used as it is simple and will fold small enough to fit within the aircraft when retracted. This retraction kinematic will be used for both the main and nose landing gear.

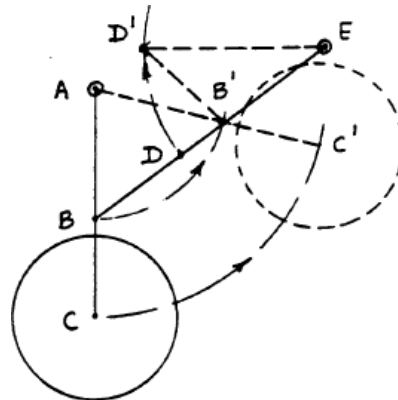


Figure 10: Stick diagram of retraction kinematic. [1]

The actuator must be placed in a position to make the proposed landing gear design may be retracted. The following figure shows the proposed position of the actuator position.

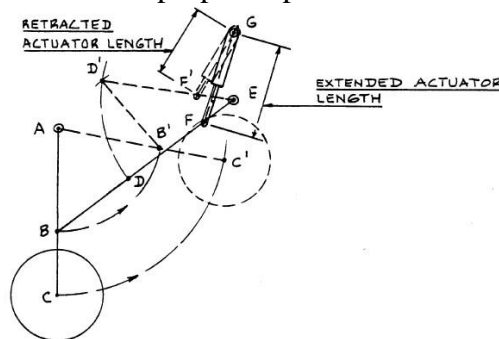


Figure 11: Proposed actuator position. [1]

The following figure shows the retraction process of the landing gear.

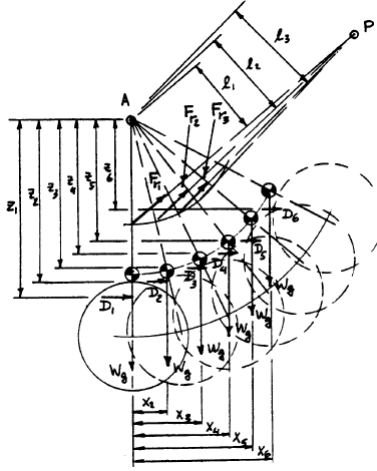


Figure 12: Expected retraction animation of landing gear. [1]

The weight of the landing gear must now be calculated for in order to determine the amount of force the actuator must generate in order to retract the landing gear. This is done with the following estimation process. The process is identified as the Torenbeek method.

$$W_g = K_{g_r} \{ A_g + B_g (W_{TO})^{3/4} + C_g W_{TO} + D_g (W_{TO})^{3/2} \} \quad (7)$$

Nose Gear:

$$W_g = [1.0 * (12 + .06(29264)^{.75})] + (0 * 29264) + [0 * (29264)^{1.5}]$$

$$W_g = 146.24 \text{ lbs}$$

Main Gear:

$$W_g = [1.0 * (33 + .04(29264)^{.75})] + (.021 * 29264) + [0 * (29264)^{1.5}]$$

$$W_g = 737.04 \text{ lbs}$$

The total weight of the landing gear is 883.28 lbs. The drag force created by the landing gear must also be determined. It was estimated the plane's landing gear will experience a coefficient of drag of .5.

Nose Gear:

$$D = C_D q S \quad (8)$$

$$D = .5 * \left(\frac{1}{2} * .0023769 * 200.5^2\right) * \frac{(2*36)+(4.85*13*2)}{12*12} = 21.804 \text{ ft} * \text{ lbs}$$

Main Gear:

$$D = .5 * \left(\frac{1}{2} * .0023769 * 200.5^2\right) * \frac{(3.98*36)+(6.5*25.3*2)}{12*12} = 78.329 \text{ ft} * \text{ lbs}$$

The landing gear total length, wheel and strut, exposed will be approximately 3.2 feet. It can be adjusted for final plane measurements if needed. This will still satisfy the plane's lateral tip over criteria. The actuator force and retraction cylinder length can now be determined. The following equations were used to determine the relation between retraction force and stroke.

$$F_{r_i} = (W_g x_i - D_i z_i) / l_i \quad (9)$$

$$l_r = \{ (z_p + R \cos \phi)^2 + (x_p - R \sin \phi)^2 \}^{1/2} \quad (10)$$

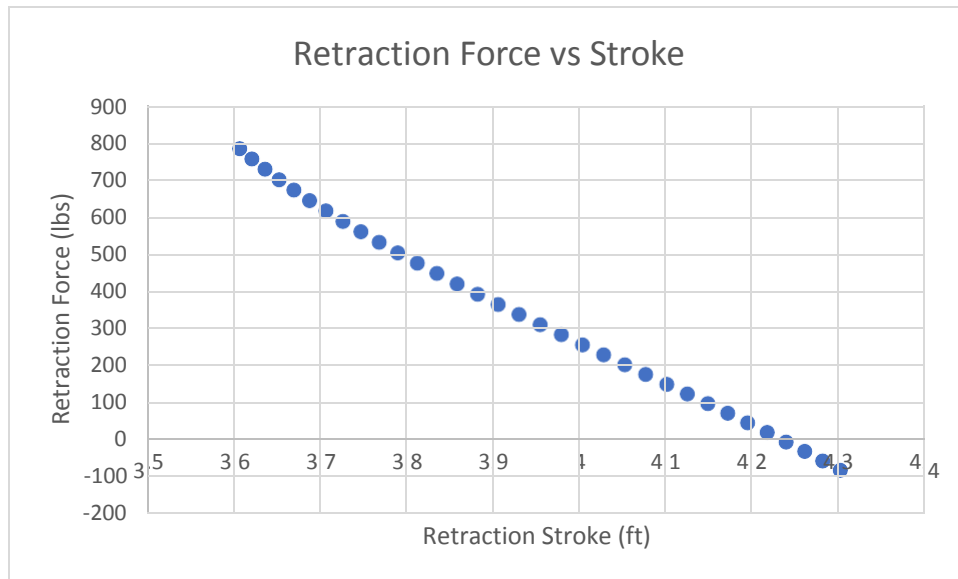


Figure 13: Retraction force versus retraction stroke

The results of this graph are acceptable as there are no peaks or valleys that rapidly occur. Another reason that warrants an accurate measurement is that as the landing gear begins to retract, the least amount of force is required as the forward progress and resistance of the landing gear is aided when retraction is in progress.

The retraction kinematics discussed are the simplistic options. The other options may include wheel rotation, strut shortening or tandem gear retraction. These options are more technologically advanced and could cause greater difficulties to maintain and operate. These options may also require extra mechanisms, which would generate extra weight which the plane not be able to takeoff with.

References

[1] Roskam, J. (1989). Airplane Design Part IV: Layout Design of Landing Gear and Systems. University of Kansas.

Chapter 4

Aircraft Subsystems

1.0 Introduction

The purpose of this chapter is to discuss and layout the business jet's subsystems. Subsystems are important as they are used to supply the plane with power, control and comfortability during flight. The subsystems which will be considered are: flight control, fuel, hydraulics, electrical, environmental, cockpit and avionics, de-icing and anti-icing, emergency escapes and water and waste systems.

2.0 Flight Control

The flight control surfaces are the components which will be used to adjust the plane's direction and movements. This includes the ailerons, rudder, elevator, and any other high lift devices which are deemed necessary, in this case plain flaps. The flight controls can be either controlled by the trim tabs or the movement of the entire control surface.

The flight controls are categorized as either reversible or irreversible components. Reversible flight controls are control surfaces which will move when the pilot controls are moved, and vis versa. While irreversible flight controls are when a hydraulic or electric system moves the controls surface. When the pilot controls are moved, the control surface moves, but the control surface movement will not move the pilot's controls.

2.1 Reversible Flight Controls

For this aircraft, the plane will not primarily consist of reversible flight controls. Since reversible controls are powered by pure pilot strength to move the control surfaces. The plausibility of a pilot being able to move control surfaces of a business jet when flying over 500 mph is highly unlikely. Thus, having reversible flight controls on this business is implausible.

2.2 Irreversible Flight Controls

Without having any reversible flight controls, the plane will consist of only irreversible flight controls. The flight controls which will be considered are ailerons, flaps, rudder and elevator. The pilot will move the controls, generating a signal that is sent to activate the actuator, which will then move the flight control surface.

2.2.1 Actuator

The actuator is the mechanism which is used for the movement of the control surface. Actuator movement is powered by either hydraulic, electromechanical or electrohydrostatic. When designing a plane, safety and maintenance must be considered. Since hydraulic actuators are most frequently used, they will be used for this business jet as well. If electromechanical or electrohydrostatic actuators were to be used, they would require special mechanics and inspectors or increased learning of how they work and how to service them. But, one benefit of an electromechanical actuator would be the weight saving factor as compared to the conventional hydraulic actuator. The following set up will be used to move the control surfaces. The figure shows the movement from a clean aileron to a deployed aileron positioning.

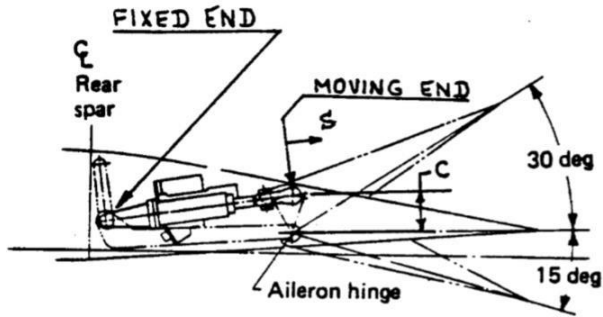


Figure 1: Actuator to surface set up. [1]

To enable the mechanism, the business jet will utilize a fly-by-wire system, a computer driven system. This will allow for the pilot to send an analog input to the computer which will convert it to a digital signal. The digital signal will then be sent to the actuator, which will then convert it back to an analog signal to move the control surface. This will help to relieve any unnecessary weights used to housed hydraulic fluid to power the control surfaces. The use of actuators will help to reduce the overall weight of the aircraft, particularly in the hydraulics subsystem, which will be discussed later in the chapter. One negative that comes from actuators is their limited range of movement. Their limited range will only allow them to control surfaces or objects that do not require free range of motion. Actuators will suffice for this business jet's control surfaces. They will be used to control the ailerons, elevator, rudder and flaps.

The hydraulic actuators will need to be sized to maintain an overall pressure of the hydraulic line to be approximately 3000 to 3500 psi, as stated by Roskam [1]. The general set up for the aileron will be similarly matched to the figure presented below for a general jet transport. The figure displays the layout of pilot input to the cables and wirings that lead to the movement of the control surface. The control surfaces show several actuators as it will cause a smaller and evenly stressed flight control structure, rather than a larger load on a single point of the structure.

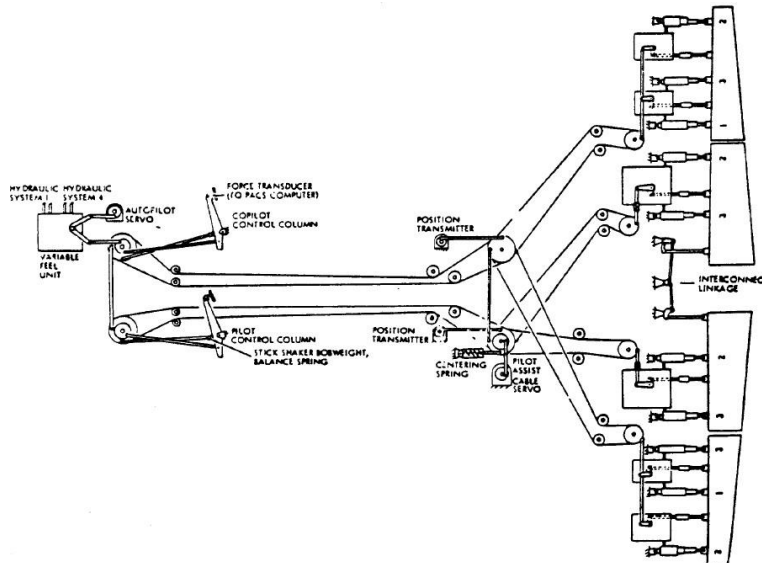


Figure 2: Hydraulic actuator set up for control surfaces. [1]

Several other factors to consider for the flight control set up include simplicity, redundancy, as well as accessibility for maintenance. The simplicity accounts for the systems accessibility and general knowledge for maintenance as well as the ability to avoid damaging

other subsystems that would affect the aircraft in a greater matter. The redundancy of the actuators that are used to move the control surfaces will ensure that if one set of the actuators was to fail, the pilot will not be put in a position where the plane is unable to maneuver for a safe emergency landing.

2.3 Trim system

For the plane to maintain a level and smooth flight, a trim system will be used to enable the plane to do so. The trim surfaces will be located on each of the ailerons, as well as the rudder and elevator. The trim system will be adjusted based off the fly-by-wire computer system. The trim panels will be sized to have a significant enough impact to adjust the plane's flight path to maintain a level flight. This trim system may also be adjusted by pilot if need be.

2.4 High lift device system

The use of high lift devices will be used primarily during either takeoff or landing for added lift when the plane's airspeed is not adequate to keep the plane in the air. The high lift device being used for this business jet are plain flaps on both wings. One important note is to ensure that asymmetric embolization of the flaps is avoided. Flap travel sensors will be used to ensure asymmetric flap deployment does not occur. This will halt the deployment of the flaps if a certain point is reached and the two flaps are not close enough in their related positional deployment to continue. The flap displayed will begin at a hinged actuator positioning, but as it is deployed, the hinge will straighten.

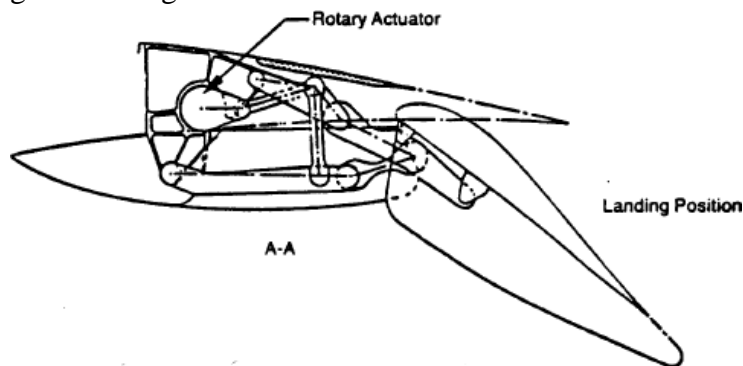


Figure 3: Flaps deployed for landing. [1]

2.5 Propulsion Control System

These control surfaces will be used to control the forward movement of the plane. The propulsion control system includes the ignition control, starter system, fuel flow and reverse thrusters. These components will be examined further as they primarily relate towards other subsystems. The ignition control and starter systems both relate towards electric. Fuel flow or the throttle control relates to the fuel subsystem to control the amount of fuel the engine is feed. The thrust reversers are used on the engine nacelles as a hydraulically powered opening to slow the plane after touchdown.

3.0 Fuel

The fuel is a necessary component for the plane as it will supply the engines the fuel needed to provide chemically react to provide forward thrust. The general fuel tanks will be placed in the wings, as well as in the small undercarriage of the aircraft if needed. As stated in the Class I design process, the amount of fuel required is 246 ft^3 . Approximately 203 ft^3 will be stored in the wings, with the remaining 43 ft^3 being stored in the remaining undercarriage of the plane. The fuel stored in the undercarriage of the plane will be placed slightly ahead of the

wing to ensure the wheel tip over criteria will be satisfied, the exact placement will be examined in the future chapter which covers weight and balance of the aircraft. This tank will be drained first, then followed by the wing sub tanks which are positioned under the fuselage of the aircraft. The fuel stored in the wing will be used from the fuselage out towards the wing tips as to help maintain the plane's center of gravity.

This subsystem will also include fuel pumps and lines, venting, measurement and management and refueling. These components are necessary in moving the fuel to the engines and knowing the amount of fuel remaining to ensure a safe landing may occur. The fuel pumps and lines must be able to supply the engines with the amount of fuel required to reach the desired air speed. The fuel line must be pressurized enough to match the amount of fuel required by the engines. The fuel pumps will regulate the amount of fuel required by the engines for its most efficient fuel economy. The measurement and management system are needed to instruct the pilot of how much fuel is remaining, as well as where the fuel is located in the tanks to ensure the plane will be able to maintain a level flight. The refueling ports must be accessible to the grounds crew to allow for a quick turnaround time if needed.

It is also important to consider a fire extinguishing system to ensure that if an accident was to occur, the plane's dire situation is not further worsened. Especially in this case of the business jet utilizing a low wing configuration, it places the plane at a greater risk of igniting the fuel tanks if the plane were to make an unconventional landing without landing gear deployment. This system is needed to limit the amount of damage with the likelihood of fire being contained. The fire extinguishing system will be self-contained within the wing and fuel tanks as these are the vulnerable positions of the aircraft.

4.0 Hydraulics

The hydraulic system is tasked with the movement of the primary and secondary flight controls, landing gear retraction and extension, steering and thrust reversers. The flight controls will be powered, as previously stated, by conventional hydraulic actuators. The landing gear movements will be hydraulically powered to be lowered and retracted. The steering will require power steering, a form of hydraulic movement, for the pilot to maneuver the plane while on the ground. Thrust reversers will be deployed, from the nacelles, when landing to help the plane brake and reduce speed to a maneuverable ground speed.

To successfully apply a hydraulic system to an aircraft, a reservoir, pumps, accumulators and hydraulic lines will need to be used. The reservoir will be used to supply the hydraulic fluid throughout the lines. The hydraulic pump will be used to supply and pressurize the actuators and hydraulic lines. Below is a figure which presents a general example of a reservoir and hydraulic pump which will be employed on this aircraft.

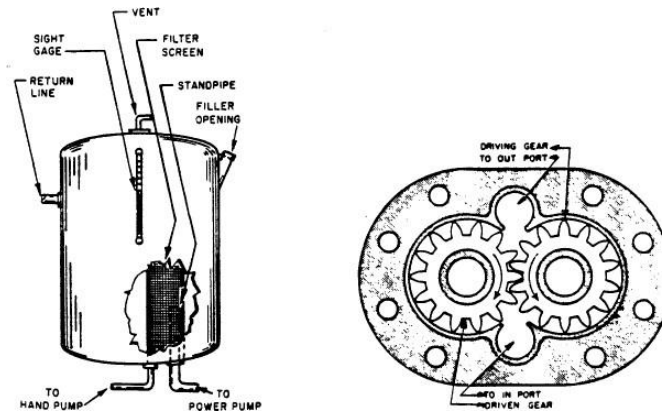


Figure 4: Example of hydraulic reservoir and pump. [1]

The system will be pressurized to 3000 psi, as most other hydraulic systems are pressurized at as well. The hydraulic system will need to operate under normal conditions, as well as under emergency flight conditions, such as hydraulic failure. Thus, a backup, or redundant, system will be needed to ensure a safe flight. As for the flight control system, the hydraulic system components should be easily accessible and maintained to ensure failure is not caused as means of a poor maintenance record.

Outlined in Roskam's book, the business jet being designed is most similar to the Gates Learjet M25 [1]. Thus, the hydraulic pressure will be 1500 psi rather than the more conventional 3000 psi. The lowered hydraulic pressure line is allowable as the business jet does not require as much force and pressure to move smaller control surfaces than a large passenger jet. The hydraulic system will have control over the plane's ailerons, flaps, rudder, elevator, landing gear movement and control, such as steering and braking. The system flow capacity will be at 4 gallons per minute to 0.3 gallons per minute, depending on the amount of pressure required per control surface and external reaction forces acting on the control surfaces.

The hydraulic system will look similar to that of the Learjet M 25. The layout shows the hydraulic pressurization will be a combination of pressurized air of the cabin and hydraulic fluid pressure. The two pressurization options will go through a pressure regulator before continuing to the actuators to move the flight control surfaces.

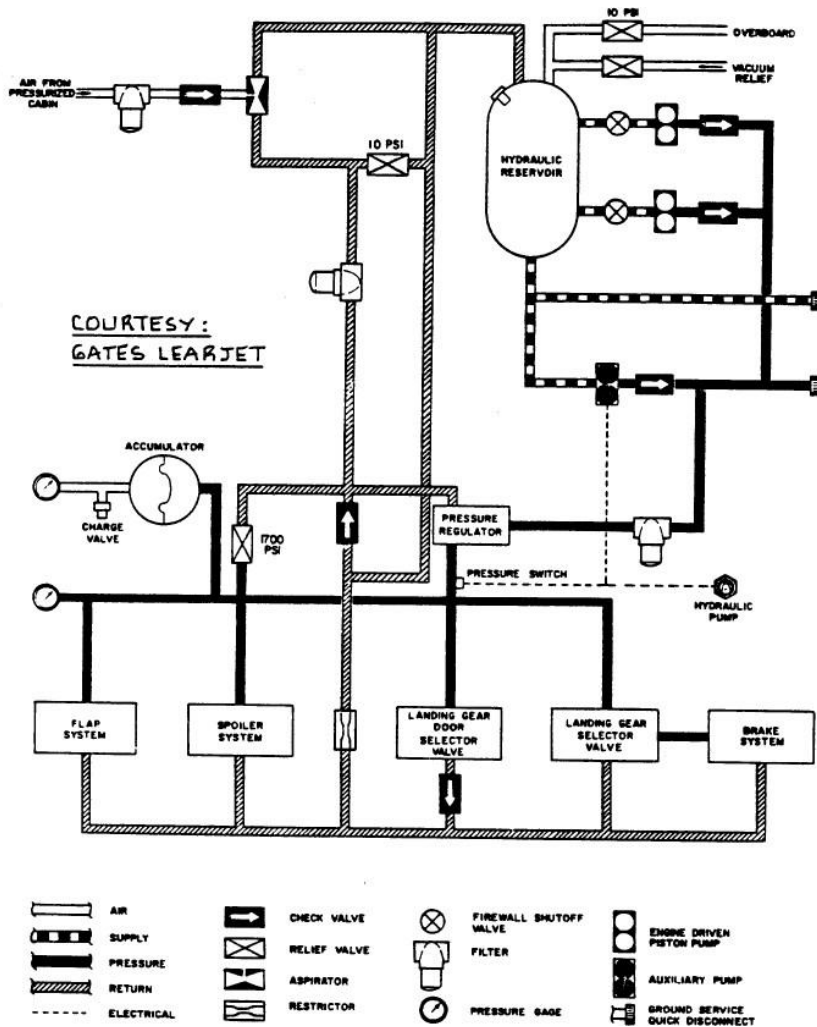


Figure 5: Example hydraulic layout of Learjet M25. [1]

The hydraulic cooling system will need to be implemented to help reduce heating of the hydraulic fluid and possible failures caused by heat. To address this issue, while keeping additional weight to a minimum, is to have several of the hydraulic lines run through or along the fuel tanks, as the fuel will be kept cold. The backup system will be used to control only the vital flight control surfaces as the likelihood of an emergency system being used is due to a lack of hydraulic feed pressure. The backup will maintain control of the rudder and elevator, if allowable, the ailerons and flaps as well. The landing gear will be gravity assisted when being deployed to land. The landing gear will take in bleed air measurements until a reasonably slow airspeed is reached to land, the hydraulic pressure holding the landing gear doors closed will be released and the landing gear will drop with the gravity assist.

5.0 Electrical

The electrical system is a vital component to all planes. For this business jet, the electrical system will be used for the following: internal and external lighting features, flight instruments and avionics displays, food and beverage heating and assisted engine start up. These components will be powered by a primary power generator, engine turbines. These components will also be equipped with a backup electrical system which will power the necessary

components, such as the flight instrument, communicational features and emergency interior and exterior lights. The backup system will be powered by a ram air turbine, as well as an additional battery if it is deemed necessary and capable of a storage position.

Determining the actual electrical requirements need by the plane is divided into sections of the flight path. The electrical usage is broken down into the loading, take-off, climb, landing and cruise phases of flight. The electrical loads are broken into essential and normal operating loads. The essential load will consist of flight deck and avionics illumination, minimum emergency lighting, necessary pneumatic systems and engine and flight control operations. The normal load requirements would be comprised of the essential loads with the addition of all remaining features which require electricity for power. The electrical backup system will only power the essential load items.

The placement and protection of the electrical system is important as the consequences of failure can be catastrophic. One note of importance to account for is the avoidance and dissipation of unwanted lightning strikes. Another avoidance is unwanted contact between two different electrical wiring systems as a short circuit could cause system failure, sparks, or in the worst case a fire. In emergency situations, when the plane must descend from its current altitude without all electronically powered devices being used, it will require that certain electrical components be power accessible always. This can be done by either utilizing a ram air turbine or a separate battery to use for power supply. The battery may also be used for standby operations when plane is still grounded. When grounded, the plane will utilize an APU, auxiliary power unit, to power the interior lighting. It must also be stated that all electrical components should be accessible for maintenance and service when necessary. Figure is a basic AC and DC power layout. Both layouts pull power from a source, in this case, a battery and generator in the engine, that will run through a set of regulators to power the internal lighting and instrumentation of the plane.

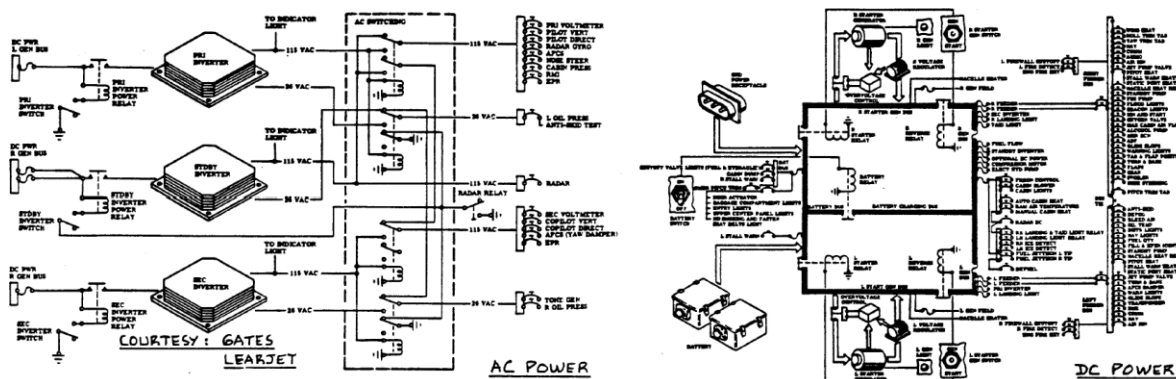


Figure 6: AC and DC power layout. [1]

6.0 Environmental

A plane's environmental system is a collection of systems which are used to control the climate within the cabin. These other systems are pressurization, pneumatic or bleed air, air conditioning and oxygen systems. The pressurization system will be used when the plane is flying to help maintain a lower altitude pressure within the cabin to allow for the comfortability of the passengers. The pneumatic system is used primarily for supplying the cabin with air flow, details will be explained later in the section. The air conditioning system is used to keep the cabin temperature at a comfortable temperature for the passengers. The oxygen system is used as a backup to the pressurization system to supply oxygen to each individual passenger.

6.1 Pressurization

The pressurization system will be utilized to maintain a comfortable cabin pressure and oxygen level as the plane flies at heights of up to 40,000 ft. The typical cabin pressure of commercial airliners is to pressurize the cabin to an altitude of 8,000 ft; thus, this standard altitude pressurization will be used for this business jet. This will be done with the help of airplane's pneumatic system. A control or metering system device will be used to adjust and measure the cabin's pressure. The pressure will be automatically set and maintained by the computer, but the cabin crew will also receive a monitor in the cockpit and cabin area to observe to ensure the cabin pressure is being maintained. The pressurization must also be able to detect and give a timely warning to the crew and passengers if the pressurization within the cabin is begins to drop or is lost. The pressurization system must be able to increase and decrease the cabin pressure for different flight conditions such as takeoff, cruise or landing. The system must also must consider that not all airports or landing strips will be at the same altitude above or below sea level.

6.2 Pneumatic

The pneumatic system is used to supply the air to the pressurize the cabin. This system will use bleed air collected from the engines. The air will be collected from the engines during flight and pass through a filtration system to ensure the air entering the cabin is clean and breathable. This air will likely need to be cooled as it has passed through the engine turbine, the air conditioning will be discussed in the next section. The bleed air can also help with engine startup. The pneumatic system will be similar to the one presented in the figure below. The bleed air taken from the engine has multiple uses, as shown in the figure. The bleed air can be recycled to help start the engine, as well as run through the cooling system to supply air to the cabin.

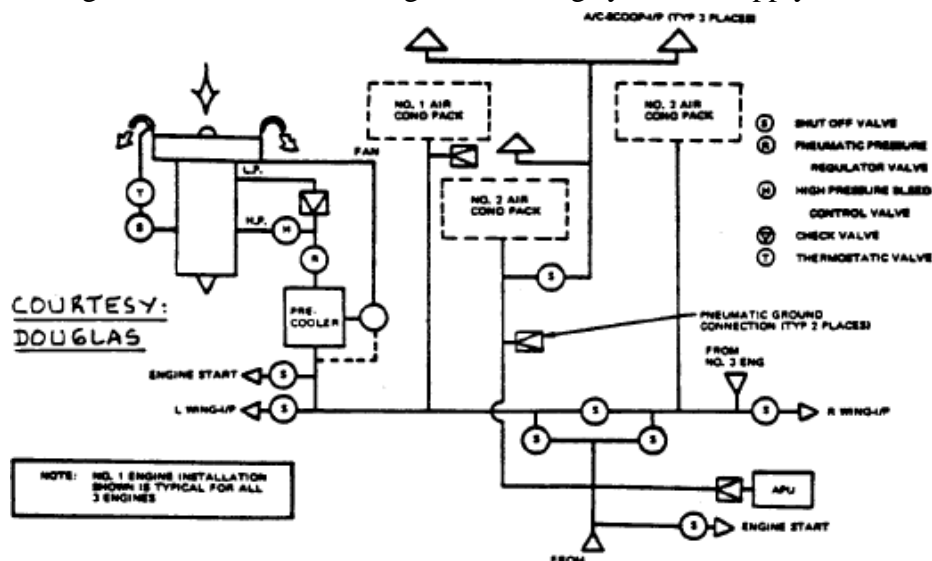


Figure 7: Example pneumatic system setup. [1]

6.3 Air Conditioning

The air conditioning system is used as it is labeled, to heat and cool the cabin temperature to ensure the passengers comfortability. The air conditioning system can also be used to control the humidity levels within the cabin. Without humidity, the air can be dry and cause bodily harms to passengers if they are exposed to dry air for extended periods of time [2]. The air conditioning set up will distribute the heated or cooled air multiple ways. The first way is through top air circulation throughout the entire cabin. The second way will be through

personalized air vents or gaspers located near each seated passenger. In the figure below, the air conditioning system takes in the air from the engine, runs it through the air filter and cooling packs and eventually into the cabin.

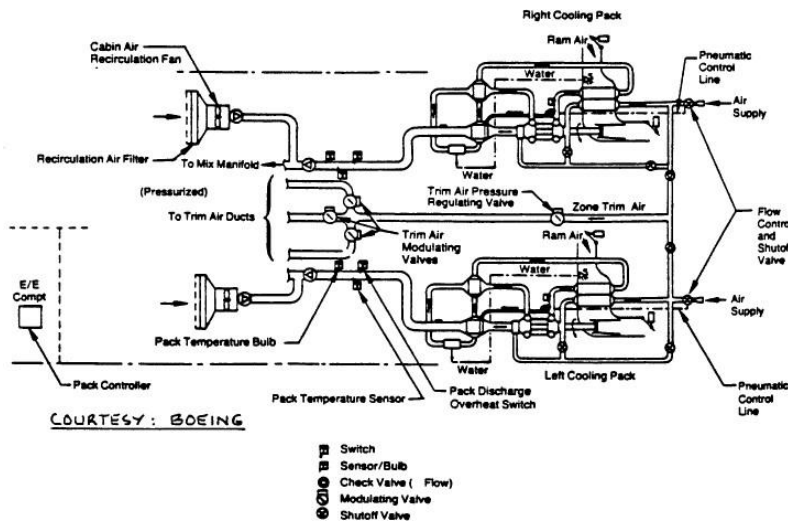


Figure 8: Air condition system layout. [1]

In the figure below, the ventilation system is for a larger passenger jet, but the same principle will apply to the business jet. The air conditioned air will run through a central air system that runs parallel to the fuselage. The air will then be distributed into several air vents along the ceiling to supply the cabin with conditioned air.

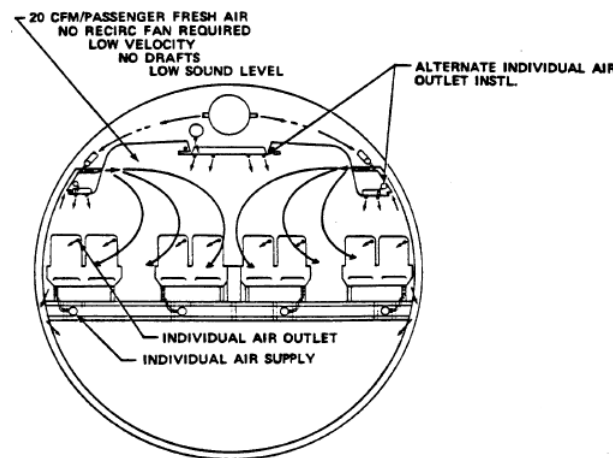


Figure 9: Air conditioning distribution. [1]

6.4 Oxygen

The final environmental system is the oxygen system. The oxygen system is necessary in providing oxygen to the passengers and crew members within the pressurized cabin. This system will operate as an assister and as a backup to the pressurization system. The oxygen is supplied to the cabin by several self-contained oxygen tanks which will provide a sufficient amount of oxygen to passengers and crew members as the bleed air from the exterior of the plane is oxygen deficient. The backup or emergency oxygen will be supplied through personalized masks as the plane will descend from high altitude to a more oxygen rich altitude to prevent further health concerns that may arise from oxygen deficiency. A conventional oxygen system setup is shown

in the figure below. The oxygen tank presented passes through a regulator and pressurization regulator to supply oxygen to the emergency masks.

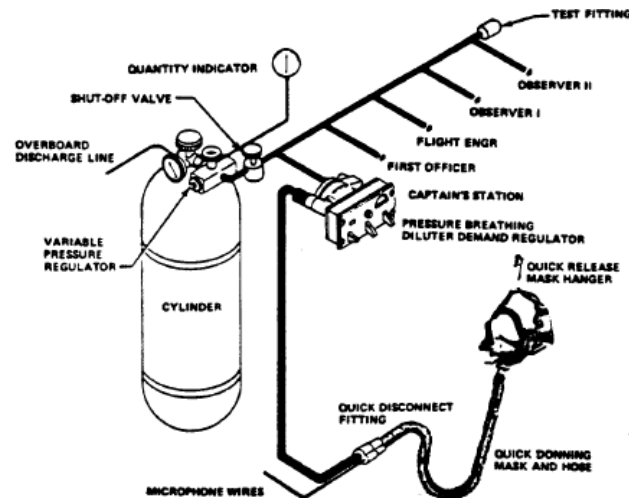


Figure 10: Oxygen system back up tank setup. [1]

7.0 Cockpit and Avionics

The cockpit and avionics are vital subsystems which are used by the crew to fly the plane safely. With the high level of complexity of cockpits and avionic measurement controls, a detailed description of each component and all controls will not be discussed fully.

For the cockpit, the most important factor to consider during the design process is the user interface between the instrumentation and the pilot. The interface between the pilot and the flight deck must be simplistic and easy to comprehend, as well as noticeable if an error or emergency arises to allow for the pilot to take immediate action to limit the damage. Several key components that the flight deck should have are weather and atmospheric conditions ahead and surrounding the airplane, the airplane's speed and fuel levels, as well as indicators of landing gear and the operational status of the subsystems discussed in this chapter. The interface should also be simple enough that if a certain emergency were to arise where the pilot is unable to fly the plane, a cabin crew member or passenger must be able to fly the plane to safely and land through communications with air traffic control.

The flight must be managed and observed either by a computer or the pilot at all times. Several instruments that should always be monitored are the flight control surface positions, autopilot engagements, thrust management, inertial positioning, flight data and communication and advisory systems. For the components and instrumentation implemented in the flight deck, the installation should consider the maintenance accessibility that the wiring and systems are up to date on software. The feedback accuracy of these components is important as it will ensure the safety of the plane and its passengers, such as fuel or other flight indicators of the subsystems.

8.0 De-Icing, Anti-Icing, Rain Removal and Defog Systems

Anti-environmental systems are important as planes will likely encounter poor weather or storms at some point in their lifetimes. Weather can be encountered at both altitude and when grounded. Anti-weather systems will allow for the pilots to have enhanced control of the plane if there was no such system installed.

8.1 Ice Removal

The first anti-weather system that will be implemented on this business jet includes the de-icing and anti-icing system. This system will be used for the wings, windshield and outer skin of the body. This will help to maintain the plane's aerodynamic properties and prevent unnecessary extra weight and stresses on the plane structure. Possible issues that may arise from ice collection include a loss of lift, increase in drag, increased stress on the structure, loss in engine performance or incorrect readings of surrounding air. There are several ways to de-ice a plane's wing, such as boots or electro-impulse. The electro-impulse method will be used as the plane will be traveling at high speeds, which may lead to the rubber boots deformation and malfunction. The electro-impulse will have isolated areas that the wing will expand at to break the ice away and the free stream velocity would push it off of the wing, as shown in the figure below. The coil will protrude outward from the wing, creating a breaking force of the ice on both the top and bottom surfaces of the leading edge of the wing.

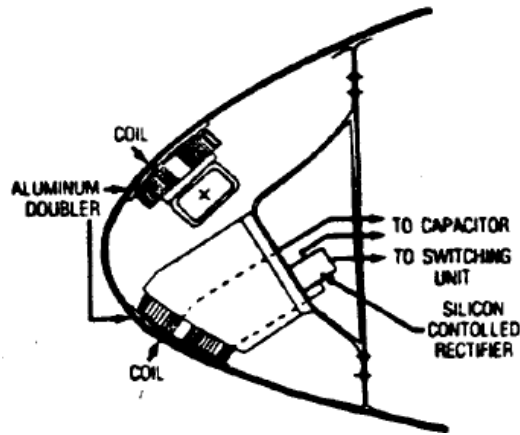


Figure 11: Electro-impulse deicing set up. [1]

The plane will use the thermal anti-icing setup as the plane will not likely exceed an altitude of 35,000 ft, thus temperatures will not be as extreme for aircraft traveling at a higher altitude. The thermal anti-icing setup utilizes bleed air from the engines and will recirculate it through the leading edge of the wings, and empennage if needed. The bleed air coming from the engines is warm, thus causing ice buildup to melt away. This setup will act as a defroster to deter the initial buildup of ice. The setup for the thermal anti-ice setup is presented in the figure below. The cross-sectional view of the anti-icing system shows the bleed air from the engine run through a centralized pipe where several cuts are made to circulate the warm air at the leading edge of the wing. This will heat the wing to prevent ice from forming.

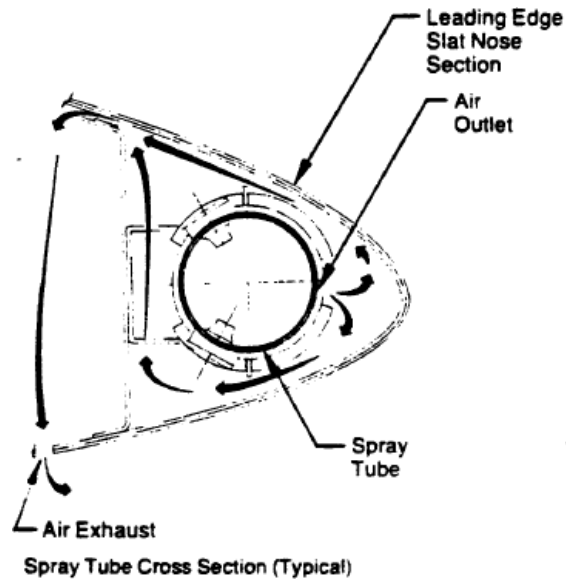


Figure 12: Thermal anti-icing setup. [1]

8.2 Water Removal

Rain removal and defogging systems typically relate to only the pilot's windows, the cockpit windshield. These systems could also be applied to the passenger viewing windows, with added weight and aerodynamic losses as the main cost. Thus, these two systems will only be employed for the windshields of the aircraft. Rain removal systems are typically the use of windshield wipers, similarly to those used in automobiles. Rain X will also be used to help with the water runoff. Water runoff is important as a backup if the wipers are to fail, the pilot is not stuck in a position where water builds up, obstructing the pilots view. For defogging, embedded heating and cooling lines will be embedded in the windshield to help with fogging and condensation buildup.

9.0 Emergency Escapes

To comply with the Federal Aviation Administration guidelines, planes must have emergency plans in place to keep the passengers and crew safe if an accident were to occur. Several of the basic requirements will be covered in this report. Exits must be properly marked, this would be the main door. In case of over water landings, lifejackets must be accessible to all passengers and crew. To save space and enhance the multipurpose uses, the seat cushions will be used as flotation devices. Lifejackets will be placed in the forward cabinets closest to the plane door. One escape hatch will be located along the ceiling to allow for a backup escape route if the main door is blocked. The main door will have an inflatable slide deployed when the door is armed. Emergency rafts will be placed in either of the two closets closest to the main door. Depending on the number of passengers and crew per flight, one emergency life raft may be sufficient.

10.0 Water and Waste Systems

The water and waste systems are two separately housed systems, yet, are closely related to one another. The water system is used to provide clean drinking water to be used in sinks and galley area. The waste system is used to hold the off run from the lavatory or galley areas.

The water system will supply the lavatory and galley sinks with both cold and hot water. The plane's water will be cold naturally when stored at altitude. To obtain warm water, such as

for the lavatory sink, an electric heating exchanger will be used to heat the water. Both systems will require a heating component to avoid freezing in the pipe.

For these systems to work, they must be pressurized. The systems will be pressurized by air, rather than a higher capacity of water. The air will come from the engine's bleed air, the plane's pneumatic system. Both systems must also be easily accessible during ground maintenance to ensure enough clean water is available to passengers, as well as to ensure the waste system does not back up into the cabin to allow for an enjoyable flight for the passengers.

11.0 Initial Structural Arrangement Drawings

The following figure shows the subsystems layout and design implemented as a part of the plane's structure. This figure shows the complexity that goes into each system. The internal structure shows that if an impact was to cause a malfunction of one subsystem, it could very easily influence the other remaining subsystems which are in the vicinity.

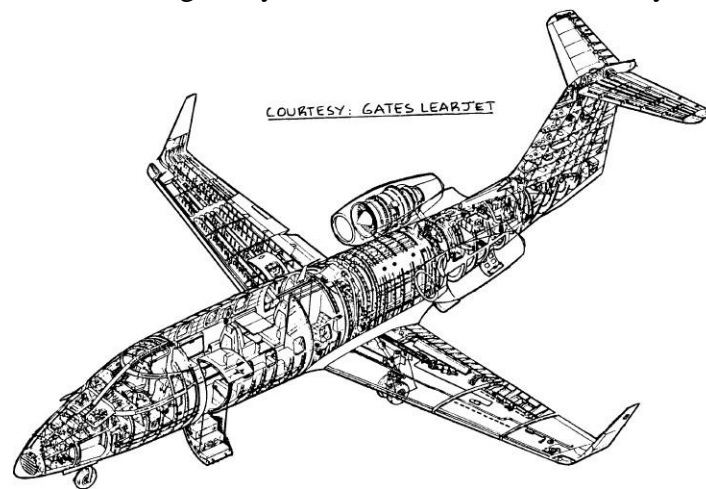


Figure 13: Initial plane subsystem layout. [1]

The flight controls subsystem will run from the cockpit's controls to the control surfaces, such as the aileron, flaps, rudder and elevator.

The fuel system will be placed within the wing and run along the fuselage to the engines. The fuel tanks in the wings is anticipated to not be able to fully hold all of the fuel for a complete range, thus some of the space under the cabin will be used as a secondary fuel tank. This tank will be used first to ensure the plane's stability throughout flight as the weight changes.

The hydraulics system will require a hydraulics reservoir, lines and actuators. The reservoir will be ahead of the fuel tank, closest to the nose of the plane. The hydraulics lines will then be fed to the actuators at the flight control surfaces. The hydraulic lines will run through the fuel tanks as a method of reducing weight. This will help to reduce weight as it acts a self-cooling system.

The electrical system will use bleed air from the engines which will lead to a generator. The generator will then spin, creating the electricity required for the plane. From this power source, a battery will be used as well to power the vital components. A secondary battery will be used to hold the extra power generated to supply the remaining electrical needs of the plane.

The environmental system is to be used to keep the cabin at a comfortable atmosphere. Thus, the system layout will be centralized around the cabin. The air pressure will be powered by

the external oxygen tanks and bleed air will be recycled into clean air after passing through several filters and temperature monitors.

The cockpit and avionics subsystem is rather common sense as this system is primarily located within the cockpit area. Other instruments such as air pressure reading or temperature may be available in the passenger cabin for either the stewardess or passengers to observe and adjust if necessary.

The deicing, anti-icing, rain removal and defog system will utilize bleed air and electrical power, depending on the system function. The deice and anti-ice systems are primarily based in the wings. The engine will provide bleed air from the rear engine placement back to the leading edges of the wings and empennage. The rain removal and anti-icing systems will be in the cockpit area, primarily the windshields. The use of wipers and heated windows will utilize an electrical battery to provide power.

The emergency escape systems are located throughout the passenger cabin. With the use of the emergency escape hatch and floating devices in case of water landings. The water and waste systems will be used in the galley and restroom area. The clean water tank will be placed in the rear, aft of the fuselage fuel tanks. The waste tank will also be placed in the rear. With the requirement of needing water for a short intercontinental flight, only a limited amount is needed. The two tanks will be placed side by side.

References

- [1] Roskam, J. (1989). Airplane Design Part IV: Layout Design of Landing Gear and Systems. University of Kansas.
- [2] Effects of Dry Air on the Body. (2018). Retrieved July 30, 2018, from <https://www.infoplease.com/science-health/weather/effects-dry-air-body>

Chapter 5

Weight Sizing

Symbols

A - Wing aspect ratio

A_{inl} – Capture area per inlet

A_v – Vertical tail aspect ratio

b_h – Horizontal tail span

b_v – Vertical tail

\bar{c}_h - Horizontal mean geometric chord

h_f – Max fuselage height

K_{buf} – Food constant

K_{ec} – Engine control constant

K_{fc} – Flight control constant

K_{fsp} – Specific weight of fuel

K_{inl} – Inlet constant

K_{lav} – Lavatory constant

l_f – Fuselage length

l_h – Dist. between wing $\frac{1}{4}$ chord and horizontal $\frac{1}{4}$ chord

l_n – Nacelle length from inlet lip to compressor face

l_v - Dist. between wing $\frac{1}{4}$ chord and vertical tail $\frac{1}{4}$ chord

M_H - Max Mach at sea level

N_{cc} – Number of cabin crew

N_{cr} – Number of crew

N_e – Number of engines

N_e – Number of engines

N_{fdc} – Number of flight deck crew

N_{inl} – Number of inlets

N_{pax} – Number of passengers

N_{pil} – Number of pilots

N_t – Number of fuel tanks

n_{ult} - Ultimate load

P_2 – Max static pressure at engine compressor face

P_c – Ultimate design cabin pressure

\bar{q} – Design dive dynamic pressure

S - Wing area

S_h – Horizontal tail wing area

S_r – Rudder area

S_v – Vertical tail wing area

t/c_m - Maximum thickness ratio

t_{r_h} - Max root thickness of horizontal

V_{pax} – Passenger cabin volume

W_{ai} – Air induction system weight

W_{api} – Air-conditioning, pressurization, anti and deicing system weight

W_{apu} – Auxiliary power unit weight

W_{aux} – Auxiliary gear weight

W_{bal} – Ballast weight

W_{bc} – Baggage and cargo handling equipment weight
 W_E – Empty weight
 W_e – Engine weight
 W_{ec} – Engine control weight
 W_{els} – Electrical system weight
 W_{emp} – Empennage weight
 W_{ess} – Engine start system weight
 W_F – Fuel weight
 W_f – Fuselage weight
 W_{fc} – flight control system weight
 W_{feq} – Fixed equipment weight
 W_{fs} – Fuel system weight
 W_{fti} – Flight test instrumentation weight
 W_{fur} – Furnishings weight
 W_g – Landing gear weight
 W_h – Horizontal tail weight
 W_{hps} – hydraulic and pneumatic system weight
 W_{iae} – Instrumentation, avionics and electronics weight
 W_n – Nacelle weight
 W_{ops} – Operational items weight
 W_{ox} – Oxygen system weight
 W_p – Powerplant weight
 $W_{payload}$ – Payload weight
 W_{pt} – Paint weight
 W_{pwr} – Powerplant weight
 W_{struct} – Structure weight
 W_{TO} – Takeoff weight
 W_{tr} – Thrust reverser weight
 W_v – Vertical tail weight
 W_w – Wing weight
 z_h – Distance between vertical tail root to horizontal tail root
 λ – Wing taper ratio
 $\Lambda_{1/2}$ – Sweep angle at $\frac{1}{2}$ chord
 $\Lambda_{1/4v}$ – Vertical tail sweep at $\frac{1}{4}$ chord
 λ_v – Vertical tail taper ratio

1.0 Introduction

In this chapter, the plane's weight will be more accurately estimated according to Class II standards, as opposed to Class I calculations. Class II calculations will use a separate set of equations and methods to obtain an accurate weight value of each component. The weight calculations will be done under the commercial transport category, rather than as a general aviation or military grade aircraft.

2.0 Known Weights

Several airplane components and structures are known or are unable to be properly estimated for, as previously found in the Class I design process. These items include the following: payload, crew, dry engines, fuel and trapped oil and fuel.

Table 1: Known weights.

System Component	Notes	Weight (lbs)
Payload*	8 Passenger, 2 bags per pass	8(200) + 8(2*25)
	*Payload Total	2000
Crew**	2 Crew (1 pilot min)	2(200)
	**Crew Total	400
Fuel	Class I Design	11050
Trapped oil and fuel	Estimate	100
Engines (dry weight)	Honeywell HTF 7500	1524
Total		15074

3.0 Estimate Weights

The following step will calculate the remaining weights of the plane's structure, powerplant and fixed equipment. The collective weights of these three categories will result in the plane's final empty weight.

3.1 Structure Weight

The plane's structure is the weight of the plane as if it were only the shell of the aircraft, without furnishings or operational mechanics. The structure weight will include the weights of the wing, empennage, fuselage, nacelles and landing gear. The total structure weight equation is shown below.

$$W_{\text{struct}} = W_w + W_{\text{emp}} + W_f + W_n + W_g \quad (1)$$

3.1.1 Wing

The weight of the wing will be calculated for an empty wing. This calculation will include the weights of ailerons and flaps, without additional subsystem. The following equation will be used.

$$W_w = \frac{\{0.00428(S^{0.48})(A)(M_H)^{0.43}(W_{TO}n_{ult})^{0.84}(\lambda)^{0.14}\}}{\{[100(t/c)_m]^{0.76}(\cos \Lambda_{1/2})^{1.54}\}} \quad (2)$$

The following equation's variables are defined below.

Table 2: Variable definition to determine wing weight.

Variable	Definition	Value
S	Wing area	416.9 ft ²
A	Wing aspect ratio	7.5
M _H	Max Mach at sea level	.69
W _{TO}	Takeoff weight	29600 lbs
n _{ult}	Ultimate load	3.8g's
λ	Wing taper ratio	.42

t/c _m	Maximum thickness ratio	.18
Λ _{1/2}	Sweep angle at ½ chord	22°

After inputting the following variables, the wing weight was calculated to be 958.387 lbs.

3.1.2 Empennage

The weight of the empennage will calculate the weight of the vertical and horizontal stabilizer as two separate weights. These two components will then be added together to obtain the complete empennage weight, as shown in the equation below.

$$W_{emp} = W_h + W_v \quad (3)$$

3.1.2.1 Horizontal Stabilizer

The following equation will be used to determine the weight of the horizontal stabilizer.

$$W_h = 0.0034 \{ (W_{TO^{n_{ult}}})^{0.813} (S_h)^{0.584} x \\ x (b_h/t_{r_h})^{0.033} (\bar{c}/l_h)^{0.28} \}^{0.915} \quad (4)$$

The following table defines the variables of the horizontal stabilizer's weight equation. Several variables have been defined previously and will be omitted from future tables.

Table 3: Variable definition to determine horizontal stabilizer weight.

Variable	Definition	Value
S _h	Horizontal wing area	99.76 ft ²
b _h	Horizontal span	21.88 ft
t _{r_h}	Max root thickness	.738 ft
\bar{c}	Wing mean geometric chord	4.56 ft ²
l _h	Dist. between wing ¼ chord and horizontal ¼ chord	27.1 ft

The horizontal tail weight was calculated to be 865.99 lbs.

3.1.2.2 Vertical Stabilizer

The following equation will be used to determine the weight of the vertical stabilizer.

$$W_v = 0.19 \{ (1 + z_h/b_v)^{0.5} (W_{TO^{n_{ult}}})^{0.363} (S_v)^{1.089} (M_H)^{0.601} x \\ x (l_v)^{-0.726} (1 + S_r/S_v)^{0.217} (A_v)^{0.337} (1 + \lambda_v)^{0.363} x \\ x (\cos \Lambda_{1/4_v})^{-0.484} \}^{1.014} \quad (5)$$

The following table defines the variables of the vertical stabilizer's weight equation.

Table 4: Variable definition to determine horizontal stabilizer weight.

Variable	Definition	Value
z _h	Dist. from vertical tail root to horizontal tail root	9.84 ft
b _v	Vertical span	10.6 ft
S _v	Vertical wing area	93.63 ft ²
l _v	Dist. between wing ¼ chord and vertical ¼ chord	19.685 ft
S _r	Rudder area	15.92 ft ²
A _v	Aspect ratio of vertical	1.2
λ _v	Vertical taper ratio	.52

$\Lambda_{1/4v}$	Vertical sweep angle at 1/4 chord	41.5°
------------------	-----------------------------------	-------

The vertical tail weight was calculated to be 370.753 lbs.

The total empennage weight, the combined weight of the vertical and horizontal stabilizer, was totaled to be 1236.74 lbs. Although the tail is heavier than the wing, the additional structural supports of the t-tail are accounted for in the vertical stabilizer equation.

3.1.3 Fuselage

The fuselage weight will be found with the following equation.

$$w_f = 2 \times 10.43 (K_{inl})^{1.42} (\bar{q}_D/100)^{0.283} (w_{TO}/1000)^{0.95} (l_f/h_f)^{0.71} \quad (6)$$

The following table defines the variables of the fuselage weight equation.

Table 5: Variable definition to determine fuselage weight.

Variable	Definition	Value
K_{inl}	Inlet constant	1
\bar{q}	Design dive dynamic pressure	460 psf
l_f	Fuselage length	47.244 ft
h_f	Fuselage height	ft

The dive dynamic pressure was assumed as it was not already defined previously. The pressure is the pressure of the jet transport example in Roskam [1]. The empty fuselage weight was calculated as 3474.57 lbs.

3.1.4 Nacelle

The weight of the nacelles, the housing compartment for the engines, will be computed for the Honeywell HTF 7500 engine size. The engine chosen was based on Class I design process' performance constraint analysis. The engine weight sizing falls under the high bypass turbofan category. The following equation is used to determine the weight of the nacelles.

$$w_n = 7.435 (N_{inl}) \{ (A_{inl})^{0.5} (l_n) (P_2) \}^{0.731} \quad (7)$$

The following table defines the variables of the nacelle weight equation.

Table 6: Variable definition to determine fuselage weight.

Variable	Definition	Value
N_{inl}	Number of inlets	2
A_{inl}	Capture area per inlet	25.52 ft ²
l_n	Nacelle length from inlet lip to compressor face	1.44 ft
P_2	Max Static pressure at engine compressor face (Avg Range: 15-50 psi)	33.5 psi

The collective weight of the two nacelles is 413.11 lbs.

3.1.5 Landing gear

The landing gear weight was previously found. The revised landing gear weight accounted for adjusted tires, shock absorbers and retraction kinematics. The weight of the nose gear is 146.24 lbs. The weight of the main landing gear is 737.04 lbs. thus, the total weight is 883.28 lbs.

3.1.6 Structure Weight Review

The total structure weight of the plane is the collective weights of the wing, empennage, fuselage, nacelles and landing gear. The total structure weight is 6966.08 lbs.

3.2 Powerplant Weight

The powerplant of the aircraft is the second of three weight categories which contribute to the plane's empty weight. The powerplant weight is compiled from the weights of the engine, air induction system, fuel system and propulsion system. The following equation lays out the powerplant weight.

$$W_{pwr} = W_e + W_{ai} + W_{fs} + W_p \quad (8)$$

3.2.1 Engine

The engine weight can be found by from manufacturers data. Honeywell defines the dry weight of the 7500E series engine to be 1364 lbs [2]. The dry weight is used as the fluids within the engine are estimated for in the trapped fuel and oil estimates.

3.2.2 Air Induction System

The air induction system is the method to supply air for buried engines. The business jet being designed will utilize a podded engine mount. The weight of the pods was accounted for in the weight calculation of the nacelles.

3.2.3 Fuel System

The fuel system, depending on its complexity and ability, will have a significant effect on the plane's overall weight. The weight will depend on whether the system is required to adjust the plane's center of gravity by moving the fuel around within the tanks to maintain a stable aircraft during flight. The business jet being designed will not have this feature based on the way the fuel is expected to be withdrawn from the tanks. The fuel system will be categorized as an integral wet wing tank. The following equation will be used to calculate the weight of the fuel system.

$$W_{fs} = 80(N_e + N_t - 1) + 15(N_t)^{0.5} (W_F / K_{fsp})^{0.333} \quad (9)$$

The following table defines the variables of the fuel system weight equation.

Table 7: Variable definition to determine fuel system weight. [3]

Variable	Definition	Value
N_e	Number of engines	2
N_t	Number of fuel tanks	3
W_F	Weight of fuel	11050 lbs
K_{fsp}	Specific weight of fuel	6.8 lbs/gal

The specific weight of fuel was found to be 6.8 lbs/gal for the generic compound. A specific compound was not defined previously or by the manufacturer. The fuel system weight was calculated to be 624.70 lbs.

3.2.4 Propulsion System

The propulsion system weight is more than just the engine. The propulsion system also accounts for the engine controls, starting system and thrust reversers. The following equation will be used to find the propulsion system weight.

$$W_p = W_{ec} + W_{ess} + W_{tr} \quad (10)$$

3.2.4.1 Engine control

The engine control weight calculation is categorized by engine mount placement. The business jet will fall under the fuselage mounted jet engine rather than wing tail mounted. The following equation will be used to determine the weight of the engine control.

$$W_{ec} = K_{ec} (1_f N_e)^{0.792} \quad (11)$$

The engine control constant, K_{ec} , falls under two categories: non- afterburning or afterburning engines. The business jet and engine will categorize the plane as a non-afterburning engine. The engine controls constant is .686. The length of the fuselage and number of engines has previously been defined. The weight of engine control components is 25.17 lbs.

3.2.4.2 Engine Starting System

The startup system to gain initial power for the engines is selected from two options: pneumatic or electrical startup. The engine will utilize a pneumatic starting system. The following equation will be used to calculate the weight of the startup system.

$$W_{ess} = 9.33(W_e/1,000)^{1.078} \quad (12)$$

The engine startup system weight was calculated to be 13.04 lbs.

3.2.4.3 Thrust Reversers

Thrust reversers are an important factor in helping the plane come to a stop in a shorter amount of time when landing. The following equation will be used to estimate the weight of the thrust reversers.

$$W_{tr} = 0.18W_e \quad (13)$$

The weight of the thrust reversers was calculated to be 245.52 lbs.

The propulsion weight, combination of engine control, startup system and thrust reversers, was calculated to be 283.72 lbs.

3.2.5 Powerplant Weight Review

The total power plant weight, combination of engine, air induction, fuel system and propulsion system, was calculated to be 2272.42 lbs.

3.3 Fixed Equipment Weight

The fixed equipment weight is a collection of subsystem weights, as well as several other important flight components. The following table and equation will make up the fixed equipment weight for the business jet.

Table 8: Fixed equipment components.

Fixed Equipment Components	
Flight control system	Hydraulic and pneumatic system
Electrical system	Instrumentation, avionics and electronics
Air-conditioning, pressurization, anti and deicing system	Oxygen System
Auxiliary power unit (APU)	Furnishings
Baggage and cargo handling equipment	Operational items
Flight test instrumentation	Auxiliary gear
Ballast	Paint

$$W_{feq} = W_{fc} + W_{hps} + W_{els} + W_{iae} + W_{api} + W_{ox} + W_{apu} + W_{fur} + W_{bc} + W_{ops} + W_{fti} + w_{aux} + W_{bal} + W_{pt} \quad (14)$$

3.3.1 Flight Control System

The flight control system weight estimation will estimate the weights of the aileron, flap, elevator and rudder. The following equation will be used.

$$W_{fc} = K_{fc} (W_{TO})^{2/3} \quad (15)$$

The flight control constant, K_{fc} , is .64. The takeoff weight will be the weight found in Class I design process, 29600 lbs. The flight control weight amounted to 612.41 lbs.

3.3.2 Hydraulic and Pneumatic System

The hydraulic and pneumatic system are a mixture of the two subsystems with overlapping duties on most planes. The proposed business jet will utilize only the hydraulic system. In determining the weight of the hydraulic system, it is typically included in the flight control system weight calculation. A range of ratios is presented to calculate the hydraulic system weight independently.

For business jets, Roskam states the hydraulic system weight can be estimated by a ratio of the plane's takeoff weight. The range is between 0.007 and 0.015 of the takeoff weight. An average of this range will be used. Thus, the hydraulic system weight, independent of the flight controls is 325.6 lbs. The independent flight control weight is then 286.81 lbs.

3.3.3 Electrical System

The electrical system weight is dependent on the passenger cabin volume, as evidenced by the following equation.

$$W_{els} = 10.8(V_{pax})^{0.7} \{1 - 0.018(V_{pax})^{0.35}\} \quad (16)$$

The passenger cabin will be assumed as a perfect cylindrical volume to simplify the process. The length of the cabin is 21.3255 ft. The height, or diameter, is 6 ft. Thus, the passenger cabin volume is 602.96 ft³. The electrical system weight is calculated as 792.74 lbs.

3.3.4 Instrumentation, avionics and electronics

The following calculation is for older model planes which do not utilize modern computer-based flight management and navigation systems. These equations will provide a conservative weight, thus lightening the plane's overall weight. A tolerance of 150 lbs will be assumed for the final weight of the modern computer system. The following equation will be used to calculate the flight avionics weight.

$$W_{iae} = \begin{matrix} flight\ instruments \\ + \\ enigne\ instruments \\ + \\ other\ instruments \end{matrix} \quad (17)$$

$$W_{iae} = [N_{pil} (15 + .032 \frac{W_{TO}}{1000})] + [N_e (5 + .006 \frac{W_{TO}}{1000})] + .15 \frac{W_{TO}}{1000} + .012W_{TO}$$

The number of pilots, N_{pil} , will be 2 at the most. This value may be adjusted depending on if the plane is employed with one pilot and one cabin crew or two pilots and no cabin crew. The maximum number of pilots will be used to calculate greatest weight of the aircraft to determine what the greatest possible takeoff weight is for the business jet. The plane will have two engines.

The calculated weight of the instrumentation, avionics and electronics is 401.89 lbs. With the added tolerance to modernize the system, the new weight will be 551.89 lbs.

3.3.5 Air-conditioning, Pressurization, Anti and Deicing System

The air-conditioning, pressurization and anti and deicing system can be calculated in relation to the passenger cabin volume, number of crew and number of passengers. The following equation will be used.

$$W_{api} = 469 \{V_{pax} (N_{cr} + N_{pax}) / 10,000\}^{0.419} \quad (18)$$

The number of crew members, N_{crew} , will be two. The number of passengers, N_{pax} , will be eight.

The calculated weight of the air-conditioning, pressurization, anti and deicing systems is 379.415 lbs.

3.3.6 Oxygen System

The oxygen system weight will be calculated by the following equation.

$$W_{ox} = 30 + 1.2N_{pax} \quad (19)$$

The weight of the oxygen system was calculated to be 39.6 lbs.

3.3.7 Auxiliary Power Unit (APU)

The auxiliary power unit will provide the plane with power while grounded. The weight of the APU should be provided by the manufacturer, however, it was unable to be found. Thus, the weight will be calculated for with the following equation.

$$W_{apu} = .0085W_{TO} \quad (20)$$

As mentioned previously the takeoff weight will be the maximum takeoff weight calculated from the Class I design process.

The APU weight was calculated to be 251.6 lbs.

3.3.8 Furnishings

Furnishing weight calculation includes the following items: interior cabin details, galley, lavatory, cockpit design and escape and firefighting equipment. The following equation will be used to determine the furnishing weight.

$$W_{fur} = \text{flight deck crew} + \text{passenger} + \text{cabin crew} + \text{lavatory and water} \\ + \text{food provisions} + \text{cabin windows} + \text{other}$$

$$W_{fur} = [55N_{fdc}] + [32N_{pax}] + [15N_{cc}] + [K_{lav}(N_{pax})^{1.33}] + [K_{buf}(N_{pax})^{1.12}] + \\ \left\{ 109 \left[\frac{N_{pax}(1+P_c)^{.505}}{100} \right] \right\} + [.771 \left(\frac{W_{TO}}{1000} \right)] \quad (21)$$

The following table defines the variables of the furnishings weight equation.

Table 9: Variable definition to determine air-conditioning, pressurization, anti and deicing system weight. [4]

Variable	Definition	Value
N_{fdc}	Number of flight deck crew	1
N_{pax}	Number of passengers	8
N_{cc}	Number of cabin crew	1
K_{lav}	Lavatory constant	3.90
K_{buf}	Food constant	3.35
P_c	Ultimate design cabin pressure	10.9 psi

The number of crew aboard the plane will be one pilot and one cabin crew. Rather than two pilots and no cabin crew, this presented configuration is what is anticipated to be chosen by the passengers. The lavatory constant is categorized based on plane category, this value is for a business jet. The food constant is an average of short range and long-range flights. The cabin pressure is set to 8000 ft, which corresponds to 10.9 psi. The weight of the plane's inner furnishings is calculated to be 551.51 lbs.

3.3.9 Baggage and Cargo Handling Equipment

With limited cargo area under the cabin subfloor, the cabin closets will be used to store the passenger and crew luggage. Thus, no extra luggage handling equipment is needed other than human power.

3.3.10 Operational Items

Operational items include food, potable water, drinks, plates and silverware and lavatory supplies. These items were accounted for in the furnishings calculation. The isolated weight of these items was found as 119.186 lbs.

3.3.11 Flight Test Instrumentation

The flight test instrumentation does not have a definitive method of calculating an accurate weight. Roskam recommends observing the weight breakdowns of several NASA X airplanes as a method of determining a range of weights for the instrumentation. The weight ranges from 100 lbs to 600 lbs of similarly powered aircraft [1]. Although these planes do not match the mission requirements of this business jet, this is the best option of determining an accurate weight. An average of this range will be used as the weight of the test instrumentations, thus, the flight test instrumentation will weigh 350 lbs.

3.3.12 Auxiliary Gear

Auxiliary gear are items which are not necessities to fly the aircraft, but serve other purposes required by law. Such items include smoke detectors, fire extinguishers, fire axes, sextants and paper maps among other items. These items are limited and an estimate weight for these items can be calculated as a ratio of the plane's proposed empty weight.

$$W_{aux} = .01W_E \quad (22)$$

The previously found empty weight, according to Class I sizing, is 16000 lbs. Therefore, the auxiliary items weight is 160 lbs.

3.3.13 Ballast

The ballast is either a movable or fixed weight to help to airplane achieve or maintain a stable center of gravity point. This will be revisited if the weight and balance analysis deems it is necessary.

3.3.14 Paint

The paint on the exterior of the plane is a minor detail in the weight calculation. The weight will be estimated based on takeoff weight rather than surface area. The surface area will not be used in the calculation as it is difficult in computing every inch with curves, indent and protrusions that can occur at any point along the plane's body. The following equation will be used to estimate the weight of paint.

$$W_{pt} = 0.003 - 0.006W_{TO} \quad (23)$$

The weight of the paint will be 177.60 lbs.

3.3.15 Fixed Equipment Weight Review

The final fixed equipment weight can now be calculated. This value will be revisited and may be changed if the plane's center of gravity becomes an issue. The final fixed equipment weight is 3516.76 lbs.

4.0 Final Weight Review

The plane's final empty weight can now be found. The empty weight is the sum of the structure, powerplant and fixed equipment weight. The business jet's empty weight is 12,755.26 lbs. The new weights are as follows in the table below.

Table 10: Revised plane weights

W_E	W_F	Max $W_{payload}$	Max W_{TO}
12755.26 lbs	11050 lbs	2400 lbs	26205.26 lbs

References

- [1] Roskam, J. (1989). Airplane Design Part IV: Layout Design of Landing Gear and Systems. University of Kansas.

- [2] HTF7000 TURBOFAN ENGINE. (2016). Retrieved July 11, 2018, from https://aerospace.honeywell.com/en/~media/aerospace/files/brochures/htf7000_turbofan_bro_low.pdf
- [3] Lawicki, D. (n.d.). [Http://www.smartcockpit.com/docs/Jet_Fuel_Characteristics.pdf](http://www.smartcockpit.com/docs/Jet_Fuel_Characteristics.pdf). Retrieved July 11, 2018, from http://www.smartcockpit.com/docs/Jet_Fuel_Characteristics.pdf
- [4] Altitude above Sea Level and Air Pressure. (n.d.). Retrieved July 11, 2018, from https://www.engineeringtoolbox.com/air-altitude-pressure-d_462.html

Chapter 6

V-n Diagram

Symbols

\bar{c} – Wing mean geometric chord length

C_{L_max} – Maximum coefficient of lift

$C_{L\alpha}$ – Coefficient of lift versus angle of attack

C_{N_max} – Maximum normal force coefficient

g – Gravity constant

GW – Gross weight

K_g – Gust alleviation factor

$n_{lim\ neg}$ – Negative limit load factor

$n_{lim\ pos}$ – Positive limit load factor

S – Wing area

U_{de} – derived gust velocities

V – True airspeed

V_A – Design Maneuvering speed

V_B – Design speed for maximum gust intensity

V_C – Design cruise speed

V_D – Design dive speed

V_{S1} – +1g stall speed

μ_g – Airplane mass ratio

ρ – Air density

1.0 Introduction

This chapter will construct a V-n diagram to display the limitations of the aircraft at different velocities. The +1g stall speed, cruising speed, design diving speed, maneuvering speed, speed for max gust, negative stall speed, limit load factor and gust load factor lines will make up the V-n diagram. The diagram will be constructed under cruising stage characteristics.

2.0 +1g Stall Speed

The +1g stall speed will be calculated using the plane's gross weight, wing area, air density and maximum normal force coefficient. The following equation will be used.

$$V_{S_1} = \{2(GW/S) / \rho C_{N_max}\}^{1/2} \quad (1)$$

The only unknown, the maximum normal force, can be found with the following equation, where the maximum coefficient of lift during cruise is 2.0.

$$C_{N_max} = 1.1C_{L_max} \quad (2)$$

The max normal force coefficient is calculated as 2.2. The +1g stall speed was calculated to be 147.78 fps, or 87.56 knots.

3.0 Design Limit Load Factor

3.1 Positive Limit Load Factor

The design limit load factor will determine the maximum speed at which the plane may safely perform a maneuver. The positive limit will be calculated first as the following equation is presented. The positive limit load must be greater than 2.5 at all times, this is a rule of thumb presented by Roskam [2]. The newly found max takeoff weight, 26205.26 lbs, will be assumed to display the effects of an extreme case.

$$n_{lim_{pos}} \geq 2.1 + \{24,000 / (W + 10,000)\} \quad (3)$$

The positive limit load factor was found to be 2.76. This value is greater than the 2.5 minimum, thus, the calculated value is acceptable.

3.2 Negative Limit Load Factor

The negative limit load factor, $n_{lim_{neg}}$, may be stated before proceeding. Roskam states that the negative limit should be set to a load factor of -1.

4.0 Design Maneuvering Speed

Determining the design maneuvering speed relates the design cruising speed and limit load factor. The following equation will be used for both positive and negative loads.

$$V_A \geq V_{S1} n_{lim}^{1/2} \quad (4)$$

The design maneuvering speed was calculated to be 145.54 knots and 87.56 knots for the positive and negative load, respectively. The maneuvering speed should be greater than the values calculated to ensure the plane is able to maintain flight.

5.0 Gust Load Factor Lines

The gust load factor lines will be used to find the remaining safety parameters for the business jet to safely perform maneuver. The following equation will be used for points, B, C and D.

$$n_{lim} = 1 + (K_g U_{de} V C_{L_{\alpha}}) / 498 (GW/S) \quad (5)$$

Where the gust alleviation factor is defined by the following equation.

$$K_g = 0.88 \mu_g / (5.3 + \mu_g) \quad (6)$$

The airplane mass ratio is defined by the following equation. The coefficient of lift versus alpha is .11 for the NACA 64008a airfoil [1].

$$\mu_g = 2 (GW/S) / \rho c g C_{L_{\alpha}} \quad (7)$$

The main determining factor of each scenario is the derived gust velocities, U_{de} .

Velocity B will be used as a reference point. Velocities C and D will be used as data points for the plane's limitations. Each velocity factor will utilize a different method for obtaining the derived gust velocities. The calculations will be conducted at cruising altitude, 35000 ft. The following table shows the different methods.

Table 1: Derived gust velocity scenarios.

Velocity	Equation
B	$U_{de} = 47.33 - 0.000933h$
C	$U_{de} = 66.67 - 0.000833h$

D	$U_{de} = 16.67 - 0.000417h$
---	------------------------------

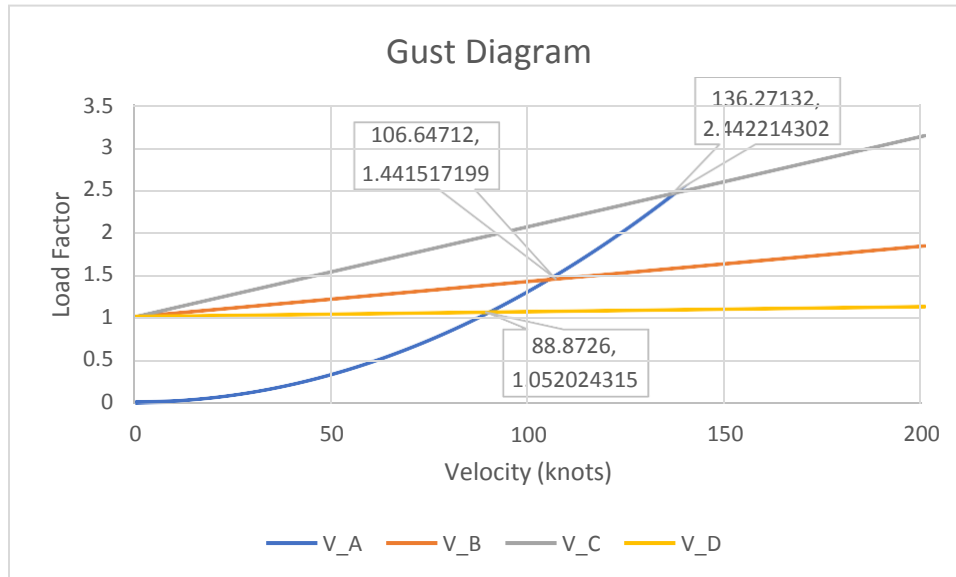


Figure 1: Gust diagram.

From this graph, the design speed for maximum gust, V_B , should not fall below 106.65 knots. The design cruise speed, V_C , should not fall below 136.27 knots. The design dive speed, V_D , should not fall below 88.87 knots.

5.1 Design Speed for Max Gust Intensity

The design speed for maximum gust intensity intersects with the $C_{N_{max}}$ line at 106.647 knots. A lower velocity during max gust than the cruise velocity is acceptable as the wind is expected to be acting against the business jet, creating, in theory, a higher cruising velocity with respect to the gust velocity than the geographical positioning.

5.2 Design Cruising Speed

The design cruise speed should not fall below the previously found value of 136.27 knots. It is recommended that the cruise speed be found in relation to the max gust intensity speed. The cruise speed should be greater as to avoid speed fluctuations likely to occur with changing atmospheric turbulence. The following equation will be used to find the new design cruise speed.

$$V_C \geq V_B + 43 \text{ kts} \quad (8)$$

The redesigned cruise speed will be 149.65 knots.

5.3 Design Diving Speed

The design dive speed will be found in relation to the plane's cruise speed, as shown in the equation below.

$$V_D \geq 1.25V_C \quad (9)$$

The new design dive speed will be 187.06 knots.

6.0 Negative Stall Speed Line

The negative stall speed line is found similarly to the +1g stall speed. As opposed to a positive maximum normal force coefficient, it will be negative. As previously stated, Roskam informs that the negative limit load factor is restricted to -1.

7.0 V-n Diagram Overview

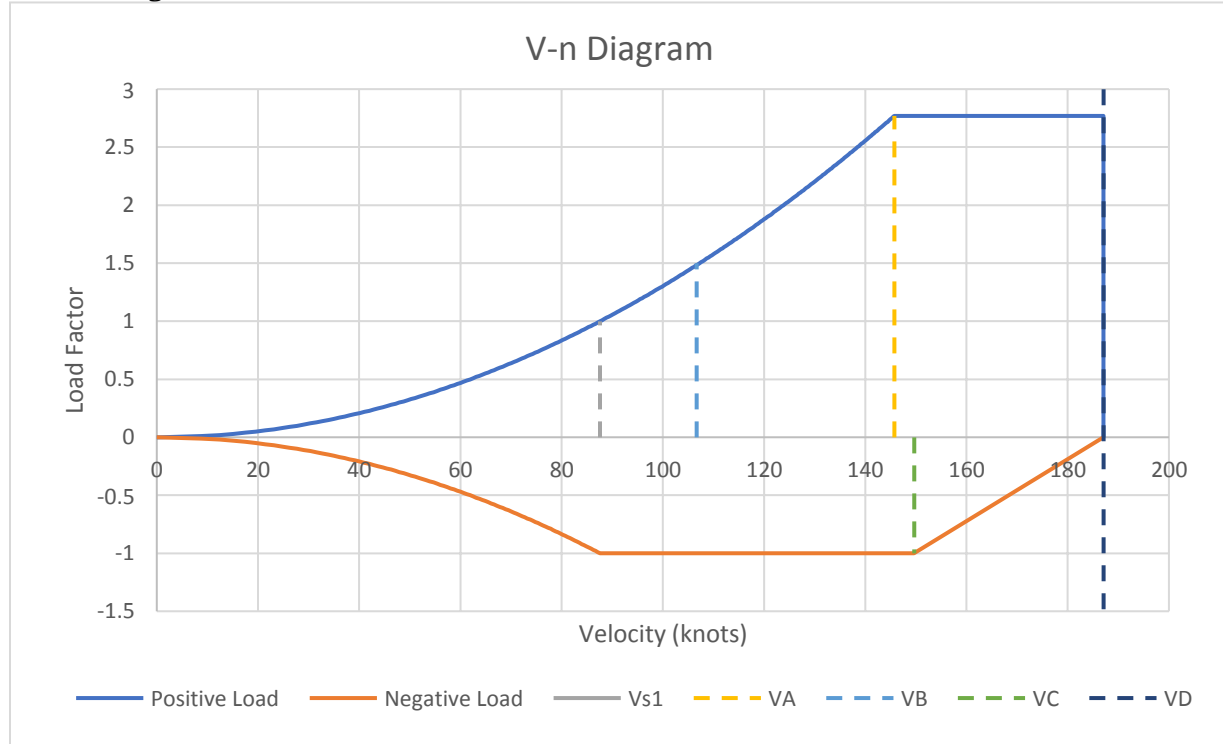


Figure 2: V-n Diagram.

The graph above shows the plane's minimal speed requirements depending on flight conditions. The illustration depicts the plane's ability to perform and maintain maneuvers during flight. The conditions laid out from the graph are minimal speed and load requirements at which the plane should fly at to maintain flight.

References

- [1] NACA 64-008A AIRFOIL. (2018). Retrieved July 11, 2018, from <http://airfoiltools.com/airfoil/details?airfoil=n64008a-il>
- [2] Roskam, J. (1989). Airplane Design Part IV: Layout Design of Landing Gear and Systems. University of Kansas.

Chapter 7

Weight and Balance Analysis

Symbols

AC – Aerodynamic center

APU – Auxiliary power unit

\bar{c} – Wing mean geometric chord length

C_1 – Aerodynamic constant one

C_2 – Aerodynamic constant two

CG – Center of gravity

$C_{L_{\alpha_h}}$ – C_L vs alpha of horizontal stabilizer

$C_{L_{\alpha_{wb}}}$ – C_L vs alpha of wing body

$\delta x_{cg}/\delta x_i$ – Change in center of gravity with movement of item i

$d\epsilon/d\alpha$ – Downwash vs angle of attack

$\Delta x_{ac_{wb}}$ – Change in aerodynamic center of wing-body

Δx_w – Change in wing position

ft – Feet

S – Wing area

S_h – Size of horizontal stabilizer

TBD – To be determined

W_i – Weight of item i

wrt – With respect to

W_w – Weight of wing

x_{ac} – Aerodynamic center long x-axis

x_{ac_h} – Aerodynamic center of horizontal stabilizer

$x_{ac_{new}}$ – New aerodynamic center along x-axis

x_{ac_w} – Aerodynamic center of wing

x_{cg} – Center of gravity along x-axis

$x_{cg_{new}}$ – New center of gravity along x-axis

$x_{cg_{old}}$ – Old center of gravity along x-axis

x_i – position of item i

X_{LE} – Position of leading edge of wing

1.0 Introduction

The purpose of this chapter is to ensure the plane's center of gravity position will not negatively affect the plane's performance before, during and after flight. All center of gravities processes are referenced from Roskam. [1]

2.0 Locating Center of Gravities

The center of gravity measurements will be found separately for the structural, powerplant and fixed equipment components. The location of the center of gravity must also

account for the plane satisfying the tip over criteria of the landing gear, both in the longitudinal and lateral directions. The y-axis center of gravity will be zero as the assumption will be made that all components will be symmetrical.

2.1 Structural

2.1.1 Wing

The wing's center of gravity position will be found based on the general geometry of the wing, either being swept or unswept. As previously stated, the business jet will utilize a swept wing. The position of the wing's center of gravity is 70% of the distance between the front and rear spar, or at 35% of the semi spar location. With the structural layout not fully designed in this process, an assumed position of the spar locations will be made to allow for the calculation. The spar locations will be at the extremes of the wing root.

The wing root chord length is 10.5 ft. The center of gravity point will be 7.35 ft behind the leading edge of the wing. With respect to the nose, the wing's leading edge begins at 17.957 ft. Thus, the wing's center of gravity with respect to the nose is 25.307 ft.

2.1.2 Horizontal Tail

Regardless of the sweep angle of the horizontal tail, the center of gravity process be the same for all horizontal tail geometries. The center of gravity location can be found as 42% of the horizontal tail chord length from the leading edge.

The horizontal tail root chord length is 6.7 ft. The center of gravity position will be 2.814 ft behind the leading edge of the horizontal tail. The position of the horizontal tail's leading edge with respect to the nose is 47.244 ft. The horizontal tail's center of gravity with respect to the nose is 50.058 ft.

2.1.3 Vertical Tail

The center of gravity location of the vertical tail can be found as 38% of the root chord length. The root chord length of the vertical stabilizer is 11.62 ft. The center of gravity point will be 4.4156 ft aft of the leading edge. With respect to the nose of the aircraft, the center of gravity position of the vertical stabilizer will be 45.43 ft.

2.1.4 Fuselage

The center of gravity of the fuselage process is categorized on the proposed propulsion system. The business jet is classified under the jet transport category and rear fuselage mounted engine subcategory. This subcategory estimates the center of gravity range to be between 47% and 50% of the total fuselage length. The average of the range will be assumed because of the lack of extreme weight concentrations to build the fuselage. The center of gravity will be at 48.5% of the fuselage length. The center of gravity of the fuselage, with respect to the nose, is 23.868 ft.

2.1.5 Nacelle

The nacelles, which house the engines, center of gravity can be found as 40% of the nacelle length. The length is from the opening of the nacelle until the end of the plug. The nacelle length total is 7.874 ft. The center of gravity of each nacelle with respect to the nacelle

opening is 3.1496 ft. With respect to the nose of the aircraft, the nacelle center of gravity is 36.942 ft.

2.1.6 Landing Gear

Roskam states that the landing gear center of gravity is 50% of the strut length, but this process will only influence the z-axis center of gravity position of the aircraft. The landing gear strut length will be 3 ft. Thus, the center of gravity of the landing gear with respect to the ground will be 1.5 ft.

The x-axis positioning does not have a definitive process on finding a location, as well as the possibility of moving the landing gear positioning to satisfy the tip over criteria. An assumption will be made based off the Class I sizing as to the location of the center of gravity along the x- axis. Knowing the weights of the nose and main landing gear, 146 lbs and 737 lbs, respectively, the center of gravity will favor the main landing gear. The center of gravity position will be estimated at 20 ft with respect to the nose.

2.1.7 Structural Center of Gravity Review

As a brief review of the structural components CG location, the following table is presented.

Table 1: Structural center of gravities.

Structural Component	Center of Gravity Location (WRT nose) (ft)
Wing	25.307
Horizontal Tail	50.058
Vertical Tail (T-tail)	45.43
Fuselage	23.868
Nacelles	36.942
Landing Gear	20

2.2 Powerplant

2.2.1 Engines

Roskam states to use the manufacturer's data to determine the engine's center of gravity. The Honeywell HTF 7500 center of gravity was unable to be obtained from the manufacturer's data. An assumption will be made that the engine's center of gravity will be estimated as the nacelle. This can be made because the areas of the nacelle which are expected to be strengthened will be used to support the engine weight concentrations. The engine's center of gravity will be 36.942 ft, with respect to the nose.

2.2.2 Fuel System

The fuel systems purpose will be to transfer the fuel from the wing and fuselage tanks to the engines. The fuel system weight will be assumed as an equally distributed weight between the fuel tanks and the engine location. The center of gravity of the fuel system will be 29.692 ft with respect to the nose of the aircraft.

2.2.3 Filled Fuel Tank

The plane will utilize three tanks when fully fueled. The center of gravity of the fuel tanks will resemble the center of gravity of the wing. The central fuselage fuel tank will be

centered under the wing to help maintain the center of gravity if the plane were to have employed only the wing fuel tanks. The filled fuel tanks will maintain a center of gravity position of 25.307 ft with respect to the nose of the aircraft.

2.2.4 Trapped Fuel and Oil

The trapped fuel and oil will account for the remaining unused or unobtainable fuel in the fuel tank and fuel lines. Roskam states that the trapped oil and fuel will primarily collect closest to the engine casing, assuming the engines are wing mounted. A new assumption must be made that the trapped oil and fuel will be located in between the fuel tanks and engines. The center of gravity of the trapped oil and fuel will be 31.168 ft with respect to the nose of the aircraft.

2.2.5 Propulsion System

The propulsion system utilizes more than just the engine. The propulsion system will use an engine control, starting system and thrust reversers. The method of determining the center of gravity is to be found based on estimations.

The engine control module is used to control actuators and internal combustion measurements to ensure maximum efficiency of the engines. This will be placed around the combustion chamber of the engine. The center of gravity of the engine control module will be 37.07 ft with respect to the nose of the aircraft.

The engine starting system is used to gain initial power for the engines. This will be placed closer to the opening and fan blades of the engine. The center of gravity of the starting system will be 36.417 ft with respect to the nose of the aircraft.

The thrust reversers are used to redirect air from the engines to help slow the plane. The thrust reversers will be after the combustion process and when the air passes through a separate set of channels and redirects the air opposite of positive thrust. The center of gravity of the thrust reversers will be 40.026 ft with respect to the nose of the aircraft.

2.2.6 Powerplant Center of Gravity Review

As a brief review of the powerplant components CG location, the following table is presented.

Table 2: Powerplant center of gravities.

Powerplant Component	Center of Gravity Location (WRT nose) (ft)
Engines	36.942
Fuel System	29.692
Filled Fuel Tank	25.307
Trapped Oil and Fuel	31.168
Engine Control Module	37.07
Engine Starting System	36.417
Thrust Reversers	40.026

2.3 Fixed Equipment

The center of gravity of most of the systems will be assumed for and estimated based on anticipated available space and location.

2.3.1 Flight Control System

The flight control system is a collection of the necessary control surfaces to maneuver the plane. These items consist of the aileron, flap, rudder and elevator. The ailerons and flaps are installed on the wing, as the rudder and elevator are a part of the empennage. The dual aileron and flap will be larger than the singular elevator and rudder. The center of gravity will favor the aileron and flaps. The center of gravity of the flight control system with respect to the nose will be 36.089 ft.

2.3.2 Hydraulic and Pneumatic System

The hydraulic and pneumatic system will be used to control the flight control system. The business jet will utilize a hydraulically powered system. The weight calculation of the hydraulic system is accounted for in the flight control system, thus it will be isolated and accounted for independently. The hydraulic system will require a reservoir for hydraulic fluid to power the movement of the flight control surfaces. The reservoir will be placed forward of the fuel tanks to help counter the position of numerous center of gravity locations previously found. The hydraulic system center of gravity will be 19.685 ft with respect to the nose of the aircraft.

2.3.3 Electrical System

The electrical system is used to power the internal electronics and lighting amongst other intended uses. The electrical system weight includes wiring and a battery to store extra generated electricity from the turbine generator. The battery will be placed ahead of the central fuselage fuel tanks to help offset several rear CGs. The center of gravity of the electrical system will be 24.6063 ft.

2.3.4 Instrumentation, Avionics and Electronics

The instrumentation, avionics and electronics will be centralized in the cockpit and forward areas of the passenger cabin. The center of gravity of the instrumentation, avionics and electronics will be 6.15 ft with respect to the nose of the aircraft.

2.3.5 Air-conditioning, Pressurization, Anti and Deicing System

The air-conditioning, pressurization, anti and deicing system will be spread throughout the cockpit and passenger cabin area. The air ventilation system will be throughout the plane with the air being provided by bleed air recycled by the engine. The center of gravity will be 15.748 ft with respect to the nose of the aircraft.

2.3.6 Oxygen System

The oxygen system will coincide with the air-conditioning and pressurization system. The main difference will be the need for tanks to supply the cabin and cockpit with extra oxygen to maintain a comfortable cabin altitude pressure. The oxygen tanks will be located in the closets as they will need to be replenished or replaced after a certain number of flight hours. The oxygen system will also provide emergency oxygen masks if cabin pressurization were to fail. The oxygen system's center of gravity will be 12.303 ft with respect to the nose of the aircraft.

2.3.7 Auxiliary Power Unit (APU)

The APU will be used when the plane is grounded and requires electricity without running the engines to conserve the fuel tanks. The APU will be placed towards the rear of the

aircraft to allow for an exhaust opening that will not negatively affect the plane's aerodynamic properties. The APU center of gravity will be 43.061 ft with respect to the nose of the aircraft.

2.3.8 Furnishings

The furnishings are spread throughout the passenger cabin area and cockpit. The center of gravity position will be based on the chair positioning, as it will be difficult to include the furnishings finishes and weight densities. The center of gravity of the furnishings will be 16.499 ft with respect to the nose of the aircraft.

2.3.9 Operational Items

Operational items include food, water plates and silverware amongst other items. These items may be moved around the cabin storage areas to enhance the plane's overall center of gravity. With the possibility of storing these items in closet A, B, C or D/bar area, the assumption will be to store these items in closet A. Closet A was chosen because if a cabin crew member were to be assigned, this area would be best for the crew to prepare food and beverages for passengers without interfering with passenger conversations and activities. The clean water however will need an area to be stored, this will be ahead of the fuselage fuel tank and electrical system battery. The center of gravity of the operational items will be 9.145 ft with respect to the nose of the aircraft.

2.3.10 Flight Test Instrumentation

The flight test instrumentation will record data of the flight, both independent and dependent quantities. This collection of data can either be stored to be analyzed in the future or can be read in live time by the crew in the cockpit. To simplify the wiring, the location of the flight test instrumentation will be positioned in the cockpit area. The center of gravity will be 3.076 ft with respect to the nose of the aircraft.

2.3.11 Auxiliary Gear

The auxiliary gear carried within the aircraft vary in desirable locations. The smoke detectors, fire extinguishers and axes should be located throughout the cabin and lavatory. The sextons, maps and external GPS should be in or near the cockpit. These items will be estimated and assumed to be stored in closet B. The smoke detectors are considerably light and non-numerous that the weight will be neglected in the center of gravity determination. The center of gravity of the auxiliary gear will be 12.310 ft with respect to the nose of the aircraft.

2.3.12 Ballast

The ballast center of gravity will not be assigned until after completing the weight and balance final analysis to determine if the center of gravity positioning must change.

2.3.14 Paint

The painted areas include the exterior of the plane. The best way to determine the center of gravity of the paint would be to treat each main structural item individually. The fuselage paint would likely be at the center of the fuselage. The wing and empennage paint will likely cancel one another out. The nacelle would be the tipping structural component that will skew the center of gravity of the plane's overall painted weight towards the rear of the plane. The plane's paint center of gravity will be 29.528 ft with respect to the nose of the aircraft.

2.3.15 Fixed Equipment Center of Gravity Review

As a brief review of the fixed equipment components CG location, the following table is presented.

Table 3: Powerplant center of gravities.

Fixed Equipment Component	Center of Gravity Location (WRT nose) (ft)
Flight Control System	36.089
Hydraulic System	19.685
Electrical System	24.606
Instrumentation, Avionics and Electronics	6.150
Air-conditioning, Pressurization, Anti and Deicing System	15.748
Oxygen System	12.303
Auxiliary Power Unit (APU)	43.061
Furnishings	16.499
Operational Items	9.145
Flight Test Instrumentation	3.076
Auxiliary Gear	12.310
Ballast	TBD
Paint	29.528

2.4 Known Weights

2.4.1 Payload

The payload carried by the aircraft is intended to be the maximum number of passengers and their baggage. To ensure the plane will remain stable at all instances when the plane is on the ground or in flight, the passenger and luggage will be centralized in the rear of the cabin area. The center of gravity of the payload will be 22.962 ft with respect to the nose of the aircraft.

2.4.2 Crew

The crew's center of gravity will be centered in the cockpit. This analysis is anticipated for two pilots rather than for the single pilot single cabin crew. The crew center of gravity will be 4.839 ft with respect to the nose of the aircraft.

3.0 Weight and Balance Analysis

The following table displays all of the component weight and center of gravity positions with respect to the nose of the aircraft.

Table 4: Collective review of center of gravities.

	Plane Component	Weight (lbs)	Center of Gravity (ft)
Known	Payload	2000	22.962
	Crew	400	4.839
Structure	Wing	958.387	25.307
	Horizontal Tail	865.99	50.058

	Vertical Tail	370.753	45.43
	Fuselage	3474.57	23.868
	Nacelle	413.11	36.942
	Landing gear	883.28	20
Powerplant	Engine (dry)	1364	36.942
	Fuel System	624.70	29.692
	Filled Fuel Tank	11050	25.307
	Trapped Oil and Fuel	100	31.168
	Engine Control Module	25.17	37.07
	Engine Starting System	13.04	36.417
	Thrust Reversers	283.72	40.026
Fixed Equipment	Flight Control System	286.81	36.089
	Hydraulic System	325.6	19.685
	Electrical System	792.74	24.606
	Instrumentation, Avionics and Electronics	551.89	6.150
	Air-conditioning, Pressurization, Anti and Deicing System	379.415	15.748
	Oxygen System	39.6	12.303
	Auxiliary Power Unit (APU)	251.6	43.061
	Furnishings	551.51	16.499
	Operational Items	119.186	9.145
	Flight Test Instrumentation	350	3.076
	Auxiliary Gear	160	12.310
	Ballast	TBD	TBD
	Paint	177.60	29.528

3.1 Effects of Moving Components

The overall plane's center of gravity will be determined first with the following equation.

$$x_{cg} = \frac{\sum_{i=1}^{i=n} W_i x_i}{\sum W_i}$$

The plane's new center of gravity location is 25.641 ft with respect to the nose of the aircraft. With a noticeably different overall center of gravity, the landing gear will need to be readjusted to satisfy the tip over criteria.

The new center of gravity was found to be 25.66 ft with respect to the nose, with a slight adjustment to set the main landing gear further aft. The new center of gravity may need to be adjusted, with an addition of ballast weight, based on further analysis. The change in the plane's center of gravity will also require a readjustment of the main landing gear to satisfy the

longitudinal tip over criteria. The new position of the main landing gear will be 27.167 ft with respect to the nose of the aircraft.

By moving components around, the plane's center of gravity will change as well. The following equation will be used to examine how each item will affect the plane's center of gravity location.

$$\partial x_{cg} / \partial x_i = (W_i) / (\sum_{i=1}^{i=n} W_i)$$

Table 5: Weight adjustment sensitivities

	Plane Component	Weight (lbs)	$\delta x_{cg} / \delta x_i$	
Known	Payload	2000	.0746	
	Crew	400	.0149	
Structure	Wing	958.387	.0357	
	Horizontal Tail	865.99	.0138	
	Vertical Tail	370.753	.0138	
	Fuselage	3474.57	.1296	
	Nacelle	413.11	.0154	
	Landing gear	883.28	.0329	
	Powerplant	Engine (dry)	1364	.0509
		Fuel System	624.70	.0233
Filled Fuel Tank		11050	.4121	
Trapped Oil and Fuel		100	.00373	
Engine Control Module		25.17	.00939	
Engine Starting System		13.04	.000486	
Thrust Reversers		283.72	.0106	
Fixed Equipment		Flight Control System	286.81	.0107
		Hydraulic System	325.6	.0121
		Electrical System	792.74	.0296
	Instrumentation, Avionics and Electronics	551.89	.0206	
	Air-conditioning, Pressurization, Anti and Deicing System	379.415	.0152	
	Oxygen System	39.6	.00148	
	Auxiliary Power Unit (APU)	251.6	.00938	
	Furnishings	551.51	.0206	
	Operational Items	119.186	.00445	
	Flight Test Instrumentation	350	.0131	
Auxiliary Gear	160	.00597		
	Ballast	TBD	TBD	

	Paint	177.60	.00662
--	-------	--------	--------

The previous table data concludes that the heavier an item is, the greater affect it has upon the plane's center of gravity position. If the center of gravity had to adjusted, the heavier items would have the greatest impact while lighter items would need to move drastically to have an effect. Roskam states that items such as air conditioning units, batteries, black boxes or flight test instrumentation and ballast are most typically moved to adjust a plane's center of gravity. [1]

3.2 Effects of Moving Wing

The plane's center of gravity with respect to the wing's mean geometric chord can be found with the following equation.

$$\bar{x}_{cg} = (x_{cg} - x_{LE}) / \bar{c}$$

The plane's center of gravity in terms of wing mean geometric chord length is 1.073 ft.

For conventional aft tail aircraft, the following equation can be used to determine the plane's aerodynamic center.

$$\bar{x}_{ac} = \{C_1 + C_2(\bar{x}_{ac_h})\} / (1 + C_2)$$

Where,

$$C_1 = \bar{x}_{ac_w} + \Delta\bar{x}_{ac_{wb}}$$

$$C_2 = (C_{L_{a_h}} / C_{L_{a_{wb}}}) (1 - d_s / d_a) (S_h / S)$$

C₁ and C₂ values were calculated to be 20.283 and .1686, respectively. These values can then be used to determine the effects of moving the plane's wing will change the plane's center of gravity and aerodynamic center.

The following equations will be used to determine the effect of the wing position changing against the plane's center of gravity and aerodynamic center.

$$\bar{x}_{cg_{new}} = \bar{x}_{cg_{old}} + (\Delta x_w W_w) / (\bar{c} (\sum_{i=1}^{i=n} W_i))$$

$$\bar{x}_{ac_{new}} = \{C_1 + C_2(\bar{x}_{ac_h} - \Delta x_w / \bar{c})\} / (1 + C_2)$$

From these two equations, the following data shows the effects of the moving the aircraft's wing.

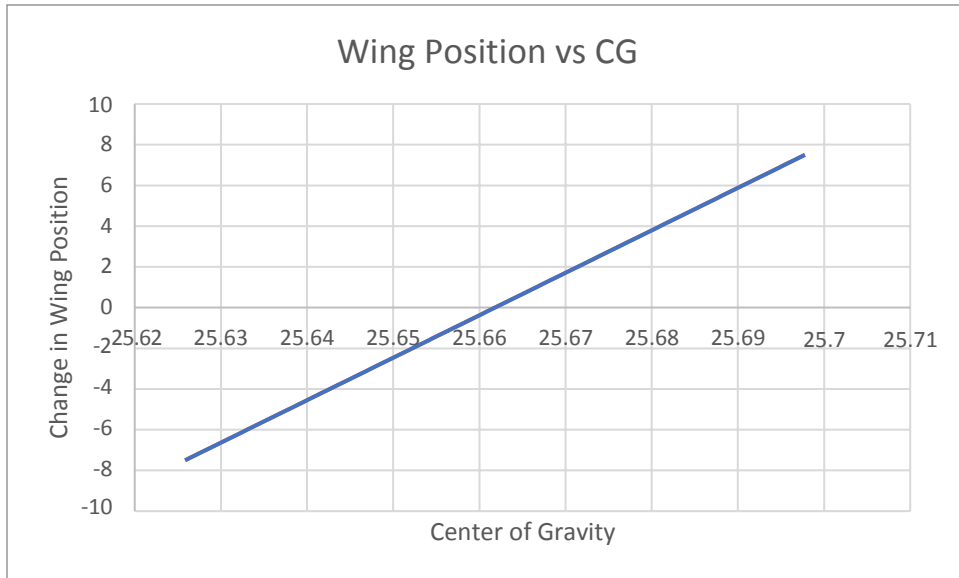


Figure 1: Change in wing position effect on CG.

From this figure, the data is plotted with the wing initially positioned at 25.307 ft with respect to the nose of the aircraft. The plane's center of gravity is located at 25.66 ft with respect to the nose. As the wing is moved forward, the plane's overall center of gravity will move forward as well. For every one foot the wing moves, the center of gravity of the aircraft will shift in the same direction as the wing by .004795 ft.

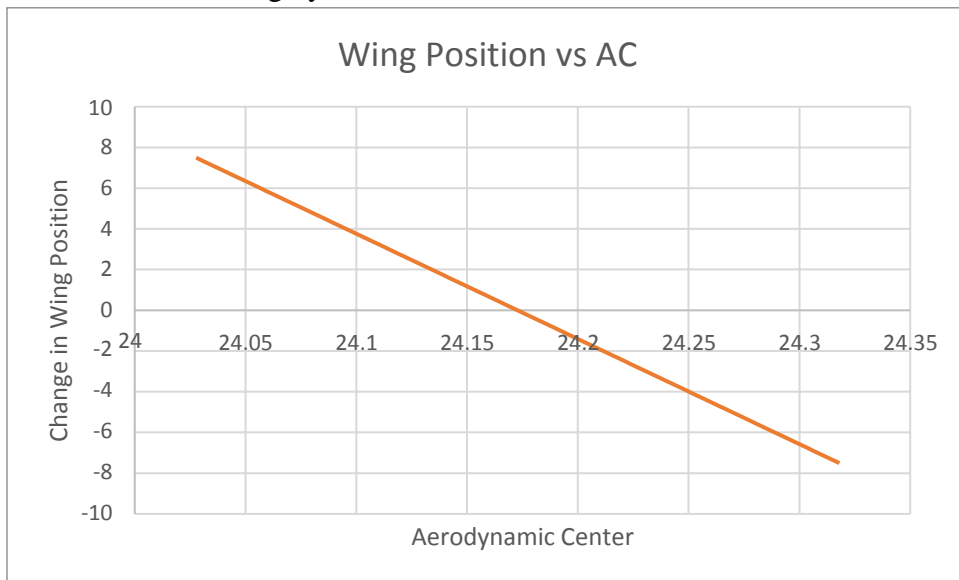


Figure 2: Change in wing position effect on AC.

From this figure, the data is plotted with the wing remaining in its original CG position of 25.307 ft with respect to the nose. The initial aerodynamic center of the aircraft was found to be 24.173 ft with respect to the nose. As the wing moves aft on the plane, the plane's aerodynamic center will shift in the opposite direction of the wing. For every one foot the wing is shifted, the plane's aerodynamic center will shift .01935 ft in the opposite direction.

References

- [1] Roskam, J. (1989). Airplane Design Part IV: Layout Design of Landing Gear and Systems. University of Kansas.

Chapter 8

Drag Polar and Trim

Symbols

° - Degrees

A – Aspect ratio

A_h – Aspect ratio of horizontal

AOA – Angle of attack

A_p – Aspect ratio of pylon

$\frac{\alpha_{o1@M}}{\alpha_{o1@M=.3}}$ – Mach number correction for zero-lift angle of attack

α_{oL_h} - Horizontal zero-lift angle of attack

α_{oL_p} – Pylon zero lift angle of attack

C_D – Coefficient of drag

c_{d_c} - Experimental steady state cross flow drag coefficient of circular cylinder

C_{D_emp} – Coefficient of drag of empennage

C_{D_flap} – Coefficient of drag of flap

C_{D_fus} – Coefficient of drag of fuselage

C_{D_gear} – Coefficient of drag of landing gear

C_{D_misc} – Coefficient of drag of miscellaneous items

C_{D_n} – Coefficient of drag of nacelle

C_{D_n'} - Fuselage/nacelle drag interference

factor C_{D_np} – Coefficient of drag of nacelle and

pylon C_{D_p} – Coefficient of drag of pylon

C_{D_trim} – Coefficient of drag of trim

C_{D_wing} – Coefficient of drag of wing

C_{f_fus} – Turbulent flat plate skin friction coefficient of fuselage

C_{f_n} - Turbulent flat plate friction coefficient of nacelle

C_{f_p} - Turbulent flat plate friction coefficient of pylon

C_{f_w} – Turbulent flat plate friction coefficient

C_{fh} – Turbulent flat plate friction coefficient of horizontal

C_{fi} – Turbulent flat plate friction coefficient of empennage surface i

C_{fv} – Turbulent flat plate friction coefficient of vertical

c_{h_r} – Horizontal tail chord at root

C_L – Coefficient of lift

C_{L_h} – Coefficient of lift of horizontal

C_{L_o} – lift coefficient at zero angle of attack

C_{L_p} – Coefficient of lift of pylon

C_{L_w} – Coefficient of lift of the wing

C_{L_α} – Lift curve slope

c_{v_t} – Vertical tail chord at tip

$C_{D_{Lh}}$ – Drag coefficient due to lift of horizontal

$C_{D_{LW}}$ – Drag coefficient due to lift of the wing

$C_{D_{Lemp_i}}$ – Drag coefficient due to lift of empennage surface i

$C_{D_{Lfus}}$ – Fuselage drag coefficient due to lift

$C_{D_{Ln}}$ – Drag coefficient due to lift of nacelle

$C_{D_{Lp}}$ – Drag coefficient due to lift of pylon

$C_{D_{bfus}}$ – Fuselage base drag coefficient

$C_{D_{bn}}$ – Nacelle base drag coefficient

$(C_{D_{gear}})_{C_{L=0}}$ – Zero-lift drag coefficient of landing gear based on own reference area of landing gear i

$C_{D_{nint}}$ – Fuselage/nacelle interference drag coefficient

$C_{D_{np_{new}}}$ – New coefficient of drag of nacelle/pylon

$C_{D_{np_{old}}}$ – Original coefficient of drag of nacelle/pylon

$C_{D_{oemp_i}}$ – Zero-lift drag coefficient of empennage surface i

$C_{D_{of}}$ – Zero-lift drag coefficient of fuselage

$C_{D_{ofus-base}}$ – Zero-lift drag coefficient of the fuselage exclusive of the base

$C_{D_{on}}$ – Zero-lift drag coefficient of nacelle

$C_{D_{op}}$ – Zero-lift drag coefficient of pylon

$C_{D_{ow}}$ – Zero-lift drag coefficient of wing

$C_{L_{owf}}$ – Zero angle of attack coefficient of the wing/fuselage combination

$C_{L_{\alpha h}}$ – Horizontal lift curve slope

$C_{L_{\alpha p}}$ – Pylon coefficient of lift with respect to α

$C_{L_{\alpha w}}$ – Wing lift curve slope

$C_{L_{\alpha w}}$ – Wing-lift curve slope

$C_{L_{\alpha wf}}$ – Wing-fuselage lift curve slope

$cl_{\alpha @ M}$ – Wing coefficient of lift versus angle of attack at Mach

\bar{c}_p – Mean geometric chord length of pylon

\bar{c} – Wing mean geometric chord length

d_b – Fuselage base diameter

d_f – Diameter of fuselage

d_{inl} – Engine inlet diameter

d_n – Widest diameter face of nacelle
 $d\epsilon/d\alpha$ – Downwash angle
 e – Span efficiency
 $F_{a,2}$ – Local area ruling constant 2
 ft – feet
 ft/s – Feet per second
 h_h – Height difference between wing and horizontal stabilizer
 i_h – Incidence angle of horizontal
 i_w – incidence angle of wing
 K - Empirical constant
 k - Wing-fuselage lift curve slope constant 2
 K_A – Downwash angle constant 1
 K_h – Downwash angle constant 3
 K_{int} – Empirical interference constant
 K_{wf} – Wing-fuselage interference factor
 K_λ – Downwash angle constant 2
 L' - Airfoil thickness location parameter
 l_f – Fuselage length
 l_f – Length of fuselage
 l_{LER} – Leading edge radius of airfoil
 l_n – Length of nacelle
 M – Mach number
 M_c – Cross flow Mach number
 mph – miles per hour
 p_i - Variation of gear drag with lift factor
 \bar{q} – Dynamic pressure
 R – Leading-edge suction parameter
 R_{hf} – Horizontal/fuselage interference factor
 R_{if} – Interference factor of empennage surface i
 R_{LS} – Lifting surface correction factor
 R_n – Reynolds number
 $R_{N_{fus}}$ – Fuselage Reynolds number
 $R_{N_{fus}}$ – Fuselage Reynolds number
 R_{N_w} – Reynolds number of the wing
 R_{nf} - Nacelle/fuselage interference factor
 R_{pf} – Pylon/fuselage interference factor
 R_{vf} – Vertical/fuselage interference factor
 R_{wf} – Wing/fuselage interference drag
 S - Wing planform area
 $S_{b_{fus}}$ – Fuselage base area

S_{b_n} – Nacelle base area
 S_{ef} - Elevator flap area
 S_{fus} – Maximum fuselage cross sectional area
 S_{gear_i} - Reference area for zero-lift gear drag coefficient of landing gear i
 S_h – Horizontal wing area
 S_h – Horizontal wing area
 S_n - Maximum frontal area of the nacelle
 S_{noz} - Nozzle cross section area
 S_p – Pylon area
 $S_{plf_{fus}}$ – Fuselage planform area
 S_{plf_n} – Nacelle planform area
 $S_{wet_{fan\ cowling}}$ – Fan cowling wetted area
 $S_{wet_{fus}}$ – Fuselage wetted area
 $S_{wet_{gas\ generator}}$ – Gas generator wetted area
 S_{wet_h} – Horizontal wetted area
 S_{wet_n} – Wetted area of nacelle
 S_{wet_p} – Wetted pylon area
 $S_{wet_{plug}}$ – Plug wetted area
 S_{wet_v} – Vertical wetted area
 S_{wet_w} - Wing wetted area
 S_{wf} – Flapped wing area
 t – distance from fuselage to nacelle center
 t/c - Thickness ratio at mean geometric chord
 t/ch – Horizontal tail thickness ratio
 t/c_{max} – Max thickness ratio at mean geometric chord
 t/c_p – Thickness ratio of pylon
 t/c_v – Vertical tail thickness ratio
 t/D – ratio of the distance from the plane's fuselage to the center of the nacelle to the maximum diameter of the nacelle
 U_1 – Free stream velocity
 v – Induced drag factor
 V_{noz}/U_1 - Ratio of average flow velocity in nozzle to steady state flight speed (High bypass jet engine)
 W – Weight of aircraft
 w – Zero-lift drag factor due to linear twist
 x_h – Distance between wing trailing edge to horizontal quarter chord
 z_h – Dynamic pressure ratio constant 1
 z_w – Dynamic pressure ratio constant 2
 α – Angle of attack
 α_h – Horizontal angle of attack

α_{o_1} – Airfoil zero-lift angle of attack
 $\alpha_{o_{LW}}$ – Wing zero-lift angle of attack
 α_p – Pylon angle of attack
 β – Wing-fuselage lift curve slope constant 1
 $\Delta\alpha_o/\varepsilon_t$ – Change in wing zero-lift angle of attack per degree of linear wing twist
 $\Delta C_{D_p \Lambda_{c/4}}$ – Profile drag coefficient due to elevator
 $\Delta C_{D_{iflap}}$ – Induced drag increment due to flaps
 $\Delta C_{D_{intflap}}$ – Interference drag increment due to flaps
 $\Delta C_{D_p \Lambda_{c/4}=0}$ – Two-dimensional profile drag increment
 $\Delta C_{D_{prof flap}}$ – Flap profile drag increment
 $\Delta C_{D_{trimlift}}$ – Trim drag due to lift
 $\Delta C_{D_{trimprof}}$ – Trim drag due to profile drag
 $\Delta C_{D_{wmj}}$ – Windmilling drag coefficient
 ΔC_{L_h} – Horizontal tail increment lift coefficient
 $\Delta C_{L_{flap}}$ – Incremental lift coefficient due to flap (Learjet M55)
 ε_t – Wing twist angle
 η – Ratio of the drag of a finite cylinder to drag of an infinite cylinder
 η_h – Dynamic pressure ratio
 λ – Taper ratio
 $\Lambda_{c/4_{max}}$ – Max wing sweep angle
 Λ_h – Horizontal wing sweep angle
 Λ_{LE} – Leading edge sweep angle
 μ – Dynamic viscosity
 ρ – Air density

1.0 Introduction

The purpose of this chapter is to determine the plane's drag characteristics for all items. From determining each component's drag coefficient, the plane will be able to be trimmed properly to allow for a straight and level flight during cruise.

2.0 Drag Polar Configuration

Roskam categorizes planes drag polar estimations by speed, subsonic, transonic or supersonic [1]. The business jet being designed is expected to cruise at 530 mph, Mach .69. This will categorize the plane as a subsonic aircraft.

The airplane's drag coefficient will be found with the following equation.

$$C_D = C_{D_{wing}} + C_{D_{fus}} + C_{D_{emp}} + C_{D_{np}} + C_{D_{flap}} + C_{D_{gear}} + C_{D_{trim}} + C_{D_{misc}} \quad (1)$$

2.1 Wing

The wing's coefficient of drag can be found with the following equation.

$$C_{D_{wing}} = C_{D_{o_w}} + C_{D_{LW}} \quad (2)$$

The equation is broken into two separate drag coefficient calculations, wing zero-lift drag coefficient and wing drag coefficient due to lift.

2.1.1 Wing Zero-Lift Drag Coefficient

The following equation is used to find the wing zero-lift drag coefficient

$$C_{D_{o_w}} = R_{wf} * R_{LS} * C_{f_w} * (1 + L \left(\frac{t}{c}\right) + 100 \left(\frac{t}{c}\right)^4) * \frac{S_{wetw}}{S} \quad (3)$$

To obtain the wing/fuselage interference drag, the following graph, from Roskam, was used.

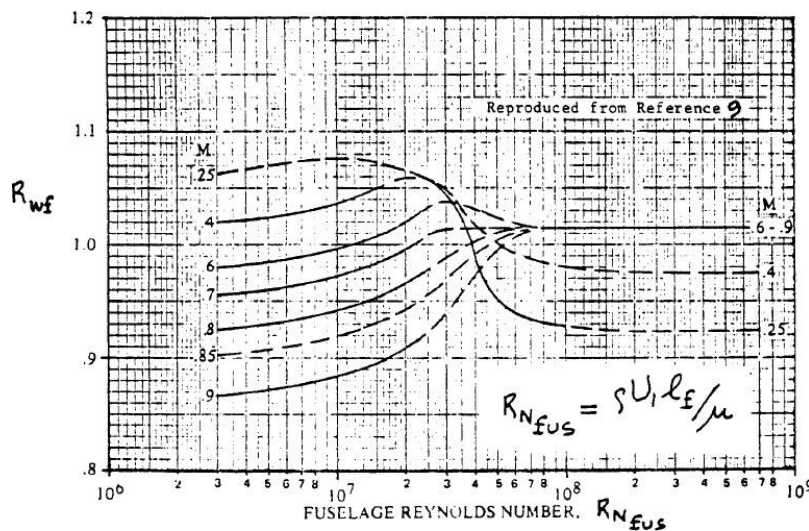


Figure 1: Wing/fuselage interference factor. [1]

The following equation was used to obtain the fuselage Reynolds number. The Mach value at which the graph was analyzed at was .69. Reynolds number will be analyzed at 777.333 ft/s.

$$R_{N_{fus}} = \frac{\rho U_{\infty} l_f}{\mu} \quad (4)$$

The density and dynamic viscosity of air were analyzed at 35,000 ft, the expected cruising altitude of the aircraft. The density of air at 35,000 feet is 7.338×10^{-4} . The dynamic viscosity of air at 35,000 ft is 2.995×10^{-7} . [2] The length of the fuselage is 47.244 ft. Reynolds number of the fuselage was calculated to be 9.0×10^7 . This corresponds to an approximated wing/fuselage interference factor of 1.02.

To find the lifting surface value, R_{LS} , the following figure from Roskam was used.

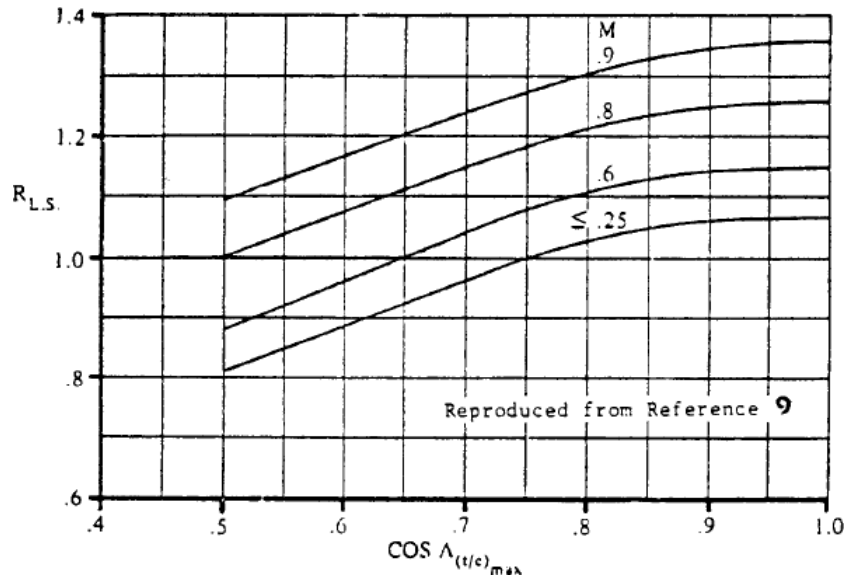


Figure 2: Lifting surface correction factor. [1]

The following expression must be used to determine the relation between wing sweep angle and lifting surface correction factor. The wing has a constant sweep angle of 22° .

$$\cos(\Lambda_{c/4_{max}}) \quad (5)$$

$$\cos(22) = .927$$

The figure was analyzed at cruise speed of Mach .69. Since the figure does not have this value plotted, it was approximated between Mach .6 and Mach .8. With a sweep angle which corresponds to .927 along the x-axis of the figure, the lifting surface correction factor was found to be 1.2.

To find the turbulent flat plate friction coefficient, C_{fw} , the Reynolds number must first be obtained with the following equation.

$$R_{N_w} = \frac{\rho U_1 c}{\mu} \quad (6)$$

The Reynolds number and friction coefficient will be analyzed at a Mach speed of .69, or 777.333 ft/s. The wing's mean geometric chord length is 7.455 ft. Reynolds number was calculated to be $1.42e7$. The following figure will be used to find the relation between the Reynolds number of multiple airplane components and their corresponding friction coefficient.

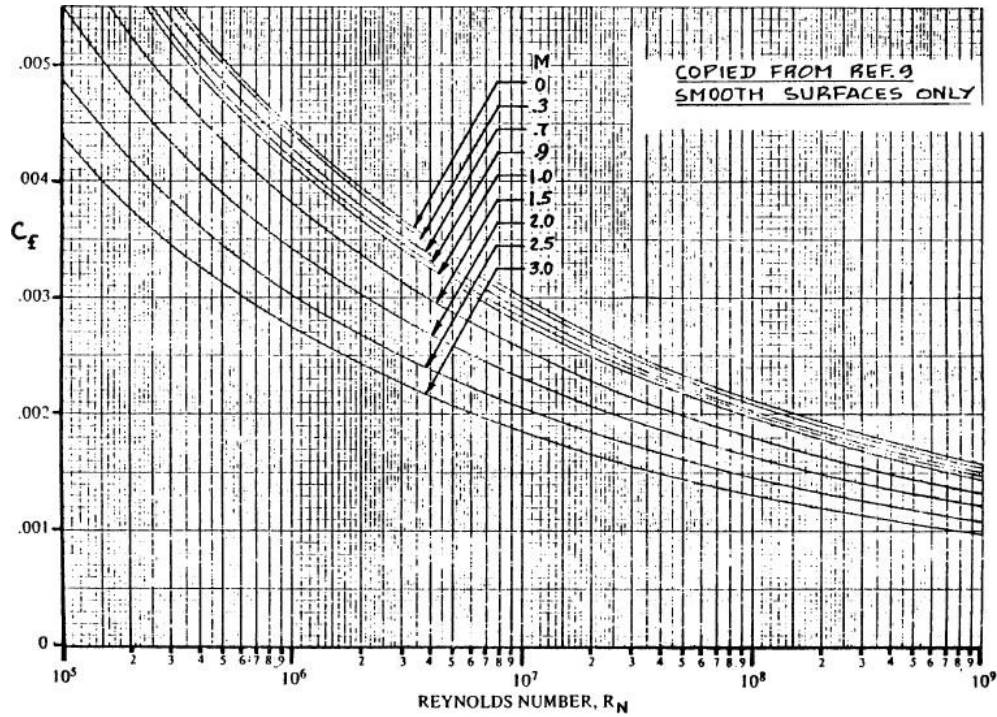


Figure 3: Reynolds number relation to skin friction coefficient. [1]

For this case, the wing, the Reynolds value corresponds to a turbulent flat plate value of .00275.

The airfoil thickness location parameter is one of two values, as shown in the figure below.

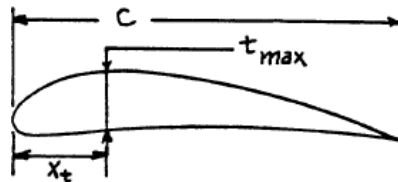


Figure 4: Airfoil thickness location parameter. [1]

If the wing chord thickness is greater than 30% of the wing chord, the airfoil thickness value will be 1.2. If the wing chord thickness is less than 30% of the wing chord, the airfoil thickness value will be 2.0. The following equation will be used for this calculation. The thickness ratio of the wing is .159.

$$(t/c)_{max} \leq .3\bar{c} \quad (7)$$

$$.159 < .3(7.455)$$

The airfoil thickness location parameter will be 2.0, based on the previous expression.

The following table defines the unknown variables of the wing-zero lift drag coefficient equation.

Table 1: Unknown variable definition for wing zero lift drag coefficient.

Variable	Definition	Value
R_{wf}	Wing/fuselage interference drag	1.02
R_{LS}	Lifting surface correction factor	1.2

C_{fw}	Turbulent flat plate friction coefficient	.00275
L'	Airfoil thickness location parameter	2.0
t/c	Thickness ratio at mean geometric chord	.159
S_{wet}	Wing wetted area	731.12 ft ²
S	Wing planform area	416.9 ft ²

The wing zero-lift drag coefficient was calculated to be .007837.

2.1.2 Wing Drag Coefficient Due to Lift

The following equation is used to find the wing drag coefficient due to lift.

$$C_{D_{LW}} = \frac{C_L^2}{\pi A e} + 2\pi C_{LW} \epsilon_t v + 4\pi^2 \epsilon_t^2 w \quad (8)$$

The coefficient of lift of the wing is found with the following equation.

$$C_{LW} = .105 C_L \quad (9)$$

From the previous Class I design, the clean wing was able to generate a clean coefficient of lift of 1.641. Thus, the coefficient of lift of the wing was calculated to be 1.72305.

The span efficiency factor is found with the following equation.

$$e = 1.1 \frac{\left(\frac{C_{L\alpha_w}}{A}\right)}{R\left(\frac{C_{L\alpha_w}}{A}\right) + (1-R)\pi} \quad (10)$$

The wing-lift curve slope was found to be .1 for a NACA 64-008A [3]. The leading-edge suction parameter, R, is found with the following figure.

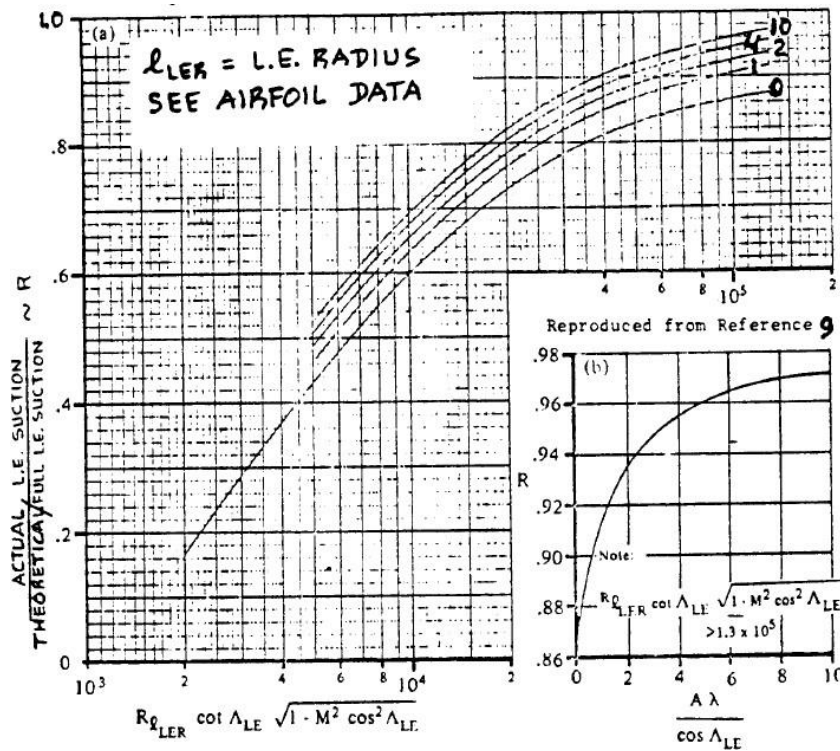


Figure 5: Leading edge suction parameter. [1]

The previous figure contains two graphs, depending on the following equation.

$$R_{LER} \cot(\Lambda_{LE}) \sqrt{1 - M^2 \cos^2(\Lambda_{LE})} \geq 1.3e5 \quad (11)$$

Where the Reynolds number of the leading-edge radius, $R_{L_{LER}}$, is found with the following equation.

$$R_{L_{LER}} = \frac{\rho U_{\infty} l_{LER}}{\mu} \quad (12)$$

Roskam informs to use airfoil's data on the leading-edge radius value [1]. Data was unavailable for this geometric value, therefore, it will be assumed to be .984 ft. This results in a Reynolds number of 1.89e6. The previous relation to determine which graph to use is recalled. The sweep angle of the wing at all points is 22°. Mach number is .69.

$$R_{L_{LER}} \cot(\Lambda_{LE}) \sqrt{1 - M^2 \cos^2(\Lambda_{LE})} \blacksquare 1.3e5$$

$$3.59e6 > 1.3e5$$

Based on this relation, the smaller of the two graphs in the figure will be used. A new x-value must be used found before proceeding. The equation is shown below.

$$\frac{\frac{A\lambda}{\cos(\Lambda_{LE})}(12)}{7.5(.42)} = 3.397$$

$$\frac{\quad}{\cos(22^\circ)}$$

With the new x-value, the figure may be used. The leading-edge suction parameter, R, is found to be .947. This value can be recycled to find the span efficiency factor, which is calculated to be .081877.

The remaining terms of the wing drag coefficient due to lift rely on wing twist, which is not utilized for this business jet. The revised equation is shown below.

$$C_{D_{L_w}} = \frac{C_{L_w}^2}{\pi A e} \quad (13)$$

The following table defines the unknown variables.

Table 2: Unknown variable definition for wing drag coefficient due to lift.

Variable	Definition	Value
C_{L_w}	Wing lift coefficient	.172305
A	Aspect ratio	7.5
e	Span efficiency factor	.081877
ϵ_t	Wing twist angle	0
v	Induced drag factor	0
w	Zero-lift drag factor due to linear twist	0

The wing drag coefficient due to lift was calculated to be .1539.

The drag coefficient of the wing, summation of zero-lift drag coefficient and wing drag coefficient due to lift, is .02323.

2.2 Fuselage

The fuselage's coefficient of drag can be found with the following equation.

$$C_{D_{fus}} = C_{D_{ofus}} + C_{D_{L_{fus}}} \quad (14)$$

The equation is broken into two separate drag coefficient calculations, fuselage zero-lift drag coefficient and fuselage drag coefficient due to lift.

2.2.1 Fuselage Zero-Lift Drag Coefficient

The following equation is used to find the fuselage zero-lift drag coefficient

$$C_{D_{ofus}} = R_{wf} * C_{f_{fus}} * \left(1 + \frac{60}{(l/d)^3} + .0025(l/d)\right) * \frac{S_{wet_{fus}}}{S} + C_{D_{b_{fus}}} \quad (15)$$

The turbulent flat plate skin friction coefficient is found similarly to the skin friction coefficient of the wing. The first step will be to find the Reynolds to relate it to the skin friction coefficient. The following equation will be reused to determine the fuselage Reynolds number.

$$R_{N_{fus}} = \frac{\rho U l_f}{\mu} \quad (4)$$

The fuselage Reynolds number was calculated to be $9.0e7$. At Mach .69, the turbulent flat plate skin-friction coefficient is .0021.

The following equation will be used to obtain the fuselage base drag coefficient.

$$C_{D_{b_{fus}}} = \frac{.029(d_b/d_f)^3}{\sqrt{C_{D_{ofus-base}}(S/S_{fus})}} * \frac{S_{fus}}{S} \quad (16)$$

The fuselage base diameter, d_b , is the area of the tail end of the fuselage. The fuselage will have an APU exhaust at the rear. The exhaust will be circular to follow the streamlines of the fuselage. The fuselage base diameter will be 1 ft.

The fuselage max diameter, d_f , is the diameter of the largest cross-sectional face of the fuselage. The fuselage is cylindrical with two conical sections to close the cylinder. The cabin region is the cylindrical section of the fuselage. The largest diameter is 6 ft.

The zero-lift drag coefficient of the fuselage exclusive of the base is the first term of the fuselage zero-lift drag coefficient. The following equation will be used to find this value.

$$C_{D_{ofus-base}} = R_{wf} * C_{f_{fus}} * \left(1 + \frac{60}{(l/d)^3} + .0025(l/d)\right) * \frac{S_{wet_{fus}}}{S} \quad (17)$$

$$C_{D_{ofus-base}} = 1.02(.0021) \left(1 + \frac{60}{(47.244/6)^3} + .0025(47.244/6)\right) * \frac{744.71}{416.9} = .00256$$

Referring to the fuselage base drag coefficient equation, the following value was obtained.

$$C_{D_{b_{fus}}} = \frac{.029(.1667)^3}{\sqrt{.002564(14.7448)}} * .00256 = 4.68 * 10^{-5}$$

The length of the fuselage, diameter of the fuselage and wetted area of the fuselage were found in the Class I design process. The following table defines the unknown variables of the fuselage zero-lift drag coefficient equation with several variables previously defined being omitted.

Table 3: Unknown variable definition for fuselage zero lift drag coefficient.

Variable	Definition	Value
$C_{f_{fus}}$	Turbulent flat plate skin friction coefficient	.0021
l_f	Length of fuselage	47.244 ft
d_f	Max fuselage diameter	6.00 ft
$S_{wet_{fus}}$	Fuselage wetted area	744.71 ft ²
$C_{D_{b_{fus}}}$	Fuselage base drag coefficient	4.68e-5

The fuselage zero-lift drag coefficient was calculated to be .004419.

2.2.2 Fuselage Drag Coefficient Due to Lift

The following equation is used to find the fuselage drag coefficient due to lift.

$$C_{DLfus} = \frac{2\alpha^2 S_b fus}{S} + \frac{\eta C_{dc} \alpha^2 S_{plf} fus}{S} \quad (18)$$

The angle of attack will be found with the following equation. It is important to note that values which are in degrees and do not utilize trigonometric functions should be converted to radians.

$$\alpha = \frac{W/\bar{q} - C_{L0}}{C_{L\alpha}} \quad (19)$$

The weight which will be used is the revised maximum takeoff weight of 26,205.26 lbs. The dynamic pressure will be computed at cruise air density and speed of 7.338e-4 and 777.333 mph, respectively.

The first unknown, lift coefficient at zero angle of attack, will be solved for as follows:

$$C_{L0} = C_{L0wf} + C_{L\alpha h} * \eta_h \left(\frac{S_h}{S} \right) (i_h - \epsilon_{oh}) \quad (20)$$

The zero angle of attack coefficient of the wing/fuselage combination is found with the following equation.

$$C_{L0wf} = (i_w - \alpha_{oLW}) C_{L\alpha wf} \quad (21)$$

The incidence angle of the wing is 1°, which is equivalent to .01745 radians. Continuing, the wing zero-lift angle of attack, α_{oLW} , is found with the following equation.

$$\alpha_{oLW} = \left[\alpha_{o1} + \left(\frac{\Delta\alpha_o}{\epsilon_t} \right) \epsilon \right] \left[\frac{\alpha_{o1@M}}{\alpha_{o1@M=3}} \right] \quad (22)$$

The airfoil zero-lift angle of attack, α_{o-1} , can be found from the tables presented in Roskam, as shown below.

Airfoil	α_{o-1} (deg)	c_{m0}	$c_{l\alpha}$ (deg ⁻¹)	a.c. (tenths c)	$\alpha_{c_{lmax}}$ (deg)	c_{lmax}	α^* (deg)
63-006	0	.005	.112	.258	10.0	.87	7.7
63-009	0	0	.111	.258	11.0	1.15	10.7
63-206	-1.9	-.037	.112	.254	10.5	1.06	6.0
63-209	-1.4	-.032	.110	.262	12.0	1.40	10.8
63-210	-1.2	-.035	.113	.261	14.5	1.56	9.6
63 ₁ -012	0	0	.116	.265	14.0	1.45	12.8
63 ₁ -212	-2.0	-.035	.114	.263	14.5	1.63	11.4
63 ₁ -412	-2.8	-.075	.117	.271	15.0	1.77	9.6
64-006	0	0	.109	.256	9.0	.8	7.2
64-009	0	0	.110	.262	11.0	1.17	10.0
64-206	-1.0	-.040	.110	.253	12.0	1.03	8.0
64-209	-1.5	-.040	.107	.261	13.0	1.40	8.9
64-210	-1.6	-.040	.110	.258	14.0	1.45	10.8
64 ₁ -012	0	0	.111	.262	14.5	1.45	11.0
64 ₁ -212	-1.3	-.027	.113	.262	15.0	1.55	11.0
64 ₁ -412	-2.6	-.065	.112	.267	15.0	1.67	8.0

Figure 6: Airfoil experimental data. [1]

From the figure, the NACA 64008 airfoil is not listed, but two other similarly listed airfoils are shown. These two other airfoil's data will be used; thus, the airfoil AOA will be 0°. The change

in wing zero-lift angle of attack per degree of linear wing twist can be found from another figure presented in Roskam.

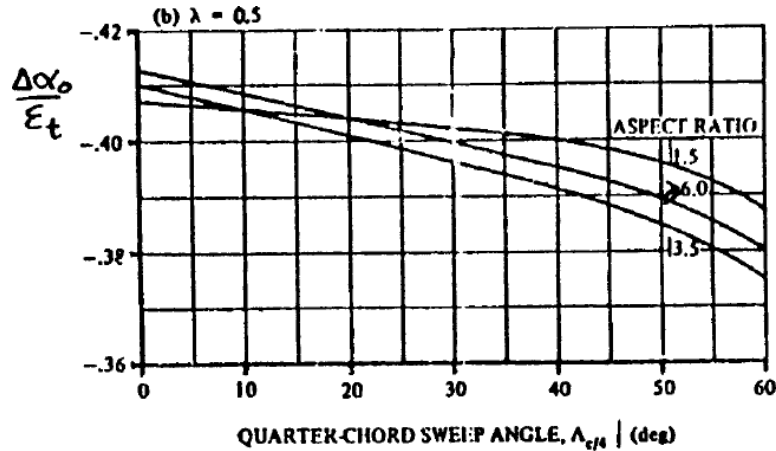


Figure 7: Effect of linear twist on wing angle of attack for zero lift. [1]

The wing sweep angle is 22°. The aspect ratio of the wing is 7.5. The aspect ratios plotted in the figure does not match that of this wing, it will be assumed to be between 6 and 13. However, the selected data point will favor the aspect ratio of 6 data. The change in wing zero-lift angle of attack per degree of linear wing twist was estimated to be -.41. The wing twist angle, declared in Class I sizing methods, is 0°. The Mach number correction for zero-lift angle of attack can be found from the following figure presented in Roskam.

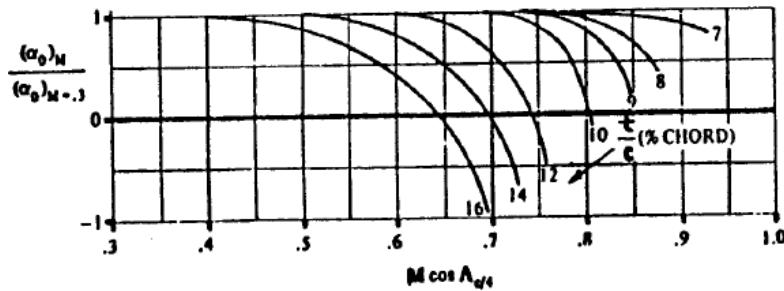


Figure 8: Mach number correction for zero-lift angle of attack. [1]

With a thickness ratio of .159, the data presented for a chord thickness of .16 will be used. The x-value will be .6398. This value corresponds to a Mach number correction value of .5. The angle wing zero-lift angle of attack can now be found.

$$\alpha_{oLW} = [0 + (-.41)0][.5] = 0$$

Continuing with zero angle of attack coefficient of the wing/fuselage combination, the wing-fuselage lift curve slope can be found with the following equation.

$$C_{L\alpha_{wf}} = K_{wf} C_{L\alpha_w} \quad (23)$$

The wing-fuselage interference factor, K_{wf} , can be found with the following equation.

$$K_{wf} = 1 + .025 \left(\frac{d_f}{b} \right) - .25 \left(\frac{d_f}{b} \right)^2 \quad (24)$$

$$K_{wf} = 1 + .025 \left(\frac{6}{55.92} \right) - .25 \left(\frac{6}{55.92} \right)^2 = .999804$$

The wing lift curve slope, $C_{L_{\alpha_w}}$, can be found with the following.

$$C_{L_{\alpha_w}} = \frac{2\pi A}{1/2} \quad (25)$$

$$2 + \left(\frac{A^2 \beta^2}{k^2 \left(1 + \frac{\tan^2(\Lambda)}{\beta^2}\right)} + 4 \right)$$

Where,

$$\beta = \sqrt{1 + M^2} \quad (26)$$

And

$$k = c_{l_{\alpha@M}} = \frac{c_{l_{\alpha@M=0}}}{\sqrt{1-M^2}} \quad (27)$$

Thus, the wing lift curve slope can be found as follows.

$$C_{L_{\alpha_w}} = \frac{2\pi(7.5)}{1/2} = 1.16905$$

$$2 + \left(\frac{7.5^2 * .723^2}{.138^2 \left(1 + \frac{\tan^2(22)}{.723^2}\right)} + 4 \right)$$

Returning to the wing-fuselage lift curve slope, the following was computed.

$$C_{L_{\alpha_{wf}}} = 1.1688$$

Returning to the zero angle of attack coefficient of the wing/fuselage combination, the following was computed. The incidence angle of the wing was converted from degrees to radians in the hand calculation process.

$$C_{L_{o_{wf}}} = (1^\circ - 0) * 1.1688 = .0204$$

The next step in the lift coefficient at zero angle of attack computation process is to find the value of the lift curve slope of the horizontal stabilizer. Similarly, the horizontal follows the same process as that of the wing.

$$C_{L_{\alpha_h}} = \frac{2\pi A_h}{1/2} = 1.1996$$

$$2 + \left(\frac{A_h^2 \beta^2}{k^2 \left(1 + \frac{\tan^2(\Lambda_h)}{\beta^2}\right)} + 4 \right)$$

The dynamic pressure ratio may be found with the following equation.

$$\eta_h = \frac{1 - \cos^2 \left(\frac{z_w}{z_w} \right) (2.42 \sqrt{C_{D_{o_w}}})}{x_h / \bar{c} + .3} \quad (28)$$

Where,

$$z_h = x_h \tan(\gamma_h + \epsilon_{cl} - \alpha_w) \text{ and } z_w = .68 \bar{c} \sqrt{C_{D_{o_w}}} (x_h / \bar{c} + .15) \quad (29) \quad (30)$$

$$\eta_h = \frac{1 - \cos^2 \left(\frac{\pi(20.0131)}{2(.851)} \right) (2.42 \sqrt{.008157})}{24.6063/7.455 + .3} = .2182$$

Returning to the lift coefficient at zero angle of attack, the following was calculated.

$$C_{L_o} = .0204 + 1.196 * .2182 \left(\frac{104}{416.9} \right) (-3.5^\circ - 0) = .01641$$

The next for the angle of attack equation was to find the airplane lift-curve slope, as shown below.

$$C = C_{L\alpha} + C_{L\alpha_{wf}} + C_{L\alpha_h} \eta_h \left(\frac{S_h}{S} \right) \left(1 - \frac{d\epsilon}{d\alpha} \right) \quad (31)$$

The downwash angle is the lone term which must be computed before continuing.

$$\frac{d\epsilon}{d\alpha} = 4.44 (K_A K_\lambda K_h (\cos(\Lambda))^2)^{1.19} \left(\frac{C_{L\alpha_w@M=.69}}{C_{L\alpha_w@M=0}} \right) \quad (32)$$

$$K_A = \left(\frac{1}{A} \right) - \frac{1}{1+A^{1.7}} \text{ and } K_\lambda = \frac{10-3\lambda}{7} \text{ and } K_h = \frac{1-h_h/b}{2l_h/b} \quad (33) \quad (34) \quad (35)$$

For these K constant equations, the values will be representative of the horizontal tail. The aspect ratio is 4.8, taper ratio of .42, height of horizontal over wing of 20.131 ft and length between the wing's quarter chord and horizontal quarter chord of 36.0892 ft. The downwash angle was calculated to be .3454.

The final calculation for the lift curve slope is as follows.

$$C_{L\alpha} = 1.1688 + 1.196(.2182) \left(\frac{104}{416.9} \right) (1 - .345) = 1.2116$$

The angle of attack may finally be calculated as follows.

$$\alpha = \frac{26205.6 / (20 * 416.9) - .01641}{1.2116} = .2191$$

To define the next term, the fuselage base area is as follows.

$$S_{b_{fus}} = \pi r^2 \quad (36)$$

$$S_{b_{fus}} = \pi * (.5^2) = .78539$$

The ratio of drag of a finite cylinder to the drag of an infinite cylinder is found with the following figure presented by Roskam.

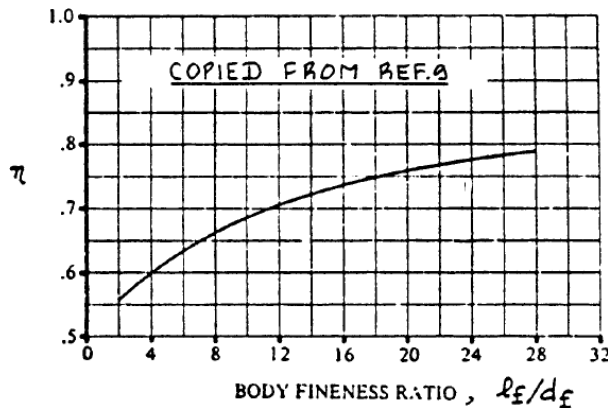


Figure 9: Ratio of drag of a finite cylinder to the drag of an infinite cylinder. [1]

The length of the fuselage is 14.4 m. The diameter of the fuselage is 1.83 m. This is a body fineness ratio of 7.8689. This will correspond to a cylinder ratio of .653.

The experimental steady state cross flow can be found from the following figure presented in Roskam.

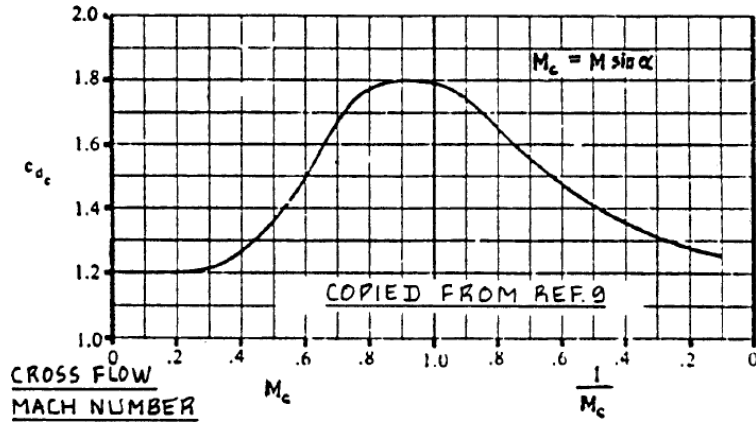


Figure 10: Steady state cross-flow drag coefficient for two dimensional circular cylinders. [1]

The cross-flow Mach number can be found with the following equation.

$$M_c = M \sin(\alpha) \quad (37)$$

Since the AOA was previously found it will be used in this calculation. The cross-flow Mach number was calculated to be .1496. This value will correspond to a cylindrical ratio of 1.2.

The planform area of the fuselage is found by treating the plane as a two-dimensional figure and finding the face area. The fuselage was divided into three areas, the cockpit, cabin and tail regions. The cockpit and tail regions were treated as triangles. The cabin was treated as a rectangle. The following equation was used to find the fuselage planform area.

$$S_{plf_{fus}} = \frac{1}{2}(6)(7.841) + (21.3253 * 6) + \frac{1}{2}(18.077)(6) = 205.707 \text{ ft}^2$$

The following table defines the unknown variables with several variables previously defined being omitted.

Table 4: Unknown variable definition for fuselage drag coefficient due to lift.

Variable	Definition	Value
α	Fuselage angle of attack	.2186 radians
$S_{b_{fus}}$	Fuselage base area	.78539 ft ²
η	Ratio of drag of finite cylinder to drag of infinite cylinder	.653
C_{d_c}	Experimental steady state cross-flow	1.2
$S_{plf_{fus}}$	Fuselage planform area	205.707 ft ²

The fuselage drag coefficient due to lift was calculated to be .004250.

The drag coefficient of the fuselage, summation of zero-lift drag coefficient and fuselage drag coefficient due to lift, is .008668.

2.3 Empennage

The empennage's coefficient of drag can be found with the following equation.

$$C_{D_{emp}} = \sum_i [(C_{D_{0emp_i}} + C_{D_{Lemp_i}})] \quad (38)$$

The equation is broken into two separate drag coefficient calculations, empennage zero-lift drag coefficient and empennage drag coefficient due to lift. The equation is also separated into the horizontal and vertical empennage sections.

2.3.1 Empennage Zero-Lift Drag Coefficient

The following equation is used to find the empennage's zero-lift drag coefficient for both the horizontal and vertical tail surfaces.

$$C_{D_{emp_i}} = R_{if} * R_{LS} * C_{f_i} * (1 + L' \left(\frac{t}{c}\right) + 100 \left(\frac{t}{c}\right)^4) * \frac{S_{wet_i}}{S} \quad (39)$$

The horizontal will be solved for first. The horizontal/fuselage interference drag, lifting surface correction factor, turbulent flat plate friction coefficient and airfoil thickness location parameter are all found in a similar process to that of the wing. The thickness ratio and wing planform area have already been established in Class I design process.

The wetted horizontal area can be found as an approximation based on the planform drawings in the Class I design process. The area of the horizontal is 104 ft², which accounts for only one side of the horizontal. The calculation must account for the area of where the horizontal is attached to the vertical tail. The following equation was used to find the horizontal wetted area.

$$S_{wet_h} = (104 * 2) - \left(\left(\frac{t}{c_v}\right) * c_{v_t}\right) (c_{h_r}) = 201.4877 ft^2 \quad (40)$$

Table 5: Unknown variable definition for horizontal stabilizer zero lift drag coefficient.

Variable	Definition	Value
R_{hf}	Horizontal/fuselage interference drag	1.0
R_{LS}	Lifting surface correction factor	1.2
C_{fh}	Turbulent flat plate friction coefficient of horizontal	.0029
L'	Airfoil thickness location parameter	2.0
t/c	Thickness ratio at mean geometric chord	.159
S_{wet_h}	Horizontal wetted area	201.4877 ft ²
S	Wing planform area	416.9 ft ²

The horizontal stabilizer zero-lift drag coefficient was calculated to be .002324.

The vertical will be solved for second. The vertical will follow the same process as that of the horizontal. The primary difference will be the vertical tail wetted area.

$$S_{wet_v} = (102 * 2) - \left(\left(\frac{t}{c_h}\right) * c_{h_r}\right) (2) = 201.8440 ft^2 \quad (41)$$

The following table defines the unknown variables with several variables previously defined being omitted.

Table 6: Unknown variable definition for vertical stabilizer zero lift drag coefficient.

Variable	Definition	Value
R_{vf}	Vertical/fuselage interference drag	1.0
R_{LS}	Lifting surface correction factor	1.13
C_{fv}	Turbulent flat plate friction coefficient	.00275
L'	Airfoil thickness location parameter	2.0
t/c	Thickness ratio at mean geometric chord	.159
S_{wet_v}	Vertical wetted area	201.8440 ft ²
S	Wing planform area	416.9 ft ²

The horizontal stabilizer zero-lift drag coefficient was calculated to be .002208.

2.3.2 Empennage Drag Coefficient Due to Lift

The following equation is used to find the horizontal stabilizer's drag coefficient due to lift alone.

$$C_{D_{L_h}} = \frac{C_{L_h}^2}{\pi A_h^2 e^2} \left(\frac{S_h}{S} \right) \quad (42)$$

Where,

$$C_{L_h} = C_{L_{\alpha_h}} (\alpha_h - \alpha_{o_{L_h}}) \quad (43)$$

To define the second term in determining the coefficient of lift in the horizontal, the angle of attack of the horizontal was found with the following set of equations

$$\alpha_h = \alpha \left(1 - \frac{d\varepsilon}{d\alpha} \right) + i_h$$

Referring to the previous section, the airplane's overall angle of attack was calculated as .2186. The downwash angle would have to be recalculated for the horizontal stabilizer rather than the wing.

$$\frac{d\varepsilon}{d\alpha} = 4.44 (K_A K_\lambda K_h \sqrt{\cos(\Lambda_{h/4})})^{1.19} = .02486$$

And,

$$\alpha_{o_{L_h}} = [\alpha_{o_l} + \left(\frac{\alpha_{o_l@M}}{\varepsilon} \right) \varepsilon t] \left[\frac{\alpha_{o_l@M}}{\alpha_{o_l@M=3}} \right] = 0 \quad (44)$$

Thus,

$$\alpha_h = .2191(1 - .02486) + (-3.5^\circ) = .1526$$

Finally, the overall drag due to lift of the horizontal stabilizer could be calculated with the following.

$$C_{D_{L_h}} = \frac{C_{L_h}^2}{\pi A_h^2 e^2} \left(\frac{S_h}{S} \right) \quad (45)$$

The following table defines the unknown variables with several variables previously defined being omitted.

Table 7: Unknown variable definition for horizontal stabilizer drag coefficient due to lift.

Variable	Definition	Value
C_{L_h}	Coefficient of lift of the horizontal stabilizer	.015
A_h	Aspect ratio of the horizontal	4.8
e	Oswald's efficiency for T-tails	.75

The horizontal stabilizer's drag coefficient due to lift was calculated to be 5.14×10^{-7} .

The vertical stabilizer's drag coefficient due to lift will be assumed to be zero. This assumption is made as Roskam states, planes are generally made to have the vertical stabilizers create zero lift [1]. The vertical stabilizer may affect the coefficient of drag if the aircraft experiences a sideslip angle. The sideslip angle would count as the angle of attack, which would then create 'lift'. This report will only cover the most basic conditions.

The total coefficient of drag of the empennage is .004537.

2.4 Nacelle/Pylon

To determine the drag coefficient of the plane's nacelles, the process will be separated into three steps: isolated, installed and windmilling.

2.4.1 Isolated Nacelle/Pylon Drag Coefficient

The isolated nacelle and pylon calculations will analyze each as if they were able to fly independently of anything. The isolated nacelle and pylon drag is found with the following equation.

$$C_{D_{np}} = C_{D_n} + C_{D_p} \quad (46)$$

The nacelle drag coefficient will be found by treating the nacelles as a fuselage, therefore, several variables have already been defined and be reused. The nacelle drag coefficient will be found with the following equations.

$$C_{D_n} = \sum_i C_{D_n}_i = C_{D_{o_n}} + C_{D_{L_n}} \quad (47)$$

The pylon drag coefficient can be found by treating the pylons as a wing. The pylon drag coefficient can be found with the following equation.

$$C_{D_p} = \sum_i C_{D_p}_i = C_{D_{o_p}} + C_{D_{L_p}} \quad (48)$$

2.4.1.1 Nacelle Zero-Lift Drag Coefficient

As previously stated, the nacelle zero lift drag coefficient will be found similarly to the fuselage, with slight modifications to the equation. The following equation will be used.

$$C_{D_{o_n}} = R_{nf} C_{f_n} * \left(1 + \frac{60}{(l_n/d_n)^3} + .0025 \left(\frac{l_n}{d_n}\right)\right) * \frac{S_{wet_n}}{S} + C_{D_{b_n}} \quad (49)$$

To obtain these new values, a similar process of the fuselage was followed. The interference factor, flat plate friction, length and diameter of the nacelle and the nacelle base drag coefficient are found similarly to the fuselage.

The wetted area of the nacelle is a combination of the fan cowling, gas generator and plug's wetted areas found in the Class I design process, as shown below.

$$S_{wet_n} = S_{wet_{fan\ cowling}} + S_{wet_{gas\ generator}} + S_{wet_{plug}} \quad (50)$$

$$S_{wet_n} = 38.62 + 12.46 + 3.34 = 54.42 \text{ ft}^2$$

The following table defines the unknown variables with several variables previously defined being omitted.

Table 8: Unknown variable definition for nacelle zero lift drag coefficient.

Variable	Definition	Value
R_{nf}	Nacelle/fuselage interference factor	1.0
C_{f_n}	Turbulent flat plate friction coefficient of nacelle	.00028
l_n	Length of nacelle	7.874 ft
d_n	Widest diameter face of nacelle	3.37457 ft
S_{wet_n}	Wetted area of nacelle	54.42 ft ²
$C_{D_{b_n}}$	Nacelle base drag coefficient	2.677e-5

The nacelle's zero-lift drag coefficient was calculated to be .002083. This value is only for one nacelle, but there are two on the aircraft. This will be accounted for in the final step in determining the overall coefficient of drag created by the nacelle.

2.4.1.2 Nacelle Drag Coefficient Due to Lift

The following equation is used to find the nacelle drag coefficient due to lift.

$$C_{D_{L_n}} = \frac{2\alpha^2 S_{b_n}}{s} + \frac{\eta C_{d_c} \alpha^2 S_{plf_n}}{s} \quad (51)$$

Most of the variables in this equation can be recycled from the fuselage calculations. The nacelle planform area must be found before continuing. The nacelle was estimated to be most similar to that of a trapezoid. The following equation was used to estimate the planform area of the nacelle.

$$S_{plf_n} = \frac{b_1 + b_2}{2} h \quad (52)$$

$$S_{plf_n} = \frac{3.37 + 4}{2} (7.874) = 14.8605 ft^2$$

The following table defines the unknown variables with several variables previously defined being omitted.

Table 9: Unknown variable definition for nacelle drag coefficient due to lift.

Variable	Definition	Value
S_{b_n}	Nacelle base area	.5027
η	Ratio of the drag of a finite cylinder to drag of an infinite cylinder	.55
C_{d_c}	Experimental steady state cross flow drag coefficient of circular cylinder	1.2
S_{plf_n}	Nacelle planform area	14.8605

The nacelle's drag coefficient due to lift was calculated to be .00036098. This is for a singular nacelle acting on the aircraft.

The total drag coefficient generated by one nacelle on the aircraft is .002444. this value will be doubled as there are two identically placed and weighted nacelles on the aircraft. The revised total drag coefficient created by the nacelles is .004889.

2.4.1.3 Pylon Zero-Lift Drag Coefficient

Before proceeding, the pylon geometries have not yet been specifically laid out as this was not an essential step in the Class I sizing process. The pylon shape will now be defined in reference to previously manufactured aircraft with similar size and mission requirements before continuing.

The pylon will be a length of 6.56168 ft, a mean chord length of 1.64042 ft, a thickness ratio of .1 and thickness of .656168 ft. The following diagram list the following values.

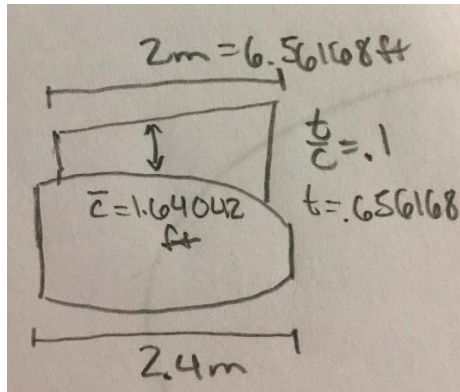


Figure 11: Geometrical lengths of pylon in reference to the nacelle size.

The pylon's drag coefficient will be found similarly to the horizontal stabilizer process, as previously stated. The following equation will be used to find the pylon's zero-lift coefficient of drag.

$$C_{D_o_p} = R_{pf} * R_{LS} * C_{f_p} * (1 + L' \frac{t}{c_p}) + 100 (\frac{t}{c_p})^4 * \frac{S_{wet_p}}{S} \quad (53)$$

The interference factor, correction factor, flat plate friction coefficient and thickness location parameter will all be found similarly to that of the horizontal stabilizer that these steps will not be written as they will be repetitive. The pylon thickness will be assumed to be .1 based on the length of the pylon chord and mean geometric chord length of the pylon being reasonable values.

The pylon wetted area must first be calculated. The pylon will be calculated as a rectangle as the exact geometry lengths are not known. The mean geometric chord of the pylon will be used as the width. The following equation will be used.

$$S_{wet_p} = 2(6.56)(1.64) = 21.5278 ft^2$$

The following table defines the unknown variables with several variables previously defined being omitted.

Table 10: Unknown variable definition for pylon zero lift drag coefficient.

Variable	Definition	Value
R_{pf}	Pylon/fuselage interference factor	1.0
R_{LS}	Lifting surface correction factor	1.2
C_{f_p}	Turbulent flat plate friction coefficient of pylon	.0028
L'	Pylon thickness location parameter	2.0
t/c_p	Thickness ratio of pylon	.1
S_{wet_p}	Wetted area of pylon	21.5278 ft ²

The zero-lift drag coefficient of the pylon was found to be .0002099. This accounts for only one of the two pylons on the aircraft. The two pylons will be accounted for in the final step.

2.4.1.4 Pylon Drag Coefficient Due to Lift

The following equation will be used to determine the plane's pylon drag coefficient due to lift.

$$C_{D_{Lp}} = \frac{C_{Lp}^2}{\pi A_p^2 e^2} \left(\frac{S_p}{S} \right) \quad (54)$$

Where,

$$C_{Lp} = C_{L\alpha_p} (\alpha_p - \alpha_{o_{Lp}}) \quad (55)$$

The pylon will not utilize an airfoil geometry, it will feature a straight support to hold the nacelle and engine. Thus, the pylon coefficient of lift with respect to α will be zero. This will effectively cancel the remaining variables in the equation, setting coefficient of lift of the pylon to zero. The pylon drag coefficient due to lift will be zero too.

The pylon drag coefficient, the summation of the zero lift drag coefficient and drag coefficient due to lift of the pylon will be .0002099. For two pylons, the plane's coefficient of drag due to the pylons is .0004199.

The isolated nacelle and pylon drag coefficient will be the summation of the zero lift drag coefficient and drag coefficient due to lift of the nacelle and pylon. This resulted in a value of .005308 for two nacelles and pylons.

2.4.2 Installed Nacelle/Pylon Drag Coefficient Increment

Depending on nacelle and engine type, the installed drag will differ. The possible options are wing/nacelle interference, fuselage/nacelle interference or cooling drag. Of these options, the fuselage/nacelle was chosen as the nacelle interferes with the streamline figure of the fuselage. The wing remains a clean wing and cooling drag is caused by propeller aircraft.

2.4.2.1 Fuselage/Nacelle Interference Drag Coefficient

The following equation will be used to solve for the fuselage/nacelle interference drag coefficient.

$$C_{D_{n_{int}}} = F_{a_2} (C_{D'_n} - .05) (S_n/S) \quad (56)$$

The local area ruling constant 2 is a given value. The maximum frontal area of the nacelle is referenced from Class I sizing process, an area of 8.943 ft². The fuselage/nacelle drag interference factor is found from the figure presented in Roskam.

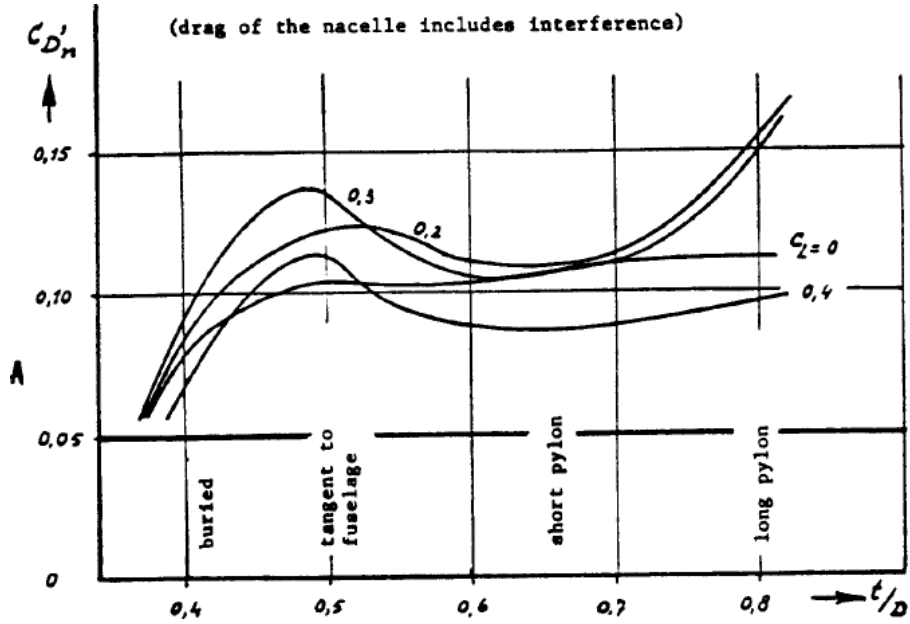


Figure 12: Fuselage/nacelle drag interference factor. [1]

The x-value of t/D is the ratio of the distance from the plane's fuselage to the center of the nacelle to the maximum diameter of the nacelle. The maximum diameter of the nacelle is at the fan cowling, which is 3.3745 ft. The distance from the fuselage to the nacelle center can be found from the following equation.

$$t = \bar{c} + \frac{d_n}{2} = 1.64 + \frac{3.3745}{2} \quad (57)$$

$$\frac{t}{D} = .985$$

The nacelle and pylon are not intended to create extra lift for the business jet, the figure will be analyzed at coefficient of lift of zero. This corresponds to an interference factor of .11

The following table defines the unknown variables with several variables previously defined being omitted.

Table 11: Unknown variable definition for fuselage/nacelle interference drag coefficient.

Variable	Definition	Value
$F_{a,2}$	Local area ruling constant 2	1.0
$C_{D,n'}$	Fuselage/nacelle drag interference factor	.11
S_n	Maximum frontal area of the nacelle	8.943 ft ²

The following calculation yielded a value of .001287.

2.4.3 Windmilling Drag Coefficient

An engine will windmill when the power to spin the fan is turned off and the fan will spin solely from the freestream flow it is interacting with. The following equation will be used to solve for the windmilling drag coefficient for a jet engine.

$$\Delta C_{D_{wmj}} = .0785 \left(\frac{t}{S} \right) + \frac{1}{1+16M^2} \left(\frac{V_{noz}}{U_1} \right) \left(1 - \frac{V_{noz}}{U_1} \right) \left(\frac{S_{noz}}{S} \right) \quad (58)$$

The following table defines the unknown variables with several variables previously defined being omitted.

Table 12: Unknown variable definition for windmilling drag coefficient.

Variable	Definition	Value
d_{inl}	Engine inlet diameter	2.0622 ft
V_{noz}/U_1	Ratio of average flow velocity in nozzle to steady state flight speed (High bypass jet engine)	.92
S_{noz}	Nozzle cross section area	.50265 ft ²

The windmilling drag coefficient was calculated to be .0002393.

The new coefficient of drag of the nacelle and pylon can now be calculated with the following equation.

$$C_{D_{np_{new}}} = C_{D_{np_{old}}} + C_{D_{nint}} + \Delta C_{D_{wmj}} \quad (59)$$

The new coefficient of drag of the nacelle and pylon was calculated to be .006835.

2.5 Flap Drag

The coefficient of drag of the flaps will be analyzed at subsonic speeds because they will be deployed during takeoff and landing to generate extra lift to compensate for the lowered speeds. The following equation will be used to solve for the coefficient of drag from the flaps.

$$C_{D_{flap}} = \Delta C_{D_{prof_{flap}}} + \Delta C_{D_{iflap}} + \Delta C_{D_{intflap}} \quad (60)$$

The equation will be solved in three steps, flap profile drag increment, induced drag increment and interference drag increment. The exact geometry of the plane's flaps was not explicitly developed under Class I sizing. The flap geometry will be defined before continuing.

The flaps will be in line with the ailerons on the wings, thus, the chord will be a ratio of .3 with respect to the wing's chord at each position along the wing. The flap will also be relocated from the outer wing towards the inner wing as to not interfere with the aileron's moments created when used.

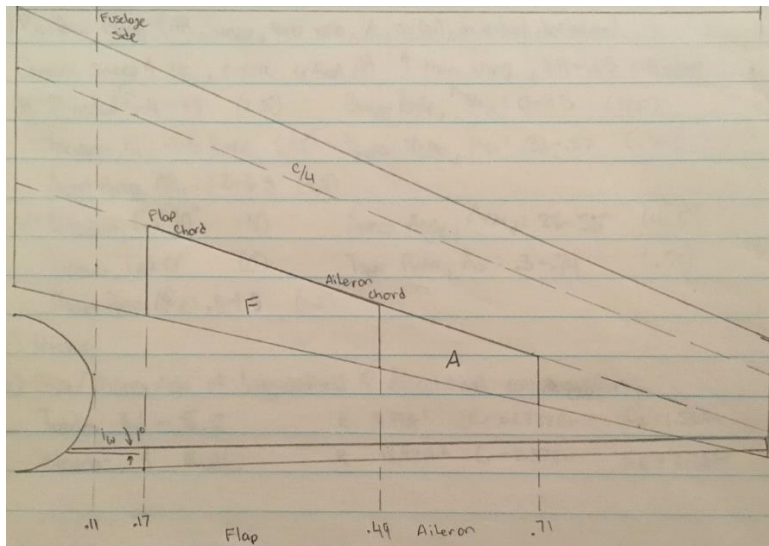


Figure 13: Revised wing control surface layout.

2.5.1 Flap Profile Drag Increment

The flap profile drag increment can be found with the following equation.

$$\Delta C_{D_{prof\ flap}} = (\Delta C_{D_p \Lambda_c/4=0}) \cos(\Lambda_c/4) (S_{wf}/S) \quad (61)$$

The two-dimensional profile drag increment is found from the figure presented below by Roskam.

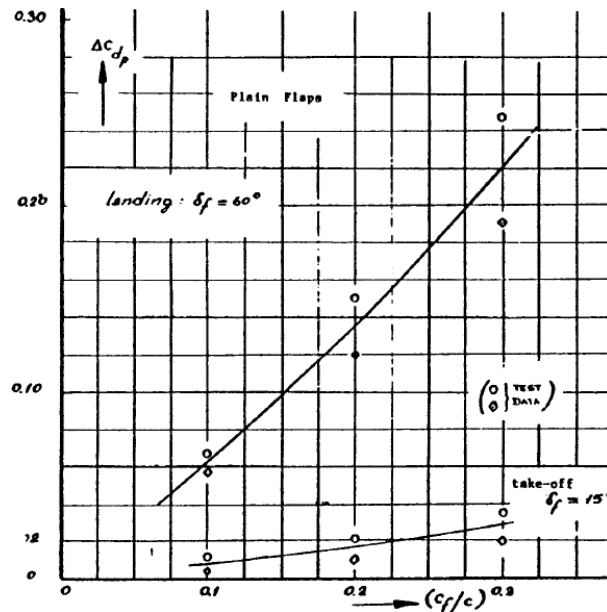


Figure 14: Profile drag increment for plain flaps. [1]

The x-value can be calculated by the ratio of the chord length of the flaps to the chord length of the wing. Since the chord length of the flaps was previously defined with respect to the wing, this value will be .32, or .09. During takeoff, the drag increment is .0085. During landing, the drag increment is .05.

The flapped wing area is the portion of the wing at which the flaps are located from leading edge to trailing edge, as shown in the figure presented by Roskam.

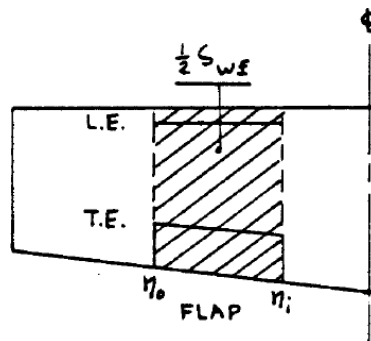


Figure 15: Flapped wing area. [1]

This area will be treated as trapezoids. The two chords will act as the bases, while the distance between the two chords will be the height. The equation below will determine the flapped wing area.

$$S_{wf} = 2 \left(\frac{b_1 + b_2}{2} h \right) \quad (62)$$

$$S_{wf} = 2 \left(\frac{9.3198 + 7.61117}{2} * 8.69848 \right) = 147.27 \text{ ft}^2$$

The following table defines the unknown variables with several variables previously defined being omitted.

Table 13: Unknown variable definition for flap drag profile increment.

Variable	Definition	Value
$\Delta C_{Dp} \Lambda_{c/4}=0$	Two-dimensional profile drag increment due to flaps	TO: 0.0085 LND: 0.05
$\Lambda_{c/4}$	Wing quarter chord sweep angle	22°
S_{wf}	Flapped wing area	147.27 ft ²

Depending on the plane's flight phase, either takeoff or landing, the plane will experience different profile drag due to the flaps. The flapped wing area is the area of two flaps. The flap drag profile increment during takeoff was calculated to be .002784. The flap drag profile increment during landing was calculated to be .01638.

2.5.2 Induced Drag Increment Due to Flaps

The induced drag increment due to flaps will be found with the following equation.

$$\Delta C_{D_{iflap}} = K^2 (\Delta C_{flap}) \cos \Lambda \quad (63)$$

The incremental lift coefficient due to flaps is determined by the distance between flaps up and flaps down C_L vs α diagram. Roskam informs that the selection of a similar aircraft will suffice for this value [1]. The Gates-Learjet M55 is the most similar aircraft as it a business jet. The following diagram will be used to obtain this value.

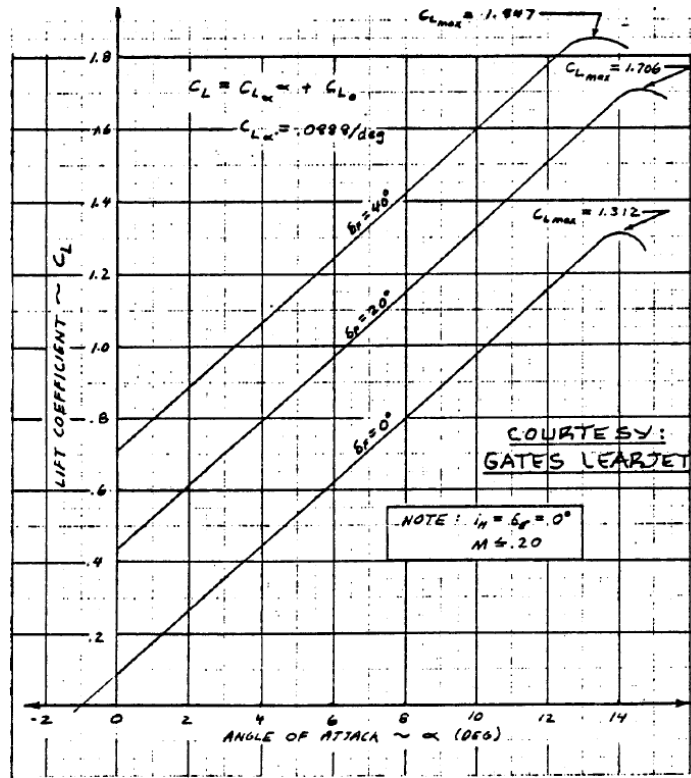


Figure 16: Gates-Learjet M55 C_L vs α . [1]

From this figure, it is important to note that the required C_{L_max} required by the business jet being designed is 1.8, not the 1.947 of the M55. The distance between the deflection of the flaps at 0° and 20° will be used. This value will be .315.

The following table defines the unknown variables with several variables previously defined being omitted.

Table 14: Unknown variable definition for induced drag increment due to flaps.

Variable	Definition	Value
K	Empirical constant	.4
ΔC_{L_flap}	Incremental lift coefficient due to flap (Learjet M55)	.315

The incremental lift coefficient due to flaps was found based on similar aircraft. Roskam provides the figures of different plane configurations which employ flaps to create lift. The Learjet M55 was the most similar out of the available aircraft. The induced drag increment was found to be .01472.

2.5.3 Interference Drag Increment Due to Flaps

The following equation will be used to solve for the interference drag increment.

$$\Delta C_{D_{intflap}} = K_{int} (\Delta C_{D_{prof\ flap}}) \quad (64)$$

The empirical interference constant, K_{int} , is categorized by flap type. The plain utilizes a plain flap configuration. This sets the constant to a value of zero. The interference drag increment will equal zero as well.

The overall drag coefficient due to the flaps is .01750 during takeoff. The overall drag coefficient due to the flaps is .03110 during landing. The landing value will be used as this will satisfy the takeoff and landing conditions for drag coefficient summation.

2.6 Landing Gear

The landing gear coefficient of drag can be calculated with the following equation.

$$C_{D_{gear}} = \sum \left\{ \left[C_{D_{gear, C_{L=0}}} + p_i C_L \right] \left(\frac{S_{gear_i}}{S} \right) \right\} \quad (65)$$

The landing gear will be a sum of the drag created by the nose and main landing gear.

The variation of gear drag with lift is based on how the landing gear is expected to be placed in reference to other objects. The landing gear is expected to be retracted without requiring extra storage to be added to take away from the streamline of the aircraft. This corresponds to an expression of $-4C_{D_{g, C_{L=0}}}$. The gear reference area is defined by the equation presented below. The variables are tire width and diameter.

$$S_{gear} = b_t * D_t \quad (66)$$

Table 15: Landing gear size calculations.

Nose Gear	Main Gear
$S_{gear} = 4.85 \text{ in} \times 13 \text{ in}$	$S_{gear} = 6.5 \text{ in} \times 25.3 \text{ in}$
$S_{gear} = .4378 \text{ ft}^2$	$S_{gear} = 1.1420 \text{ ft}^2$

The coefficient of lift will be the same for both the nose and main landing gear, however, it will differ during each phase of flight. To take off the plane will require a coefficient of lift of 1.8. During landing the plane requires a coefficient of lift of 2.0.

2.6.1 Landing Gear Zero-Lift Drag Coefficient.

2.6.1.1 Nose Gear

The nose landing gear's zero-lift drag coefficient based on reference area is found based on the figure provided by Roskam.

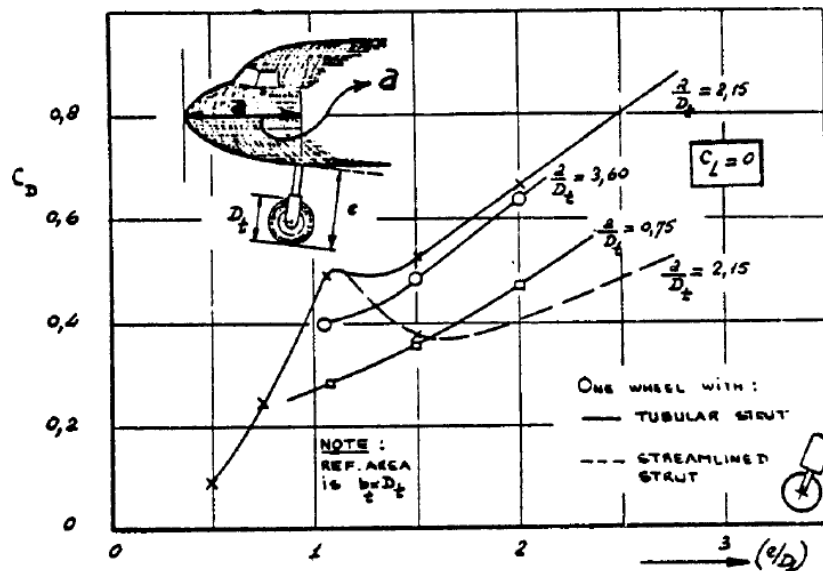


Figure 17: Nose gear drag increments. [1]

From this figure, the x-value can be found from the height of the landing gear divided by the diameter of the tire. This value will be 3.2 ft/13in, which will equal 2.95. The selection of which data line to reference is found by the distance of the landing gear aft of the nose divided by the tire diameter. This value will be 6.15 ft/13 in, which equals 5.68. Since there is not a reference point at which the business jet being designed fits under, the assumption will be made that the drag coefficient of the nose gear is .8.

2.6.1.2 Main Gear

The main landing gear’s zero-lift drag coefficient based on reference area is found based on the figure provided by Roskam. This value is representative of both legs of the main landing gear.

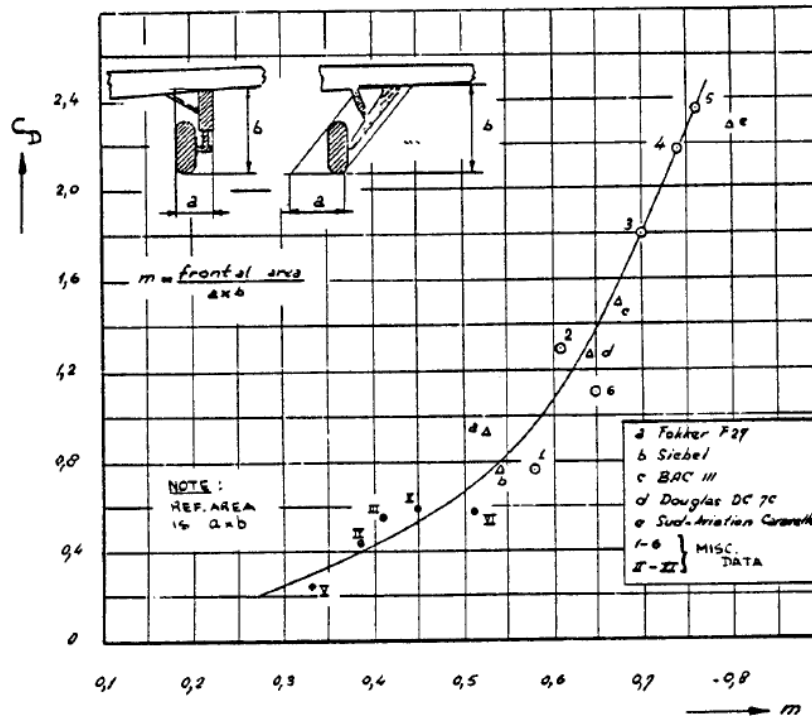


Figure 18: Gear drag increments for retractable landing gear. [1]

It is important to note the main landing gear will be comprised of two tires and a strut. The x-value is found with the following equation. The frontal area of the landing gear is representative of the 2-D side view of the landing gear.

$$m = \frac{\text{frontal area}}{a*b} \quad (67)$$

$$m = \frac{3.49}{4.53} = .77$$

This corresponds to a zero-lift drag coefficient of 2.3.

The following table defines the unknown variables with several variables previously defined being omitted.

Table 16: Unknown variable definition for coefficient of drag due to landing gear.

Variable	Definition	Value
----------	------------	-------

$C_{D_{gear}}_{C_{L=0}}$	Zero-lift drag coefficient of landing gear based on own reference area (Nose LNDG)	.8
	Zero-lift drag coefficient of landing gear based on own reference area (Main LNDG)	2.3
pi	Variation of gear drag with lift factor	$-.4C_{D_{gear}}_{C_{L=0}}$
C_L	Coefficient of lift (Takeoff)	1.8
	Coefficient of lift (Landing)	2.0
S_{gear}	Reference area for zero-lift gear drag coefficient (Nose)	.4378 ft ²
	Reference area for zero-lift gear drag coefficient (Main)	1.1420 ft ²

The coefficient of drag of the landing gear was analyzed during takeoff and landing, as these two instances are the most common flight profile the landing gear is expected to be deployed. The coefficient of drag of the landing gear during takeoff was calculated to be .001802. The coefficient of drag of the landing gear during landing was calculated to be .001209. The takeoff value will be used to determine the largest possible coefficient of drag experienced by the aircraft at any instance during flight. This will provide a safety barrier in future calculations to account for extra lift or speed to be added to the aircraft.

2.7 Trim

Although the airplane is yet to be fully trimmed, the drag coefficient will be estimated for with the following equation.

$$C_{D_{trim}} = \Delta C_{D_{trimlift}} + \Delta C_{D_{trimprof}} \quad (68)$$

2.7.1 Trim Drag Due to Lift

The trim drag due to lift will be calculated for with the following equation.

$$\Delta C_{D_{trimlift}} = \frac{\Delta C_{L_h}^2}{\pi A_{heh}} \left(\frac{S}{S_h} \right) \quad (69)$$

The horizontal tail increment lift coefficient will be calculated for before continuing. Since the trim of the horizontal tail has not been explicitly defined, it will remain at its original incidence angle of -3.5° . The following equation will be used.

$$\Delta C_{L_h} = C_{L_{\alpha_h}}(i_h) \quad (70)$$

The horizontal tail incremental lift coefficient required for trim was calculated to be $-.006109$. The remaining variables can be recalled from the empennage coefficient of drag calculations. This resulted in a final calculation for the trim drag due to lift of $1.322e-5$.

2.7.2 Trim Drag Due to Profile Drag

The trim drag due to profile drag will be found with the following equation.

$$\Delta C_{D_{trim}}_{prof} = \Delta C_{D_p}_{\Lambda_{c/4}} \cos(\Lambda_{c/4}) \left(\frac{S_{ef}}{S} \right) \left(\frac{S}{S_h} \right) \quad (71)$$

Before continuing, the profile drag coefficient due to an elevator must first be established. Roskam states that in order to find this value, it is best to treat the elevator as a flap and find its flap profile drag increment [1]. The elevator will be treated as plain flap, as the actual flaps used on the wing are plain flaps as well. The mean geometric chord length of the elevator and

horizontal will be used. The chord ratio was calculated to be .127. The profile drag during takeoff was found to be .011. The profile drag during landing was found to be .081.

The elevator wing flap area is found the same as the flaps. It is the area of the wing at which the elevator spans across, from the leading edge to the trailing edge. The following equation was used to find this value.

$$S_{ef} = \frac{2.34 + 6.5}{2} * 21 = 92.82 \text{ ft}^2$$

The following table will outline this value, as well as the omission of several previously established variables.

Table 17: Unknown variable definition for coefficient of drag due to landing gear.

Variable	Definition	Value
$\Delta C_{D_p} \Lambda_{c/4}$	Profile drag coefficient due to elevator (Takeoff)	.011
	Profile drag coefficient due to elevator (Landing)	.081
S_{ef}	Elevator flap area	92.82 ft

The calculated value for trim drag due to profile drag during takeoff was calculated to be .002271. The calculated value for trim drag due to profile drag during landing was calculated to be .01672.

The total drag coefficient due to trim during takeoff was calculated to be .002284. The total drag coefficient due to trim during landing was calculated to be .01673. The drag coefficient during the landing process will be used to determine the plane's overall coefficient of drag as it is the greatest of the two flight conditions. It will also provide extra room for error during takeoff.

2.8 Miscellaneous Item Drag

Miscellaneous drag may be caused from a number of different factors. Such instances when an extra item causes drag include spoilers, speed brakes and surface roughness amongst other things. Since Roskam is limited in the depth of this topic, only surface roughness will be covered.

2.8.1 Surface Roughness

The grade of surface roughness ranges depending on materials used on the outer most shell of the aircraft. The original coefficient of drag calculations for the wing and fuselage were assuming smooth surfaces. Since the material choice for either surface has not been made, it will be best to err on the side of caution and assume the skin is not free of imperfections which will create extra drag on the plane. The following figure is presented from Roskam showing the possible materials that may affect the plane's aerodynamic performance.

<u>Type of Surface</u>	<u>Equivalent Sand Roughness, k, in ft</u>
Aerodynamically smooth	0.0
Polished metal or polished wood	0.00000167 to 0.00000667
Natural sheet metal	0.00001333
Smooth matte paint, carefully applied	0.00002083
Standard camouflage paint, average application	0.00003333
Camouflage paint, mass-production spray	0.0001
Dip-galvanized metal surface	0.0005
Natural surface of cast iron	0.00083

Figure 19: Material's equivalent sand roughness. [1]

As most other business jets use polished metal as an exterior skin, it will be selected as the outer skin of this business jet as well. There is however a special case for business jets which utilize polished sheet metal, which has a roughneck of .000005 ft. An average of the two types of material will now be used as a revised material choice for the aircraft. The average equivalent sand roughness to be analyzed will be .000004585. This value lead to a new Reynolds number cutoff of approximately $6.0e7$.

The skin roughness will be analyzed for the fuselage and wings are the main surfaces that will be analyzed and reviewed. Roskam states to use the lowest Reynolds number to obtain the structure's turbulent flat plate friction coefficient. [1]

The wing will be analyzed first. The Reynolds number of the wing and cutoff will be observed to which of the two is the lowest. The lowest Reynolds value will be used to obtain the turbulent flat plate skin friction coefficient. The Reynolds number of the wing is $1.4e7$. This value is lower than the cutoff Reynolds number, thus, the computation of the drag coefficient will remain unchanged for the wing.

The fuselage's Reynolds number is calculated as $9.0e7$. This value is greater than the cutoff Reynolds number, thus, the calculation to find the fuselage's zero-lift drag coefficient will be revised. The new turbulent flat plate skin friction coefficient value will be .0022, rather than the original value of .0021. This will affect the fuselage zero lift drag coefficient. The new value will be .004627. The new coefficient of drag of the overall fuselage will now be .008877. The difference between the old and new values are shown in the table below.

Table 18: Old versus new values for coefficient of drag of fuselage.

Fuselage		
	Old Values	New Values
R_n	$9.0e7$	$6.0e7$
C_{f_fus}	.0021	.0022
$C_{D_o_fus}$.004419	.004627
C_{D_fus}	.008668	.008877

The empennage will be examined next. The empennage is separated into two separate calculations, one for the horizontal and the other for the vertical. The horizontal stabilizer's Reynolds number is recalled having been $9.4e6$. This value is less than the cutoff Reynolds number of $6.0e7$, Thus, the original drag coefficient calculation will remain the same. The vertical stabilizer's Reynolds number is recalled having been $1.7e7$. This value too is less than the cutoff Reynolds number. The vertical stabilizer drag coefficient calculation will not have to be revised either.

2.8.2 Other Items

Other items besides skin friction may also affect the drag coefficient of the plane. Such items include exhaust nozzles, antennas, area ruled structures, exposed bolts or external damages that may have created dings in the outer structure during flight. These items may add up, but for the most part, are so small in reference to the other vital components of the plane that they will have only a miniscule effect on the plane's overall coefficient of drag.

2.9 Coefficient of Drag Review

The drag coefficients of components of the plane are presented in the table below.

Table 19: Coefficient of drag of plane components.

Component	Value
Wing	.02323
Fuselage	.008668
Empennage	.004537
Nacelle/pylon	.006835
Flap (Takeoff)	.01750
Flap (Landing)	.03110
Gear (Takeoff)	.001802
Gear (Landing)	.0012
Trim (Takeoff)	.002284
Trim (Landing)	.01673
Miscellaneous (Revised Fuselage)	.008877

The plane will have several different coefficient of drag values: clean during cruise, takeoff, landing and max.

2.9.1 Clean Coefficient of Drag

For a clean aircraft's coefficient of drag, the original coefficient of drag equation will be modified to the following for a clean aircraft.

$$C_{D_{clean}} = C_{D_{wing}} + C_{D_{fus}} + C_{D_{emp}} + C_{D_{np}} + C_{D_{trim}} \quad (72)$$

In this equation, the coefficient of drag of the fuselage is replaced with the newly found miscellaneous drag coefficient. Although the trim drag coefficients are found during takeoff and landing, the coefficient of lift during takeoff and cruise are equal, allowing for the takeoff trim drag coefficient value to be used. The coefficient of drag of the clean aircraft is .04576.

2.9.2 Takeoff Coefficient of Drag

During takeoff, the landing gear and flaps will be deployed. The following equation will be used to determine the drag coefficient of the plane during takeoff.

$$C_{D_{TO}} = C_{D_{wing}} + C_{D_{fus}} + C_{D_{emp}} + C_{D_{np}} + C_{D_{flap_{TO}}} + C_{D_{gear_{TO}}} + C_{D_{trim_{TO}}} \quad (73)$$

The fuselage coefficient of drag is replaced by the miscellaneous drag coefficient of the fuselage. The drag coefficient during takeoff is .06507.

2.9.3 Landing Coefficient of Drag

During the landing phase of the flight profile, the landing gear and flaps will be deployed. The flaps and landing gear will differ from takeoff as the plane will require a different amount of lift than during takeoff. The following equation will be used to find the landing coefficient of drag.

$$C_{D_{LND}} = C_{D_{wing}} + C_{D_{fus}} + C_{D_{emp}} + C_{D_{np}} + C_{D_{flap_{LND}}} + C_{D_{gear_{LND}}} + C_{D_{trim_{LND}}} \quad (74)$$

The fuselage coefficient of drag will be replaced with the miscellaneous coefficient of drag which provided a revised value for the fuselage to include the added skin friction roughness. The landing coefficient of drag is .09252.

2.9.4. Max Coefficient of Drag

The maximum coefficient of drag is the greatest drag coefficient the plane may experience at any instance during flight. The following equation will be used to find this value.

$$C_{D_{MAX}} = C_{D_{wing}} + C_{D_{fus}} + C_{D_{emp}} + C_{D_{np}} + C_{D_{flap_{LND}}} + C_{D_{gear_{TO}}} + C_{D_{trim_{LND}}} \quad (75)$$

This value will be used as a safety net if for some reason the plane was forced to deploy the flaps and landing gear at cruising altitude. This value is .09311.

2.10 Drag Polar

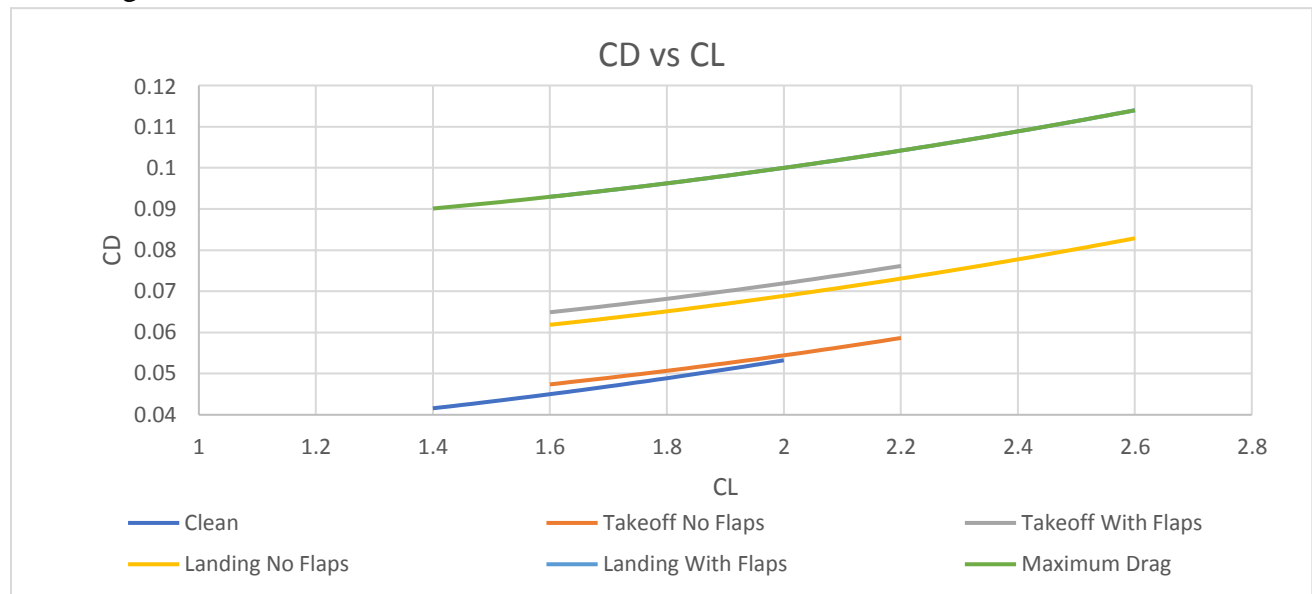


Figure 20: Drag polar diagram for business jet.

The drag polar ranges were chosen based off of Roskam's general coefficient of lift a business jet should generate. From this graph, the clean aircraft will generate the least amount of

drag, as expected. When flaps are enabled, they will increase the plane's coefficient of drag, as expected. If the plane were to experience a malfunction when flaps and landing gear are enable at cruising altitude, the coefficient of drag would largely increase. This large increase could cause the pilot to briefly lose control of the aircraft.

References

- [1] Roskam, J. (1989). Airplane Design Part IV: Layout Design of Landing Gear and Systems. University of Kansas.
- [2] Properties of US standard atmosphere ranging -5000 to 250000 ft altitude. (n.d.). Retrieved July 29, 2018, from https://www.engineeringtoolbox.com/standard-atmosphere-d_604.html
- [3] NACA 64-008A AIRFOIL (n64008a-il). (2018). Retrieved July 29, 2018, from <http://airfoiltools.com/airfoil/details?airfoil=n64008a-il>